UNIVERSITY OF CALIFORNIA

SANTA CRUZ

MODELING THE REPRODUCTIVE POTENTIAL OF ROCKFISHES (*SEBASTES* SPP.)

A dissertation submitted in partial satisfaction
of the requirements for the degree of

DOCTOR OF PHILOSOPHY

in

OCEAN SCIENCES

by

Edward Joseph Dick

March 2009

The Dissertation of Edward Joseph Dick
is approved:

Professor Marc Mangel, Chair

Stephen Ralston, Ph.D.

Professor Christopher A. Edwards

Professor Raquel Prado

Lisa C. Sloan
Vice Provost and Dean of Graduate Studies

Table of Contents

LIST OF TABLES

Tables

LIST OF FIGURES

Figures

ABSTRACT

Edward Joseph Dick

Modeling the reproductive potential of rockfishes (*Sebastes* spp.)

Understanding the reproductive potential of exploited fish populations is critical in the development of sustainable harvest practices. Models that characterize female fecundity often assume that the number of eggs produced per unit body weight (relative fecundity) is independent of size or age. Estimates of average lifetime egg production per female are used to determine target harvest rates for several fish species off the west coast of the United States, and are clearly sensitive to changes in relative fecundity with size. Relative fecundity in rockfishes (genus *Sebastes*) commonly increases with size, but to a varying degree among species. The extent to which this pattern alters our perception of target harvest rates for rockfish depends on the rate at which relative fecundity changes with size, and rates of somatic growth and natural mortality. The reproductive biology of several rockfish species remains poorly understood, and advice is needed regarding proper characterization of fecundity to aid fisheries managers in the development of harvest guidelines. I develop Bayesian hierarchical models to predict fecundity of data-poor rockfish species. The models use information from closely related (congeneric) species to inform predictions of fecundity at size, quantify uncertainty about those predictions, and provide predictive distributions of model parameters for unobserved species. Trends in size-specific relative fecundity are part of an organism's life history strategy. I use state dependent life history models for optimal resource allocation to evaluate potential mechanisms driving these trends. Patterns of growth, maturation and reproduction observed in rockfishes are consistent with the hypothesis of a trade-off between reproduction and natural mortality.

For Julie and Gannon

ACKNOWLEDGMENTS

My wife, Julie, and son, Gannon, deserve my greatest thanks. They are first in my heart, my inspiration, and my greatest teachers. I thank my mother and father for always encouraging me to pursue my dreams, and for providing support in so many ways. As with my family, my thanks to Marc Mangel can't be summarized on this page, but will hopefully become apparent through our continued friendship and future collaboration. Chris Edwards, Raquel Prado, and Steve Ralston provided advice and encouragement as part of my reading committee, and I greatly appreciate your individual contributions and support. The members of the Mangel and Wilmers labs, past and present, have provided companionship that made it easier to navigate through grad school and suggestions that significantly improved the quality of this work.

I have been fortunate to have the opportunity to learn from my NMFS mentors, friends, and fellow flatfish, Alec MacCall and Steve Ralston. I am indebted to all members of the Groundfish Analysis Team (Ken Baltz, John Field, Xi He, Don Pearson, and Keith Sakuma), who have unselfishly shared their knowledge of many topics related to this work, and who make it fun to come to work each day. My work also benefitted from several discussions with Sue Sogard, Bruce MacFarlane, and Mary Yoklavich, our resident experts on rockfish reproduction. My thanks also go to Churchill Grimes for supporting this research.

My fecundity meta-analysis would not have been possible without the researchers who have collected rockfish fecundity data over the years and who agreed to share it with me: Don Gunderson, University of Washington; Dan Ito, National Marine Fisheries Service (NMFS); Neosha Kashef, University of California, Santa Cruz (UCSC); Lisa Lacko, Fisheries and Oceans Canada (DFO); Milton Love, University of California, Santa Barbara; Bruce MacFarlane, NMFS; Dan Nichols, NMFS; Steve Ralston, NMFS; Laura Richards, DFO; Susan Sogard, NMFS; David Stafford, UCSC; Rick Stanley, DFO; Farron Wallace, Washington Department of Fish and Wildlife; and Lynn Yamanaka, DFO.

CHAPTER 1

INTRODUCTION

The earliest studies of reproduction in marine fishes were motivated by concerns over commercially exploited populations (e.g. Sars, 1876; Fulton, 1898; Raitt, 1933; Bagenal, 1957). Clearly, if our goal is to understand a population's resilience to harvesting, then we must consider factors that influence reproductive output, e.g. annual egg production (fecundity), sex ratios, size and age at maturity, viability of eggs and larvae, and biological responses to changes in population density. Together, these elements determine what has been referred to as the reproductive potential of a population (Goodyear, 1993; Trippel, 1999). Although this is the conceptual basis for setting harvest levels in many fisheries off the west coast of North America (Ralston 2002), recent studies continue to emphasize the need to improve our understanding and representation of reproductive biology in the context of managed fisheries (Trippel et al., 1997; Hunter and Macewicz, 2003; Morgan, 2008).

Reproductive potential and recent management of west-coast rockfishes

Excellent examples of the development of our understanding of stock productivity can be found in efforts to manage fisheries for rockfish (genus *Sebastes*, Cuvier 1829) off the west coast of the United States. Ralston (1998) highlighted severe declines in abundance of many rockfish populations over a

period of 2-3 decades. In 2000, the U.S. Secretary of Commerce declared the west-coast groundfish fishery a failure (Dorn, 2002).

Several aspects of rockfish life history are thought to have contributed to the failure of previous harvest policies (Yoklavich, 1998). The size of cohorts entering the adult population (recruitment) varies tremendously from year to year, and may be small for long periods of time, even decades (Ralston and Howard, 1995). Populations are often dominated by individuals from infrequent, large cohorts that are often subjected to substantial fishing mortality upon reaching a marketable size. Estimates of age at maturity among species vary from one to over twenty years, and many species become vulnerable to the fisheries prior to or upon reaching maturity (Love et al., 2002).

The longevity of rockfishes was severely underestimated historically, until methods were accepted that provide more accurate age estimates (Chilton and Beamish, 1982). Many species are now known to live longer than 50 years, and some are estimated to live over 200 years (Love et al., 2002). Longevity in general is thought to be an adaptation to highly variable environments affecting reproductive success in any given year (Murphy, 1968; Mangel, 2003).

In 1992, the Pacific Fisheries Management Council (PFMC), based on the work of Clark (1991), adopted a fishing mortality rate for rockfish that was estimated to reduce the expected lifetime egg production of a female rockfish to 35% of that in an unfished population (referred to as $F_{35\%}$). Using a simulation

approach, Clark (1991) showed that by fishing at this rate yields close to the maximum sustainable yield can be obtained from a range of assumptions about life history parameters and stock productivity. To clarify the terminology, $F_{100\%}$ corresponds to no fishing, i.e. individual lifetime egg production is not reduced by fishing mortality, but rather it remains at 100% of the expected amount in an unfished population. Continuing declines in rockfish abundance prompted the PFMC to adopt a further reduction in the fishing mortality rate to $F_{40\%}$ in 1997. The Council again reduced the harvest rate to the current target of $F_{50\%}$ based on a meta-analysis of productivity among rockfish stocks (Dorn, 2002; PFMC, 2006).

A brief overview of reproduction in rockfishes

To develop useful models of reproductive potential in fishes, it is important to understand the reproductive strategy of the species of interest. Most fish species release eggs and sperm into the water column, resulting in external fertilization and development of embryos (oviparity). In contrast, rockfishes have internal fertilization and bear live young. Studies have shown that in some rockfish species embryos obtain nutrients directly from the mother in addition to from the yolk, a process known as matrotrophic viviparity (Boehlert and Yoklavich, 1984; MacFarlane and Bowers, 1995). When embryos derive all their energy from egg yolks, this is known as lecithotrophic viviparity (also known as ovoviviparity). The extent to which embryos obtain energy directly from the mother differs among

species of rockfish, ranging from 92% in *S. schlegeli* to 3% in *S. flavidus* (Love et al., 2002).

Rockfishes are iteroparous, i.e. able to reproduce multiple times throughout their lives. Their annual reproductive cycles include egg development (vitellogenesis), copulation, delayed fertilization, gestation, and parturition (release of larvae into the water), but the timing and length of each stage may vary among species, years, and age groups (Wyllie Echeverria, 1987; Love et al., 2002; Bobko and Berkeley, 2004). Pelagic larvae are immediately able to feed on a diet that includes larval copepods and invertebrate eggs. Parturition is followed by pelagic larval and juvenile stages, often lasting several months before juveniles associate with benthic habitats.

Some species of rockfish appear to produce multiple broods of larvae in a year, particularly in the southern portion of their range. Moser (1967) found advanced embryos together with vitellogenic ova in bocaccio (*S. paucispinis*) and seven other species. MacGregor (1970) reported evidence of multiple broods in three species, and Love et al. (1990) identified twelve species with ovaries containing both advanced embryos and maturing ova. The *Sebastes* are most often considered to be determinate spawners, meaning that potential fecundity (the number of advanced yolked oocytes in the ovary) is fixed prior to the onset of the reproductive season (Eldridge et al., 1991; Murua and Saborido-Rey, 2003). The evidence of multiple broods therefore suggests that rockfishes are determinate batch

spawners (following the classifications of Murua and Saborido-Rey, 2003), and mature batches of the standing stock of yolked oocytes throughout the season until the stock of oocytes is exhausted for that year. Murua and Saborido-Rey (2003) classify the Atlantic *Sebastes* species as determinate total spawners, which ovulate the entire stock of yolked oocytes at one time and release a single brood of larvae. Total spawning is the dominant pattern among rockfishes from central California (Wylie Echeverria, 1987) to British Columbia (B. Leaman, personal communication cited in Love et al., 1990).

Age of maturation is a major factor determining lifetime reproductive success and must be considered in models of life-history strategies and population dynamics alike. Age of maturation in rockfishes varies considerably. The dwarf species Puget Sound rockfish (*S. emphaeus*) typically matures between 1-2 years, whereas approximately 50% of yelloweye rockfish (*S. rubberimus*) are thought to be mature after 22 years (Love et al., 2002). When differences in size at maturity have been found between male and female rockfish of the same species, males most often mature at smaller sizes (Love et al. 1990).

Recent literature has reported age-specific variation in aspects of rockfish reproduction. For example, larvae from older females have been found to survive longer under starvation conditions, suggesting differential survival of larvae from different age classes in wild populations (Berkeley et al., 2004; Sogard et al., 2008). This result is an example of a maternal effect in which offspring benefit from a

phenotypic characteristic of the mother. Truncation of older age classes due to fishing could therefore have a negative effect on reproductive potential of the population for a given level of spawning biomass, relative to the assumption that larvae from all age classes are equally viable.

Variability in rockfish fecundity

Estimates of rockfish fecundity can be highly variable among individuals and populations. Factors contributing to this variability are numerous and often poorly understood, but some general patterns have been observed. Size (length or weight) is a primary factor affecting fecundity in most fish species (Bagenal, 1967) and this includes rockfishes (Love et al., 2002). Haldorson and Love (1991) tabulated fecundity for lengths at which 50% of fish were mature in their review of rockfish maturity and fecundity. They found the number of eggs or larvae to vary from 1,700 to 417,000 among a collection of 45 species. Estimates of fecundity at maximum length among species ranged from 35,000 to 5,600,000 eggs or larvae.

Fecundity estimates for *Sebastes* also depend on the stage of ovarian development of the mother. Oocytes often cease to develop and are resorbed by the mother (atretic loss of oocytes). Estimates of absolute fecundity based on pre-fertilized oocytes are greater than post-fertilization estimates (Boehlert et al., 1982; Kusakari, 1991; Bobko and Berkeley, 2004). Methods for counting eggs and larvae are also not consistent among studies.

Within species, several studies have reported differences in fecundity among geographic regions and among years. Raitt and Hall (1967) studied fecundity of an Atlantic redfish (*S. norvegicus*, then called *S. marinus*), and estimated fecundity of fish taken near the Faroe Islands to be 15% higher than that of individuals caught near Iceland. Gunderson (1977) found greater fecundity at length for of Pacific Ocean Perch (*S. alutus*) off Oregon-Washington compared to Queen Charlotte Sound. Temporal and spatial variation in absolute fecundity was observed for yellowtail rockfish (*S. flavidus*) by Eldridge and Jarvis (1995), although significant spatial differences only applied to younger fish.

The effect of the environment, specifically conditions related to food availability for mature females, is also an important source of variability in egg production. Ventresca et al. (1995) found that the 1982-83 and 1992-93 El Niño events reduced body condition and gonadal indices in blue rockfish caught off central California. The study did not specify whether the reduction in gonadal indices was due to a reduction in egg number, size, or both. Lenarz and Echeverria (1986) saw a reduction in visceral and gonadal fat volumes in female yellowtail rockfish (*S. flavidus*) during the 1983 El Niño compared to observed volumes from 1980. Eldridge and Jarvis (1995) reported greater fat reserves in yellowtail rockfish from Washington, along with increased fecundity, relative to a California population. In a study of lipid dynamics and their connection to reproduction of yellowtail rockfish, MacFarlane et al. (1993) showed that females accumulate lipids

during summer months and then channel the accumulated energy into ovarian development, illustrating the importance of female condition at the beginning of the reproductive cycle.

Characterizing fecundity in models of fish population dynamics

The types of models used to monitor and manage exploited fish populations are very diverse, and the determination of which model to choose is usually based on the nature of the available data. The current state of the art for data-rich stocks is an age-structured approach which uses a mathematical model of a population (demographic structure, growth, reproduction, etc.) to generate predictions that are compared to various types of observations in a statistical framework. These models are known as stock assessments (Quinn and Deriso, 1999).

A common simplifying assumption about fish reproduction in stock assessment models is that the number of eggs or larvae produced per gram of body mass (relative fecundity) is assumed to be constant among all mature females. Put another way, the population's annual egg production is assumed to be directly proportional to the biomass of its spawning females with no direct influence from its age structure per se. Beverton and Holt (1957, pp. 61-64) were among the first to question this assumption in the context of quantitative fisheries science, and developed a simple model for mean annual yield that accounted for age-specific differences in relative fecundity. The effects of misspecification of reproductive

potential on management advice have been considered for at least 50 years, with consistent recommendations for more accurate representations of reproductive biology in population dynamics models (Beverton and Holt, 1957; Rothschild and Fogarty, 1989; Trippel et al., 1997; MacCall, 1999; Murawski et al., 1999; Beamish et al., 2006; Morgan, 2008).

The assumption that spawning output is directly proportional to female spawner biomass is often adopted when little or no fecundity data are available. Data on fish reproduction are often scarce, but are most plentiful for species that are the objects of large-scale commercial fisheries. Information related to age and size at maturity and sex ratios are most common, followed by data on fecundity and the viability of eggs and larvae (Morgan, 2008). Little or no data on reproduction may exist for species targeted by small fisheries, or for bycatch species that are simply less abundant in the catch. In these data-poor situations, it is necessary to consider alternative strategies until data become available for the species of interest. For example, closely-related species may provide a basis for reasonable assumptions about reproductive potential when data are limited or lacking.

Reproductive potential as an optimal life history strategy

A life history strategy is a collection of traits (e.g. growth, reproduction, and age at maturity) that co-evolve in the presence of trade-offs affecting individual expected reproductive success. The process of natural selection favors certain

combinations of traits, and we can represent this process as a series of developmental pathways (trade-offs) made by an organism to maximize its lifetime reproductive success. Although the true number of trade-offs is large, we can use life history models to identify the primary factors that reproduce the patterns we observe and consider them as testable hypotheses of what drives the evolution of life histories.

An intuitive example is the trade-off between growth and mortality. Organisms require food to grow, but foraging can be risky due to exposure to predators. Another commonly studied trade-off is that between growth and reproduction. Metabolic energy allocated to reproduction can not be allocated to growth. However, it is well established that fecundity per spawning increases with size in most fish species (Wooten, 1998). Another developmental consideration in models of reproductive strategies is age at maturity. The timing of maturity is a trade-off between future reproduction (growth) and current reproduction (allocation of energy to gonads). Of course, both of these decisions must be made in consideration of the probability that the individual will survive to reproduce later.

The diversity of life-history strategies among fishes has made them a focus of evolutionary biologists for several decades (Svärdson, 1949; Beverton and Holt, 1959; Roff, 1983, 1984; Beverton, 1992; Roff et al., 2006). The genus *Sebastes*, in particular, is well-suited for studies of life history evolution due to their incredible diversity of life history strategies (Beverton, 1992; Love et al., 2002). Among the

Sebastes, estimates of asymptotic length range from about 15 cm to 100 cm. The length at which 50% of females are mature varies from 10 – 45 cm. Growth rates are highly variable and maximum ages range from about 15 years to over 200 years for rougheye rockfish, *S. aleutianus* (Love et al., 2002).

Other components of reproductive potential among rockfishes are also highly variable. Average fecundity among species ranges from over a million eggs per female to less than 50,000. Relative fecundity (eggs per gram of body weight) increases with size in some species, but is independent of size in others. Optimal life history models provide a framework to help us understand how these mechanisms might interact to produce the observed patterns in reproductive potential.

Life-history models for optimal growth and resource allocation

The difficulties associated with collection of fecundity data, combined with the considerable uncertainty in resulting estimates, suggest that future research could benefit greatly from application of theoretical models designed to focus that research. These models provide a means to conduct virtual experiments, exploring hypothetical mechanisms to generate predicted patterns and motivate testable hypotheses.

We are interested in developing a life-history model of resource allocation that generates predicted patterns in relative fecundity that reflect observed patterns among the *Sebastes*. Kozlowski et al. (2004) assert that models of resource

allocation require a minimum of two sinks for surplus energy: growth and reproduction. We also require a description of factors contributing to mortality, and flexibility of the model with respect to the timing of maturation.

In choosing a growth model, we adopt a modification of the von Bertalanffy growth model (von Bertalanffy, 1938). The growth model of Stamps et al. (1998) is consistent with the advice of Day and Taylor (1997), who advocate models with separate specifications of pre- and post-maturity growth. I recast the continuous growth model of Stamps et al. (1998) as two possible discrete growth increments, one for juvenile growth (the same as von Bertalanffy growth), and one for adult growth that exhibits decreased potential growth for individuals that mature at smaller lengths. In order to first explore parsimonious explanations for our question, we represent reproduction as the fraction of potential gain in mass allocated to gonads. The remainder of potential growth is allocated to somatic growth in weight. Mortality rates are allowed to be constant, or functions of length and/or reproductive effort.

My model illustrates trade-offs between growth, age at maturity, and allocation to reproduction for a given hypothesis (set of input parameters and model structure) based on the common currency of expected lifetime egg production. The optimal allocation decisions represent a life-history strategy that would be favored by natural selection, given the model assumptions. I identify these decisions using a state-dependent framework, stochastic dynamic programming, that predicts optimal

behavior for all combinations of the state variables over time (Mangel and Clark, 1988; Mangel and Ludwig, 1992; Houston and McNamara, 1999; Clark and Mangel, 2000).

Evolutionary history of rockfishes

Closely-related species often have similar life-history strategies. When comparing life-history traits, it is therefore important to consider interspecific relations (evolutionary history and phylogeny) as this can provide insight regarding broad, interspecific patterns. Beverton and Holt (1959) recognized this in their work relating growth characteristics to longevity in fish, identifying patterns common to several orders of fish. Beverton (1987) explicitly considered the evolutionary record in his review of longevity in fish, singling out the genus *Sebastes* as a remarkable example of extreme longevity.

Classification of *Sebastes* subgroups originally relied on morphological characteristics such as variations in the number and size of spines on the head, or counts of vertebrae, fin rays, gill rakers, or lateral line pores (Kendall, 2000; Love, 2002). Beginning in the 1960s, researchers began using biochemical methods such as protein electrophoresis to examine rockfish systematics (Seeb, 1986; cited in Kendall, 2000). In the late 1990s, researchers increased this focus on genetic identification methods in hopes of better understanding rockfish taxonomy (Johns and Avise, 1998; Rocha-Olivares et al. 1999a, b). Using this approach, Rocha-

Olivares et al. (1999a) presented strong evidence that the subgenus *Sebastomus* (as defined by Chen, 1971) is monophyletic, i.e. that all descendents of the common ancestor are included in this group.

Two studies of rockfish evolutionary relationships (Hyde and Vedder, 2007; Li et al., 2007) found that the current subgeneric assignments for *Sebastes* species (reviewed by Kendall, 2000) are either paraphyletic (contained some, but not all, species descendent from a common ancestor) or polyphyletic (did not contain the most recent common ancestor). Both studies corroborated the results of Rocha-Olivares et al. (1999a) concerning the monophyly of *Sebastomus*. The study by Hyde and Vetter (2007) is arguably the most comprehensive study of *Sebastes* evolutionary relationships to date.

Hyde and Vetter (2007) group some rockfish species from the Northeast Pacific ocean with species from the North Atlantic. According to their reconstruction of rockfish evolution, species of redfish from the North Atlantic (*S. norvegicus/S. marinus*, *S. fasciatus*, *S. mentella*, and *S. viviparus*) are closely related to some of the Northeastern Pacific species, e.g. *S. alutus* (Pacific Ocean Perch) and *S. crameri* (darkblotched rockfish). Kendall (2000) cited the genus *Sebastes* as only containing the Atlantic species, and associated *S. alutus* and *S. crameri* with the subgenera *Acutomentum* and *Eosebastes*, respectively. Hyde and Vetter (2007) attribute the close relationship between these currently isolated species to a common ancestor that colonized the Bering Sea and North Atlantic during a period of high-

latitude warming (the "trans-arctic interchange") that occurred 4 – 3.5 million years ago (Vermeij, 1991; cited in Hyde and Vetter, 2007).

The focus of this dissertation is on species from the Northeastern Pacific, and specifically areas off the west coast of the United States and Canada. The majority of rockfish species occur in this area (Love et al., 2002), but comparison of these results with data for species from other regions (e.g. Northwest Pacific, North Atlantic, Southern Hemisphere) may improve our understanding of mechanisms driving differences in life history strategies among the members of this speciose group.

Chapter summaries

In the chapters that follow, I will discuss three topics related to fecundity in rockfishes. In the second chapter, I use simple age-structured models to quantify the consequences of incorrectly assuming that relative fecundity is constant with respect to size. I also review the assumptions of models commonly used to describe fecundity in fishes. Finally, I examine a collection of rockfish fecundity data sets to look for size-specific trends in relative fecundity, in the context of our current understanding of their evolutionary histories.

In chapter three, I develop a Bayesian hierarchical model to quantify the strength of evidence for size-dependent relative fecundity in rockfishes, and to improve our estimates of fecundity parameters used in stock assessments. This

approach generates predictive distributions of fecundity parameters that could be used for assessment of data-poor species.

If larger fish allocate an increasing fraction of their available energy to reproduction, this implies an energy cost to some other biological process (e.g. growth, maintenance, energy storage). In chapter four, I develop a state-dependent model for energy allocation to investigate processes that influence changes in relative fecundity. I describe a stochastic dynamic programming algorithm that identifies developmental pathways (age at maturity and energy allocation to growth and reproduction) that optimize lifetime reproductive success under alternative assumptions about growth and mortality.

CHAPTER 2

SIZE-SPECIFIC RELATIVE FECUNDITY IN ROCKFISHES AND IMPLICATIONS FOR FISHERIES MANAGEMENT

Early studies of the reproductive biology of Northeastern Pacific rockfishes (*Sebastes* spp.) coincided with the rapid expansion of the Pacific Ocean Perch (*S. alutus*) fishery during the 1950s and 1960s (Westrheim, 1958; Phillips, 1964; Moser, 1967; MacGregor, 1970). Recently, commercial and recreational rockfish fisheries off the west coast of North America have been severely restricted, the result of a generally poor understanding of the productivity of rockfish populations, failure to adequately limit fishing capacity, and several years of low recruitment since the 1990s (Ralston, 1998; Love *et al*, 2002). Seven *Sebastes* species are currently classified as overfished, i.e. the biomass of female spawners is estimated to be below 25% of the theoretical unfished biomass. Recent calls for improved characterization of reproductive biology in stock assessments are intended to help fishery managers to better understand the timelines necessary to rebuild overfished stocks, and to avoid overfishing stocks that are currently above overfished thresholds (Hunter and Macewicz, 2003; Morgan *et al*., 2008).

Reproductive biology and its role in determining how stocks replenish themselves is of great interest to fishery scientists who are asked to provide advice regarding harvest levels that maintain desired catches over time. Simple age-structured models ("per-recruit" models) have long been used to provide valuable information about the effect of fishing on the expected yield and lifetime egg

production per recruit (Beverton and Holt, 1957; Sissenwine and Shepherd, 1987). These models are the conceptual basis for the target fishing mortality rates currently adopted for rockfish populations managed by the Pacific Fishery Management Council (PFMC, 2006). I use per-recruit models to demonstrate that failure to account for size-specific trends in relative fecundity alters our perceptions of the reproductive output per recruit, and may lead to adoption of unsustainable target fishing mortality rates.

Fecundity models in stock assessments are typically functions of length, weight, or age. The use of an allometric relationship between absolute fecundity (number of eggs) and fish length is perhaps the most common approach. By focusing on length alone, this model ignores the relationship between fish condition and egg production, as condition likely reflects food availability and energy available for reproduction. In this study I propose and evaluate a simple alternative model for relative fecundity in stock assessments. I show how the alternative model relates absolute fecundity and fish condition, and then compare model fits between allometric models for absolute and relative fecundity, as well as a linear model for relative fecundity.

Early studies of fecundity in marine fishes found that a stock's annual egg production is often roughly proportional to the biomass of its spawning females, i.e. the number of eggs produced per gram of body weight (relative fecundity) is constant with respect to size or age (Raitt, 1933; Simpson, 1951). Among the

Sebastes, studies have shown that this assumption is not accurate for all species. Boehlert *et al*. (1982) showed that relative fecundity increases with age for widow rockfish (*S. entomelas*). Haldorson and Love (1991) calculated estimates of relative fecundity using predictions from published maturity and growth models, and found that the ratio of relative fecundity at maturity to relative fecundity at maximum size is less than one for 17 out of 18 species examined (Table 2 in Haldorson and Love, 1991). Similar patterns are implied by other studies, but relative fecundity in recent rockfish stock assessments has more often than not been assumed constant with respect to size and age (Table 1). A primary goal of this study is to evaluate size-specific trends in relative fecundity among rockfishes, and to consider similarities in these patterns based on evolutionary relatedness of species in the genus.

Estimates of relative fecundity (eggs per gram) do not fully characterize reproductive investment in fishes. Differences in the quality of eggs or larvae may also contribute to differential reproductive success within and among populations (Svärdson, 1949; Bagenal, 1973). Murawski *et al*. (1999) found that if fish body size affects larval quality, then removal of larger females from the population will adversely affect reproductive potential. Berkeley *et al*. (2004) found that progeny of older female black rockfish (*S. melanops*) survived starvation over twice as long as progeny from younger females. They showed that larvae from older females had significantly larger oil globules at the time of parturition, and that oil globule size was positively correlated with larval growth rates (length and mass) and median

time to starvation. Increased growth rates during the larval stage are thought to help individuals avoid predation, and increased survival without food may provide a buffer against short-term periods of low food availability. Sogard *et al*. (2008) found similar maternal effects in three of five other *Sebastes* species, noting stronger trends among species in the *Sebastosomus* subgenus and no apparent trend among the *Pteropodus* species. Differences in egg and larval quality have not been studied for most rockfish species included in this study, so I focus solely on the number of eggs and larvae as an approximate indicator of relative investment.

In this study I demonstrate the importance of properly characterizing size-specific relative fecundity in rockfish stock assessments. I use simple age-structured cohort models to quantify potential bias in target reference points currently used in management of rockfish fisheries. I evaluate alternative models for fish fecundity, and demonstrate how it is important to collect information on length, weight, and gonad maturation stage as a minimum set of covariates in rockfish fecundity studies. Finally, I compile fecundity data from over forty rockfish species and look for evidence of broad-scale trends among studies, species, and sub-generic groups.

Methods

Per-recruit models

Per-recruit models are simple age-structured models with a long history in quantitative fisheries science. These models describe the abundance of a single cohort using a discrete-time model

$$N_{a+1} = N_a \cdot e^{-(M+F_a)} = R \cdot e^{-\left(M\cdot(a+1)+\sum_{a=0}^{a+1} F_a\right)}. \quad (2.1)$$

The number of fish surviving to the next age class, N_{a+1}, is determined by the number of fish in the previous age class, N_a, reduced by the combined forces of fishing and natural mortality.

The natural mortality rate, M, characterizes deaths not caused by fishing (e.g. predation) and is often assumed constant with respect to age. If age-specific information about natural mortality is available, it is easily accommodated by this framework. Age-specific fishing mortality rates, F_a,

$$F_a = F \cdot S_a. \quad (2.2)$$

are defined as the product of a full fishing mortality rate (F) and "selectivity" at age, S_a, which represents the proportion of full fishing mortality experienced by fish of age *a.* Simple examples of selectivity curves are 1) constant selectivity for all ages, 2) "knife-edge" selectivity, which assumes that fish are immediately exposed to the full fishing mortality rate as soon as they reach a given age or size, and 3) a gradual

increase or decrease in selectivity with age or size, which is often approximated by a logistic function

$$S_a = \frac{1}{1+\exp\left(-\theta\left(a-a_{50}\right)\right)}. \tag{2.3}$$

The parameter a_{50} determines the age at which 50% of individuals are vulnerable to the fishery (the inflection point), while θ controls the slope of the selectivity curve at age a_{50}. Selectivity is likely to be a function of length *S(l)*, but age-specific values can be approximated by calculating predicted length at age and using that value in a length-specific selectivity function, $S(l_a)$.

Length at age in fish is often well described by the von Bertalanffy growth model

$$L_a = L_\infty\left(1-e^{-k(a-t_0)}\right) \tag{2.4}$$

where L_∞ is asymptotic size, k determines the rate at which the fish approaches L_∞, and t_0 is a location parameter.

The average proportion of mature individuals at each age, p_a, is often characterized by a logistic equation

$$p_a = \frac{1}{1+\exp\left(-\theta'\left(a-a'_{50}\right)\right)}. \tag{2.5}$$

where a'_{50} is age at 50% maturity and θ' is the slope of the maturity curve at that age. Mean fecundity at age, Φ_a, is represented by an allometric function of length at age

$$\Phi_a = \alpha L_a^{\beta}. \tag{2.6}$$

The schedules of mortality, fecundity, and maturity are used to estimate lifetime egg production (*LEP*) of the average female recruit

$$LEP = \sum_{a=0}^{a_{\max}} e^{-\left(M \cdot a + \sum_{a=0}^{a} F_a\right)} \cdot \Phi_a \cdot p_a \tag{2.7}$$

Often, weight at age, W_a,

$$W_a = cL_a^{\beta} \tag{2.8}$$

is substituted for fecundity at age in Equation 2.7, based on the assumption that the population's egg production is directly proportional to female spawning biomass. In other words, relative fecundity is assumed constant with respect to age (and size), which also implies that the exponent of the fecundity-length relationship is identical to the exponent of the weight-length relationship.

The management strategy employed by the PFMC for *Sebastes* species includes specification of a constant harvest rate known as $F_{x\%}$, defined as the fishing mortality rate that reduces *LEP* of a cohort to *x*% of what it would be in the absence of fishing (Clark, 1991, 2002). This value is called the spawning potential ratio, *SPR,* and is the ratio of *LEP* in a fished population to *LEP* in an unfished population.

$$SPR = \frac{LEP_{fished}}{LEP_{unfished}} = \frac{\sum_{a=0}^{a_{\max}} e^{-\left(M \cdot a + \sum_{a=0}^{a} F_a\right)} \cdot \Phi_a \cdot p_a}{\sum_{a=0}^{a_{\max}} e^{-M \cdot a} \cdot \Phi_a \cdot p_a} \tag{2.9}$$

The derivation of the $F_{x\%}$ reference point was based on efforts to identify harvest rates that achieve high levels of yield while simultaneously maintaining a sufficient level of spawning to ensure stock replacement (e.g. Sissenwine and Shepherd, 1987; Clark ,1991, 2002; Ralston, 2002; Dorn, 2002). Since the true relationship between the number of spawners and the expected number of recruits (the stock-recruitment curve) is unknown, Clark (1991, 2002) sought to identify sustainable harvest rates that come close to maximizing expected yield under a range of assumptions about overall stock productivity. Rockfish fisheries off the west coast of the United States currently use the reference point $F_{50\%}$ as a proxy for F_{MSY}, the fishing mortality rate that produces maximum sustainable yield (*MSY*).

Size-specific relative fecundity and per-recruit analyses

If we incorrectly assume that relative fecundity is constant with respect to fish length, our estimates of SPR and target fishing rates will be biased. To quantify this effect, I plotted contours of realized ("true") equilibrium SPR that would result from fishing at $F_{50\%}$ as defined by the "false" model with constant relative fecundity. I present this surface of realized SPR values as a function of two independent variables: the natural mortality rate (*M*) and the exponent of the true fecundity-length allometric model (R code for contour plots by *M*. Prager, 2006). I chose values for natural mortality (*M*) and the true fecundity exponent that are representative of the genus *Sebastes*, ranging from 0.02 – 0.3 and 2.5 – 7,

respectively. For each combination of M and the 'true' fecundity exponent, I used a numerical optimization routine in the statistical language R (R Development Core Team, 2008) to find $F_{50\%}$ based on the assumption that the fecundity exponent and the weight-length exponent were both fixed at 3. I followed this process for two sets of von Bertalanffy growth parameters (k and L_∞) to illustrate the effect of growth on the extent of bias in SPR. The first set of growth parameters is close to the average value for each parameter as reported in Love *et al*. (2002), representing a "typical rockfish" ($k = 0.15$ yr^{-1}, $L_\infty = 40$ cm). The second set of parameters is intended to represent a large, slow-growing species ($k = 0.05$ yr^{-1}, $L_\infty = 80$ cm).

Fecundity models

Fish fecundity (Φ) is most often modeled as a power function of length.

$$\Phi = cL^d e^{\varepsilon} \tag{2.10}$$

$$\varepsilon \sim N\left(0, \sigma^2\right) \tag{2.11}$$

Parameter estimates of c, d, and σ^2 are obtained via simple linear regression following natural-log transformation of the variables.

$$\log\left(\Phi\right) = \log(c) + d\log\left(L\right) + \varepsilon \tag{2.12}$$

$$E\left\{c\right\} \approx \exp\left\{\log\left(c\right) + \sigma^2 / 2\right\} \tag{2.13}$$

Life history studies commonly examine other fecundity covariates such as weight and age, but usually one covariate is selected as the 'best' predictor in a linear model due to the correlations between fish length, weight, and age. Weight is

known to affect reproductive output, since weight at a given length is an indicator of condition (e.g. fat reserves). A fish that is too thin for its length is at risk of starvation, or may skip spawning for lack of energy resources. A fish that is too heavy for its length would presumably suffer from reduced mobility and possibly increased predation risk (Noren and Mangel, 2004).

The condition of a fish is sometimes evaluated using the ratio of observed weight (W_{obs}) to the estimated average weight at the observed length (W_{pred}). This ratio is commonly referred to as a relative condition factor, *K* (Fulton, 1904; Le Cren, 1951).

$$K = \frac{W_{obs}}{W_{pred}} \tag{2.14}$$

Several studies have considered how fish fecundity varies with condition (Bagenal, 1957; Wooton, 1979; Ventresca *et al*., 1995). It makes sense, therefore, to incorporate both length and weight information into models of fish fecundity. As noted above, the choice to use one or the other is usually an attempt to avoid correlations between these covariates in the normal linear model.

We can model length-specific trends in relative fecundity by simply taking the ratio of the fecundity-length and weight-length models. This ratio is another power function, with parameters that are functions of the fecundity-length and weight-length relationships.

$$\frac{\Phi}{W} = \frac{cL^d}{aL^b} = \left(\frac{c}{a}\right) L^{(d-b)} e^{\varepsilon}, \quad \varepsilon \sim N\left(0, \sigma^2\right) \tag{2.15}$$

The ratio of two lognormally distributed variables is also lognormal (Crow and Shimizu, 1988). Therefore, if the assumptions of the component models are reasonable, we can retain the assumption of lognormally-distributed errors for the allometric relative fecundity model.

Plotting eggs per gram body weight as a function of length illustrates how relative investment in reproduction changes with size. By rearranging Equation 2.15, we see that this model implies that absolute fecundity is directly proportional to the condition factor, *K*.

$$\Phi = cL^d\left(\frac{W}{aL^b}\right) = cL^d\left(\frac{W_{obs}}{W_{pred}}\right)$$

$$\Phi = cL^d(K) \tag{2.16}$$

In other words, a fish that is x% heavier or lighter than the population average will produce x% more or fewer eggs, respectively. Using the available data, I evaluated the adequacy of this assumption by plotting the ratio of observed fecundity to predicted fecundity against the ratio of observed weight to predicted weight. Equation 1.15 suggests that points on this graph would follow a line with a zero intercept and a slope of one.

I model the relative fecundity model (Equation 2.15) under log-transformation of the variables. In this model, however, the logarithm of weight is included as an "offset" term, i.e. a covariate with coefficient set equal to 1.

$$\frac{\Phi}{W} = \left(\frac{c}{a}\right)L^{(d-b)} = \alpha L^{\beta} e^{\varepsilon} \tag{2.17}$$

$$\log(\Phi) - \log(W) = \log(\alpha) + \beta \log(L) + \varepsilon \tag{2.18}$$

$$\log(\Phi) = \log(W) + \log(\alpha) + \beta \log(L) + \varepsilon \tag{2.19}$$

$$\varepsilon \sim N(0, \sigma^2) \tag{2.20}$$

$$E\{\alpha\} \approx \exp\{\log(\alpha) + \sigma^2 / 2\} \tag{2.21}$$

This model requires measurement of fecundity, length and weight for each fish. Predicted weights from an allometric model cannot be used because they are perfectly correlated with length under log transformation. Since the regression coefficient for the offset term (*log(W)*) is fixed rather than estimated, the correlation between length and weight has no influence on the variance of the estimated regression coefficients.

The characterization of fecundity in the most commonly used stock assessment model for U.S. west-coast rockfish is a model for relative fecundity (eggs per kg) as a linear function of weight (Methot, 2005).

$$\frac{\Phi}{W} = a + bW + \varepsilon; \quad \varepsilon \sim N(0, \sigma^2) \tag{2.22}$$

To identify if a single model consistently outperforms other alternative models, I calculated Akaike's Information Criterion (Akaike, 1973) for a set of six models for absolute fecundity. The model with the minimum AIC value is considered to be best supported by the data. I present the difference between the minimum AIC value and the AIC for alternative models (Δ-AIC) which assigns the preferred model a Δ-AIC value equal to zero by definition. The linear model for

relative fecundity was not included in the set of candidate models due to the change in the response variable (relative fecundity versus absolute fecundity).

I fit fecundity data for yellowtail rockfish (Eldridge *et al*., 1991) using the length-based allometric model for absolute fecundity (Equation 2.10), the length-based allometric model for relative fecundity (Equation 2.19), the weight-based allometric model (similar to Equation 2.10, but with weight as a covariate), and the linear model for relative fecundity (Equation 2.22). I examined regression results and residual plots from the three models to evaluate model fit and assumptions.

Since the allometric model for relative fecundity assumes that absolute fecundity is proportional to the relative condition factor (Equation 2.16), I plotted the ratio of observed fecundity over predicted fecundity at length against the ratio of observed weight to predicted weight at length. I did this for three stages of gonad development using the yellowtail rockfish data from Eldridge *et al*. (1991) and S. Sogard *et al*. (unpublished data).

Length and weight data

I converted all fish lengths to total length (mm) using published conversion equations (Echeverria and Lenarz, 1984; Lea *et al*., 1999). Stanley and Kronlund (2005) reported fork lengths of silvergrey rockfish (*S. brevispinis*) and since I found no published length-conversion equations I assumed that this was equal to total length based on visual examination of published photographs.

Because fish length is easier to measure than fish weight (especially at sea), weights of individual fish are not always recorded in fecundity studies. Ideally, we want to estimate relative fecundity based on the measured weight of a fish. Many studies report only fish fecundity and length, making it is necessary to calculate relative fecundities from predicted weights. When this was necessary, I first attempted to predict weight based on weight-length relationships given in the same study (e.g. Phillips, 1964; Love *et al*., 1990). If no weight-length model was reported in the fecundity study, I attempted to use a published model from the same region.

Measured and predicted weights collected from fisheries are usually total weight (i.e. weight of the entire fish, including gonads). This measurement type presents a problem when estimating relative investment in terms of eggs per gram. Some publications report gonad weights, allowing me to compare total weight with somatic weight (total weight minus gonad weight) and evaluate the effect of using total weight to estimate relative fecundity. I used this approach to adjust reported weights of post-parturition fish in the study by Sogard *et al*. (2008), providing a more accurate comparison of relative fecundity among studies. This procedure of adjusting weight with a linear model does not affect the estimate of the exponent when fitting a power function to the data, but it does scale the result.

Assigning stages of development

The annual cycle of gonad development in rockfishes has been shown to affect estimates of absolute fecundity in some species. Raitt and Hall (1967) were among the first to identify the potential importance of maturity state on estimates of fecundity. Kusakari (1991) showed that fecundity decreased with subsequent stages of embryonic development for the Northwestern Pacific species *S. schlegeli*. Bobko and Berkeley (2004) found that estimates of fecundity for black rockfish (*S. melanops*) were reduced on average by 160,000 eggs (approximately 16-40% of absolute fecundity) when measured from females with fertilized eggs relative to measurements based on pre-fertilized eggs.

Several classification schemes exist for the maturation state of rockfish gonads. In order to identify stages among the studies in the fecundity database, I re-assigned all reported stages into one of three stages: pre-fertilized eggs, fertilized eggs, and eyed larvae.

Comparison of relative fecundity estimates based on different stages of gonad development is complicated by the same factors that confound the interpretation of variability over space and time: differences in relative fecundity among studies may be methodological, rather than biological in origin. I used a general linear model fit to the data of Eldridge *et al*. (1991) on stage 1 and stage 2 yellowtail rockfish to evaluate the effect of stage on relative fecundity for this species.

Gunderson (1976) estimated *S. alutus* fecundity based on his criterion for mature oocytes (>0.3 mm) prior to fertilization. His estimates were assigned to stage 1. Westrheim (1958) counted yolked eggs from *S. alutus* ovaries described as yellow-orange in color and not translucent or clear. These observations were assigned to stage 1, because fertilized eggs in rockfish typically appear clear or transparent (Bowers, 1992). MacGregor (1970) provided separate counts of eggs and embryos. I assigned all counts reported as eggs to stage 1. MacGregor identified embryo stage XI as the beginning of eye-pigment formation (my stage 3) and therefore I classified stages I - X as stage 2 (fertilized, but not yet eyed larvae). Romero (1988) counted "ripening" eggs, described as large, yellow, and opaque, in 68 kelp rockfish. These gonads were classified as stage 1 based on the descriptions of Bowers (1992). The observations of DeLacy *et al*. (1964) were described as un-eyed embryos, and classified as stage 2. Stanley and Kronlund (2005) stated that all *S. brevispinis* gonads in their study were in a pre-fertilized condition. Four fish in their study had high parasite loads and reduced fecundity, and were excluded from the analysis. Ito (1977) based his classification on that of Westrheim (1975) and counted pre-fertilized oocytes described as large, yellow, and opaque. The Department of Fisheries and Oceans, Canada, provided *S. maliger* and *S. caurinus* data from Richards and Emmett (1988) along with maturity codes. Almost all oocytes from that study were in a pre-fertilized condition, with a small number of fertilized samples. Fecundity estimates for *S. chlorostictus* (Benet *et al*., in prep)

were in stage 2 (D. Pearson, pers. comm., 2008). Love *et al*. (1990) stated that all fecundity estimates were based on unfertilized eggs. Nichol and Pikitch (1994) estimated fecundity of *S. crameri* samples based on pre-fertilized oocytes, excluding pre-vitellogenic and atretic oocytes. Phillips (1964, p. 8) described the samples in his study as "ovaries with developing eggs still attached." These estimates were assigned to stage 1. Moulton (1975) described all *S. emphaeus* specimens as "ripe," which is a term often used for fish containing eyed larvae. These observations were assigned to stage 3. Corlett (1964) did not provide information about stages of gonad development, but Raitt and Hall (1967) cited a personal communication with Corlett confirming that egg counts were of fertilized eggs. Fish identified as "mentella type" by Corlett (1964) were excluded from his analysis, due to the possibility of species misidentification. Eldridge *et al*. (1991; B. MacFarlane, pers. comm., 2008) used the developmental stages described in Bowers (1992). Samples from their study provided stage 1 and stage 2 fecundity estimates for *S. flavidus*. Sogard *et al*. (unpublished data) estimated fecundity from stage 2 and stage 3 samples (S. Sogard, pers. comm., 2008).

Snytko and Borets (1973, p. 3) described gonad development in their samples as "maturity stages III and IV." Fortunately, Westrheim (1975, Table 1) describes the gonad-condition criteria used at the time by U.S.S.R. scientists, confirming that the Snytko and Borets data are based on pre-fertilized eggs. Snytko and Borets (1973) report fecundities for *S. rubrivinctus*, but this species is rare north

of San Francisco and it is generally accepted that early reports of *S. rubrivinctus* caught in Oregon and north were actually *S. babcocki* (Love *et al*., 2002). The data in this study are mainly reported as the number of fish in each 2-cm length bin, with an associated range of fecundities. I retained all data reported for individual fish, and when a length bin contained only 2 fish I assumed that the reported minimum and maximum fecundities were individual observations. I then assigned both fish a length equal to the mid-point of the length bin. Therefore, lengths for these fish are only known with +/- 1 cm accuracy. Given that no other fecundity information appears to exist for some of these species (e.g. *S. babcocki*), I chose to retain these data in the analysis, although this source of observation error is not accounted for in the results. Data from Snytko and Borets' (1973) length bins that contained more than 2 fish were not included in this analysis.

Sogard *et al*. (2008) had a unique set of fecundity estimates, based on larvae extruded in laboratory tanks. These were assigned to stage 3, but the experimental conditions required estimation of total weight from somatic weight (fish sacrificed after parturition). To maintain consistency with the rest of the weight data (total weights) I regressed somatic weight against total weight for each species in their study, by gonad stage when possible, to estimate total weight prior to parturition.

Relative fecundity by species group

This study is based on a collection of rockfish fecundity data from 24 sources, comprised of 2048 fecundity observations from 41 species of rockfish (Table 2). Most of the studies were conducted off the west-coast of North America, ranging from northern Mexico to British Columbia. Data were also available for one Atlantic species, golden redfish (*S. norvegicus*, also called *S. marinus*), from an early study off East Greenland (Corlett, 1964). Previous studies have compared parameter estimates from fitted fecundity-length relationships (see review by Haldorson and Love, 1991). This study focuses primarily on original data to assist in evaluating trends in light of the observed variability within and among data sets. I categorized fecundity observations by study, species, relationship with other species (e.g. subgenus), date of capture, area, and stage of gonad development.

I grouped species according to the phylogenetic tree generated by Hyde and Vetter (2007, their Figure 3). Some species in our database (*S. levis*, *S. elongatus*, and *S. melanostomus*) were not given a group assignment by Hyde and Vetter, and those species were left unassigned. I classified *S. brevispinis*, *S. emphaeus*, and *S. proriger* as clade "A-B", given the low degree of confidence associated with the node separating clades A and B, and Hyde and Vetter's statement that Bayesian posterior probabilities may overestimate support in this context.

Data recovery (digitization)

The numerical data from three sources (noted in Table 2) were no longer available in electronic or print format, so estimates of the original data were recovered by digitizing points from figures using the program GraphClick (Arizona Software, 2008). Love *et al*. (1990) plotted fecundity (1000s of eggs) against total length (cm) for 16 rockfish species collected in the southern California bight. Their study also reported minimum and maximum values of fecundity and length for *S. ensifer*, *S. melanostomus*, and *S. ovalis*. Love and Westphal (1981) plotted fecundity estimates as a function of total length from olive rockfish (*S. serranoides*) captured in central California, and Romero (1988) reported fecundity as a function of standard length for kelp rockfish (*S. atrovirens*) captured in Monterey Bay (central California). For the kelp rockfish data, I converted standard length to total length as per Lea *et al*. (1999). A detailed description of digitized data sets is provided as an appendix.

Length at 50% maturity

Fish smaller than a certain size, or younger than a certain age, are likely to be immature. Haldorson and Love (1991) reported the length at which 50% of fish are expected to be mature for 42 *Sebastes* species (Table 3). I obtained similar data for a few other species not included in the Haldorson and Love study, and added a vertical line representing length at 50% maturity to the plots of relative fecundity

versus length. For *S. emphaeus*, Love *et al*. (2002) cite reports that some fish are mature at 11 cm, and all fish were mature by 13 cm. For this species, I used the mid-point (12 cm) as a point estimate of length at 50% maturity. Maturity data for swordspine rockfish (*S. ensifer*) are also sparse, but Love *et al*. (2002) report that a few fish are mature at 11 cm.

Although fish mature over a range of lengths, length at 50% maturity is a common summary statistic for comparing length at maturation among populations. A thorough evaluation of maturity differences between populations or species should consider the entire range of possible lengths at which individual fish mature (Wyllie Echeverria, 1987). When maturity data were not available from the same study as the fecundity data, I attempted to locate maturity information that was based on similar regions and time periods as the available fecundity data.

Results

Per-recruit analyses

The realized value of the spawning potential ratio can deviate significantly from the target SPR if we incorrectly assume that relative fecundity is constant (i.e. that female spawner biomass is proportional to egg production). The extent of this bias is affected by several factors, including the natural mortality rate, size-dependent trends in relative fecundity, and growth characteristics (Figures 1 and 2).

The target fishing rate ($F_{50\%}$) under the constant relative fecundity model achieves the intended SPR value of 0.5 when the exponent of the fecundity-length relationship equals the exponent of the weight-length relationship. In this case, the assumption of constant relative fecundity is the true model (Figures 1 and 2, fecundity-length exponent = 3). If the fecundity-length exponent was less than the weight-length exponent, the realized SPR value would be greater than the target of 0.5 and we would overestimate the reduction in spawning output per recruit. This pattern is rarely seen among rockfish, and the few observed cases may be the result of small sample sizes and/or truncated sampling of mature length ranges. For rockfishes, estimated values of the fecundity-length exponent commonly exceed the weight-length exponent (Haldorson and Love, 1991), suggesting that relative fecundity typically increases with size, although to varying degrees.

The realized SPR plot for the "typical" rockfish (the one with average growth characteristics) shows that by assuming constant relative fecundity, we underestimate the reduction in spawning output by up to 20% (or more if M>0.25 and the fecundity exponent is >6.5) for a "typical" rockfish, depending on the values of M and the true fecundity-length exponent (Figure 1). This bias is magnified for larger rockfish with slower growth, as indicated by a steeper gradient in realized SPR (Figure 2).

Fecundity models

AIC differences among alternative models suggest that absolute fecundity of rockfish is best modeled as a power function of weight (Table 4). The allometric model for length with weight as an offset was the best model according to AIC for *S. chlorostictus* and performs almost as well as the AIC-best model. Interestingly, the allometric function of length (with or without an additive offset for gonad maturation stage) was consistently one of the worst of the six candidate models.

The value of the exponent from the allometric fecundity-weight model was larger than one for seven of the eight species with relatively large sample sizes (Table 5). This evidence strongly suggests that relative fecundity increases with mass in several of the *Sebastes*, and that the assumption of egg production being proportional to female spawning biomass is inappropriate for these species.

A log-log regression of absolute fecundity (eggs) versus total length for yellowtail rockfish showed a significant relationship with length and gonad development stage (Table 6). The model explained about 73% of the variation relative to an intercept-only model. The model suggests that estimates of absolute fecundity based on stage 2 ovaries are 88% of estimates based on stage 1 ovaries (i.e. $0.88 = \exp\{-0.16904 + 0.3058^2 / 2\}$). The interaction term between length and stage in the model was not significant (result not shown).

The allometric model for relative fecundity (eggs per gram total weight) is consistent with the model for absolute fecundity, in that the effect of developmental

stage is also significant in this model (Table 7). An improvement in fit is suggested by an increase in the R^2 value (79%) and a 30-point reduction in AIC relative to the traditional fecundity-length model. The model suggests that relative fecundity based on stage-2 ovaries is 84% of that based on stage-1 ovaries ($0.84 = \exp\{-0.20996 + 0.2678^2/2\}$). The interaction term between length and stage in the model was again not significant (result not shown).

The relative fecundity model assumes that absolute fecundity is proportional to the relative condition factor (Eq. 1.16), but the data suggest that this may not be an adequate adjustment of the fecundity estimate given information on fish condition. As fish of a given length deviate from the population's average weight at length, there is a disproportionate increase in fecundity relative to the population average, as indicated by exponents greater than one in Figure 3.

The AIC-best model was the allometric fecundity-weight model with a categorical variable for gonad development stage (Tables 4 and 8). The model for yellowtail rockfish suggests that relative fecundity based on stage-2 ovaries is 82% of that based on stage-1 ovaries.

Residual plots for both allometric functions of length are similar (Figures 4 and 5). Residuals plotted against fitted values do not show consistent patterns or trends, although there appears to be a some departure from the normality assumption for this species. The residual plots from the model for absolute

fecundity as an allometric function of weight are similar to the length-based models (Figure 6).

The model for relative fecundity as a linear function of weight is consistent with the multiplicative models in that a significant relationship between relative fecundity and size is detected, and that gonad stage affects estimates of relative fecundity (Table 9). For yellowtail rockfish, this additive model suggests that relative fecundity based on fertilized eggs is 72 eggs per gram less than relative fecundity based on pre-fertilized eggs. The interaction between stage and weight was not significant (result not shown). The model explains about 40% of the variability in the data, although this is not comparable to the results from the log-log regressions due to differences in the response variable. Regression diagnostics suggest a possible increase in residual variance for larger predicted values, and the model over-predicts relative fecundity for heavy fish, as seen by the negative residuals for the three fish greater than 2 kg in the upper right panel of Figure 7.

Length and weight data

In Figure 8 I show the relationship between total and somatic weight for six *Sebastes* species. In all cases, coefficients of determination (R^2) show that a linear model through the origin explains over 97% of the variability in the data.. These data suggest that total weight is 3% - 17% greater than somatic weight, depending on the species.

Relative fecundity by species group

Subgenus *Acutomentum*

No strong trends in size-specific relative fecundity were evident among this group of species (Figure 9, panels A, B, and C). Measured weight data were not available for bank rockfish, so estimates of relative fecundity were based on predicted total weights (Love *et al*., 1990). Data for speckled rockfish (*S. ovalis*) showed no size-specific trend or indication of reduced fecundity with advancing stages of gonad development, but sample sizes were very small (<4 per study). Predicted weights were used for estimates from Love *et al*. (1990), and measured weights were provided by MacGregor (1970).

Clade A-B

I grouped species from clades A and B in Hyde and Vetter (2007) into clade "A-B" (Figure 10, panels A, B, and C). An increasing trend is suggested for Puget Sound rockfish, but the number of observations is small (5 fish) and the range of observed lengths is limited. Only two observations were available for redstripe rockfish. Relative fecundity for silvergrey rockfish appears to have an increasing trend with length, based on a sample of 126 fish.

Clade D

Data from Love *et al*. (1990) suggest increasing trends in relative fecundity with size for both *S. semicinctus* and *S. saxicola* (Figure 11, panels A and B).

Samples of *S. saxicola* from Phillips (1964), thought to be pre-fertilized oocytes, show no clear trend over the range of observed lengths. Estimates of length at 50% maturity vary considerably between fish captured north and south of Point Conception.

Subgenus *Eosebastes*

Splitnose rockfish (*S. diploproa*) show a strong trend in relative fecundity across a wide range of lengths, based on the results of Phillips (1964) (Figure 12). Relative fecundity of a single, large specimen reported by Snytko and Borets (1973) was consistent with the largest specimens in the Phillips study. No data were located for the other seven species assigned to this subgenus in Hyde and Vetter (2007).

Subgenus *Pteropodus*

Three species in this group (*S. auriculatus*, *S. dalli*, and *S. carnatus*) show no apparent trend in relative fecundity with size (Figure 13, panels A through G). However, data for these species are from a limited size range and often don't include fish near the length at 50% maturity. Grass rockfish (*S. rastrelliger*) data suggest a slight increase in RF with length, but this is based on only seven observations. The three species with larger sample sizes and more extensive length coverage display clear, but highly variable, trends in RF with size. Copper rockfish from British Columbia appear to produce more eggs per gram body weight than fish from Washington (DeLacy *et al*., 1964; Ito, 1977), although this apparent regional difference may be a result of differences among studies or among years.

Subgenus *Rosicola*

Vermillion rockfish (*S. miniatus*) has one of the strongest trends observed (Figure 14a), based on two studies from California (Phillips, 1964; Love *et al*., 1990). Results of both studies are highly consistent for vermilions. Phillips (1964) estimated fecundity for canary rockfish (*S. pinniger*), and estimates of relative fecundity based on predicted weights suggest that this species may exhibit a similar trend to its sister taxon (Figure 14b).

Subgenus *Sebastes*

This group of species is unique in that it contains species from the Pacific and Atlantic (Figure 15, panels A through D). Trends for Pacific species were much clearer than for *S. norvegicus*. However, St.-Pierre and de Lafontaine (1995) studied the fecundity-length relationship for the Atlantic redfish *S. fasciatus* and estimated an exponent greater than 4. Gunderson's (1976) data for Pacific Ocean Perch are the only example among the available sources that demonstrate clear spatial differences in fecundity within a species.

Subgenus *Sebastichthys*

Redbanded rockfish (*S. babcocki*) is the only species representing the subgenus *Sebastichthys* in this analysis, apart from one 285 mm treefish (*S. serriceps*) with an estimated 192 eggs per gram total body weight (MacGregor, 1970). Relative fecundity of redbanded rockfish is highly variable, with no apparent

trend. However, the range of lengths does not represent the full range of mature individuals (Figure 16).

Subgenus *Sebastodes*

This group contains two of the most important species in the historical rockfish catch (*S. paucispinis* and *S. goodei*), and one species who's value is described as a forage species for other organisms (*S. jordani*). Results from different studies are not entirely consistent for bocaccio (Figure 17, panels A1 and A2). Relative fecundity estimated from Phillips' (1964) data suggest a strong increasing trend with increasing length. Bocaccio data from Love *et al*. (1990) cover a similar size range and show little change in eggs per gram with length. Observations from Ralston and MacFarlane (in prep.) suggest an increasing trend based on fish from northern Mexico, but MacGregor (1970) found little evidence of any trend in RF with length for bocaccio. Finally, the small number of bocaccio samples taken from the Oregon-Vancouver area by Snytko and Borets (1973) suggest an increasing trend. Similar to bocaccio, different studies appear to support different conclusions for chilipepper rockfish (*S. goodei*) (Figure17, panels B1 and B2). The data from Phillips (1964) suggest an increasing trend for chilipepper, Love *et al*. (1990) found no change in relative fecundity with length, and observations by Sogard *et al*. (unpublished data) suggest the possibility of a length-specific trend. Data on fecundity per gram for shortbelly rockfish (*S. jordani*) do not adequately cover the

range of mature lengths, but the small amount of data do not provide any evidence of a trend for this species (Figure 17C).

Subgenus *Sebastomus*

The subgenus *Sebastomus* includes more species than any other *Sebastes* subgenus. None of the species are major targets of the commercial or recreational fisheries, but several are caught as part of the mixed rockfish fisheries characteristic of the North American west coast. No strong trends are evident for greenblotched rockfish (*S. rosenblatti*) or rosy rockfish (*S. rosaceus*) (Figure 18, panels A and C). Two species, *S. helvomaculatus* and *S. ensifer*, have sample sizes of 4 and 2 respectively, preventing us from drawing any strong conclusions for either species (Figure 18, panels D and F). The observations of Love *et al*. (1990) and the NOAA Fisheries Groundfish Ecology program (Benet *et al*., in prep.) show a strong size-dependent pattern in relative fecundity for *S. chlorostictus* (Figure 18B). The data from Love *et al*. (1990) for *S. constellatus* also imply that the number of eggs per gram increases with size for this species, but too few samples were taken by MacGregor (1970) to inform any size-related trends from his study (Figure 18E).

Subgenus *Sebastopyr*

MacGregor (1970) is the only study known to the author with estimates of fecundity for yelloweye rockfish, apart from one observation taken by Clemens (1949). Based on two observations, relative fecundity for this species is consistent

with the scale of other rockfishes, but further studies will be required to determine if relative fecundity is dependent on size or age (Figure 19).

Subgenus *Sebastosomus*

Species of the subgenus *Sebastosomus* exhibited some of the strongest trends in relative fecundity with length (Figure 20). Observations of relative fecundity at length for blue rockfish (*S. mystinus*) suggest a strong increasing trend (Figure 20, panel A). Results for *S. serranoides* are consistent among studies and gonad development stages, with a strong increasing trend (Figure 20, panel B). Data from Love *et al*. (1990) and Phillips (1964) suggest an increasing trend for widow rockfish (*S. entomelas*), but results from Snytko and Borets (1973) and Sogard *et al*. (unpublished data) are inconclusive (Figure 20, panels C1 and C2). Data from five studies on yellowtail rockfish fecundity consistently show increasing trends in size-specific relative fecundity (Figure 20, panels D1, D2, and D3). Data for black rockfish suggest an increasing trend, but the stage of gonad development does not appear to have a strong influence on the number of eggs per gram (Figure 20, panel E).

Species without a group assignment

Cowcod, greenstriped rockfish, and blackgill rockfish were not assigned to groups by Hyde and Vetter (2007). No strong trends are apparent with respect to length, given the available data for these species (Figure 21).

CHAPTER 3

HIERARCHICAL MODELS FOR FECUNDITY OF ROCKFISHES (GENUS *SEBASTES*)

The analyses I present in Chapter 2 highlight three issues related to the reproductive potential of rockfishes. First, improper characterization of size-specific relative fecundity will result in biased estimates of target harvest rates based on spawning potential ratios (the current standard for *Sebastes* species managed by the Pacific Fisheries Management Council). Second, the most common method for modeling rockfish fecundity (as an allometric function of length) appears to perform poorly relative to a set of alternative models. Third, relative fecundity for several species shows an increasing trend with length, the magnitude of which may vary among groups of closely-related species. Together, these results underscore the need to re-evaluate existing fecundity models for commercially important rockfish species, to develop methods that appropriately characterize reproduction for data-poor species, and to improve our ability to quantify uncertainty in those predictions.

Studies of rockfish reproduction are not uncommon, but the types of data collected and the manner in which they are reported vary considerably from study to study. The most abundant data are size at maturity and sex ratio, as is often the case among fish species (Tomkiewicz et al., 2003). Fecundity studies are often short-term, localized efforts, or the results are highly aggregated over space and time. Results of regression analyses are often reported as parameter point estimates, with little information about parameter uncertainty. Detailed fecundity data are generally

sparse or lacking for many rockfish species that are not of major commercial or recreational importance.

Stock assessments for species with available fecundity data do not always incorporate this information, and sometimes assume that fecundity is proportional to spawning biomass (Chapter 2, Table 1). The analysis of data-rich stocks in Chapter 2 (Table 5) suggests that this assumption may be inappropriate for several rockfish species, and is not consistent with a precautionary approach to fisheries management. A meta-analytic approach is a reasonable alternative to this default assumption, as it incorporates information from all available sources. This method has been used in the absence of species-specific data to provide management advice for data-poor stocks. For rockfish, Dorn used a hierarchical Bayesian model (Dorn, 2002) to estimate parameters for models connecting the size of the parent population (in spawning biomass or egg production) to the number of fish entering the adult population (recruits). Helser et al. (2007) conducted a meta-analysis of growth (length at age) models among 46 *Sebastes* species, also using a hierarchical approach.

Alternative approaches to estimating reproductive output are needed to better inform science-based management efforts. In this chapter, I propose using hierarchical (multi-level) models to describe the relationship between size and fecundity in rockfishes. I compare a set of candidate models that share this general framework, and show that the weight of evidence does not support the use of

spawning biomass as a proxy for egg production for rockfishes. The product of these models is a set of distributions for the parameters of fecundity-size relationships. I provide these distributions for species with available data, as well as for species not yet observed, and extend the model to consider evolutionary relationships between species.

Methods

Data and preliminary analyses

I compiled a rockfish fecundity database that contains 2048 fecundity estimates from 24 studies and 41 rockfish species (Chapter 2, Table 2). For the meta-analysis I excluded 17 observations. These include one observation for canary rockfish (Fraser, 1923) that was reported with only one significant digit and one observation for yelloweye rockfish (Clemens and Wilby, 1949) that lacked a methodological description. I excluded the single datum for treefish (*S. serriceps*) as it does not allow for estimation of a slope parameter. Stanley and Kronlund (2005) identified fecundities for 2 silvergrey rockfish (*S. brevispinis*) as anomalous points and 4 others as questionable due to large parasite loads. I removed these six records and one additional observation that was inconsistent with the remaining 126 observations based on preliminary analyses (result not shown). Corlett (1964) identified 6 redfish in his study as "mentella type" which I excluded because of uncertainty in species identification at the time. Finally, I removed a single

observation of a Pacific Ocean Perch from the Washington-Oregon region (Gunderson, 1976) because it was highly influential in preliminary regression analyses and the standardized residual was 4.8 standard deviations from the mean (result not shown). I pooled data from both regions for the meta-analysis. The final fecundity data set used in the meta-analyses consisted of 2031 observations from 40 species and 22 studies.

All records in the database contain length information (standardized to total length in mm), and about half (1006) of the records have measured weights (grams) as well. I predict total body weight from length for the remaining 1025 records using published length-weight allometries. I use the combined set of measured and predicted weights in the hierarchical models.

There are several methods for estimating fecundity in fishes (Murua et al., 2003). Most methods involve taking multiple subsamples from the ovaries, counting eggs in each subsample, and extrapolating an average from the subsamples to the entire ovary. Rockfishes have paired ovaries, so this process is repeated for each. Researchers often discard highly variable estimates, and rarely report the subsample data and associated variability. I do not model this source of error, but it contributes to the observed variability in fecundity.

The main effects of interest in this chapter are whether and how relative fecundity varies among species, subgenera, and as a function of size. To summarize patterns in the scale of relative fecundity, I examined the distribution of relative

fecundity by species and sub-generic group. I also compared relative fecundity among 3 gonad maturity stages (1 = pre-fertilized, 2 = fertilized (not eyed larvae), and 3 = eyed larvae) for the 14 species having data from more than one stage. This approach pools information across studies and does not account for possible differences in average length among stages, but provides a simple means for comparison. Since maturity stage does not have a consistent effect on fecundity estimates (Chapter 2, Table 4), I pooled data from all maturity stages for the hierarchical models, which may result in increased variance of the predictions. I also refer to fecundity and relative fecundity in terms of "eggs" in order to simplify the presentation of the results, although some fecundity estimates are counts of embryos or larvae.

The model selection results I showed in Chapter 2 suggest that mass is a better predictor of fecundity than length (Chapter 2, Table 4). I plotted relative fecundity against mass for each species, grouping them according to the sub-generic assignments of Hyde and Vetter (2007). I labeled species that were not associated with a named group (e.g. *S. levis*, *S. elongatus*, and *S. melanostomus*) as 'unassigned' in this analysis.

Hierarchical models for rockfish fecundity

In Chapter 2, I showed that the estimated exponents from the allometric fecundity-mass models are frequently greater than 1, indicating that it is common

for relative fecundity to increase with size (Chapter 2, Table 5). However, this is not true for all species, and our ability to accurately detect a trend is affected by the amount of available data. Fitting separate models for each species (no pooling of data) can lead to questionable, and sometimes biologically implausible, parameter estimates. This situation can easily occur when sample sizes are small or the range of observed sizes is narrow. Combining all of the data (complete pooling) is not desirable in this situation because in doing so we ignore potentially important variability among species. The hierarchical modeling framework is an intermediate alternative to the no-pooling and complete-pooling models, in that hierarchical models allow for partial pooling of the data (Gelman et al., 2004). Parameters are allowed to vary by species, but estimates for data-poor species are drawn toward the mean value for all species to an extent that varies according to the amount of variability in the data and the distance from the population mean. This effect is sometimes referred to as "shrinkage." Species with more information retain estimates that are more similar to the estimates from separate models fit to each group (no pooling).

I created hierarchical versions of two models described in Chapter 2: the model for relative fecundity (Φ/W, measured in eggs per gram) as a linear function of weight

$$\frac{\Phi}{W} = a + bW + \varepsilon \qquad (3.1)$$

and the model for absolute fecundity as an allometric function of weight,

$$\Phi = cW^{d}e^{\varepsilon} \tag{3.2}$$

which I fit as a linear model under log-transformation of the variables.

$$\log(\Phi) = \log(c) + d\log(W) + \varepsilon \tag{3.3}$$

In both models the error term, ε, is assumed to be normally distributed with a zero mean. I chose these two models because the first is commonly used in current assessments of rockfish and the second was usually the best fit among allometric models compared in Chapter 2 (Table 4). An increase in relative fecundity with mass is represented by a positive slope (b) in Equation 3.1 and by an exponent (d) greater than 1 in Equation 3.2.

Since both models take the same form ($y = a + bx$), I fit each of them using the same 2-level hierarchical linear model (HLM). The first level of the HLM predicts the dependent variable (in this case either relative or absolute fecundity), y_{ij}, for fish i of species j as a linear function of the independent variable, x_{ij}, with normally distributed errors.

$$\begin{aligned} y_{ij} &= \alpha_j + \beta_j x_{ij} + \varepsilon_{ij} \\ \varepsilon_{ij} &\sim N(0, \sigma^2) \end{aligned} \tag{3.4}$$

The index i takes values from 1 to n_j, the number of fish observed for species j, and the index j takes values from 1 to the total number of species, J. Prior to fitting the model, I centered the independent variable by subtracting the group-specific mean values.

The second level models the species-specific intercept and slope parameters as draws from independent normal distributions.

$$\alpha_j \sim N\left(\mu_\alpha, \tau_\alpha^2\right) \tag{3.5}$$

$$\beta_j \sim N\left(\mu_\beta, \tau_\beta^2\right) \tag{3.6}$$

This approach to modeling the regression parameters can be seen as a generalization of an analysis of covariance (Kutner et al., 2005), in which the no-pooling model is similar to setting the hierarchical variance terms (τ_α^2 and τ_β^2) to very large values, and the complete-pooling model (in which all species share the same intercept and slope) is equivalent to setting the hierarchical variance terms to zero.

I chose diffuse conjugate prior probability distributions for the data variance, σ^2

$$\sigma^2 \sim Inv-\chi^2\left(0.001,1\right) \tag{3.7}$$

and the parameters of the 2nd-level model

$$\mu_\alpha \sim N\left(0,10^4\right) \tag{3.8}$$

$$\mu_\beta \sim N\left(0,10^4\right) \tag{3.9}$$

$$\tau_\alpha^2 \sim Inv-\chi^2\left(0.001,1\right) \tag{3.10}$$

$$\tau_\beta^2 \sim Inv-\chi^2\left(0.001,1\right). \tag{3.11}$$

Conjugate priors are those which share the same parametric form as their respective posterior distributions. This set of priors (Equations 3.7 through 3.11) facilitates the use of a Gibbs sampling algorithm (described below) to generate draws from the

posterior distributions of the parameters. The scaled inverse Chi-squared (*Inv*-χ^2) distribution, $p(\theta)$, for a random variable, θ,

$$\theta \sim Inv-\chi^2\left(\nu, s^2\right)$$
$$p(\theta)=\frac{(\nu/2)^{\nu/2}}{\Gamma(\nu/2)} s^{\nu}\theta^{-(\nu/2+1)}e^{-\nu s^2/2\theta} \tag{3.12}$$

is the conjugate prior for the variance parameters in the model (Gelman et al., 2004).

Gibbs sampler for the2-level hierarchical linear model

The joint posterior distribution for the parameters of the hierarchical linear model is proportional to the product of the likelihood and the priors (Gelman et al., 2004).

$$
\begin{aligned}
& p\left(\vec{\alpha},\vec{\beta},\sigma^2,\mu_\alpha,\mu_\beta,\tau_\alpha^2,\tau_\beta^2 \middle| y\right) \\
& \propto \prod_{j=1}^{J}\prod_{i=1}^{n_j} \frac{1}{\left(2\pi\sigma^2\right)^{1/2}} \exp\left\{\frac{-\left(y_{ij}-\left(\alpha_j+\beta_j x_{ij}\right)\right)^2}{2\sigma^2}\right\} \\
& \times \prod_{j=1}^{J} \frac{1}{\left(2\pi\tau_\alpha^2\right)^{1/2}} \exp\left\{\frac{-\left(\alpha_j-\mu_\alpha\right)^2}{2\tau_\alpha^2}\right\} \\
& \times \prod_{j=1}^{J} \frac{1}{\left(2\pi\tau_\beta^2\right)^{1/2}} \exp\left\{\frac{-\left(\beta_j-\mu_\beta\right)^2}{2\tau_\beta^2}\right\} \\
& \times \exp\left\{\frac{-\left(\mu_\alpha-\mu_{\alpha 0}\right)^2}{2\tau_{\alpha 0}^2}\right\} \exp\left\{\frac{-\left(\mu_\beta-\mu_{\beta 0}\right)^2}{2\tau_{\beta 0}^2}\right\} \\
& \times \left(\sigma^2\right)^{-(\nu_0/2+1)} \exp\left\{-\left(\frac{\nu_0 s_0^2}{2\sigma^2}\right)\right\} \\
& \times \left(\tau_\alpha^2\right)^{-(\nu_1/2+1)} \exp\left\{-\left(\frac{\nu_1 s_1^2}{2\tau_\alpha^2}\right)\right\} \\
& \times \left(\tau_\beta^2\right)^{-(\nu_2/2+1)} \exp\left\{-\left(\frac{\nu_2 s_2^2}{2\tau_\beta^2}\right)\right\}
\end{aligned}
\tag{3.13}
$$

Line by line, Equation 3.13 is interpreted as 1) the joint posterior probability distribution is proportional to the product of 2) the likelihood for the data, 3) the 'likelihood' for the species-specific intercepts, 4) the 'likelihood' for the species-specific slopes, 5) priors for the means of the intercept and slope distributions, 6) a

prior for the data variance, 7) a prior for the variance of the intercept parameters, and 8) a prior for the variance of the slope parameters. I assigned values to the parameters of the prior probability distributions for the 2nd-level model and data variance (Equation 2.13). I chose these values so that the prior distributions would have minimal influence relative to the data ($\mu_{\alpha 0} = \mu_{\beta 0} = 0$, $\tau_\alpha^2 = \tau_\beta^2 = 10^4$, $\nu_0 = \nu_1 = \nu_2 = 0.001$, and $s_0^2 = s_1^2 = s_2^2 = 1$).

To obtain samples from the posterior conditional distributions of the parameters I use a Markov chain sampling algorithm known as the Gibbs sampler (Gelman et al., 2004). This approach requires derivation of the full conditional distribution for each parameter by taking the product of all terms in Equation 3.13 that contain the parameter of interest. I show that these are distributions of known form, a requirement of the Gibbs sampler.

The conditional posterior distribution of the intercept parameter for species *j* is normally distributed.

$$\alpha_j \left| \beta, \sigma^2, \mu_\alpha, \tau_\alpha^2, y \sim N\left(m_\alpha, \nu_{\alpha_j}\right) \right. \tag{3.13}$$

where

$$m_{\alpha_j} = \nu_{\alpha_j}\left(\frac{n_j\left(\bar{y}_j - \beta_j \bar{x}_j\right)}{\sigma^2} + \frac{\mu_\alpha}{\tau_\alpha^2}\right) \tag{3.14}$$

$$\nu_{\alpha_j} = \left(\frac{n_j}{\sigma^2} + \frac{1}{\tau_\alpha^2}\right)^{-1} \tag{3.15}$$

$$\bar{y}_j = \frac{1}{n_j}\sum_{i=1}^{n_j} y_{ij} \tag{3.16}$$

$$\bar{x}_j = \frac{1}{n_j}\sum_{i=1}^{n_j} x_{ij} \tag{3.17}$$

The full conditional distribution of the slope parameter for species *j*

$$\beta_j \left| \alpha, \sigma^2, \mu_\beta, \tau_\beta^2, y \sim N\left(m_\beta, v_{\beta_j}\right)\right. \tag{3.18}$$

is also normally distributed, with mean

$$m_{\beta_j} = v_{\beta_j}\left(\frac{n_j\left(\overline{xy}_j - \alpha_j \bar{x}_j\right)}{\sigma^2} + \frac{\mu_\beta}{\tau_\beta^2}\right) \tag{3.19}$$

and variance

$$v_{\beta_j} = \left(\frac{n_j \overline{x_j^2}}{\sigma^2} + \frac{1}{\tau_\beta^2}\right)^{-1} \tag{3.20}$$

where

$$\overline{xy}_j = \frac{1}{n_j}\sum_{i=1}^{n_j} x_{ij} y_{ij} \tag{3.21}$$

$$\overline{x_j^2} = \frac{1}{n_j}\sum_{i=1}^{n_j} x_{ij}^2 \,. \tag{3.22}$$

The means of the 2nd-level model, μ_α and μ_β, have identical forms for their full conditional distributions. I show the distribution for the mean of the intercept parameters,

$$\mu_\alpha \left| \alpha, \sigma^2, \tau_\alpha^2, \mu_{\alpha 0}, \tau_{\alpha 0}^2, y \sim N\left(m_{\mu_\alpha}, v_{\mu_\alpha}\right) \right. \tag{3.23}$$

where

$$m_{\mu_\alpha} = v_{\mu_\alpha}\left(\frac{J\overline{\alpha}}{\tau_\alpha^2} + \frac{\mu_{\alpha 0}}{\tau_{\alpha 0}^2}\right) \tag{3.24}$$

$$v_{\mu_\alpha} = \left(\frac{J}{\tau_\alpha^2} + \frac{1}{\tau_{\alpha 0}^2}\right)^{-1} \tag{3.25}$$

$$\overline{\alpha} = \frac{1}{J}\sum_{i=1}^{J}\alpha_j \tag{3.26}$$

but substitution of β for α gives the full conditional for the mean of the slope parameters. The conditional posterior distribution for the data-level variance is a scaled-Inverse-χ^2 distribution (Gelman et al., 2004)

$$\sigma^2 \left| y \sim Inv - \chi^2\left(v_0 + n, \frac{v_0 s_0^2 + n s^2}{v_0 + n}\right)\right. \tag{3.27}$$

where

$$s^2 = \frac{1}{n - 2J}\sum_{i=1}^{n}\left(y_{ij} - \left(\alpha_j + \beta_j x_{ij}\right)\right)^2 . \tag{3.28}$$

The conditional posterior distributions for the hierarchical variance components are similar scaled-Inverse-χ^2 distributions. For example, the variance of the distribution of intercept parameters is

$$\tau_\alpha^2 \left| \alpha, v_1, s_1^2, y \sim Inv - \chi^2\left(v_1 + J, \frac{v_1 s_1^2 + J s_\alpha^2}{v_1 + J}\right)\right. \tag{3.29}$$

where

$$s_{\alpha}^{2} = \frac{1}{J-1}\sum_{i=1}^{J}\left(\alpha_{j} - \mu_{\alpha}\right)^{2}. \qquad (3.30)$$

Implementation

To sample from these distributions, the Gibbs sampler proceeds as follows:

1. Initialize the intercepts, slopes, and data variance with their maximum likelihood estimates from a separate linear model fit
2. Initialize the hierarchical variance parameters with the variances of the MLEs estimated in step 1
3. Draw values of the hierarchical variance parameters from their respective scaled-Inverse-χ^2 distributions, e.g. Equation 3.29
4. Draw values of the hierarchical means (slope and intercept distributions) from their respective normal distributions, e.g. Equation 3.23
5. Draw a value of the data variance (Equation 3.27)
6. Simultaneously draw *J* intercept parameters from their full conditional distributions (Equation 3.13)
7. Simultaneously draw *J* slope parameters from their full conditional distributions (Equation 3.18)

I used the R programming language/environment (R core team, 2008) to program the Gibbs sampler. The program repeats steps 3 – 7 for 10,000 iterations. I then generated a second set of 10,000 simulations, starting from different initial

values. I ran diagnostic checks of the resulting posterior simulations using the "coda" package (Plummer et al., 2008) in R to assess burn-in, degree of autocorrelation, and evidence of convergence (Appendix B).

I compared quantiles of the posterior distributions from the relative fecundity model (Equation 3.1) and the absolute fecundity model (Equation 3.3) to their respective maximum likelihood estimates (MLEs). For the allometric model I summarized the distributions for the coefficients of the allometric model on the log scale (natural log transformed, but no longer centered) as well as on the original scale. Due to the skewness of the posterior distributions for the back-transformed coefficients of the allometric model, I provide means and quantiles (2.5%, 25%, 50%, 75%, and 97.5%) in tabular form. I evaluated residual plots from the non-hierarchical models to look for patterns inconsistent with the model assumptions (homogeneity of variance, normally distributed errors, etc.).

Using the simulations from the hierarchical models, I estimated posterior predictive distributions of the parameters (intercept and slope, or coefficient and exponent) for an unobserved species. An advantage of the hierarchical framework is that these predictive distributions incorporate uncertainty in the parameters, and may be interpreted as prior probability distributions for as yet unobserved species (Gelman et al., 2004).

Results

Data and preliminary analyses

The minimum and maximum observed values for absolute fecundity retained in the meta-analysis were 1,245 eggs for a 9.5 cm stripetail rockfish (*S. saxicola*) and 2,900,100 for a 75 cm bocaccio (*S. paucispinis*) (Love et al., 1990; Snytko and Borets, 1973). The range of relative fecundities was bounded by a 53 cm golden redfish (*S. norvegicus*) with approximately 9.7 eggs per gram total body weight, and a 20 cm stripetail rockfish (*S. saxicola*) with 906 eggs per gram (Corlett, 1964; Phillips, 1964). The interquartile range of relative fecundity among all observations in the database is 170 to 344 eggs per gram total body weight. The median and mean values are 252 and 263 eggs per gram, respectively.

Relative fecundity varies considerably among some species (Figure 22). Well-sampled species occur at both ends of the range of this crude measure of reproductive investment, suggesting that the observed variability is not due to chance alone. Samples for the three members of the subgenus *Sebastes* (two Pacific and one Atlantic species) have low relative fecundity, whereas silvergrey rockfish (*S. brevispinis*) and yellowtail rockfish (*S. flavidus*) are among the well-represented species that have high relative fecundity. Some sub-generic groups appear to have consistently low or high relative fecundity among species (*Sebastes*, clade A, and *Rosicola*), while other groups span the observed range for the genus (e.g. *Sebastosomus* and *Sebastodes*). Relative fecundity of bocaccio (*S. paucispinis*) is

notably higher than the two other *Sebastodes* species, chilipepper rockfish (*S. goodei*) and shortbelly rockfish (*S. jordani*).

Differences in relative fecundity are also evident among sub-generic groups (Figure 22). The data suggest that the *Sebastosomus* and *Sebastes* subgenera appear to have quite different strategies in terms of mass-specific egg production. However, the range for other groups may not be representative due to small sample sizes (e.g. clade A, *Sebastichthys*, *Sebastopyr*, *Eosebastes*).

At least one species (yellowtail rockfish, *S. flavidus*) shows strong evidence of differences in fecundity among stages of gonad maturation (Chapter 2, Tables 6 – 9). I restricted that analysis to data from single studies to control for potential bias due to methodological differences. In this chapter, I extend that analysis to a greater number of species with a visual comparison and the assumption that there is no effect of study on fecundity estimates (Figure 23). However, this comparison does not control for length. While maturation stage appears to be an important consideration for some species (e.g. *S. entomelas*, *S. flavidus*, *S. paucispinis*), other species for which reasonable amounts of data are available show little change in estimates of relative fecundity, such as *S. caurinus*, *S. goodei*, and *S. melanops*.

Trends in relative fecundity with respect to mass for rockfish are highly variable (Figures 24 – 37). Most species of the subgenus *Sebastosomus* share increasing trends (Figure 36), but other subgenera are not as consistent. Individual species show increasing trends that they do not share with closely related species.

For example, relative fecundity of *S. caurinus*, *S. maliger*, and *S. atrovirens* appears to increase with mass, but this trend does not hold for other members of the *Pteropodus* group (Figure 29). Small sample sizes sometimes suggest declining trends (*S. ovalis*, *S. proriger*, and *S. ruberrimus*), but this is likely due to chance given the observed levels of variability and the biological implications of such rapid decreases in reproductive output (Figures 24, 25 and 35). Similarly, relative fecundity of some species increases at rates that are difficult to believe (*S. ensifer*, *S. mystinus* and *S. melanostomus*) (Figures 34, 36 and 37). Predictions of expected relative fecundity for these species quickly exceed the most extreme observed values. This effect is sometimes the result of observations being limited to a very small range of sizes. Extreme predictions such as these become a problem for assessment models, because extrapolation to all mature sizes is required to model the effect of truncated size distributions that result from fishing.

Hierarchical linear model for relative fecundity

I present the posterior distributions (species-specific slopes and intercepts) from the hierarchical relative fecundity model (Equations 3.1 and 3.4) as boxplots for each species (Tables 10 and 11, Figures 38 and 39). The posterior median slopes are "shrunken" from the MLE toward the population median (solid vertical line, Figure 38). Slopes for species with very little data have estimates equal to the population-level distribution, with similar variability. The mean and median values

from the posterior slope distributions are all greater than zero (Table 10). According to this model, the posterior probability that the slope parameter is greater than zero is greater than 90% for 14 species and greater than 50% for all species (Table 12). In Figure 40 I show histograms of the posterior distributions of the variance components.

Model diagnostics (residual plots) from a non-hierarchical analysis of covariance model suggest that the assumption of equal variance does not hold for these data (Figure 41, upper right panel). The model also consistently under-predicts relative fecundity (Figure 41, upper left panel), and the distribution of the residuals appears to have a heavier right tail relative to the assumed normal distribution (Figure 41, lower right panel).

Hierarchical allometric model for absolute fecundity

Under log-transformation the data were more consistent with the assumptions of the linear model (Figure 42). Some evidence of variance heterogeneity and skewed residuals remained, but given the improvement relative to the linear model for relative fecundity I chose to fit the linearized allometric model for absolute fecundity as a hierarchical model. Posterior slope distributions from the linearized model are equivalent to the exponent of the multiplicative model, and values greater than 1 provide evidence of increasing relative fecundity with increasing weight (Table 13, Figure 43). The posterior distributions for the log-scale

intercept parameters were quite variable (Table 14, Figure 44). The variance components of this model structure are quite large as well, with a log-scale root mean square error greater than 1.4 (Figure 45). Compared to the linear model for relative fecundity, this model suggests that the probability that relative fecundity increases with size is higher, ranging from 82% - 99% (for *S. ovalis* and *S. flavidus*, respectively) (Table 15).

In summary, the data suggest that the characterization of size-dependent relative fecundity can be improved, with potentially important implications for rockfish stock assessments. For most species and subgenera, the weight of evidence suggests that relative fecundity is not independent of size. I examined the available data using three hierarchical model structures, finding important sources of variability at the species and sub-generic level. This framework is easily extended to accommodate new data and covariates, and provides predictive distributions of parameters for data-poor species.

CHAPTER 4

STATE DEPENDENT LIFE HISTORY THEORY FOR GROWTH AND REPRODUCTION IN *SEBASTES* SPP.

Introduction

In Chapter 2, I show that proper characterization of reproductive potential can have important implications for management of harvested fish stocks. Hierarchical statistical models provide a framework for modeling fecundity of individual species and sharing information among species while taking into account phylogenetic relationships (Chapter 3). The next step toward improving our understanding of reproductive potential is to identify mechanisms driving the observed patterns in fecundity, growth, and age at maturity. Specifically, we want to understand how trade-offs between these life-history traits affect lifetime reproductive success.

Organisms have a finite supply of energy to distribute among life history traits such as reproduction and growth. The life history strategies we observe have been and continue to be shaped by trade-offs associated with resource allocation (Stearns, 1992). Given that individuals vary in their allocation decisions, natural selection will favor strategies that maximize an individual's long-term genetic representation (Fisher, 1930).

Several definitions of fitness have been used in evolutionary studies. These include expected lifetime reproductive success, R_0,

$$R_0 = \sum_{a=0}^{\infty} m(a)l(a)$$

which is the product of age-specific fecundities, *m(a)*, and survival rates, *l(a)*, accumulated over the life of the individual.

Maximizing R_0 to identify evolutionarily optimal strategies is appropriate for stable populations ($R_0 = 1$) in constant environments (Clark and Mangel, 2000). Mylius and Diekmann (1995) discuss alternative fitness measures such as population growth rate, and emphasize that all fitness criteria make implicit assumptions, including the nature of density dependence in the population. No single measure of fitness is appropriate for all life histories (Stearns, 1992). For this study I use maximum lifetime expected allocation of energy to reproduction as a fitness measure that is analogous to R_0, and my conclusions are conditioned on the associated assumptions.

Dynamic state variable models (Mangel and Clark, 1988; Clark and Mangel, 2000) are well suited for the study of life-history strategies because they evaluate trade-offs associated with allocation of resources and predict optimal allocation based on the current state of the organism. This modeling framework also provides a common currency (expected lifetime reproductive success) for maximizing fitness over several decision variables (Clark and Mangel, 2000). This approach does not imply that organisms are making rational decisions based on their age, length, or some other state. Rather, model predictions can be interpreted as evolutionary

outcomes that would be favored by natural selection as a result of maximization of expected lifetime reproductive success.

Kozlowski et al. (2004) argue that while models of resource allocation can include an arbitrarily large number of sinks for energy, two sinks cannot be removed: growth and reproduction. I adopt this approach, examining allocation of resources to growth and reproduction given the state of the organism (e.g. age, length, maturity). Of course, optimal allocation decisions will be affected by the model assumptions regarding energy dynamics, so I consider alternative hypotheses to help determine which assumptions are consistent with observed patterns for organisms with life histories similar to rockfish.

Modeling potential somatic growth (surplus energy)

Growth rates for fish, reptiles and amphibians often decrease with size and growth continues after maturity (Beverton, 1992). This growth pattern is consistent with the strategy of allocating energy to both growth and reproduction after maturity, with an increasing fraction being used for reproduction over time (Ware, 1980; Kozlowski, 1996). If observed somatic growth patterns are the result of resource allocation, then the function describing energy acquisition must represent the sum of energy allocated to either somatic tissue or gonads (Kozlowski and Uchmanski, 1987). I define surplus energy as resources in excess of maintenance

costs that are available for allocation to either somatic growth or reproduction (Ware, 1980; Roff, 1983).

Studies of resource allocation often define the dynamics of surplus energy (the "production function") as a function of body size, but many differ with respect to the functional form. To simplify calculations, the units of "energy" are often in terms of mass (Ware, 1980). The production function

$$dW/dt = aW^b, \tag{4.1}$$

is used in many studies based on empirical fits to somatic growth which generally conclude that $2/3 < b < 1$ (Ware, 1980; Myers and Doyle, 1983; Kozlowski, 1996; Lester et al. 2004). However, Parker and Larkin (1959, pg. 742) noted that "…the interpretation attached to the constants [a and b] is complicated in the case of growth rate because both ecological and physiological factors act as determinants." Since the production function is describing the dynamics of energy allocated to reproduction in addition to that used for somatic growth, it is important to consider the sensitivity of model results to alternative hypotheses.

Miller et al. (2008) use an exponential production function to model reproductive allocation for an iteroparous cactus. They define a discrete model for potential growth in terms of the number of cactus segments, x

$$x_{t+1} = x_t + \left(a + bx_t\right), \tag{4.2}$$

$$x_{t+1} - x_t = a + bx_t, \tag{4.3}$$

$$\Delta X\left(x\right) = a + bx. \tag{4.4}$$

For an exponential model, the growth increment function, ΔX, is a linear function of size.

For many organisms, the true production function is unknown and difficult to observe. My first goal in this study is to evaluate how the assumed form of the production function affects predictions from resource allocation models. I develop models that bracket a range of functional forms for surplus energy acquisition, and compare model predictions with observable patterns such as growth and mass-specific fecundity.

Growth after maturity and diminishing returns of reproductive effort

Simple models of resource allocation often predict that the optimal strategy is to allocate all surplus energy to reproduction after maturity, resulting in no somatic growth after maturity (Kozlowski, 1992; Perrin and Sibly, 1993). Factors that favor growth after maturity have been reviewed by Heino and Kaitala (1999). These include seasonal switching between periods of growth and reproduction (Kozlowski, 1996), diminishing returns from increased reproductive effort (Taylor et al., 1974; Myers and Doyle, 1983; Miller et al., 2008), and rates of production and mortality that either both increase or both decrease with body size (Perrin et al. 1993).

Myers and Doyle (1983) identify two categories of biological mechanisms that result in growth after maturity due to diminishing returns from increased

reproductive effort (Taylor et al., 1974). The first category is the "concave egg conversion function." For example, if eggs are developed primarily from energy reserves, and energy storage has a cost that increases with respect to the amount of energy stored, then reproductive success in the current time period will be a concave function of reproductive effort. The second category is a convex relationship between mortality and reproductive output. Myers and Doyle (1983) suggest that reproduction may be accompanied by increased mortality due to either predation or susceptibility to disease.

In this study I evaluate different hypotheses concerning 1) size-dependent acquisition of surplus energy, 2) the relationship between reproductive effort and current reproduction, and 3) schedules of natural mortality. I use state dependent life history models to identify optimal resource allocation strategies, and compare model predictions with observed patterns for size at age, age at maturity, and weight-specific fecundity.

Methods

State dependent life history models are implemented using stochastic dynamic programming (Clark and Mangel, 2000). Prior to discussing the algorithm, I first describe the submodels that characterize the dynamics of length, surplus

energy, and natural mortality, with the hope that this approach will clarify details of execution and simplify my notation.

Models for potential growth in length

I develop three models for the dynamics of potential length which, when combined with an assumed length-weight relationship, determine the dynamics of surplus energy. The first model describes the potential for exponential growth, for which length at time $t+1$ (l_{t+1}) is the sum of length in the previous time step (l_t) and an increment function ($\Delta L(l)$) that is proportional to current length.

$$l_{t+1} = l_t + \Delta L(l_t) \tag{4.5}$$

$$\Delta L(l) = gl \tag{4.6}$$

This model can be considered one end of a continuum of potential growth models for resource allocation studies, in that potential growth in length is smallest at small sizes (Figure 46).

The other end of the continuum is a model in which maximum potential growth in length declines linearly with length. The von Bertalanffy (VB) growth model (Figure 46)

$$\frac{dL}{dt} = q - kL, \tag{4.7}$$

fits this description, with its maximum growth rate, q, occurring at $L=0$ and size approaching an asymptotic value of q/k (von Bertalanffy, 1938; Mangel *et al.*, 2007). Thinking of this as a recursive relationship, we can write Equation 4.7 as

$$L(t+dt) = L(t) + (q - kL)dt \quad (4.8)$$

The VB model is not commonly used to describe potential growth dynamics, but it has an attractive feature in this new context: potential growth is asymptotic, rather than unbounded. The solution to the VB equation is a function of three parameters: the maximum growth rate (q), a rate constant (k), and a location parameter ($L(t_0)$=0)

$$L(t) = \frac{q}{k}\left(1 - e^{-k(t-t_0)}\right) \quad (4.9)$$

Day and Taylor (1997) reasoned that growth must change after maturity due to the cost of reproduction. This reduction in somatic growth rate is thought to arise from energy allocated to reproductive products, but may also include increased costs associated with maintenance of reproductive structures or participation in breeding behavior (e.g. migration). In the state variable models I consider, energy used for reproductive products is determined by the optimal allocation decision, but the production function can allow for the possibility of reduced surplus energy due to increased fixed maintenance costs after maturation. Therefore, I adopt a modified version of the VB model (Stamps et al., 1998) in which the potential growth rate (in length) of mature individuals is reduced relative to immature individuals of the same size (Figure 46).

$$\frac{dL}{dt} = \begin{cases} q - kL & \text{immature} \\ q - \left(k + \dfrac{d}{l_m}\right)L & \text{mature}, d > 0 \end{cases} \quad (4.10)$$

In this model, individuals incur a greater lifetime potential growth cost for smaller lengths at maturity (l_m), and the parameter d scales the effect of this potential growth cost.

The asymptotic size for immature individuals (q/k) is therefore larger than the asymptotic size for mature individuals, $L_\infty(l_m)$, which is an increasing function of length at maturity for d>0.

$$L_\infty(l_m) = q / (k + d/l_m) \tag{4.11}$$

It is important to remember that these asymptotic models do not determine somatic growth in the life history models I develop. Rather, they describe the dynamics of surplus energy. For that reason, the reduction in somatic growth rate after maturity described by Stamps et al. (1998) is interpreted here as reduced potential growth rate. This change can be interpreted as an increase in maintenance costs associated with reproductive structures.

Gulland (1983) showed that the VB model can be recast as a length-increment equation. The same is true for the more complicated model, but it requires separate expressions for immature and mature individuals. The length increment function for immature individuals, $\Delta L_0(l)$, is identical to VB growth

$$L(t+1) = L(t) + \Delta L_0(l), \tag{4.12}$$

$$\Delta L_0(l) = (q/k - l)\left(1 - e^{-k}\right). \tag{4.13}$$

The increment function for mature individuals, $\Delta L_1(l, l_m)$, is a function of current length, length at maturity. A growth-cost parameter ($d \geq 0$, assumed constant)

determines the extent to which growth rate is reduced for a given value of length at maturity l_m.

$$\Delta L_1(l, l_m) = \max\left\{0, \quad \left(\frac{q}{(k + d/l_m)} - l\right)\left(1 - \exp\{-(k + d/l_m)\}\right)\right\} \tag{4.14}$$

The maximization function in Equation 4.14 ensures that potential growth (and current reproduction) is zero for mature fish if length exceeds the asymptotic mature size (Equation 4.11). Hereafter I refer to the Stamps et al. (1998) model simply as the "asymptotic" production function, since the VB model is a special case ($d = 0$).

Different values of d in the asymptotic production function are not easily interpreted (apart from $d = 0$), so I reparameterized the model such that a fish that matures at the smallest size in the model (l_{min}) would grow to a fraction, c, of the immature asymptotic size. The relationship between c and d for $0 < c \leq 1$ is

$$d = k \cdot l_{\min}\left(\frac{1}{c} - 1\right). \tag{4.15}$$

The third model I consider for the dynamics of potential length defines the length increment as constant with respect to length (Lester et al., 2004) (Figure 46).

$$l_{t+1} = l_t + C \tag{4.16}$$

$$\Delta L(l) = C \tag{4.17}$$

Parker and Larkin (1959) show that when weight is proportional to a cubic function of length, Equation 4.17 is equivalent to the allometric production function in terms of weight with $b = 2/3$ (Equation 4.1). Specifically, if we differentiate a weight-length relationship that is assumed proportional to the cube of length

$$W(L) = uL^3, \tag{4.18}$$

$$\frac{dW}{dt} = 3uL^2 \frac{dL}{dt}, \tag{4.19}$$

then equate Equation 4.19 to the allometric production function, Equation 4.1,

$$3uL^2 \frac{dL}{dt} = aW^{2/3}, \tag{4.20}$$

$$3uL^2 \frac{dL}{dt} = a\left(uL^3\right)^{2/3}, \tag{4.21}$$

and rearrange terms

$$\frac{dL}{dt} = \frac{au^{-1/3}}{3}, \tag{4.22}$$

we see that a constant length increment function (Equation 4.22) is equivalent to a mass increment function with an exponent of 2/3 (Equation 4.1) when we assume a cubic weight-length relationship (Equation 4.18).

Dynamics and allocation of surplus energy

The dynamics of surplus energy, rather than length, are key to decisions regarding optimal resource allocation. The cubic relationship between length and mass (energy) provides a simple link. Since immature fish do not devote resources to reproduction, their growth in length is fully characterized as either exponential (Equation 4.6), asymptotic (Equation 4.13), or linear (Equation 4.17). Mature fish allocate a fraction of surplus energy to gonads, so their growth in length is dependent on optimal allocation decisions. I now describe the equations which

characterize reproduction, somatic weight, and length as functions of the allocation decision.

The potential mass increment, ΔW, which is equivalent to surplus energy, is derived from a length increment function (Equations 4.6, 4.13, 4.14 or 4.17) and the weight-length relationship (Equation 4.18)

$$\Delta W(l) = u[l + \Delta L]^3 - ul^3 . \tag{4.23}$$

Examining the production functions in terms of mass (Figure 47) emphasizes the bounded growth potential associated with the asymptotic VB and Stamps et al. (1998) length models, compared to the unbounded growth potential of the exponential and linear length models. The mass increment function for the Stamps et al. model is a function of both current length and length at maturity, but length at maturity is omitted in the increment equations to simplify the notation among models.

The decision variable (over which fitness is optimized) is the fraction of surplus energy allocated to reproduction, ρ. I define current reproduction

$$R(\rho, \Delta W(l), \mu) = \rho \Delta W(l) \exp\{-\mu\rho\Delta W(l)\} \tag{4.24}$$

in terms of ρ , $\Delta W(l)$ and an additional parameter, μ, which provides the option of a concave relationship between current reproduction and the allocation decision (Myers and Doyle, 1983). When $\mu = 0$ reproduction is a linear function of surplus energy (Figure 48). Values of $\mu > 0$ define reproduction as a concave function of

allocation, with the amount of curvature depending also on the amount of surplus energy, $\Delta W(l)$ (Figure 49).

Energy not allocated to gonads is used for creation of somatic tissues. The the fraction of surplus energy allocated to somatic growth is (1 - ρ). Somatic weight (now a function of ρ) is the sum of current weight and the fraction of the potential mass increment that is not allocated to gonads.

$$W(\rho,l) = \min\left\{ul^3 + (1-\rho)\Delta W(l), W(L_{limit})\right\} \tag{4.25}$$

The minimization ensures that length will not exceed the dimensions of the model, where L_{limit} is the maximum possible length, but allows fish at that size to continue acquiring resources. Solving the allometric weight-length relationship for length then gives an equation for updating length in each time step, based on the current length and allocation decision.

$$L(\rho,l) = \exp\left\{\frac{1}{3}\log\left(\frac{W(\rho,l)}{u}\right)\right\} \tag{4.26}$$

Mass-specific reproductive output, which is sometimes referred to as the gonadosomatic index (γ) is analogous to relative fecundity (e.g. eggs per gram).

$$\gamma(\rho,l,\mu) = \frac{R(\rho,\Delta W(l),\mu)}{ul^3 + \Delta W(l)} \tag{4.27}$$

Natural mortality

I define the rate of natural mortality, *M*, as one of two possible relationships.

$$M(l) = m_0 + \frac{m_1}{l} \tag{4.28}$$

$$M(l, \gamma) = m_0 + \frac{m_1}{l} + \gamma^{m_2} \tag{4.29}$$

The first (Equation 4.28) contains size-independent and size-dependent components, and the second (Equation 4.29) specifies a relationship between mortality and reproductive effort. I define m_0 as the size-independent mortality rate, m_1 as a scalar of size-dependent mortality, and m_2 as a power function of relative reproductive effort, γ.

Stochastic dynamic programming algorithm

To implement the state dependent life history models, I define a lifetime fitness function in terms of the state variable $L(t)$, length at time t.

$$F(l, t) = \text{maximum expected total reproduction from age t to T, given that } L(t) = l \tag{4.30}$$

The fitness function for the asymptotic production model (Stamps et al., 1998) also includes a state variable for maturity, which I develop in a later section. The models with exponential and linear production functions have length as the only state variable. The maximum age, T, can be interpreted as the end of an organism's life so fitness of the maximum age in the model is set equal to zero.

$$F(l, T) = 0 \tag{4.31}$$

I specify a time step of one year, and assume that reproduction occurs once per year. This assumption is consistent with the reproductive patterns observed in most

rockfish, although multiple spawning events have been observed in some species (Love et al., 2002).

The lifetime fitness function is the sum of two terms, current reproduction (Equation 4.24) and future fitness, $F(l,t+1)$, discounted by the probability of surviving from age *t* to *t+1*, maximized over the set of possible allocation decisions.

$$F(l,t) = \max_{\rho}\{R(\rho,l,\mu) + \exp(-M(l,\gamma))F(l,t+1)\} \tag{4.32}$$

Recall that we previously defined fitness for all lengths at the maximum age, *T* (Equation 4.31). Therefore we can calculate fitness of the penultimate age, *F(l,T-1)*. Once we have obtained values for *F(l, T-1)*, we can evaluate *F(l, T-2)*, *F(l, T-3)*, and so on back to age t=1 in the model. This backward iterative procedure is the stochastic dynamic programming (SDP) algorithm, which identifies the optimal allocation strategy for every length and every age, assuming that the individual behaves optimally from that time forward (Clark and Mangel, 2000).

Computer implementation of the SDP algorithm for the models with exponential and linear production functions proceeds as follows:

1. Assign values for model parameters
2. Define a vector of possible allocation decisions ($0 \le \rho \le 1$)
3. Specify fitness at length for the maximum age, *F(l, T)*
4. Set the age variable *t = T-1*
5. For each length at time *t*
    a. Calculate potential length, $l_{pot} = l_t + \Delta L(l_t)$

b. Calculate potential weight, ul^3_{pot}

c. Calculate surplus energy, $\Delta W(l_t) = ul^3_{pot} - ul^3_t$

d. For each allocation decision, ρ_i

i Compute current reproduction $R(\rho_i, \Delta W(l_t), \mu)$ (Equation 4.24) and store its value in a vector, $R(\rho_i)$

ii Calculate the gonadosomatic index (Equation 4.27) and store its value, $\gamma(\rho_i)$

iii Calculate updated somatic weight $W(\rho_i, l)$ (Equation 4.25)

iv Convert $W(\rho_i, l)$ into an updated length, $l(\rho_i)$ (Equation 4.26)

v Compute fitness given ρ_i as the sum of current reproduction and mortality-discounted future fitness* and store its value, $V(\rho_i)$

$$V(\rho_i) = R(\rho_i, \Delta W(l), \mu) + \exp\{-M(l, \gamma(\rho_i))F(l(\rho_i), t+1)\}$$

**evaluation of future fitness usually requires interpolation, see Appendix C*

e. Identify the allocation decision (ρ^*) at maximizes V

f. Set $V(\rho^*) = F(l, t)$

g. Store ρ^* and the associated optimal values of $R(\rho^*)$, $\gamma(\rho^*)$, and $M(l, \gamma(\rho^*))$

6. Define the age variable t as $t-1$

7. If $t \geq 1$ go to step 5, otherwise stop.

This algorithm generates a matrix of optimal allocation decisions, and the associated values of fitness, for each length at each age in the model. The gonadosomatic index and current reproduction (analogous to fecundity) are also recorded. For the exponential and linear production models, I define age (size) at

maturity as the youngest age (smallest size) at which optimal allocation to gonads is greater than zero.

The state variable models based on the exponential and linear production functions are simple applications of the dynamic programming algorithm. I extend these models to accommodate the Stamps et al. (1998) production function. This model for surplus energy acquisition requires length at maturity as an input so it is necessary to explicitly model maturity as an additional state variable. In addition, the fitness of all lengths at maturity that are equal to or less than the current length must be evaluated.

To reflect the role of length at maturity, l_m, in the fitness of mature individuals, I redefine the equations for surplus energy dynamics, reproduction, and the gonadosomatic index (Equations 4.23 – 4.27) to include the new state variable. I use the subscripts 0 and 1 for functions associated with immature and mature individuals, respectively.

$$\Delta W_1(l, l_m) = u\left[l + \Delta L_1(l, l_m)\right]^3 - ul^3 \tag{4.33}$$

$$R(\rho, \Delta W_1(l, l_m), \mu) = \rho \Delta W_1(l, l_m) \exp\{-\mu\rho \Delta W_1(l, l_m)\} \tag{4.34}$$

$$W_1(\rho, l) = \min\left\{ul^3 + (1-\rho)\Delta W_1(l, l_m), W(L_{limit})\right\} \tag{4.35}$$

$$l_1(\rho, l, l_m) = \exp\left\{\frac{1}{3}\log\left(\frac{W_1(\rho, l)}{u}\right)\right\} \tag{4.36}$$

$$\gamma = \frac{R(\rho, \Delta W_1(l, l_m), \mu)}{W(l) + \Delta W_1(l, l_m)} \tag{4.37}$$

As with the simpler models, the lifetime fitness function of mature individuals

$$F_1(l, l_m, t) = \max_{\rho}\{R(\rho, \Delta W_1(l, l_m), \mu) + \exp(-M(l, \gamma))F_1(l_1(\rho, l, l_m), t+1)\} \quad (4.38)$$

is the maximum over allocation decisions of the sum of current reproduction (Equation 4.34) and discounted future fitness.

Fitness of immature individuals, $F_0(l,t)$, is the greater of two choices: remain immature and grow at the faster rate (ΔL_0), or mature and grow at the slower rate (ΔL_1), but with the ability to reproduce in the future.

$$F_0(l,t) = \max\begin{cases} \exp(-M(l, \gamma = 0))F_0[l + \Delta L_0(l), t+1] \\ \exp(-M(l, \gamma = 0))F_1[l + \Delta L_1(l, l), t+1] \end{cases} \quad (4.39)$$

When the decision is to mature (lower expression), note that reproduction does not occur in the year of maturation ($\gamma = 0$) and that length at maturity equals current length in the mature growth increment, $\Delta L_1(l,l)$.

Computer implementation of the state variable model with the asymptotic production function is similar to the algorithm for the exponential and linear models. The differences are in step 5, within which an additional loop over possible lengths at maturity is required, and an evaluation of the decision to mature.

5. For each length at time *t,*
    a. For each length at maturity, l_m, from L_{min} to the current length
        I. Calculate potential length, $l_{pot} = l_t + \Delta L_1(l_t, l_m)$
        II. Calculate potential weight, ul_{pot}^3

III. Calculate surplus energy, $\Delta W_1(l, l_m) = ul_{pot}^3 - ul^3$

IV. For each allocation decision, ρ_i

i. Compute current reproduction $R(\rho_i, \Delta W_1(l, l_m), \mu)$ (Equation 4.34) and store its value in a vector, $R(\rho_i)$

ii. Calculate the gonadosomatic index (Equation 4.37) and store its value, $\gamma(\rho_i)$

iii. Calculate updated somatic weight $W_1(\rho_i, l)$ (Equation 4.35)

iv. Convert $W_1(\rho_i, l)$ into an updated length, $l_1(\rho_i, l, l_m)$ (Equation 4.36)

v. Compute fitness given ρ_i as the sum of current reproduction and mortality-discounted future fitness* and store its value, $V(\rho_i, l_m)$

$$V(\rho_i, l_m) = R(\rho_i, \Delta W_1(l, l_m), \mu) + \exp\{-M(l, \gamma(\rho_i))F(l_1(\rho_i, l, l_m), t+1)\}$$

**evaluation of future fitness usually requires interpolation, see Appendix C*

vi. Identify the allocation decision (ρ^*, l_m) at maximizes V

vii. Set $V(\rho^*, l_m) = F_1(l, l_m, t)$

viii. Store ρ^* and the associated optimal values of $R(\rho^*, l_m)$, $\gamma(\rho^*, l_m)$, and $M(l, \gamma(\rho^*))$

V. Calculate the fitness of an immature fish choosing to remain immature

$$V_{immature} = \exp(-M(l, \gamma = 0))F_0[l + \Delta L_0(l), t+1]$$

VI. Calculate the fitness of an immature fish choosing to mature

$$V_{mature} = \exp(-M(l, \gamma = 0))F_1[l + \Delta L_1(l, l), t+1]$$

VII. Calculate fitness of immature individual (Equation 4.39)

$$F_0(l,t) = \max\{V_{immature}, V_{mature}\}$$

VIII. Record optimal maturity decision, $\pi(l, t)$

if $V_{mature} > V_{immature}$, then $\pi(l, t)=1$, else $\pi(l, t)=0$

6. Define the age variable t as $t-1$

7. If $t \geq 1$ go to step 5, otherwise stop.

The stochastic dynamic programming algorithm for the asymptotic production function returns a 3-dimensional array of optimal allocation decisions (for each age, length, and length at maturity), the associated values of fitness, optimal age and size at maturity, and other quantities of interest (e.g. gonadosomatic index, current reproduction). To evaluate model predictions regarding optimal growth trajectories requires an additional step: forward simulation of individuals that behave optimally according to the results of the SDP algorithm.

Forward simulation algorithm

State-dependent predictions regarding growth, maturation and reproduction are valuable outputs of the SDP algorithm. To determine what the models predict regarding the patterns we observe for rockfish, we reverse the order of time steps and 'grow' virtual organisms forward in time according to the optimal strategies obtained from the backward algorithm. These results are assessed to evaluate the adequacy of model assumptions.

The forward simulation algorithm for the exponential and linear production functions proceeds as follows:

1. Set the age variable $t = 1$
2. Set the initial length, $L(t=1) = l_{true}(1)$, as the first value in a vector that will store realized lengths from the simulation, $l_{true}(t)$
3. Read the optimal allocation decision, ρ^*, given the current length and time from the array of optimal decisions generated by the SDP algorithm (this may require interpolation if $l_{true}(t)$ is between the discrete length values evaluated by the SDP algorithm; see Appendix 3.A)
4. Calculate available surplus energy (potential growth in mass)

   $l_{pot} = l_{true}(t) + \Delta L(l_{true}(t))$

   $\Delta W\left(l_{true}(t)\right) = u l_{pot}^3 - u l_{true}^3$
5. Calculate and store somatic weight and length in the next time step given the current size and optimal allocation, ρ^*

   $$W\left(\rho^*, l_{true}(t+1)\right) = \min\left\{u l_{true}(t)^3 + (1-\rho^*)\Delta W\left(l_{true}(t)\right), W\left(L_{limit}\right)\right\}$$

   $$L\left(\rho^*, l_{true}(t+1)\right) = \exp\left\{\frac{1}{3}\log\left(\frac{W\left(\rho^*, l_{true}(t)\right)}{u}\right)\right\}$$
6. Interpolate (see Appendix 3.A) optimal values of the gonadosomatic index, $\gamma(\rho^*, l_{true}(t))$, and reproduction at the current length, $R(\rho^*, l_{true}(t))$, from the arrays stored during the SDP algorithm
7. If $t < T$, set the age variable $t = t + 1$; otherwise stop

Forward simulation for the asymptotic production function is similar, with the additional step of retrieving the optimal maturity state and recording the length at which the individual matures during the forward simulation. Length at maturity determines the growth for that time step (Equations 4.13 and 4.14), but subsequent allocation decisions are similar to the exponential and linear models.

Model evaluation

To compare alternative hypotheses concerning the dynamics of surplus energy (production functions) and the effect of reproductive effort on current reproduction, I plotted three relationships (optimal allocation at length, optimal gonadosomatic index at length, and length at age) to check for consistency of trends with patterns observed in rockfishes. I generated 6 figures for each relationship, based on pairwise combinations of the 3 alternative production functions and 2 reproduction assumptions. Specifically, I compare predictions from the exponential, linear, and asymptotic production functions, with the assumption that current reproduction, $R(\rho, \Delta W(l), \mu)$, is either proportional to the optimal allocation strategy ($\mu = 0$) or that $R(\rho, \Delta W(l), \mu)$ is a concave function of allocation ($\mu > 0$). Combinations of model assumptions that produce trends consistent with those observed for rockfish can be considered viable hypotheses for mechanisms shaping reproductive patterns among the *Sebastes*. Tables 16-18 report the parameter values I use for these analyses.

To understand how differences in natural mortality affect optimal resource allocation and growth patterns, I compare results from a model with constant mortality (Equation 4.28; $m_0 = 0.05$, $m_1 = 0$) to one that allows for increasing mortality associated with increasing reproductive effort (Equation 4.29; $m_0 = 0.05$, $m_1 = 0$, $m_2 = 2$). Since the concave reproduction function and convex mortality functions can both generate growth after maturity (Myers and Doyle, 1983), I limit the analysis to the proportional reproduction assumption ($\mu = 0$).

Finally, as a general evaluation of model properties, I compare models with different levels of baseline mortality but the same assumptions about production and reproduction. I evaluate the response of model predictions to changes in natural mortality and compare these patterns to well-supported relationships in the literature on life-history theory.

Results

Given the large amount of empirical support for the existence of trade-offs between growth and reproduction (Stearns, 1992), we can assume that for post-maturation growth to exist the optimal fraction of surplus energy allocated to reproduction (ρ^*) must increase gradually as a function of length. This graded response is evident in the predictions from several combinations of production and growth-increment functions (Figure 50). Only the models with proportional reproduction and either linear or asymptotic production functions (Figures 50c and

50e, respectively) predict an abrupt increase in allocation with respect to length. These models predict that maturation is optimal at sizes just below the maximum predicted size. The exponential production function produces a graded response in optimal allocation for both hypotheses about the relationship between reproductive output and effort (Figures 50A and 50B). The optimal allocation strategy is also a graded response for the linear and asymptotic production functions when reproduction is a concave function of allocation (Figures 50D and 50F).

The gonadosomatic index, $\gamma(\rho^*, l, \mu)$, is an increasing function of length for several rockfish species (Gunderson, 1997). The predicted pattern for $\gamma(\rho^*, l, \mu)$ versus length for the model with exponential production and proportional reproduction is consistent with this empirical observation, in that it increases with size (Figure 51a). All models with a concave reproduction relationship predict that $\gamma(\rho^*, l, \mu)$ increases at first, but then declines with increasing size (Figure 51, panels B, D, and F). The linear and asymptotic production models with proportional reproduction increase with size, but rapidly approach their maximum value after maturation (Figure 51, panels C and E). In fact, the trends in gonadosomatic index versus length in models with proportional reproduction (Figure 51, panels A, C, and E) are directly proportional to the trends in allocation strategies (Figure 50).

Based on size-dependent optimal allocation strategies (Figure 50) and gonadosomatic indices (Figure 51), it would appear that the model with the exponential production function and proportional reproduction is the only one

consistent with the observed patterns in the *Sebastes*. The results of the forward simulation show us however, that the predicted somatic growth trajectory associated with this model shows no growth after maturity (Figure 52A). In fact, all models with proportional reproduction (Figure 52, panels A, C, and E) show little evidence of growth after maturity. This result is consistent with the allocation strategy shown in Figure 50A, and emphasizes the importance of evaluating predictions based on forward simulations. When the growth increment increases exponentially with length, the organism rapidly "grows through" the range lengths over which intermediate allocations are optimal, and growth is only bounded by the maximum length in the model, L_{limit}. The concave reproduction function succeeds in generating patterns of growth after maturity (Figure 52, panels B, D, and F) as predicted by Taylor et al. (1974), but the associated trends in gonadosomatic index are inconsistent with the patterns of fecundity and size in rockfish (Haldorson and Love, 1991).

Sibly et al. (1985) found that if mortality is a convex function of allocation to reproduction, then post-maturation growth can result. Models based on the linear and asymptotic production functions predict a graded response for optimal allocation as a function of length (Figure 53, panels C and D). The associated trajectories of natural mortality at age (Figure 53, panels A and B) show that mortality under the linear growth model increases rapidly at first from the baseline level (prior to maturity) of 0.05, stopping abruptly at a maximum value of

approximately 0.06 (Figure 53A). The progression of change in mortality for the asymptotic production model is more gradual (Figure 53B). Examination of predicted lengths at age from the forward simulations reveals that, although there is post-maturation growth in the linear production model, it reaches the boundary of the model dimensions. Reduced the growth increment (C) does avoid this problem (results not shown), but maturity in Figure 54 is already predicted to occur at 20 years of age, and a reduced growth rate pushes that important event even farther into the future.

The asymptotic production model with the convex mortality function predicts an increase in $\gamma(\rho^*, l, \mu)$ with length (Figure 54B). This model also predicts maturity at an age of 16 years, which is at the high end of observed values for rockfish, but well within the observed range (Figure 54D). Love et al. (2002) report that 50% of yelloweye rockfish are mature at 22 years of age. Maximum length is 45 cm, and length at maturity (32 cm) is about 71% of this maximum size.

As an additional diagnostic test, I used the asymptotic production model with the convex mortality function as a baseline for examining the effect of varying the size-independent mortality rate (m_0) on model predictions (Table 19). An important feature of the state dependent life history model is that maximum size, L_{max}, (equivalent to L_∞ in the VB length at age model) is not an input to the growth model, but rather emerges as a function of optimal allocation decisions and the rate of natural mortality (Table 19). A existence of a negative correlation between

maximum size and *M* has long been recognized in ecology and fisheries (Beverton and Holt, 1959). Since age is correlated with size, age at maturity also declines with increasing *M*. Beverton (1992) reports a range of values (0.66 – 0.82) for the ratio of length at maturity to maximum length for the Pacific *Sebastes* species. By varying m_0 in the life history model between 0.05 and 0.125 (values consistent estimated *M* for rockfish), the predicted ratio takes values from 0.56 – 0.71 (Table 19). Predicted values of the gonadosomatic index (relative reproductive investment) also vary with *M* as predicted by life history theory (Stearns, 1992), ranging from 9% to 18% of somatic weight and well within the range of observed values (Love et al., 1990).

I conclude that the asymptotic production function, coupled with proportional reproduction and a convex mortality curve is the hypothesis that is most consistent, among the models I have examined, with trends observed among the *Sebastes*. Other mechanisms may be responsible for the observed patterns, but this simple resource allocation model is a parsimonious hypothesis for mechanisms driving patterns of reproductive potential in rockfish that is broadly consistent with rockfish life history strategies.

CHAPTER 5

SYNTHESIS OF FINDINGS REGARDING THE REPRODUCTIVE POTENTIAL OF ROCKFISHES

For over 50 years fisheries scientists have emphasized the importance of an accurate representation of reproductive biology in population dynamics models (Beverton and Holt, 1957; Bagenal, 1973; Rothschild and Fogarty, 1989; Trippel et al., 1997; MacCall, 1999; Murawski et al., 1999; Beamish et al., 2006; Morgan, 2008). Studies of fecundity in some fish species have found that the number of eggs produced per gram body weight (relative fecundity) is constant with respect to size and age (Raitt, 1933; Simpson, 1951). For these species, the spawning output of a population can be considered proportional to the biomass of female spawners. In other species, including many members of the genus *Sebastes*, there is evidence of increasing relative fecundity with size or age (Boehlert, 1982; Haldorson and Love, 1991; Bobko and Berkeley, 2004). In exploited populations it is necessary to consider how this pattern affects population dynamics and resilience to harvesting.

Increasing reproductive effort with size is also interesting from an evolutionary standpoint. Life history theory suggests that allocation of an increasing amount of energy to reproduction must come at some cost, e.g. slower growth or reduced survival (Stearns, 1992). To evaluate alternative hypotheses about the nature of these costs I develop state dependent life history models that identify optimal evolutionary pathways based on the criterion of maximizing lifetime expected reproductive success. I evaluate each hypothesis by comparing trends in

model predictions with observed patterns of growth, reproduction, and maturity seen in rockfishes.

Implications for management: estimation of target harvest rates

Stock assessments of many *Sebastes* species continue to assume that egg production is proportional to female spawning biomass (Table 1). The per-recruit analysis I present in Chapter 2 indicates that management decisions based on the assumption of constant relative fecundity are risk-prone, potentially underestimating the effects of fishing on the reproductive potential of the stock. I demonstrate that realized spawning potential ratio (SPR) can substantially differ from target SPR when fecundity is incorrectly characterized, and I show that the extent of this difference is a function of the natural mortality rate and the magnitude of size-dependent changes in relative fecundity (Figures 1 and 2).

The SPR analysis is a simple description of the problem, based on a management reference point that is used for rockfish off the U.S. west coast ($F_{50\%}$). I chose values of the natural mortality rate, M, the fecundity-length exponent (b), and the von Bertalanffy growth coefficient (k) that are consistent with estimated values for rockfish. If trade-offs exist between reproductive effort and survival, then species may be constrained with respect to what combinations of mortality, fecundity exponent, and growth coefficient (k) are possible (Stearns, 1992; Gunderson, 1997). Each set of SPR contours are conditioned on a single value of the

growth parameter, *k*, which is positively correlated with natural mortality (Beverton and Holt, 1959). As a result, faster growing species may experience similar differences in realized SPR. Species with lower natural mortality rates appear to be less affected by the incorrect assumption of constant relative fecundity, but these species are often more susceptible to overharvesting due to lower innate productivity. As a result, even small errors in estimating SPR remain a concern due to the regulatory consequences of exceeding management thresholds (Ralston, 2002).

Beamish et al. (2006) used an age-structured simulation model with variable recruitment to demonstrate how the absence of older individuals with greater reproductive potential ("longevity overfishing") increases the time needed to rebuild populations after periods of poor ocean conditions. Murawski et al. (1999) simulated a change in realized SPR ("%MSP") for Atlantic cod (*Gadus morhua*) that is similar to my result, but motivated by size- or age-dependent differences in the number of hatched eggs or viable larvae. Increased viability of larvae from older females may also be a characteristic of rockfish; Berkeley et al. (2004) found that larvae from older female rockfish were more resistant to starvation than larvae from younger females. If offspring from older fish have enhanced survival, then my analysis which is based on fecundity (numbers) alone would underestimate the reduction in realized SPR relative to the target. Moreover, my results assume that fecundity at size or age does not change with population density, which may not be

true. Rothschild and Fogarty (1989) considered the role of density on fecundity, particularly as a stabilizing mechanism for population egg production, and suggested that it contributes to the resilience of fish populations.

The structure of age classes in population dynamics models must also be considered carefully for species with size-dependent relative fecundity. These models sometimes incorporate a "plus group," an age class that approximates the dynamics of all individuals equal to or older than a given age. If all age classes in the plus group are assumed to share the same biological characteristics as the youngest age in the group, and a substantial proportion of the population occurs in the plus group, then reproductive output of older age classes will be underestimated.

A biological aspect of rockfish reproduction that deserves further study is the prevalence of females that spawn (parturate) two or more times per year. Multiple spawning (parturition) events have the potential to dramatically increase the reproductive output of rockfish populations. Increased egg production would only result if additional broods within a spawning season were the result of *de novo* vitellogenesis within the season (indeterminate spawning). Release of several broods from a fixed stock of mature oocytes (group synchronous determinate spawning) would not have an affect on annual egg production. Evidence of multiple broods has been reported for *S. paucispinis, S. ovalis, S. constellatus , S. chlorostictus, S. elongatus, S. ensifer, S. goodei, S. hopkinsi, S. levis, S. rosaceus, S. rosenblatti,* and *S. rufus* (Moser, 1967; MacGregor, 1970; and Love et al., 1990).

Multiple broods appear to be more common in the southern portion of these species' ranges, and two broods per year is typical with a possibility of three broods in large cowcod (*S. levis*) and bocaccio (*S. paucispinis*) (Love et al., 1990). Love et al. (1990) observed that smaller mature females were mostly single brooders, and larger females were almost exclusively multiple brooders. If species with multiple broods are capable of indeterminate spawning, this size-dependent pattern could potentially amplify the effects of fishing on reproductive output due to selective removal of larger fish.

Love et al. (1990) found no evidence of multiple broods in the other seven species examined in their study (*S. dalli, S. entomelas, S. flavidus, S. melanostomus, S. miniatus, S. saxicola*, and *S. semicinctus*). Multiple broods may still occur in these species, perhaps at lower frequencies. Miller and Geibel (1973) found evidence of multiple broods in 1 out of 648 blue rockfish (*S. mystinus*). The proportion of multiple spawners in each population may also vary by region and among years, in addition to the observed variability among size classes. Establishing criteria for identifying multiple spawning events is another source of uncertainty related to this phenomenon. Love et al. (1990) considered the presence of eyed larvae along with large numbers of eggs as an indicator of multiple broods.

Data sources and model selection

The database of rockfish fecundity estimates provides an opportunity to 1) examine patterns in relative fecundity among groups of closely related species, 2) compare alternative models for rockfish fecundity, and 3) examine other covariates (e.g. gonad maturation stage) that may relate to larval production. Previous studies suggest that size-specific trends in relative fecundity may be common among the rockfishes (Haldorson and Love, 1991; Gunderson, 1997) but no attempts have been made to provide a quantitative, genus-wide description of sources of variability.

The results of model selection based on AIC for six species indicate that an allometric fecundity model in terms of weight is preferred among the set of candidate models (model 2, Table 4). The data for these six species were chosen due to relatively large sample sizes and the availability of measured weights and lengths. The allometric model with weight as an offset (model 3, Table 4) is nearly as effective, with small AIC differences between it and the weight-only model, and has an intuitive interpretation related to condition factor. Richards and Schnute (1990) examined the data for quillback rockfish used in this study, and found that the length-based allometric model for absolute fecundity failed to adequately represent both curvature in the response and homogeneity of the residuals. They proposed a five-parameter dose-response model that contained simpler allometric and linear models as special cases. However, they did not evaluate weight as a covariate, and the AIC differences in Table 4 suggest a substantial improvement in fit relative to

the length-only model. Residual plots for the fecundity-weight allometric model (result not shown) did not indicate any major deviations from model assumptions, except for evidence of heavier tails in the distribution of residuals relative to the Gaussian assumption. It is possible that the Richards and Schnute model would further improve the fit of the weight-based model and warrant the additional model complexity, but I restricted my analysis to the set of more parsimonious models based on the substantial improvement in fit of the weight-based alternatives.

Bagenal (1973) noted that estimating fecundity as a function of total weight may be misleading because ripe gonads may weigh more than maturing gonads, and that it is important to consider which type of weight data are available from market data. Catch statistics for *Sebastes* are in units of total weight and population dynamics models for *Sebastes* seldom differentiate between total and somatic weights. Somatic weight data are less available than total weights, but conversion between the two can be accomplished with reasonable accuracy (Figure 8). I fit all models using total weight as the explanatory variable because the data for many species only included lengths, and published weight-length relationships are almost always based on total weight. The current analysis could benefit from species-specific adjustment of weights to reflect somatic weight.

In addition to models for absolute fecundity in terms of weight or length alone, I consider a model for relative fecundity as a function of length. This model requires measured weight and length for each fish, and is equivalent to the

assumption that absolute fecundity is proportional to condition factor (Equation 2.19). My results suggest, however, that the assumption of direct proportionality between fecundity and condition factor does not adequately represent the change in fecundity associated with deviations from the population average weight (Figure 3). The effect of condition factor on reproductive effort could occur in the earlier stages of egg development, determining the number of maturing eggs. Alternatively, condition factor could affect the viability of larvae through differences in available energy stores during gestation.

Bobko and Berkeley (2004) found that gonad development stage affects estimates of egg counts for black rockfish (*S. melanops*) and Kusakari (1991) found a similar result for *S. schlegelii*. Eldridge et al. (1991) found no difference between pre-fertilized and fertilized eggs as a semi-logarithmic function of age, but a difference is evident based on the allometric function of length or weight (Tables 6, 7, and 8). This difference is also found for yellowtail rockfish (*S. flavidus*) data collected by Sogard et al. (in prep.) (result not shown). Rockfish ages are difficult to estimate, especially for older fish, which may have masked the effect of stage on fecundity at age.

If relative fecundity is constant with respect to mass, then the exponent of the allometric fecundity-weight model will be equal to one. Maximum likelihood estimates (MLEs) of the exponents from allometric fecundity-weight models (Table 5) are consistently larger than 1 for the larger data sets, except for brown rockfish

(*S. auriculatus*). An exponent less than 1 would suggest that relative fecundity declines with increasing mass (e.g. the MLE for *S. ovalis*, Table 13). Values less than 1 might be interpreted as reproductive senescence, but is most likely an artifact due to small sample sizes. A study by de Bruin et al. (2004) reports no evidence of reproductive senescence in Pacific Ocean Perch (*S. alutus*) and rougheye rockfish (*S. aleutianus*).

Haldorson and Love (1991) reviewed maturation and fecundity of 45 rockfish species, comparing point estimates of life history parameters reported by 27 sources. Their approach provides important insights into qualitative trends among life history parameters for the *Sebastes*. The variability of fecundity estimates makes comparisons based on point estimates of model parameters difficult to evaluate, because uncertainty in the parameter estimates is not available. The database I compiled of rockfish fecundity estimates provides an opportunity to compare results among species and subgenera in a formal statistical framework (Chapter 3) as well as examine qualitative trends among species and subgenera.

Hierarchical Bayesian models for meta-analysis of rockfish fecundity

One of the striking patterns in the data is differences in relative fecundity by species and subgenus (Figure 22). Although these figures do not control for length, the data suggest that species in the subgenus *Sebastes* have very low relative fecundity, even though its members are found in different oceans (*S. norvegicus* is

an Atlantic species). Estimates of relative fecundity for another Atlantic species (*S. fasciatus*), based on reported fecundity-length and weight-length relationships, suggest that relative fecundity is also low for this species and increases with size (St-Pierre and de Lafontaine, 1995). Some species cluster together with close relatives (e.g. *Sebastes*, clade A, *Rosicola*), while others are quite different (*Sebastosomus*, *Pteropodus*, *Sebastomus*). Relative fecundity of bocaccio (*S. paucispinis*) is markedly different from its closest relatives, the shortbelly rockfish (*S. jordani*) and chilipepper rockfish (*S. goodei*). If relative fecundity is a measure of differences in reproductive effort among species, then there may be correlations with other life history parameters, e.g. natural mortality. This effect may be masked by imprecise estimates of mortality or other factors that influence realized reproductive effort such as differences in survival rates of larvae.

Raitt and Hall (1967) were the first to consider the effect that gonad maturity stages might have on rockfish fecundity estimates. In their study of the fecundity of *S. norvegicus* (then called *S. marinus*), they classify fecundity estimates into three categories: pre-fertilized fecundity, fertilized fecundity, and larval fecundity. Very few studies report fecundity estimates from multiple stages, and those that do often have small sample sizes from eyed larvae, probably due to the short duration of this stage prior to parturition. As mentioned earlier, the data on yellowtail rockfish from Eldridge et al. (1991) suggest that there is a difference in fecundity among stages (Tables 6 – 9). Since most studies are based on a single

maturity stage, and the effect of stage is inconsistent among species (Figure 23), I combined the data from all stages in my analysis. Ignoring this effect adds uncertainty to the fecundity estimates. Future comparative studies of rockfish fecundity would benefit from standardization of stages and increased sampling to acquire females in later stages of gonad development (e.g. fertilized eggs or eyed larvae). Fecundity estimates based on fertilized eggs and eyed larvae, while likely to be most representative of the number of larvae ultimately extruded, may be biased low if eggs or larvae are liberated upon capture (Raitt, 1933).

All of the fecundity estimates compiled for this study are reported as a single number when in fact, most values are estimates based on an average count from multiple subsamples of known weight taken from the ovaries. This source of measurement error in the response variable is absorbed into the error term in my analyses. As I note in Chapter 2, weight data were not available for all fish in the fecundity database. Fecundity was better predicted by weight than length, based on my analysis of species for which both lengths and weights are available. Therefore, I used length data to predict weights for about half of the individuals in the database. This source of measurement error in the explanatory variable is potentially more of a concern than measurement error in the response. The hierarchical framework can accommodate errors in explanatory variables by the additional of another 'level' to the hierarchy. If data from the same population of fish are available to predict weight from length, then the regression of log-fecundity against log-weight could be

based on simultaneous predictions of log-weight from log-length and thereby propagate uncertainty in weight at length through the fecundity-weight relationship. This approach requires that available weight-length data are representative of the population that generated the fecundity data, or that published weight-length relationships are available which report necessary variance estimates. Unfortunately, these two types of data are not always available. Nevertheless, variability in weight at length is likely small relative to variability in fecundity at weight, so the effect of errors in variables on the parameter estimates may be small (Kutner et al., 2005). Incorporation of this source of uncertainty would better characterize the variability in the data.

Spatial and temporal coverage in most fecundity studies is quite limited, and as a result I could not evaluate this source of variation although studies have shown that these can be important factors in determining fecundity of rockfishes (Gunderson, 1977, 1980; Eldridge and Jarvis, 1995). Among studies, the effect of region is potentially confounded with temporal or methodological differences. The only data obtained for this analysis that considered regional and/or spatial effects was from a study of the biology and population dynamics of Pacific Ocean Perch (*S. alutus*) by Gunderson (1976) which identified differences in fecundity among populations in the Washington-Oregon region and Queen Charlotte Sound, British Columbia. Fecundity estimates for some species differ among regions and years (reviewed by Haldorson and Love, 1991), but this result is potentially confounded

by methodological differences. Eldridge and Jarvis (1995) found evidence of temporal trends in fecundity in a thorough analysis of yellowtail rockfish (*S. flavidus*), and Gunderson et al. (1980) detected regional differences in the fecundity of chilipepper rockfish (*S. goodei*).

Differences in oceanographic conditions are likely to produce spatial and temporal fluctuations in fecundity, which are not captured by short-term regional studies. Gonadosomatic indices for *S. mystinus* are lower in El Nino years, possibly due to reduced food availability associated with lower levels of primary productivity (VenTresca et al., 1995). Differences in fecundity that are associated with ocean conditions are assumed to be part of the random component in my models. Collection of fecundity data over longer time periods and with greater spatial coverage may provide opportunities to include environmental covariates in the models and potentially reduce predictive uncertainty.

I make the assumption that there is an underlying relationship between rockfish fecundity schedules, either among all species or within individual subgenera. The data suggest that closely related species (e.g. the *Sebastosomus* species) may have similar trends. To develop predictions of fecundity for data-poor species, it seems reasonable to inform these predictions using data from close relatives of the species of interest. In the hierarchical modeling framework, the extent to which information is borrowed from other species is determined in part by the variability in the data. Species with few observations will have parameter

distributions similar to the population average (genus or subgenus, depending on the model). Data that suggest extreme or biologically implausible fecundity relationships are 'shrunken' toward the population mean if the data are highly variable. If these extraordinary patterns are in fact real, then the model will "self-correct" and assert the proper relationship with the arrival of additional data.

The model for relative fecundity as a linear function of weight (Equation 2.22) predicts that the probability of an increasing relationship (positive slope) is greater than 90% in 14 species (Table 12), and greater than 80% in 30 of the 40 species examined. The weight of evidence, therefore, suggests that representing relative fecundity as constant (slope = 0) with respect to weight is not in agreement with the data. One might assign a threshold probability to these estimates (similar to a p-value) and only accept those that exceed this value. This approach may explain why so many stock assessments for *Sebastes* assume proportionality between spawning biomass and egg production. This study illustrates why it is sometimes important to inform decisions based on the best available science rather than statistical tests of no change (Waples et al., 2008). Regarding relative fecundity as constant can overestimate the resiliency of stocks to fishing pressure, and is therefore not a precautionary choice for the null hypothesis.

The hierarchical modeling framework provides estimates that are similar to MLEs if the data are informative (e.g. *S. paucispinis*, Figures 43 and 44). Estimates obtained by maximum likelihood for other species suggest very rapid changes in

relative fecundity (e.g. *S. mystinus* and *S. proriger*; Table 13). Notice, however, that the data for *S. mystinus* are constrained to a small size range, and therefore extrapolation beyond this range is questionable. In the case of *S. proriger*, only two observations are available and suggest a negative relationship. One could choose to either remove these data sets from the analysis or pool information across species. The HLM framework allows us to retain the data, which even in the case of *S. proriger* provides information about the general scale of relative fecundity. The predicted parameters for each species differ from the population (species-wide) averages to an extent determined by the variability in the data and the size of the effect. In the case of *S. mystinus*, the extremely high slope parameter is shrunken toward the population mean, but retains a relatively high value. *S. proriger*, given the fact that only two observations are available, has parameter distributions almost identical to the posterior predictive distributions for a species not included in the analysis.

State dependent life history theory for growth and reproduction of Sebastes *spp.*

Predictions of the state dependent life history model I develop in Chapter 4 are qualitatively consistent with patterns of growth, reproduction, and maturity observed for rockfish. The inputs to this model are simple: a description of the dynamics of surplus energy, a relationship between length and weight, and a mortality schedule. It is important to note that the model does not pre-specify the

dynamics of somatic growth, characterize the timing of maturity, or define reproduction from an empirical fecundity-size relationship or as a fixed proportion of body mass. Rather, these features are emergent predictions of the model based on resource allocation decisions that maximize lifetime expected reproductive success.

I use stochastic dynamic programming to identify the resource allocation strategy that maximizes lifetime reproductive success for each time and length, conditioned on the inputs. This framework is well-suited for the purpose of evaluating alternative hypotheses about the mechanisms driving the pattern of increasing relative fecundity with size seen in rockfish.

Each model assumes there is a trade-off between reproduction and somatic growth, i.e. these processes compete directly for a finite supply of surplus energy. Empirical support for this trade-off has been reported in many studies across a wide range of organisms (Stearns, 1992). In contrast, the specification of the dynamics of surplus energy is rarely given much attention in studies of optimal resource allocation.

Miller et al. (2008) used an exponential production function to model resource allocation in an iteroparous cactus. Ware (1980) used an allometric production function (Equation 4.1) with an exponent of 0.98 (very similar to exponential growth) to develop a bioenergetic mechanism for the relationship between stock and recruitment in fish. Although this model can generate a graded response of optimal allocation as a function of size (Figure 50, panels A and B), and

increasing GSI with size (Figure 50A), forward simulation reveals that growth patterns associated with this hypothesis are inconsistent with patterns of growth after maturity observed in rockfishes (Figure 52A). The exponential production function combined with a concave reproduction relationship (Figure 52B) predicts growth after maturity, but maximum size is only constrained by the artificial limit of the maximum size category in the model, and GSI is predicted to decline under this set of assumptions (Figure 51B).

Empirical studies have shown that fish assimilate energy according to a power function of mass (Equation 4.1) with an exponent typically less than one (Cui, 1987, cited in Wooton, 1998). Many studies of optimal resource allocation adopt this functional form for total energy assimilation to represent surplus energy, defined as energy available for growth or reproduction after maintenance costs (e.g. Ware, 1980; Roff, 1983; Kozlowski, 1996).

The linear production function in terms of length (Equation 4.17) is equivalent to the allometric model in terms of mass (Equation 4.1, given an exponent value of 2/3). Post-maturation growth is predicted by this model when reproduction is a concave function of allocation (Figure 52D) and when mortality is a convex function of allocation (Figure 54C). The former case is not representative of rockfish data because GSI increases, then decreases with size (Figure 51D). The latter case is also inconsistent, in that allocation to reproduction only occurs at 80% of maximum length, which happens to be the length boundary (100cm). Slowing the

growth rate prevents the model from hitting the boundary (result not shown), but also predicts a delay in age at maturity beyond the already large value of 20 years (Figure 54C).

The exponential and linear production functions imply that surplus energy and therefore potential growth is unbounded for organisms that do not reproduce. This assumption is made in many resource allocation models (Ware, 1980; Myers and Doyle, 1983; Heino and Kaitala, 1996; Kozlowski, 1996; Gunderson, 1997; Miller et al., 2008). Instead, it seems reasonable to consider a model in which immature individuals can not grow without bound. This idea was the biological motivation for the von Bertalanffy (VB) growth equation: growth rate is a difference between assimilated energy and maintenance costs. Growth ceases when these two processes are balanced. If we adopt the VB growth function as a model for surplus energy (potential growth), then we can retain this interpretation for juveniles.

Surplus energy for mature individuals may be reduced relative to juveniles of the same size due to the cost of maintaining reproductive structures. The growth model of Stamps et al. (1998) (which I refer to simply as asymptotic production) fits this description if used to model surplus energy rather than somatic growth.

The asymptotic production function can produce somatic growth trajectories with and without growth after maturity, similar to the linear production function (Figure 52, panels E and F). Growth after maturity is selected when either reproduction is a concave function (Figure 52F) or mortality is a convex function

(Figure 54D). GSI, however, is asymptotic or slightly declines near the maximum size when reproduction is a concave function of allocation. The convex mortality function (hypothesis), combined with the asymptotic production function, is therefore the combination of assumptions that best matches the qualitative patterns seen in rockfishes of length at age, size and age at maturity, and GSI at length.

I have evaluated two mechanisms that result in growth after maturity: 1) a concave relationship between reproductive output and energy allocation to gonads, and 2) a convex relationship between natural mortality and energy allocation to gonads. Myers and Doyle (1983) consider biological mechanisms that motivate these relationships, which can be considered in the context of rockfish life histories. Although some mechanisms they consider may apply to rockfish, the predictions of the life history model (declining GSI) do not support this approach to maintaining post-maturation growth.

Sibly et al. (1985) examined the theory of trade-offs between mortality and reproduction leading to growth after maturity. Myers and Doyle (1983) suggested possible biological mechanisms including increased predation with increasing reproductive effort or an increased susceptibility to disease. Empirical evidence of a reproduction-survival trade-off is less conclusive than the trade-off between reproduction and growth (Stearns, 1992). Gunderson (1997) showed a correlation between GSI and the natural mortality rate in a study of several fish species.

However, the support for this pattern was less strong among viviparous species (including several *Sebastes* spp.).

Other hypotheses have been suggested regarding mechanisms that select for growth after maturity (Heino and Kaitala, 1999). There is empirical support for seasonal switching between growth and reproduction for species in highly seasonal environments (e.g. pike and sticklebacks) (Wooton, 1999). Kozlowski and Uchmanski (1987) found post-maturation growth to be optimal in a two-season model in which growth and/or reproduction occur during the first season, and no growth or reproduction occurs during the second. Growth after maturity is optimal under this model if the length of the season during which growth occurs decreases with age. Rockfish may experience seasonal changes in food abundance associated with oceanographic conditions (e.g. upwelling). The allocation model of Lester et al. (2004) also required a seasonal strategy to produce post-maturation growth. However, their model fixes allocation to growth at a constant proportion. The data presented in Chapter 2 and the hierarchical models from Chapter 3 suggest that GSI is not always constant for rockfish, but increases with size in many species. They show that the constant allocation assumption generates VB somatic growth after maturity.

Many studies of optimal resource allocation and age at maturity assume that the gonadosomatic index (GSI) is a constant fraction of body weight (Roff, 1983; Day and Taylor, 1997; Lester et al., 2004). If the number and mass of eggs does not

change, this is equivalent to a constant number of eggs produced per gram. This assumption appears to be appropriate for some fish species (Raitt, 1933; Simpson, 1951), but not for many rockfish species (Boehlert *et al.*, 1982; Haldorson and Love, 1991; analyses in Ch. 1 and Ch. 2, this study). For this reason, predictions regarding the relationship between GSI and size are an important diagnostic for identifying reasonable model of rockfish life history. Models that assume a constant GSI should not be considered for analysis of resource allocation in rockfishes.

The life history model I develop predicts an increase in reproductive effort with size. Apart from an increase in relative fecundity, rockfish larvae from older females are thought to have better survival capabilities. This sequential optimization of egg number and size (quality) seems to contradict predictions of life history theory (Svardson, 1949) and deserves further study.

I evaluated how model predictions (based on the asymptotic production model with convex mortality) change in relation to different baseline mortality rates (parameter m_0, Table 18). Maximum size is an emergent property of the model, as opposed to a model input, and varies with the strength of mortality risk (Table 19). Beverton and Holt (1959) were among the first to identify this pattern among fish species. Another intuitive result is a decrease in age (and length) at maturity with increasing natural mortality. If the probability of surviving decreases, then it is optimal to mature earlier and begin reproducing. The ratio of length at maturity to maximum length (0.56 – 0.71) is consistent with the findings of Beverton (1992),

who reported a range of values from 0.66 to 0.82 for Pacific *Sebastes*. GSI is also positively correlated with mortality, as observed by Gunderson (1997).

These diagnostic tests show that the asymptotic model with the convex mortality function has predictions that respond to changing mortality in a way that is consistent with empirical observations and life history theory. Of the models I consider in this analysis, this is the best supported hypothesis for the presence of increasing relative fecundity with size given the presence of growth after maturity and realistic ratios of size at maturity to maximum size.

The life history models I evaluate in this study do not include the effects of fishing. There is experimental evidence that fishing may act as a selective force on heritable traits in some fish populations (Conover and Munch, 2002), but the extent to which this occurs in wild populations is unclear. The time scale of significant exploitation of rockfishes (decades or perhaps a century) is small relative to the estimated temporal scale of evolution (Hyde and Vetter, 2007). Therefore, mortality associated with fishing is unlikely to affect predictions of evolutionary outcomes from the state dependent models.

TABLES

Table 1. Fecundity models used in recent rockfish stock assessments from the U.S. west coast. W = weight, L = length, and C = assumed constant number of eggs per unit weight of female spawning biomass. Units vary among assessments. Parameters a and b are estimated separately for each assessment, but treated as fixed values.

species	assessment year	fecundity model
S. alutus	2007	Eggs/W = C
S. carnatus	2005	Eggs/W = C
S. crameri	2007	$Eggs = aW + bW^2$
S. entomelas	2007	Eggs = a + bW
S. flavidus	2005	Eggs/W = C
S. goodei	2007	Eggs/W = C
S. jordani	2007	Eggs/W = C
S. levis	2007	Eggs/W = C
S. melanops (CA & OR)	2007	Eggs/W = a + bW
S. melanops (north)	2007	Eggs/W = a + bW
S. melanostomus	2005	Eggs/W = C
S. miniatus	2005	Eggs/W = C
S. mystinus	2007	Eggs/W = a + bW
S. paucispinis	2007	Eggs/W = a + bW
S. pinniger	2007	Eggs/W = C
S. ruberrimis	2007	Eggs/W = C
S. rufus	2000	$Eggs = aL^b$

Table 2. Species and data sources. If sample sizes recovered from digitized sources differed from the reported sample size, the recovered sample size is noted in parentheses. If measured weights of individual fish were not provided, round weight was predicted from published weight-length relationships (from the same region if available).

species	common name	source	sample size (recovered)	region(s)	digitized	weight data
S. alutus	pacific ocean perch	Gunderson (1976)	79	WA-OR, Queen Charlotte Sound		predicted
		Westrheim (1958)	13	OR		predicted
S. atrovirens	kelp rockfish	MacGregor (1970)	2	CA, S.		measured
		Romero (1988)	68 (67)	CA, N.	Yes	predicted
		Sogard et al. (2008)	17	CA, N.		measured
S. auriculatus	brown rockfish	DeLacy et al. (1964)	35	WA		measured
S. babcocki	redbanded rockfish	Snytko and Borets (1973)	13	Vancouver-OR		predicted
S. brevispinis	silvergray rockfish	Snytko and Borets (1973)	8	Vancouver-OR		predicted
		Stanley and Kronlund (2005)	126	British Columbia		measured
S. carnatus	gopher rockfish	MacGregor (1970)	4	CA, S.		measured
		Sogard et al. (2008)	12	CA, N.		measured
S. caurinus	copper rockfish	DeLacy et al. (1964)	33	WA		measured
		Ito (1977)	23	WA		measured
		Richards and Emmett (1988)	21	British Columbia		measured
S. chlorostictus	greenspotted rockfish	NOAA Fisheries (SWFSC/FED)	47	CA, N.		measured
		Love et al. (1990)	16	CA, S.	Yes	predicted
S. constellatus	starry rockfish	Love et al. (1990)	21	CA, S.	Yes	predicted
		MacGregor (1970)	5	CA, S.		measured
S. crameri	darkblotched rockfish	Nichol and Pikitch (1994)	43	OR		combination
		Phillips (1964)	12	CA (statewide)		predicted
		Snytko and Borets (1973)	5	Vancouver-OR		predicted
S. dalli	calico rockfish	Love et al. (1990)	23	CA, S.	Yes	predicted
S. diploproa	splitnose rockfish	Phillips (1964)	15	CA (statewide)		predicted
		Snytko and Borets (1973)	1	Vancouver-OR		predicted
S. elongatus	greenstriped rockfish	Love et al. (1990)	25	CA, S.	Yes	predicted
		Snytko and Borets (1973)	8	Vancouver-OR		predicted
S. emphaeus	puget sound rockfish	Moulton (1975)	5	WA		measured
S. ensifer	swordspine rockfish	Love et al. (1990)	2	CA, S.	Yes	predicted
S. entomelas	widow rockfish	Love et al. (1990)	27	CA, S.	Yes	predicted
		Phillips (1964)	20	CA (statewide)		predicted
		Snytko and Borets (1973)	2	Vancouver-OR		predicted
		Sogard et al. (in prep.)	18	CA, N.		measured
S. flavidus	yellowtail rockfish	Eldridge et al. (1991)	126	CA, N.		measured
		Love et al. (1990)	34	CA, S.	Yes	predicted
		Phillips (1964)	15	CA (statewide)		predicted
		Snytko and Borets (1973)	2	Vancouver-OR		predicted
		Sogard et al. (2008)	19	CA, N.		measured
		Sogard et al. (in prep.)	50	CA, N.		measured

Table 2 (continued). Species and data sources. If sample sizes recovered from digitized sources differed from the reported sample size, the recovered sample size is noted in parentheses. If measured weights of individual fish were not provided, round weight was predicted from published weight-length relationships (from the same region if available).

species	common name	source	sample size (recovered)	region(s)	digitized	weight data
S. goodei	chilipepper	Love et al. (1990)	37 (39)	CA, S.	Yes	predicted
		Phillips (1964)	23	CA (statewide)		predicted
		Sogard et al. (in prep.)	112	CA, N.		measured
S. helvomaculatus	rosethorn rockfish	Snytko and Borets (1973)	4	Vancouver-OR		predicted
S. hopkinsi	squarespot rockfish	Love et al. (1990)	39	CA, S.	Yes	predicted
S. jordani	shortbelly rockfish	Phillips (1964)	10	CA (statewide)		predicted
S. levis	cowcod	Love et al. (1990)	27	CA, S.	Yes	predicted
S. maliger	quillback rockfish	Richards and Emmett (1988)	253	British Columbia		measured
S. melanops	black rockfish	Wallace et al. (unpublished)	38	WA		measured
S. melanostomus	blackgill rockfish	Love et al. (1990)	2	CA, S.	Yes	predicted
S. miniatus	vermilion rockfish	Love et al. (1990)	45 (46)	CA, S.	Yes	predicted
		Phillips (1964)	12	CA (statewide)		predicted
S. mystinus	blue rockfish	Sogard et al. (2008)	17	CA, N.		measured
S. norvegicus	golden redfish	Corlett (1964)	26	Atlantic (East Greenland)		predicted
S. ovalis	speckled rockfish	Love et al. (1990)	2	CA, S.	Yes	predicted
		MacGregor (1970)	5	CA, S.		measured
S. paucispinis	bocaccio	Love et al. (1990)	52	CA, S.	Yes	predicted
		MacGregor (1970)	13	CA, S.		measured
		Phillips (1964)	24	CA (statewide)		predicted
		Ralston and MacFarlane (in prep.)	10	Northern Baja, Mexico		measured
		Snytko and Borets (1973)	4	Vancouver-OR		predicted
S. pinniger	canary rockfish	Fraser (1923)	1	British Columbia		measured
		Phillips (1964)	10	CA (statewide)		predicted
S. proriger	redstripe rockfish	Snytko and Borets (1973)	2	Vancouver-OR		predicted
S. rastrelliger	grass rockfish	Love and Johnson (1998)	8	CA, S.		predicted
S. rosaceus	rosy rockfish	Love et al. (1990)	23	CA, S.	Yes	predicted
		MacGregor (1970)	7	CA, S.		measured
S. rosenblatti	greenblotched rockfish	Love et al. (1990)	26	CA, S.	Yes	predicted
S. ruberrimus	yelloweye rockfish	Clemens (1949)	1	British Columbia		measured
		MacGregor (1970)	2	CA, S.		measured
S. rufus	bank (red-widow) rockfish	Love et al. (1990)	27	CA, S.	Yes	predicted
S. saxicola	stripetail rockfish	Love et al. (1990)	33 (31)	CA, S.	Yes	predicted
		Phillips (1964)	13	CA (statewide)		predicted
S. semicinctus	halfbanded rockfish	Love et al. (1990)	46	CA, S.	Yes	predicted
S. serranoides	olive rockfish	Love and Westphal (1981)	83	CA, N.	Yes	predicted
		MacGregor (1970)	1	CA, S.		measured
		Sogard et al. (2008)	7	CA, N.		measured
S. serriceps	treefish	MacGregor (1970)	1	CA, S.		measured

Table 3. Estimates of length at 50% maturity by species and region. All lengths are from Haldorson and Love (1991), except as indicated. The estimate for *S. emphaeus* is the mid-point of values presented in Love *et al*. (2002), and the estimate for *S. ensifer* is a length at which a few individuals are known to be mature (Love *et al*., 2002).

species	length 50% mat.	region	source (if different)
S. alutus	26	CA_N	
S. alutus	30	GOA	
S. alutus	36	WA_OR	
S. alutus	37	BC	
S. alutus	38	BC	
S. atrovirens	17	CA_N	Romero, 1988
S. auriculatus	26	CA_S	Love & Johnson, 1998
S. auriculatus	31	CA_N	
S. babcocki	34	CA_N	
S. babcocki	43	BC	
S. brevispinis	46	BC	
S. carnatus	17	CA_N	
S. carnatus	24	CA_S	Love & Johnson, 1998
S. caurinus	34	CA_N	
S. chlorostictus	22	CA_S	
S. chlorostictus	28	CA_N	
S. constellatus	22	CA_S	
S. constellatus	27	CA_N	
S. crameri	27	CA_N	
S. crameri	39	OR_WA	
S. dalli	9	CA_S	
S. diploproa	19	CA_N	
S. diploproa	28	BC	
S. elongatus	19	CA_S	
S. elongatus	23	CA_N	
S. elongatus	24	OR_WA	
S. elongatus	35	CA_S	
S. elongatus	37	CA_N	
S. elongatus	38	WA_OR	
S. elongatus	41	BC	
S. emphaeus	12	WA_OR	Love et al., 2002
S. ensifer	11	CA	Love et al., 2002
S. flavidus	36	CA_S	
S. flavidus	36	CA_N	
S. flavidus	43	BC	
S. flavidus	43	BC	
S. flavidus	46	WA_OR	
S. goodei	30	CA_S	
S. goodei	34	CA_N	
S. goodei	39	OR_WA	
S. helvomaculatus	21	BC	
S. helvomaculatus	23	CA_N	
S. hopkinsi	14	CA_S	
S. hopkinsi	18	CA_N	
S. jordani	14	CA_N	
S. jordani	16	CA_S	
S. levis	32	CA_N	
S. levis	43	CA_S	
S. melanostomus	34	CA_S	
S. melanostomus	35	CA_N	
S. miniatus	37	CA_S	
S. miniatus	37	CA_N	
S. mystinus	27	CA_N	
S. mystinus	29	CA_N	
S. norvegicus	41	ATL	
S. norvegicus	43	ATL	
S. ovalis	25	CA_S	
S. ovalis	28	CA_N	
S. paucispinis	36	CA_S	
S. paucispinis	48	CA_N	
S. paucispinis	50	CA_N	
S. pinniger	44	CA_N	
S. pinniger	51	BC	
S. pinniger	52	OR_WA	
S. proriger	30	BC	
S. rosaceus	15	CA_S	
S. rosaceus	20	CA_N	
S. rosenblatti	28	CA_S	
S. rubberimus	40	CA_N	
S. rubberimus	52	BC	
S. rufus	34	CA_N	
S. rufus	36	CA_S	
S. saxicola	10	CA_S	
S. saxicola	16	CA_N	
S. semicinctus	11	CA_S	
S. serranoides	34	CA_N	
S. serriceps	20	CA_S	Colton & Larson, 2007

Table 4. Comparison of AIC differences (Δ-AIC) for six models of absolute fecundity. Analyses were restricted to species with at least 30 observations from a single study, with measured weights and lengths. F = absolute fecundity [eggs], L = total length [mm], W = total body weight [g], stage = gonad stage (categorical variable), error term (e) is distributed $N(0, \sigma^2)$. Models 3 and 6 include the logarithm of weight as an offset term.

Model #	Description
1	log(F) = log(a) + b*log(L) + e
2	log(F) = log(a) + b*log(W) + e
3	log(F) = log(W) + log(a) + b*log(L) + e
4	log(F) = log(a) + b*log(L) + stage + e
5	log(F) = log(a) + b*log(W) + stage + e
6	log(F) = log(W) + log(a) + b*log(L) + stage + e

				Model					
Sci. name	**Common name**	**Source**	**n**	1	2	3	4	5	6
S. flavidus	yellowtail rockfish	Eldridge et al. 1991	126	48.92	14.60	21.36	44.80	**0**	11.34
S. flavidus	yellowtail rockfish	Sogard et al. (in prep)	50	16.17	8.37	10.18	12.06	**0**	3.69
S. melanops	black rockfish	Wallace et al. (unpublished)	38	15.37	**0**	3.31	16.63	0.05	4.03
S. goodei	chilipepper rockfish	Sogard et al. (in prep)	112	5.37	**0**	0.19	7.22	0.56	1.27
S. brevispinis	silvergrey rockfish	Stanley and Kronlund, 2005	126	20.35	**0**	1.75	na	na	na
S. chlorostictus	greenspotted rockfish	NMFS GF Ecology program	47	18.57	1.34	**0**	na	na	na
S. maliger	quillback rockfish	Richards and Emmett, 1988	253	47.61	**0**	3.83	na	na	na
S. auriculatus	brown rockfish	DeLacy et al., 1964	35	8.04	**0**	0.03	na	na	na
S. caurinus	copper rockfish	DeLacy et al., 1964	33	2.23	0.87	**0**	na	na	na

Table 5. Maximum likelihood estimates and 95% confidence intervals of the exponent parameter from allometric fecundity-weight models (no stage effect). Values greater than one indicate that relative fecundity increases with size.

Sci. name	Common name	Source	n	2.5%	MLE	97.5%
S. flavidus	yellowtail rockfish	Eldridge et al. 1991	126	1.58	1.73	1.89
S. flavidus	yellowtail rockfish	Sogard et al. (in prep)	50	1.44	1.79	2.14
S. melanops	black rockfish	Wallace et al. (unpublished)	38	1.27	1.61	1.95
S. goodei	chilipepper rockfish	Sogard et al. (in prep)	112	1.14	1.42	1.69
S. brevispinis	silvergrey rockfish	Stanley and Kronlund, 2005	126	1.13	1.26	1.38
S. chlorostictus	greenspotted rockfish	NMFS GF Ecology program	47	1.33	1.54	1.75
S. maliger	quillback rockfish	Richards and Emmett, 1988	253	1.19	1.29	1.40
S. auriculatus	brown rockfish	DeLacy et al., 1964	35	0.86	1.04	1.22
S. caurinus	copper rockfish	DeLacy et al., 1964	33	1.50	1.69	1.88

Table 6. Regression analysis results from the allometric fecundity-length model for yellowtail rockfish (*S. flavidus*).

```
Coefficients:
             Estimate Std. Error t value Pr(>|t|)
(Intercept) -15.32759    1.63559  -9.371 4.47e-16 ***
log(length)   4.65510    0.26377  17.648  < 2e-16 ***
stage        -0.16904    0.06833  -2.474   0.0147 *
---
Signif. codes:  0 ‘***’ 0.001 ‘**’ 0.01 ‘*’ 0.05 ‘.’ 0.1 ‘ ’ 1

Residual standard error: 0.3058 on 123 degrees of freedom
Multiple R-squared: 0.7358,     Adjusted R-squared: 0.7315
F-statistic: 171.2 on 2 and 123 DF,  p-value: < 2.2e-16
```

AIC
63.992

Table 7. Regression analysis results from the allometric fecundity-length model for yellowtail rockfish (*S. flavidus*). Including weight as an offset term is equivalent to modeling eggs per gram total body weight (relative fecundity).

```
Coefficients:
            Estimate Std. Error t value Pr(>|t|)
(Intercept) -5.45120    1.43223  -3.806 0.000221 ***
log(length)  1.88243    0.23097   8.150 3.50e-13 ***
stage       -0.20996    0.05984  -3.509 0.000629 ***
---
Signif. codes:  0 ‘***’ 0.001 ‘**’ 0.01 ‘*’ 0.05 ‘.’ 0.1 ‘ ’ 1

Residual standard error: 0.2678 on 123 degrees of freedom
Multiple R-squared: 0.7889,     Adjusted R-squared: 0.7855
F-statistic: 229.8 on 2 and 123 DF,  p-value: < 2.2e-16
```

AIC
30.535

Table 8. Regression analysis results from the allometric fecundity-weight model for yellowtail rockfish (*S. flavidus*).

```
Coefficients:
            Estimate Std. Error t value Pr(>|t|)
(Intercept)  0.86429    0.55051   1.570    0.119
log(weight)  1.70002    0.07626  22.293  < 2e-16 ***
stage2      -0.23602    0.05671  -4.162 5.87e-05 ***
---
Signif. codes:  0 ‘***’ 0.001 ‘**’ 0.01 ‘*’ 0.05 ‘.’ 0.1 ‘ ’ 1

Residual standard error: 0.256 on 123 degrees of freedom
Multiple R-squared: 0.8148,     Adjusted R-squared: 0.8118
F-statistic: 270.6 on 2 and 123 DF,  p-value: < 2.2e-16
```

AIC

19.1945

Table 9. Regression analysis of relative fecundity as a linear function of weight for yellowtail rockfish (*S. flavidus*).

```
Coefficients:
             Estimate Std. Error t value Pr(>|t|)
(Intercept) 245.28796   36.29659   6.758 4.98e-10 ***
weight        0.15027    0.01895   7.928 1.15e-12 ***
stage       -72.67953   18.22823  -3.987 0.000114 ***
---
Signif. codes:  0 ‘***’ 0.001 ‘**’ 0.01 ‘*’ 0.05 ‘.’ 0.1 ‘ ’ 1

Residual standard error: 82.58 on 123 degrees of freedom
Multiple R-squared: 0.4054,     Adjusted R-squared: 0.3957
F-statistic: 41.93 on 2 and 123 DF,  p-value: 1.301e-14
```

Table 10. MLE, posterior mean, and percentiles of posterior slope distributions for each species in the 2-level hierarchical model for relative fecundity as a linear function of weight, $\Phi/W = a + bW$. Estimates based on 500,000 samples.

			percentiles of marginal posterior distribution				
	MLE	**mean**	**2.5%**	**25%**	**50%**	**75%**	**97.5%**
S.alutus	0.0825	0.0691	-0.0130	0.0407	0.0687	0.0975	0.1552
S.atrovirens	0.0821	0.0623	-0.0455	0.0265	0.0618	0.0974	0.1749
S.auriculatus	0.0020	0.0261	-0.0537	0.0002	0.0269	0.0531	0.1032
S.babcocki	0.0030	0.0348	-0.0600	0.0046	0.0361	0.0666	0.1262
S.brevispinis	0.0318	0.0337	0.0023	0.0230	0.0338	0.0446	0.0652
S.carnatus	-0.0908	0.0475	-0.0774	0.0089	0.0482	0.0869	0.1718
S.caurinus	0.0375	0.0403	-0.0037	0.0254	0.0405	0.0554	0.0842
S.chlorostictus	0.2791	0.1367	0.0374	0.0977	0.1328	0.1715	0.2552
S.constellatus	0.0856	0.0593	-0.0596	0.0206	0.0588	0.0977	0.1836
S.crameri	0.0412	0.0447	-0.0099	0.0261	0.0448	0.0634	0.0990
S.dalli	1.3184	0.0575	-0.0707	0.0165	0.0568	0.0974	0.1893
S.diploproa	0.1762	0.0743	-0.0375	0.0357	0.0725	0.1111	0.1981
S.elongatus	0.1049	0.0639	-0.0489	0.0265	0.0633	0.1015	0.1848
S.emphaeus	6.5971	0.0581	-0.0687	0.0178	0.0576	0.0983	0.1915
S.ensifer	1.7370	0.0573	-0.0719	0.0170	0.0571	0.0976	0.1901
S.entomelas	-0.0175	0.0020	-0.0584	-0.0179	0.0026	0.0224	0.0604
S.flavidus	0.1725	0.1531	0.1052	0.1365	0.1529	0.1696	0.2016
S.goodei	0.0108	0.0174	-0.0255	0.0028	0.0175	0.0321	0.0594
S.helvomaculatus	1.2816	0.0639	-0.0606	0.0231	0.0628	0.1033	0.1975
S.hopkinsi	-0.1531	0.0550	-0.0734	0.0154	0.0552	0.0955	0.1858
S.jordani	0.1002	0.0576	-0.0705	0.0173	0.0570	0.0976	0.1891
S.levis	-0.0015	0.0027	-0.0272	-0.0075	0.0027	0.0129	0.0323
S.maliger	0.0564	0.0564	0.0076	0.0398	0.0565	0.0731	0.1051
S.melanops	0.1631	0.0956	0.0019	0.0618	0.0941	0.1277	0.2002
S.melanostomus	0.1843	0.0705	-0.0458	0.0316	0.0686	0.1079	0.1971
S.miniatus	0.0893	0.0854	0.0474	0.0724	0.0854	0.0985	0.1237
S.mystinus	1.2203	0.0901	-0.0299	0.0463	0.0861	0.1291	0.2349
S.norvegicus	0.0014	0.0120	-0.0379	-0.0048	0.0125	0.0295	0.0622
S.ovalis	-0.1575	0.0366	-0.0904	-0.0009	0.0384	0.0762	0.1548
S.paucispinis	0.0488	0.0492	0.0233	0.0404	0.0493	0.0581	0.0752
S.pinniger	0.0017	0.0214	-0.0497	-0.0024	0.0217	0.0450	0.0894
S.proriger	-1.5616	0.0544	-0.0747	0.0142	0.0545	0.0946	0.1850
S.rastrelliger	0.0306	0.0473	-0.0502	0.0155	0.0478	0.0795	0.1445
S.rosaceus	0.0518	0.0571	-0.0703	0.0169	0.0565	0.0965	0.1874
S.rosenblatti	0.0488	0.0532	-0.0337	0.0238	0.0530	0.0823	0.1411
S.ruberrimus	-0.0396	0.0352	-0.0777	0.0003	0.0365	0.0713	0.1418
S.rufus	0.0527	0.0551	-0.0405	0.0236	0.0551	0.0874	0.1532
S.saxicola	0.3340	0.0905	-0.0238	0.0491	0.0868	0.1278	0.2231
S.semicinctus	1.1903	0.0597	-0.0672	0.0187	0.0586	0.0993	0.1921
S.serranoides	0.1190	0.0942	0.0218	0.0684	0.0934	0.1192	0.1704

Table 11. MLE, posterior mean, and percentiles of posterior intercept distributions (original scale) for each species in the 2-level hierarchical model for relative fecundity as a linear function of weight, $\Phi/W = a + bW$. Estimates of posterior distributions based on 500,000 samples.

			percentiles of marginal posterior distribution				
	MLE	**mean**	**2.5%**	**25%**	**50%**	**75%**	**97.5%**
S.alutus	109.2	50.3	-33.0	22.5	50.6	78.0	130.0
S.atrovirens	299.9	274.6	221.7	257.0	274.6	292.2	326.3
S.auriculatus	138.7	111.2	-1.9	71.6	110.3	149.6	227.8
S.babcocki	391.5	279.5	22.3	189.8	276.6	364.9	545.5
S.brevispinis	363.7	267.1	175.0	235.2	267.0	298.6	358.6
S.carnatus	209.9	193.9	105.0	163.3	193.5	223.5	283.1
S.caurinus	192.8	142.9	78.2	120.5	142.7	164.8	208.0
S.chlorostictus	309.6	232.4	158.5	209.7	234.0	256.9	298.0
S.constellatus	263.8	237.1	160.9	211.7	237.2	262.7	312.4
S.crameri	149.4	101.0	27.8	75.9	101.1	126.4	173.9
S.dalli	223.9	225.7	169.3	206.3	225.5	244.7	281.4
S.diploproa	282.0	237.5	141.1	205.9	238.1	269.5	329.5
S.elongatus	398.6	371.1	312.0	350.8	371.2	391.0	429.4
S.emphaeus	547.8	459.4	350.1	421.1	458.7	496.9	570.3
S.ensifer	219.4	237.4	98.1	189.4	237.6	284.4	375.3
S.entomelas	289.9	286.5	203.9	257.8	286.2	315.1	371.8
S.flavidus	336.4	128.3	60.2	105.1	128.5	151.8	195.8
S.goodei	150.5	130.7	74.8	111.4	130.6	149.9	187.0
S.helvomaculatus	342.0	300.1	183.4	259.1	299.4	340.3	417.8
S.hopkinsi	178.8	177.5	131.9	161.8	177.5	193.3	223.3
S.jordani	126.9	139.9	54.0	110.3	139.9	169.2	224.8
S.levis	226.9	217.8	72.5	167.5	217.6	268.3	364.0
S.maliger	252.7	196.2	144.4	178.2	196.0	214.0	248.2
S.melanops	409.5	272.9	125.3	226.8	274.7	321.0	407.8
S.melanostomus	252.7	148.4	-94.1	70.1	150.4	227.0	378.8
S.miniatus	335.5	115.7	12.3	80.2	115.5	151.1	219.1
S.mystinus	232.9	197.7	109.0	169.2	198.3	227.0	281.2
S.norvegicus	42.6	36.9	-95.4	-9.0	35.8	80.9	169.3
S.ovalis	153.3	151.0	18.1	105.3	150.7	196.0	288.0
S.paucispinis	301.9	192.7	129.6	171.0	192.5	214.2	256.1
S.pinniger	346.2	262.5	29.6	181.3	261.9	344.3	505.8
S.proriger	558.2	373.1	209.1	316.4	372.4	428.6	540.0
S.rastrelliger	271.1	213.2	66.5	162.7	212.4	262.5	359.1
S.rosaceus	296.6	286.1	233.0	267.9	286.0	304.3	339.1
S.rosenblatti	241.4	173.1	46.0	130.3	173.2	215.6	299.0
S.ruberrimus	306.8	141.9	-318.1	-13.4	137.9	293.6	626.3
S.rufus	239.3	174.0	44.1	130.5	173.8	217.0	302.0
S.saxicola	408.8	388.3	342.4	372.7	388.3	403.9	433.4
S.semicinctus	307.4	301.9	260.6	287.7	301.8	316.0	343.3
S.serranoides	214.0	124.3	45.7	98.4	125.0	151.3	200.5

Table 12. Species ranked by posterior probability that the slope parameter is greater than zero, based on the 2-level relative fecundity model, $\Phi/W = a + bW$.

S.flavidus	100%
S.miniatus	100%
S.paucispinis	100%
S.chlorostictus	100%
S.serranoides	99%
S.maliger	99%
S.brevispinis	98%
S.melanops	98%
S.caurinus	96%
S.alutus	95%
S.crameri	95%
S.saxicola	94%
S.mystinus	93%
S.diploproa	91%
S.melanostomus	89%
S.rosenblatti	89%
S.atrovirens	88%
S.rufus	87%
S.elongatus	87%
S.helvomaculatus	85%
S.constellatus	85%
S.rastrelliger	84%
S.semicinctus	84%
S.emphaeus	83%
S.rosaceus	83%
S.dalli	83%
S.jordani	83%
S.ensifer	83%
S.hopkinsi	82%
S.proriger	81%
S.carnatus	79%
S.goodei	79%
S.babcocki	78%
S.auriculatus	75%
S.ruberrimus	75%
S.ovalis	74%
S.pinniger	73%
S.norvegicus	68%
S.levis	57%
S.entomelas	53%

Table 13. MLE, posterior mean, and percentiles of posterior slope distributions for each species in the 2-level hierarchical model for absolute fecundity as an allometric function of weight, $\log(\Phi) = \log(c) + d\log(W)$. Estimates of posterior distributions based on 500,000 samples.

			percentiles of marginal posterior distribution				
	MLE	**post.mean**	**2.5%**	**25%**	**50%**	**75%**	**97.5%**
S.alutus	1.754	1.439	0.864	1.245	1.428	1.622	2.072
S.atrovirens	1.174	1.277	0.764	1.120	1.283	1.440	1.760
S.auriculatus	1.037	1.294	0.643	1.104	1.301	1.490	1.907
S.babcocki	1.002	1.337	0.611	1.129	1.339	1.547	2.048
S.brevispinis	1.392	1.361	0.821	1.188	1.360	1.532	1.905
S.carnatus	0.764	1.305	0.589	1.102	1.311	1.516	1.981
S.caurinus	1.344	1.345	0.934	1.209	1.345	1.480	1.754
S.chlorostictus	1.546	1.414	0.895	1.240	1.408	1.583	1.963
S.constellatus	1.196	1.328	0.662	1.129	1.331	1.529	1.984
S.crameri	1.555	1.410	0.876	1.231	1.402	1.582	1.981
S.dalli	1.215	1.337	0.632	1.130	1.337	1.545	2.036
S.diploproa	1.491	1.369	0.744	1.175	1.366	1.560	2.009
S.elongatus	1.122	1.267	0.718	1.100	1.276	1.441	1.779
S.emphaeus	1.606	1.348	0.627	1.140	1.347	1.558	2.070
S.ensifer	1.960	1.345	0.611	1.133	1.347	1.556	2.072
S.entomelas	1.071	1.260	0.685	1.087	1.268	1.442	1.793
S.flavidus	1.787	1.546	1.094	1.380	1.534	1.701	2.055
S.goodei	1.200	1.278	0.803	1.128	1.283	1.431	1.733
S.helvomaculatus	1.843	1.363	0.660	1.153	1.360	1.569	2.080
S.hopkinsi	0.926	1.301	0.619	1.104	1.309	1.505	1.955
S.jordani	1.049	1.312	0.627	1.114	1.318	1.514	1.963
S.levis	1.032	1.284	0.635	1.097	1.293	1.482	1.887
S.maliger	1.282	1.311	0.884	1.173	1.313	1.452	1.729
S.melanops	1.607	1.365	0.683	1.161	1.361	1.566	2.060
S.melanostomus	2.178	1.356	0.633	1.145	1.354	1.564	2.085
S.miniatus	1.819	1.480	0.942	1.292	1.468	1.655	2.086
S.mystinus	2.518	1.388	0.701	1.175	1.380	1.592	2.115
S.norvegicus	1.142	1.320	0.646	1.121	1.325	1.523	1.970
S.ovalis	0.382	1.290	0.555	1.087	1.300	1.502	1.962
S.paucispinis	1.468	1.405	0.963	1.256	1.401	1.551	1.860
S.pinniger	1.316	1.344	0.634	1.135	1.344	1.554	2.057
S.proriger	-0.779	1.343	0.606	1.130	1.344	1.557	2.072
S.rastrelliger	1.089	1.307	0.642	1.113	1.313	1.507	1.946
S.rosaceus	0.988	1.271	0.632	1.085	1.282	1.467	1.858
S.rosenblatti	1.353	1.346	0.701	1.150	1.346	1.541	1.992
S.ruberrimus	0.477	1.340	0.596	1.129	1.340	1.553	2.075
S.rufus	1.319	1.341	0.674	1.142	1.340	1.542	2.001
S.saxicola	1.177	1.238	0.868	1.116	1.241	1.363	1.594
S.semicinctus	1.338	1.342	0.703	1.148	1.342	1.535	1.982
S.serranoides	1.714	1.467	0.945	1.287	1.455	1.636	2.041

Table 14. MLE, posterior mean, and percentiles of posterior intercept distributions (log scale) for each species in the 2-level hierarchical model for absolute fecundity as an allometric function of weight, $\log(\Phi) = \log(c) + d\log(W)$. Estimates of posterior distributions based on 500,000 samples.

			percentiles of marginal posterior distribution				
	MLE	**post.mean**	**2.5%**	**25%**	**50%**	**75%**	**97.5%**
S.alutus	-0.486	1.657	-2.639	0.409	1.728	2.970	5.562
S.atrovirens	4.607	4.008	1.143	3.040	3.975	4.942	7.044
S.auriculatus	4.656	2.813	-1.604	1.392	2.761	4.187	7.487
S.babcocki	5.884	3.030	-2.596	1.352	3.016	4.691	8.778
S.brevispinis	2.758	2.982	-1.315	1.625	2.993	4.351	7.240
S.carnatus	6.748	3.472	-0.745	2.145	3.431	4.741	7.910
S.caurinus	2.785	2.773	-0.104	1.816	2.770	3.729	5.659
S.chlorostictus	2.267	3.091	-0.346	2.030	3.130	4.185	6.356
S.constellatus	4.317	3.537	-0.480	2.299	3.519	4.767	7.620
S.crameri	1.027	2.040	-1.945	0.831	2.091	3.290	5.773
S.dalli	4.604	4.367	1.772	3.577	4.361	5.147	6.987
S.diploproa	2.524	3.290	-0.766	2.070	3.304	4.536	7.248
S.elongatus	5.258	4.478	1.597	3.497	4.431	5.422	7.555
S.emphaeus	3.840	5.278	2.151	4.324	5.281	6.234	8.400
S.ensifer	0.782	4.518	0.727	3.344	4.515	5.689	8.331
S.entomelas	5.071	3.707	-0.089	2.418	3.650	4.947	7.798
S.flavidus	0.107	1.828	-1.836	0.709	1.916	3.016	5.074
S.goodei	3.562	3.013	-0.198	1.927	2.980	4.076	6.372
S.helvomaculatus	1.199	4.022	-0.060	2.797	4.041	5.265	8.015
S.hopkinsi	5.513	3.849	0.766	2.880	3.816	4.788	7.078
S.jordani	4.560	3.432	-0.102	2.303	3.401	4.531	7.143
S.levis	5.131	2.916	-2.127	1.255	2.839	4.497	8.376
S.maliger	3.557	3.351	0.486	2.384	3.337	4.306	6.288
S.melanops	1.622	3.309	-1.697	1.858	3.337	4.783	8.213
S.melanostomus	-3.168	2.469	-3.078	0.824	2.479	4.128	7.958
S.miniatus	-0.634	1.949	-2.766	0.585	2.047	3.421	6.150
S.mystinus	-3.965	2.934	-1.532	1.655	2.984	4.250	7.150
S.norvegicus	2.521	1.199	-3.831	-0.381	1.159	2.745	6.400
S.ovalis	9.041	3.108	-1.447	1.647	3.046	4.501	8.059
S.paucispinis	2.066	2.526	-0.949	1.415	2.548	3.664	5.878
S.pinniger	3.225	2.729	-3.085	1.012	2.727	4.448	8.498
S.proriger	17.768	3.721	-1.234	2.225	3.711	5.214	8.707
S.rastrelliger	4.969	3.357	-1.174	1.926	3.328	4.747	8.077
S.rosaceus	5.712	4.390	1.438	3.405	4.342	5.327	7.594
S.rosenblatti	2.929	2.939	-1.695	1.523	2.935	4.351	7.583
S.ruberrimus	10.056	1.954	-4.316	0.073	1.947	3.803	8.275
S.rufus	3.185	2.996	-1.686	1.561	2.994	4.420	7.743
S.saxicola	5.127	4.901	3.216	4.311	4.890	5.479	6.651
S.semicinctus	4.333	4.392	1.751	3.584	4.392	5.205	7.031
S.serranoides	0.427	2.106	-1.818	0.940	2.183	3.335	5.665

Table 15. Species ranked by posterior probability that the slope (exponent) parameter is greater than one, based on the 2-level absolute fecundity model, $\log(\Phi) = \log(c) + d\log(W)$.

S.flavidus	99%
S.paucispinis	96%
S.serranoides	96%
S.miniatus	96%
S.caurinus	95%
S.chlorostictus	94%
S.alutus	94%
S.crameri	94%
S.maliger	93%
S.brevispinis	92%
S.saxicola	90%
S.diploproa	89%
S.goodei	89%
S.mystinus	88%
S.melanops	88%
S.rosenblatti	87%
S.semicinctus	87%
S.atrovirens	87%
S.helvomaculatus	87%
S.rufus	87%
S.melanostomus	86%
S.emphaeus	86%
S.constellatus	86%
S.pinniger	86%
S.ensifer	85%
S.dalli	85%
S.proriger	85%
S.babcocki	85%
S.norvegicus	85%
S.ruberrimus	85%
S.elongatus	85%
S.rastrelliger	85%
S.jordani	84%
S.auriculatus	84%
S.hopkinsi	84%
S.entomelas	84%
S.levis	84%
S.carnatus	83%
S.rosaceus	83%
S.ovalis	82%

Table 16. Parameter values for state variable models with exponential potential growth functions ($\Delta L = gL$)

Parameter	Description [units]	Value
T	maximum age [yrs]	100
L_{min}	minimum length [cm]	1
L_{max}	maximum length [cm]	100
g	growth rate proportionality constant [unitless]	0.25
a	coefficient of weight-length allometric relationship [kg×cm^{-b}]	0.00001
b	exponent of weight-length allometric relationship [unitless]	3
m_0	baseline mortality rate [1/yr]	0.05
m_1	length-dependent mortality rate [cm/yr]	0
m_2	reproduction-dependent mortality rate [1/yr]	2[a]
μ	concave conversion parameter [1/kg]	0.1[b]

[a] models with increasing mortality as a function of GSI, otherwise this term is omitted

[b] models with reproduction as a concave function of allocation, otherwise $\mu = 0$

Table 17. Parameter values for state variable models with linear potential growth functions ($\Delta L = C$)

Parameter	Description [units]	Value
T	maximum age [yrs]	100
L_{min}	minimum length [cm]	1
L_{max}	maximum length [cm]	100
C	growth increment [cm]	4
a	coefficient of weight-length allometric relationship [kg×cm^{-b}]	0.00001
b	exponent of weight-length allometric relationship [unitless]	3
m_0	baseline mortality rate [1/yr]	0.05
m_1	length-dependent mortality rate [cm/yr]	0
m_2	reproduction-dependent mortality rate [1/yr]	2[a]
μ	concave conversion parameter [1/kg]	0.8[b]

[a] models with increasing mortality as a function of GSI, otherwise this term is omitted

[b] models with reproduction as a concave function of allocation, otherwise $\mu = 0$

Table 18. Parameter values for state variable models with asymptotic potential growth functions (Equations 4.13 and 4.14)

Parameter	Description [units]	Value
T	maximum age [yrs]	100
L_{min}	minimum length [cm]	1
q	maximum growth rate in asymptotic growth model [cm/yr]	2.5
k	Brody growth coefficient [1/yr]	0.025
L_{pan}	asymptotic size of immature fish [cm]	q / k
c	cost fraction; $c \times L_{pan}$ is maximum size of fish maturing at L_{min} [unitless]	0.8
a	coefficient of weight-length allometric relationship [kg×cm^{-b}]	0.00001
b	exponent of weight-length allometric relationship [unitless]	3
m_0	baseline mortality rate [1/yr]	0.05
m_1	length-dependent mortality rate [cm/yr]	0
m_2	reproduction-dependent mortality rate [1/yr]	2[a]
μ	concave conversion parameter [1/kg]	0.004[b]

[a] models with increasing mortality as a function of GSI, otherwise this term is omitted

[b] models with reproduction as a concave function of allocation, otherwise $\mu = 0$

Table 19. Predictions of maximum realized length (L_{max}), length at maturity (L_{mat}), age at maturity (A_{mat}), the ratio of length at maturity to maximum size (L_{mat} / L_{max}), and the gonadosomatic index (γ) at L_{max}. Results are based on an asymptotic production function with natural mortality specified as a quadratic function of relative investment in reproduction (γ).

	Baseline Natural Mortality (m_0)			
	0.050	**0.075**	**0.100**	**0.125**
L_{max}	45.0	39.0	34.0	30.0
L_{mat}	32.0	24.8	20.9	16.9
A_{mat}	16	12	10	8
L_{mat}/L_{max}	0.711	0.636	0.616	0.563
$\gamma(L_{max})$	0.093	0.120	0.150	0.182

FIGURES

Figure 1. Realized spawning potential ratio (*SPR*) resulting from the fishing mortality rate that would achieve a 50% reduction in unfished spawning output under the assumption of constant relative fecundity. The exponent of the weight-length power function is set equal to 3, L_∞ = 40 cm, k = 0.15 yr^{-1}, length at 50% maturity = 20 cm, length at 50% selection by the fishery = 25 cm.

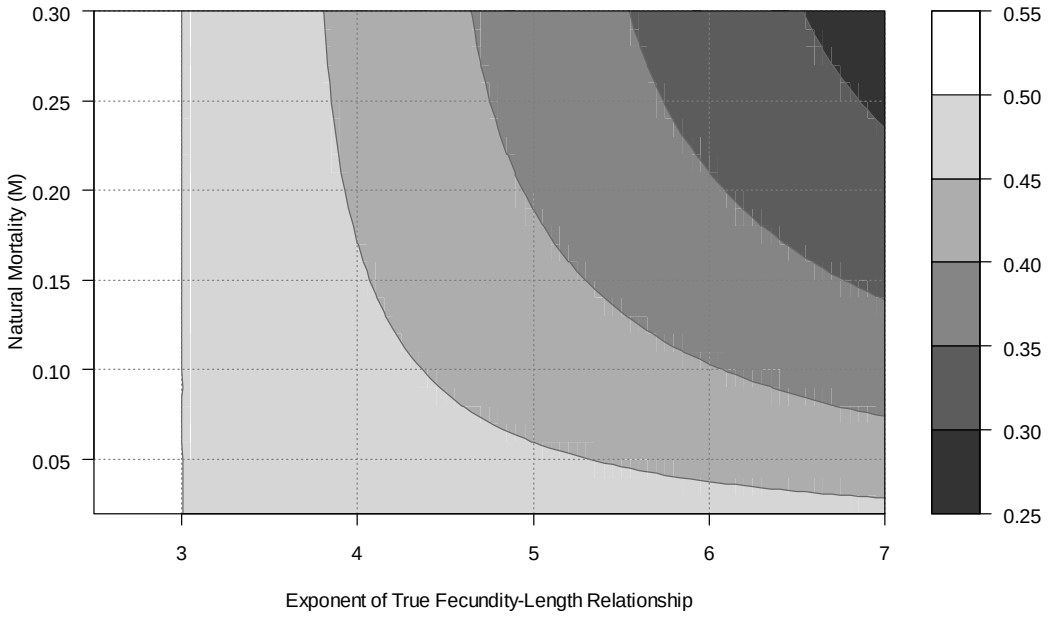

Figure 2. Realized spawning potential ratio (*SPR*) resulting from the fishing mortality rate that would achieve a 50% reduction in unfished spawning output under the assumption of constant relative fecundity. The exponent of the weight-length power function is set equal to 3, L_∞ = 80 cm, k = 0.05 yr^{-1}, length at 50% maturity = 30 cm, length at 50% selection by the fishery = 35 cm.

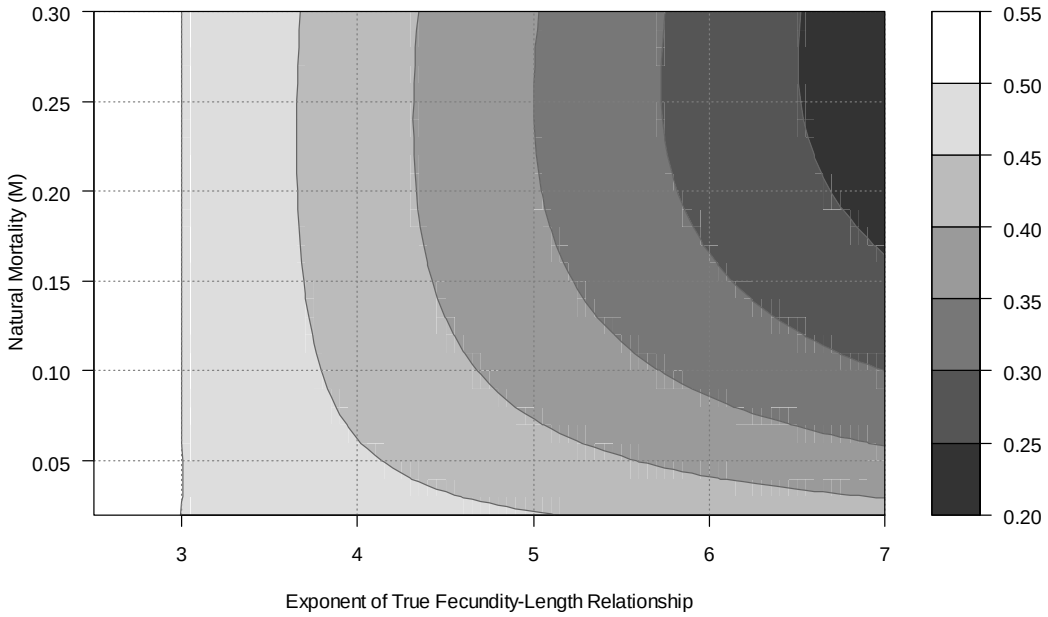

Figure 3: Evaluation of the assumption that fecundity is directly proportional to condition factor. Data for panels A and B are from Eldridge *et al*. (1991), data for panel C is from Sogard *et al*. (in prep.).

A)

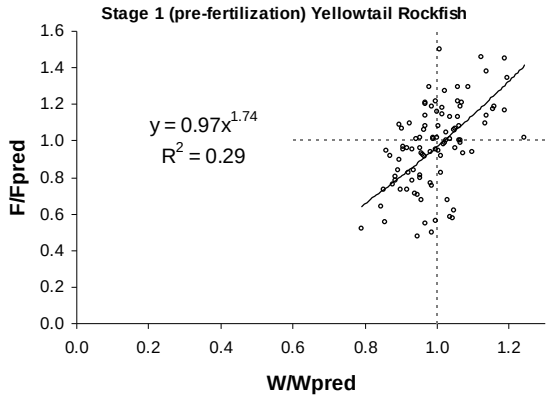

B)

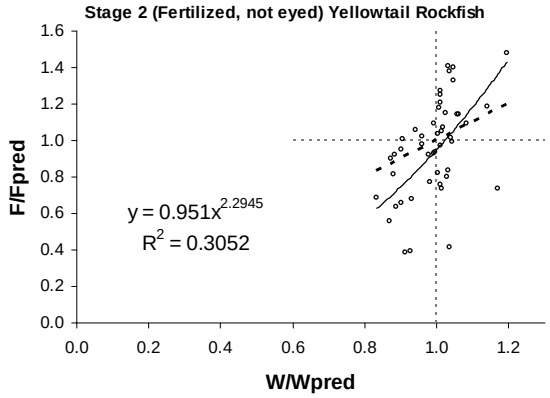

C)

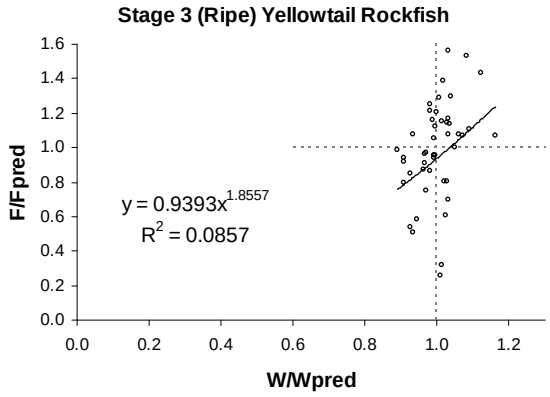

Figure 4. Residual plots from the model for absolute fecundity as an allometric function of length for yellowtail rockfish (*S. flavidus*).

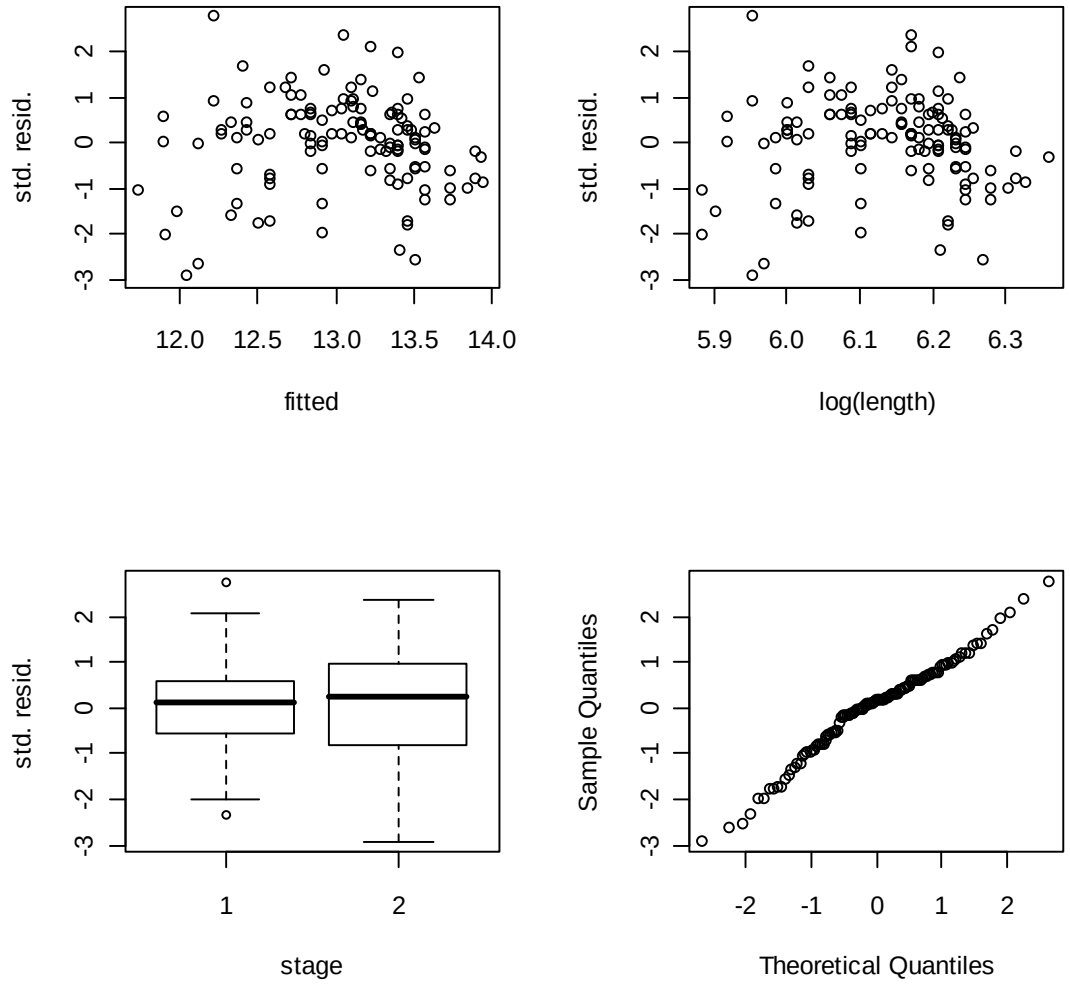

Figure 5. Residual plots from the model for absolute fecundity as an allometric function of length, including weight as an offset term, for yellowtail rockfish (*S. flavidus*).

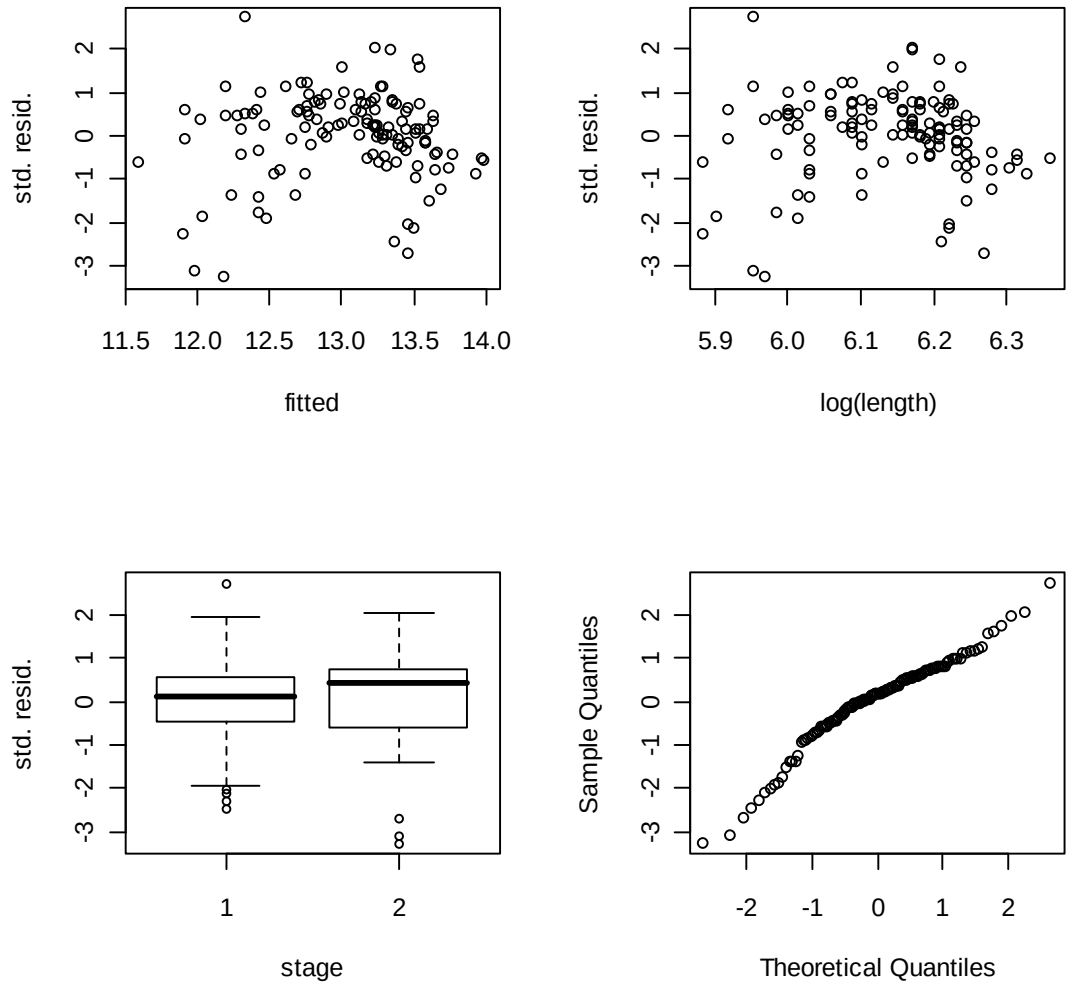

Figure 6. Residual plots from the model for absolute fecundity as an allometric function of weight for yellowtail rockfish (*S. flavidus*).

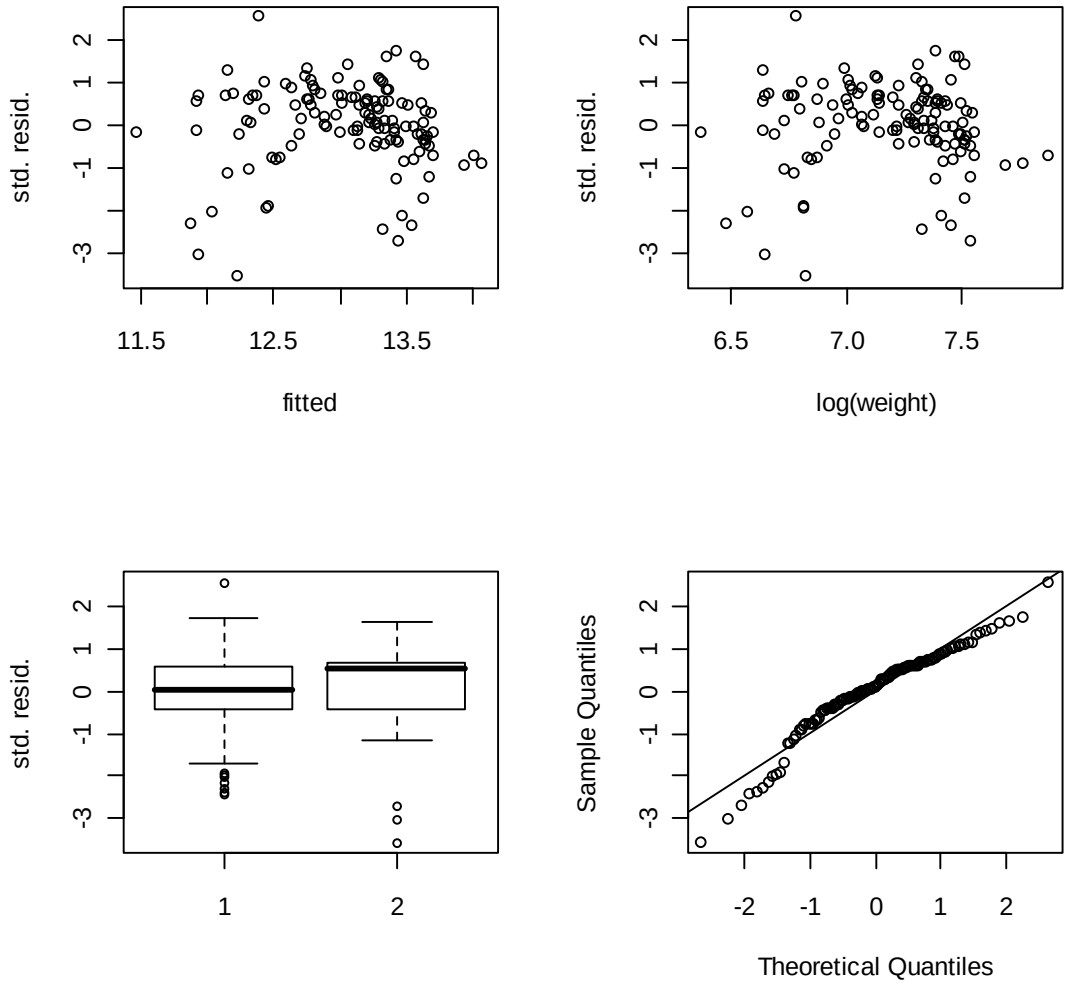

Figure 7. Residual plots from model for relative fecundity as a linear function of weight for yellowtail rockfish (*S. flavidus*).

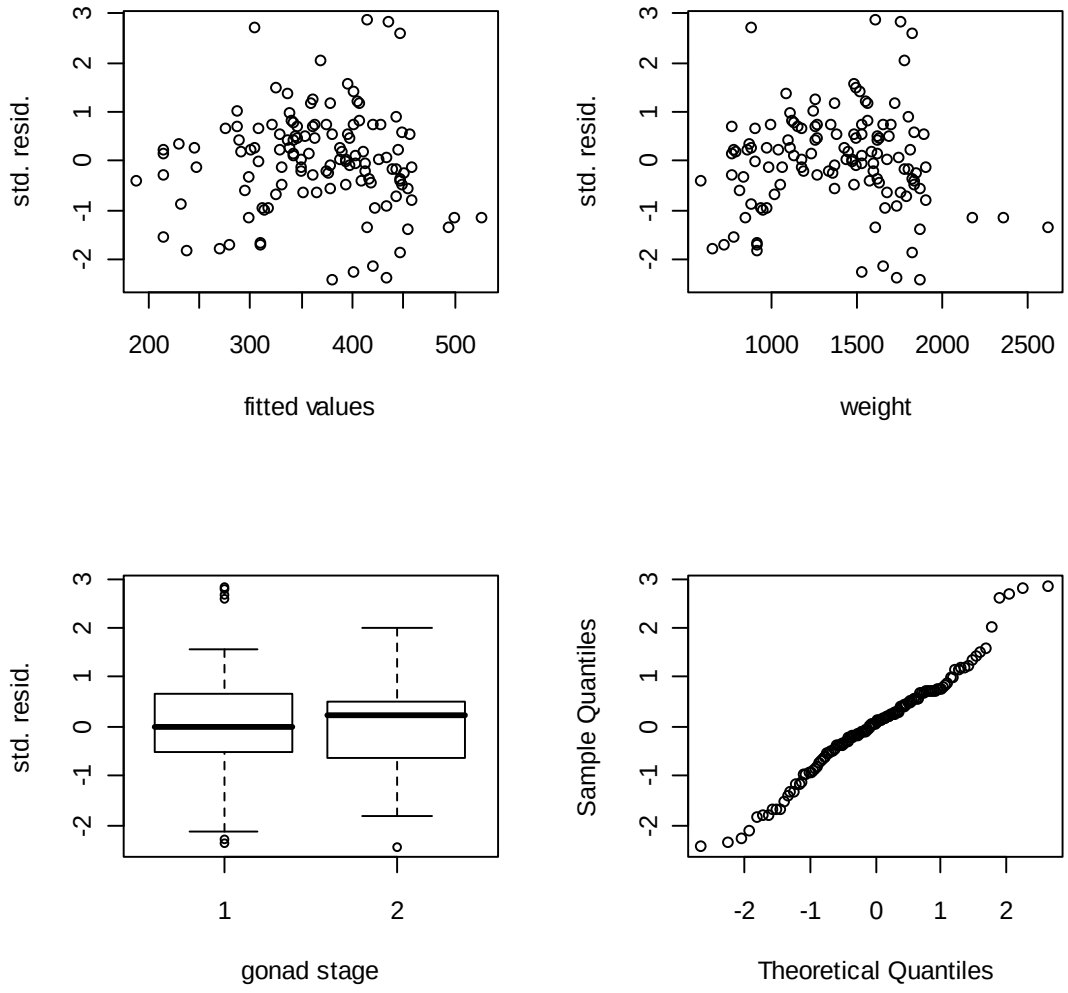

Figure 8: Total body weight versus somatic weight (total weight minus gonad weight) for six *Sebastes* species, with estimated parameters from regressions through the origin.

A)

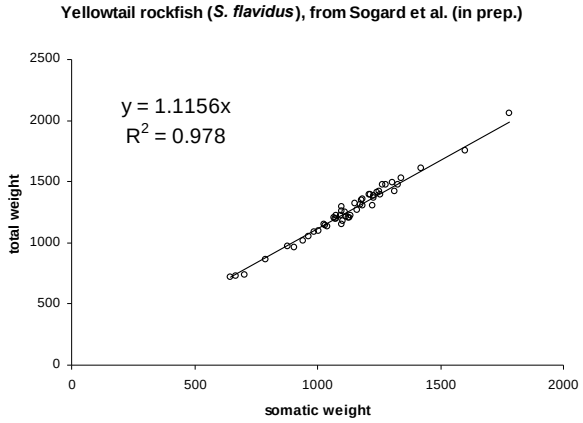

B)

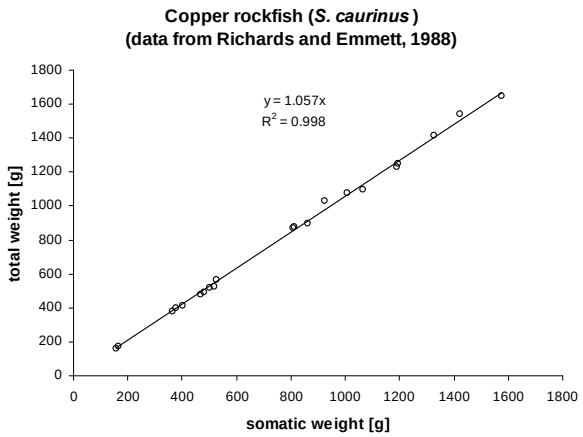

C)

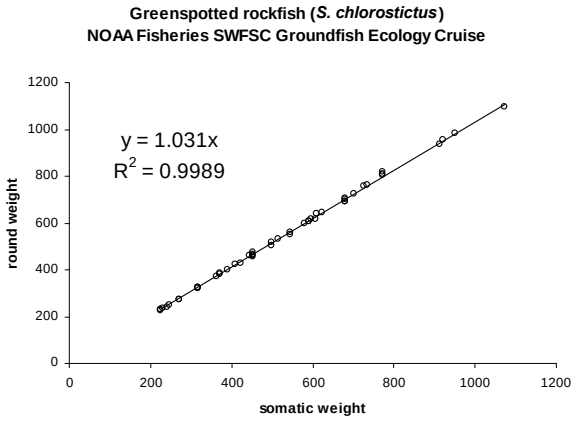

Figure 8 (continued): Total body weight versus somatic weight (total weight minus gonad weight) for six *Sebastes* species, with estimated parameters from regressions through the origin.

D)

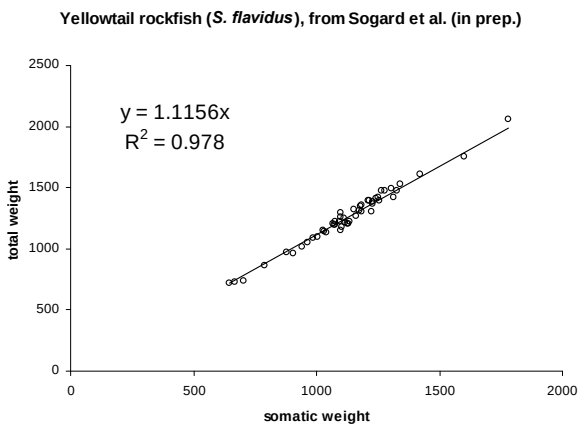

E)

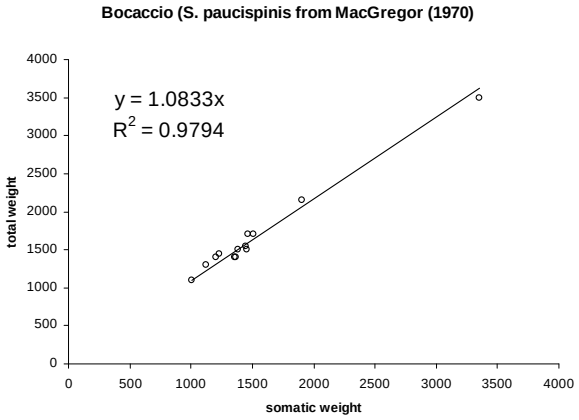

F)

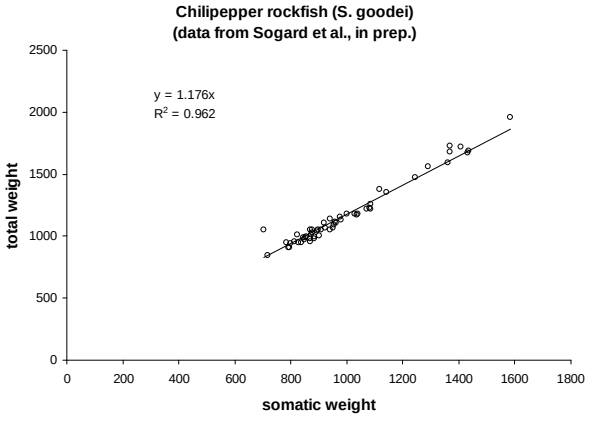

Figure 9. Eggs per gram total body weight versus total length (mm) for species assigned to Subgenus *Acutomentum* following Hyde and Vetter (2007), by data source and stage of gonad development. Vertical lines are estimates of length at which 50% of individuals are mature.

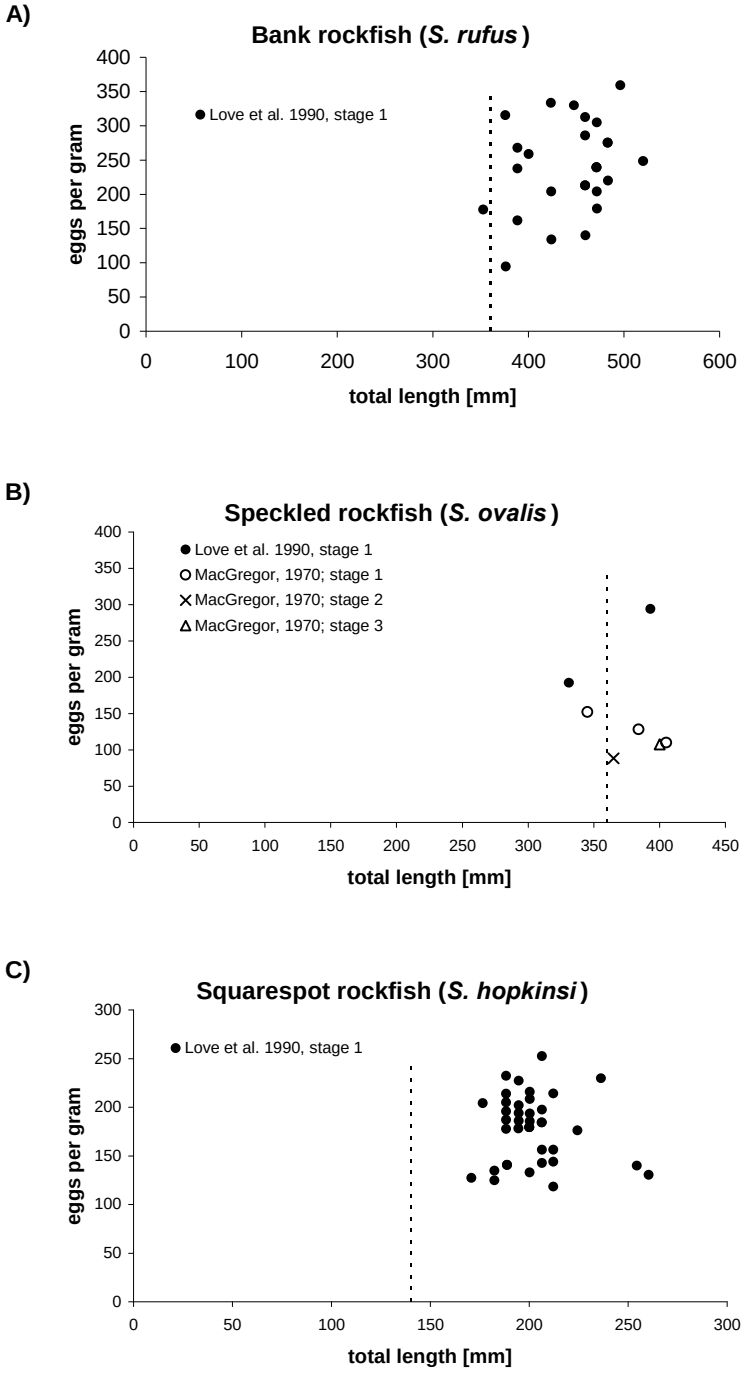

Figure 10. Eggs per gram total body weight versus total length (mm) for species assigned to clades A-B following Hyde and Vetter (2007), by data source and stage of gonad development. Vertical lines are estimates of length at which 50% of individuals are mature.

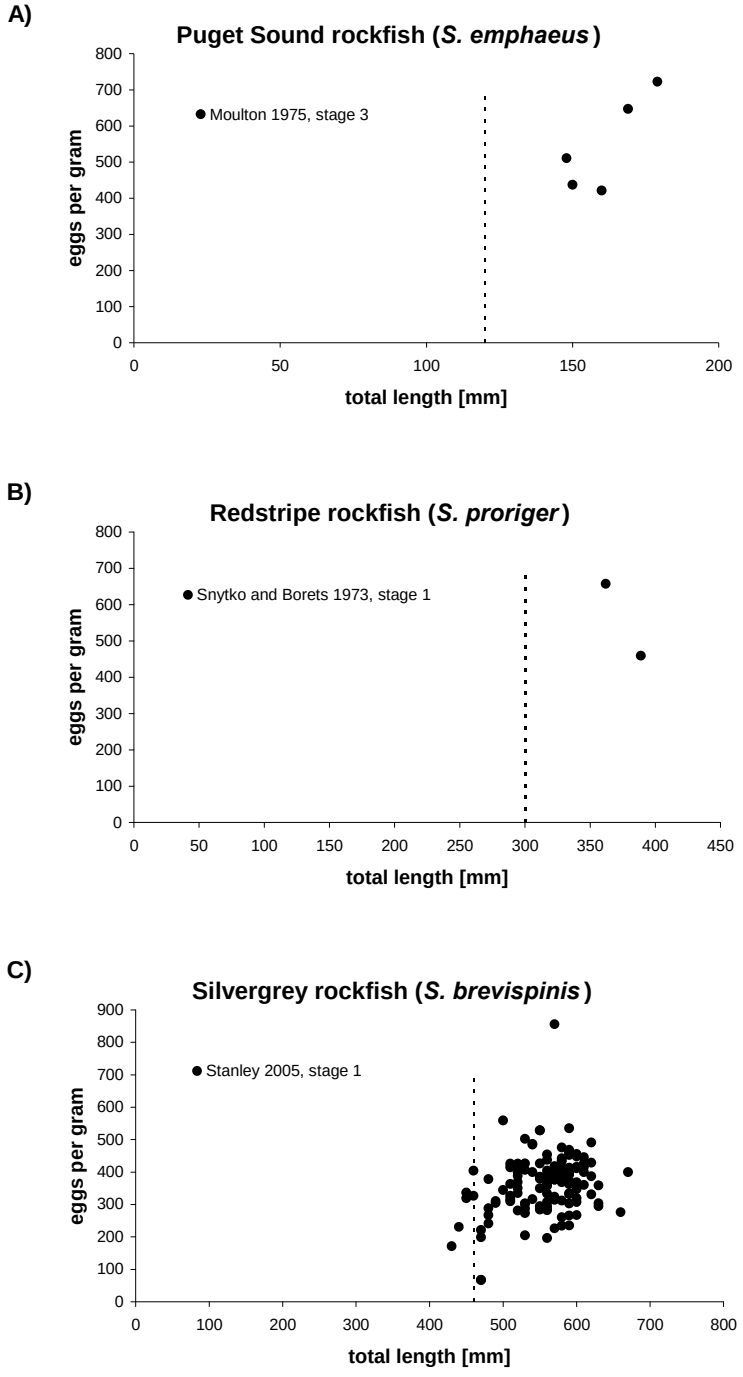

Figure 11. Eggs per gram total body weight versus total length (mm) for species assigned to clade D following Hyde and Vetter (2007), by data source and stage of gonad development. Vertical lines are estimates of length at which 50% of individuals are mature.

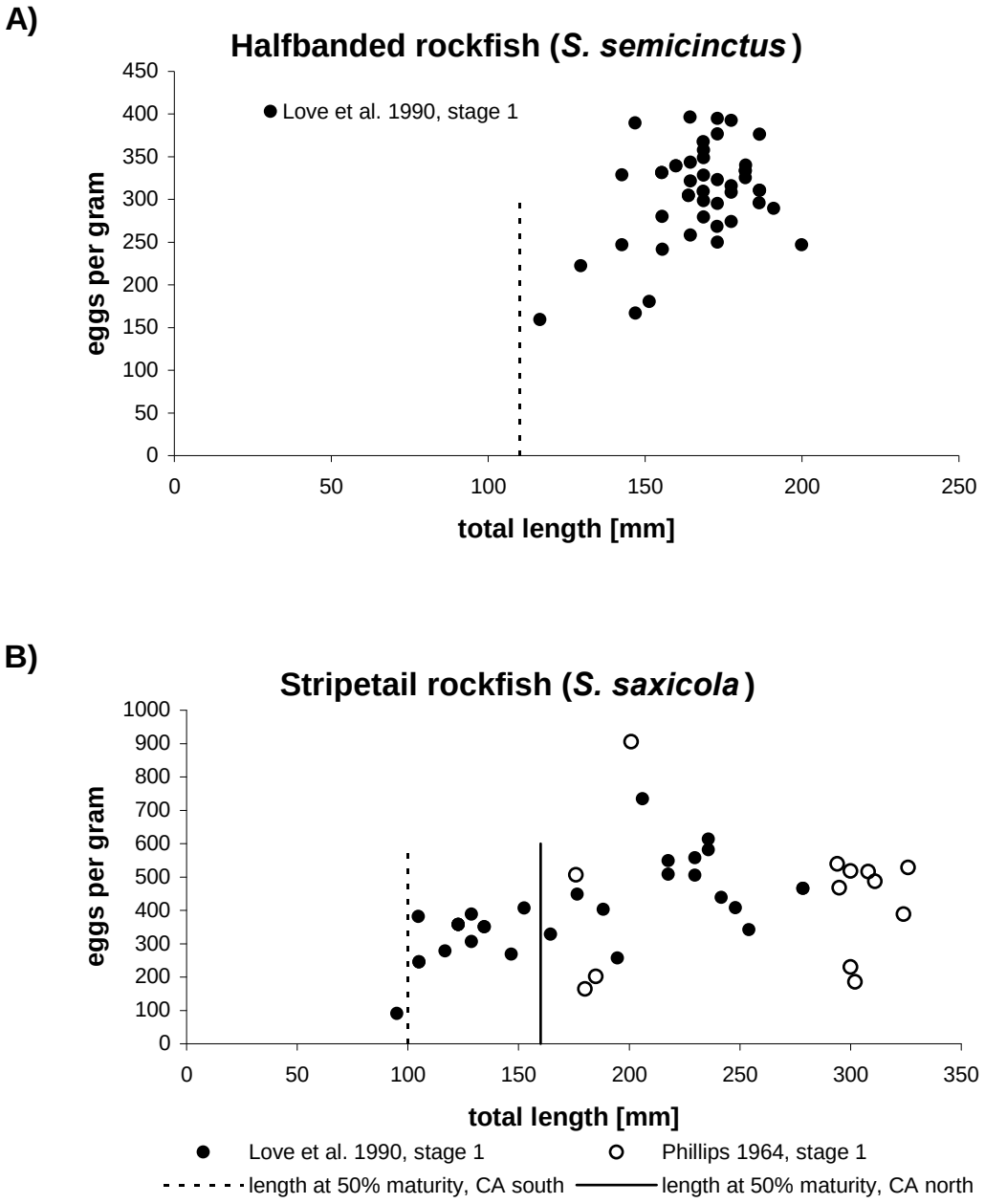

Figure 12. Eggs per gram total body weight versus total length (mm) for *Sebastes diploproa*, assigned to subgenus *Eosebastes* following Hyde and Vetter (2007). Vertical lines are estimates of length at which 50% of individuals are mature.

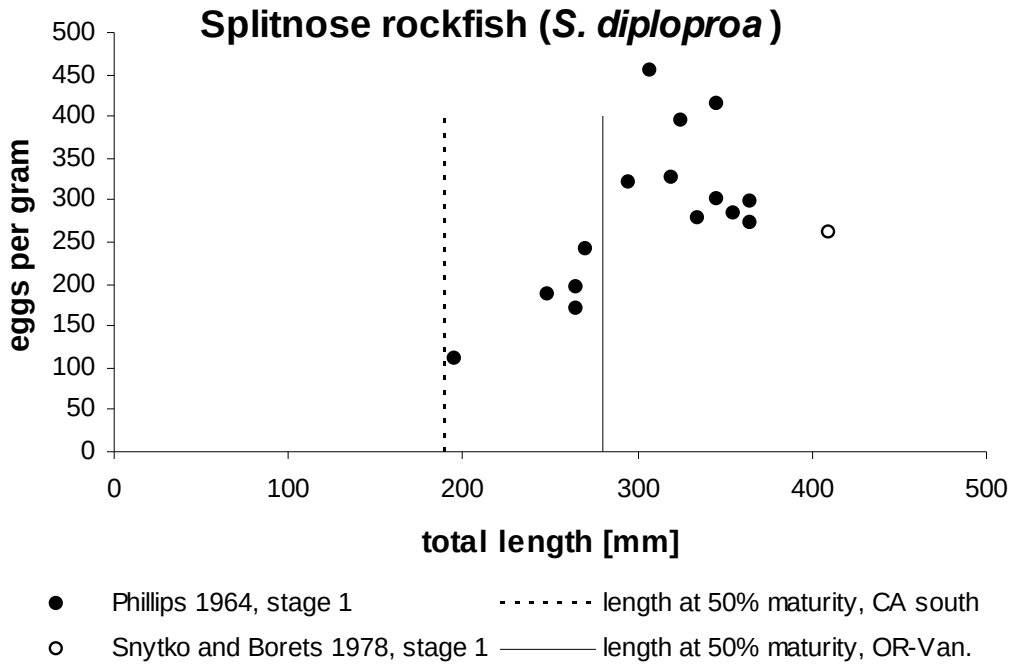

Figure 13. Eggs per gram total body weight versus total length (mm) for species assigned to subgenus *Pteropodus* following Hyde and Vetter (2007), by data source and stage of gonad development. Vertical lines are estimates of length at which 50% of individuals are mature.

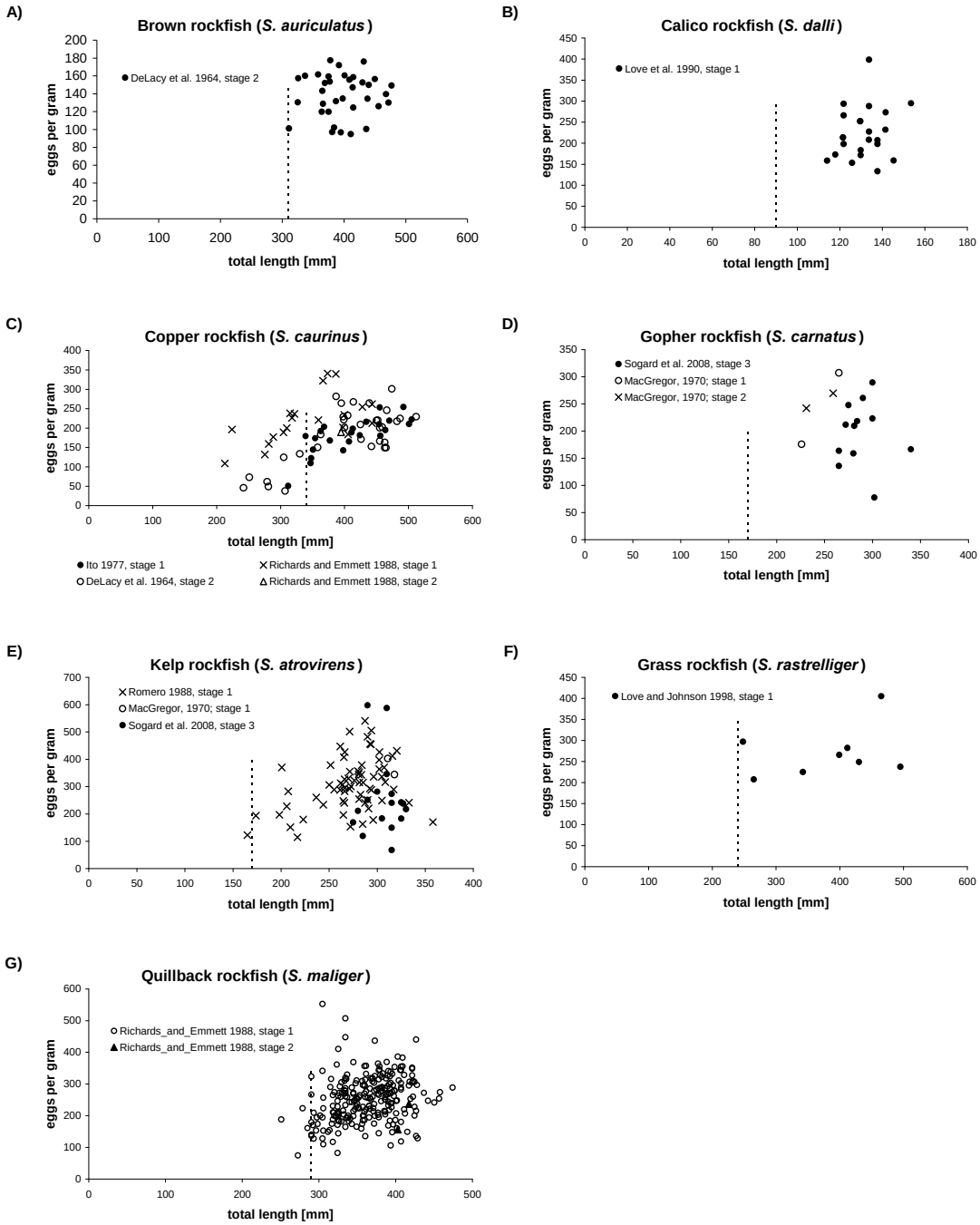

Figure 14. Eggs per gram total body weight versus total length (mm) for species assigned to subgenus *Rosicola* following Hyde and Vetter (2007), by data source and stage of gonad development. Vertical lines are estimates of length at which 50% of individuals are mature.

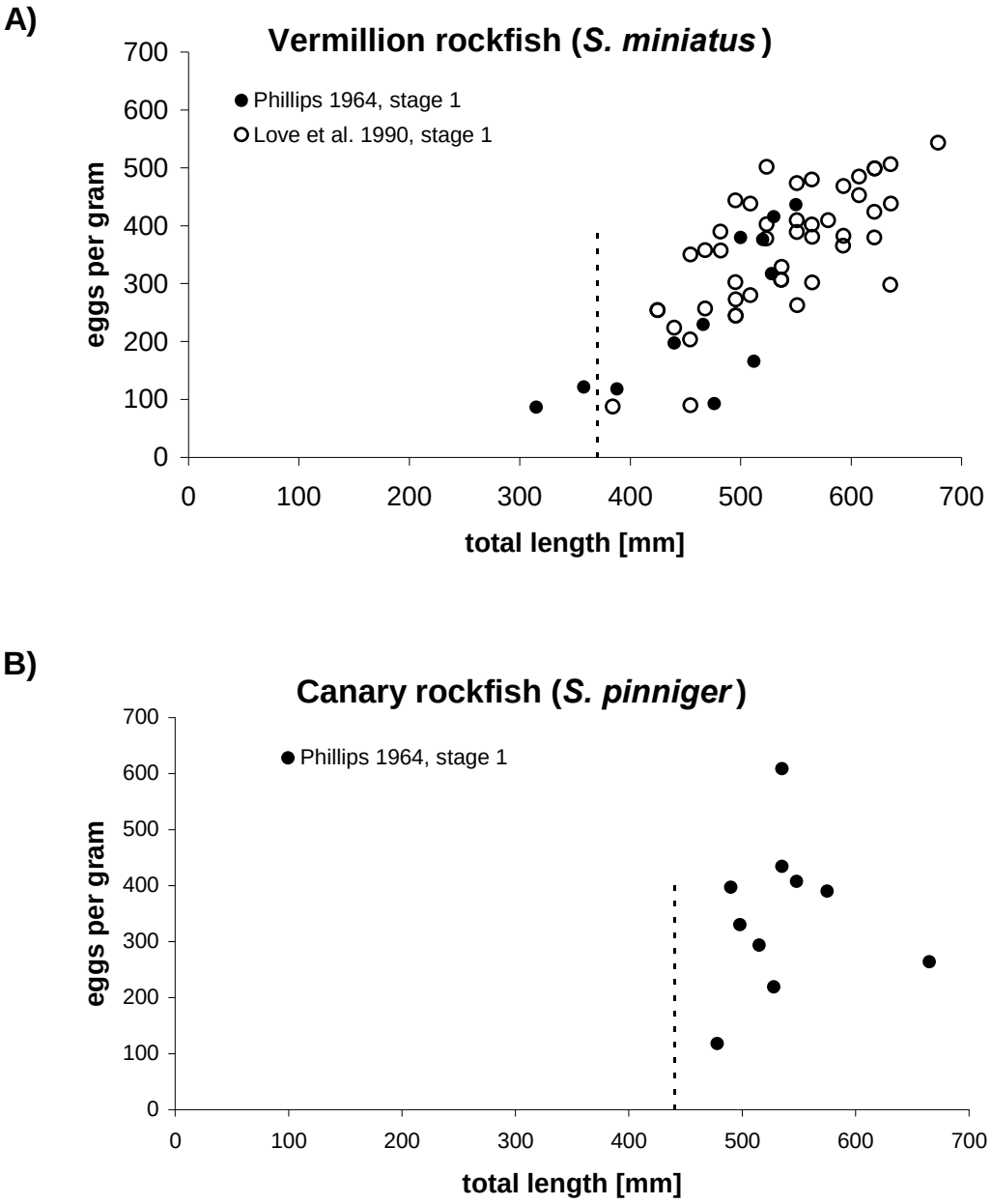

Figure 15. Eggs per gram total body weight versus total length (mm) for species assigned to subgenus *Sebastes* following Hyde and Vetter (2007), by data source and stage of gonad development. Vertical lines are estimates of length at which 50% of individuals are mature.

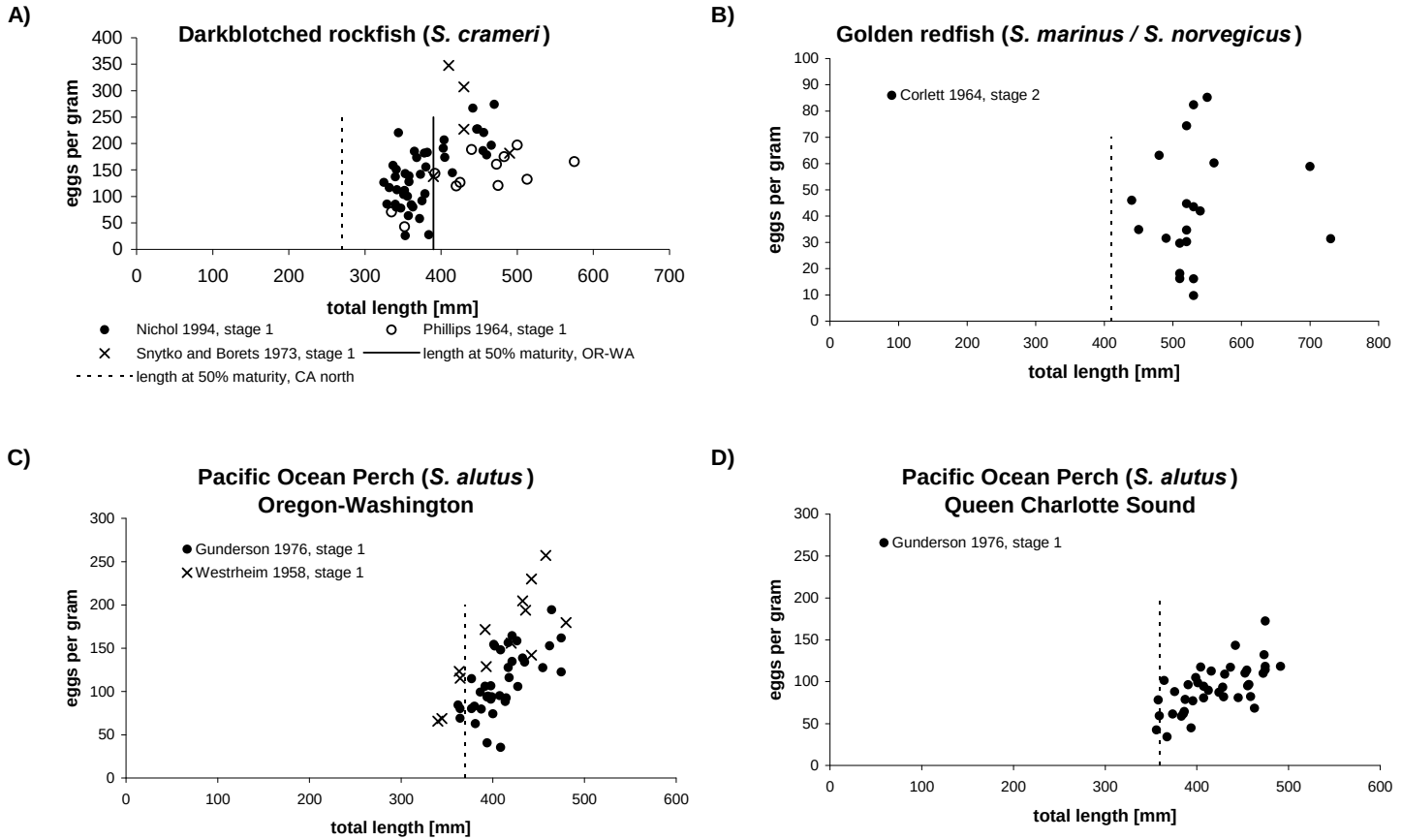

Figure 16. Eggs per gram total body weight versus total length (mm) for *S. babcocki*, assigned to subgenus *Sebastichthys* following Hyde and Vetter (2007). Vertical line is estimate of length at which 50% of individuals are mature. The only other relative fecundity sample from this subgenus was one 285 mm treefish (*S. serriceps*), with an estimated 192 eggs per gram total body weight (MacGregor, 1970).

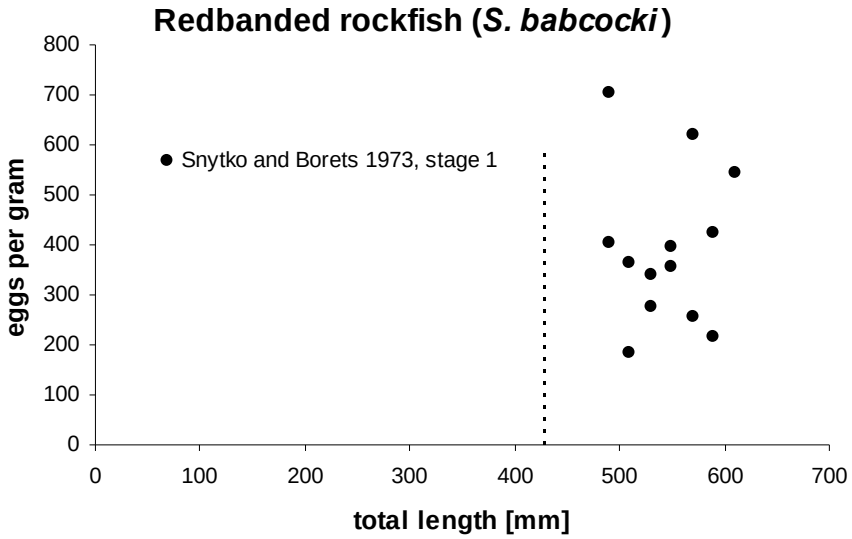

Figure 17. Eggs per gram total body weight versus total length (mm) for species assigned to subgenus *Sebastodes* following Hyde and Vetter (2007), by data source and stage of gonad development. Vertical lines are estimates of length at which 50% of individuals are mature.

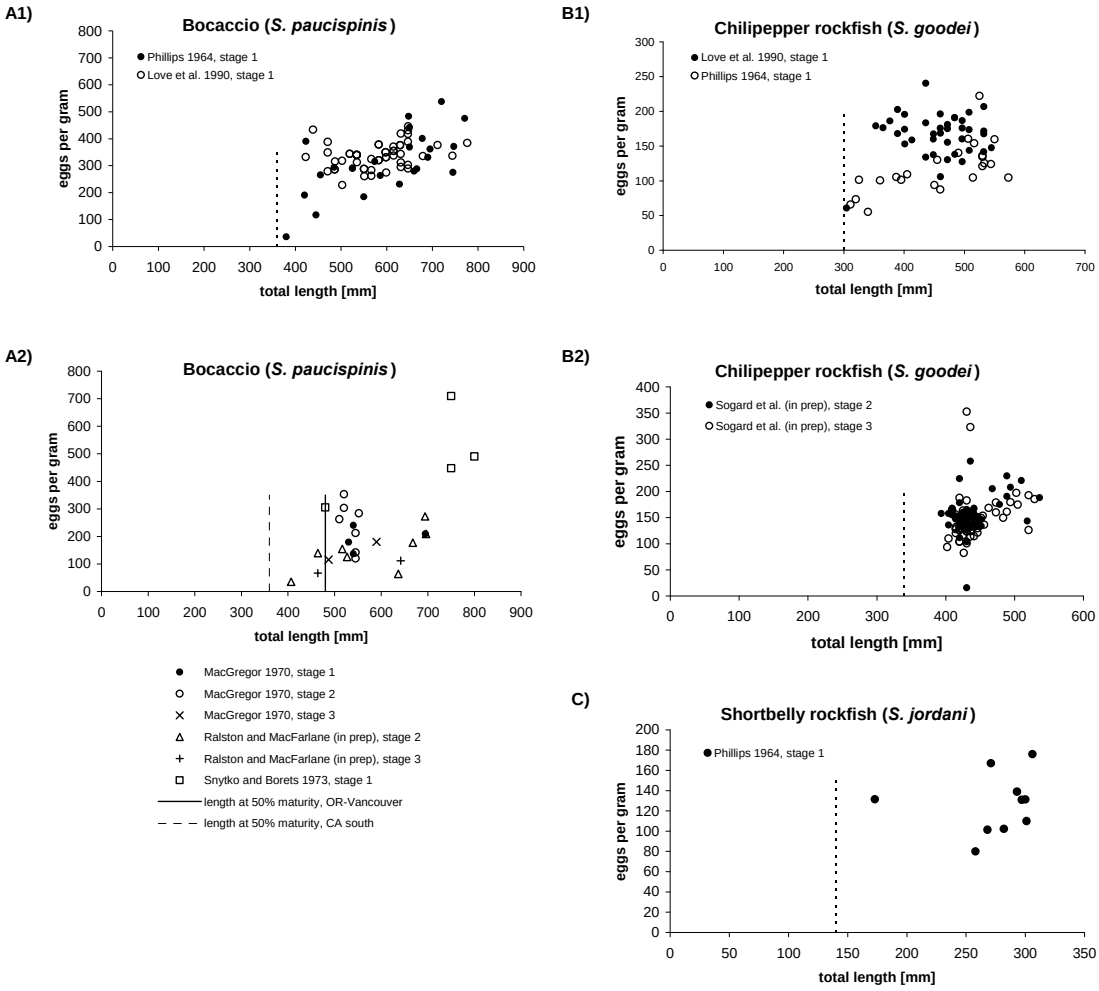

Figure 18. Eggs per gram total body weight versus total length (mm) for species assigned to subgenus *Sebastomus* following Hyde and Vetter (2007), by data source and stage of gonad development. Vertical lines are estimates of length at which 50% of individuals are mature, except for *S. ensifer* due to a lack of sufficient data.

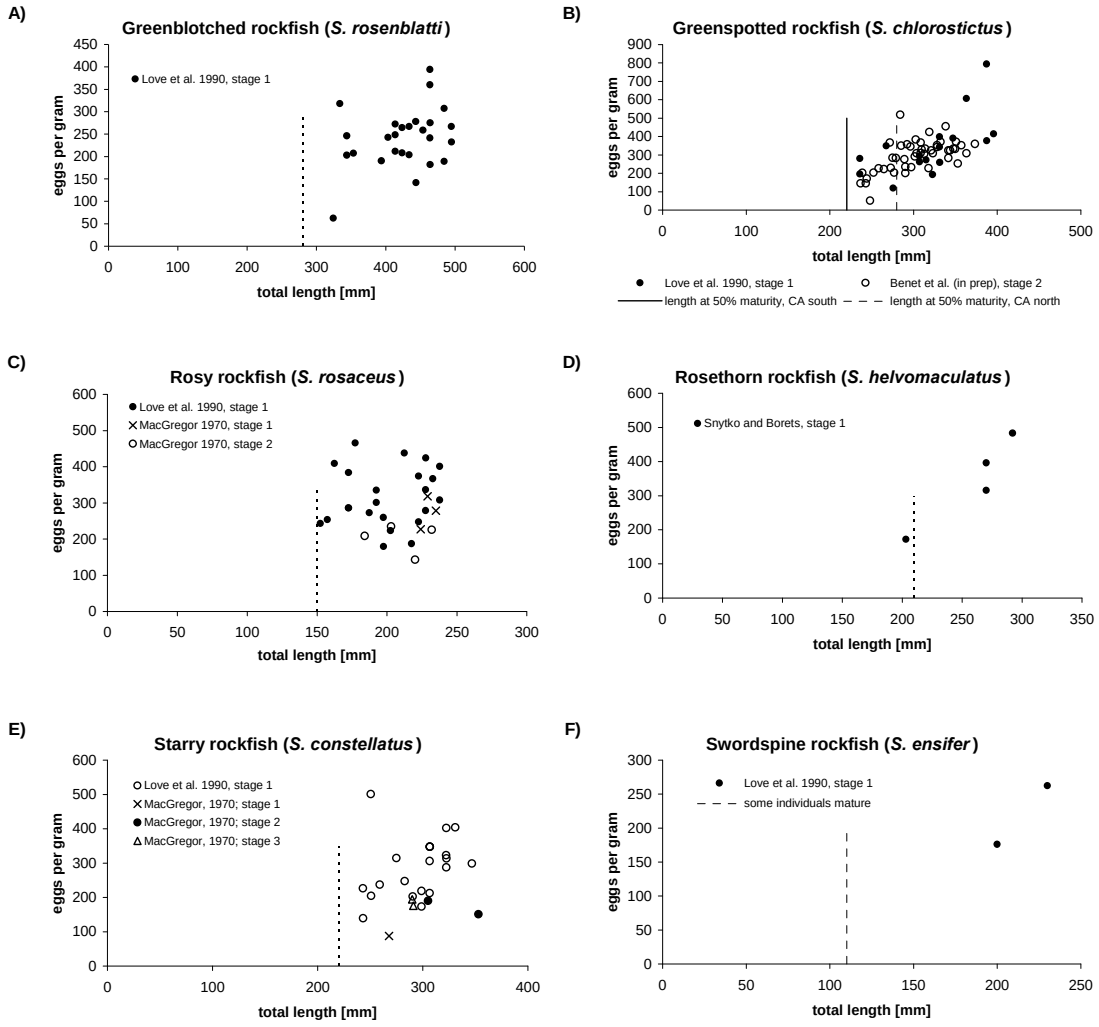

Figure 19. Eggs per gram total body weight versus total length (mm) for *S. rubberimus*, assigned to subgenus *Sebastopyr* following Hyde and Vetter (2007). Vertical line is estimate of length at which 50% of individuals are mature.

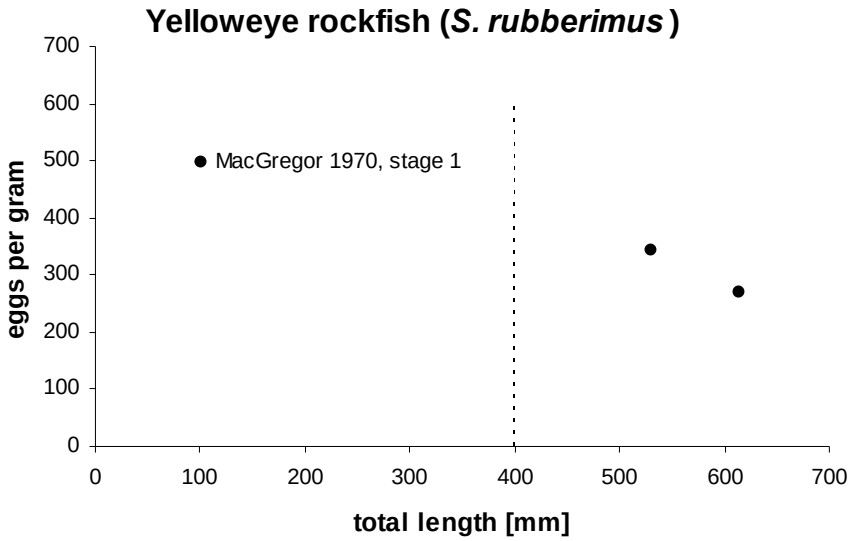

Figure 20. Eggs per gram total body weight versus total length (mm) for species assigned to subgenus *Sebastosomus* following Hyde and Vetter (2007), by data source and stage of gonad development. Vertical lines are estimates of length at which 50% of individuals are mature.

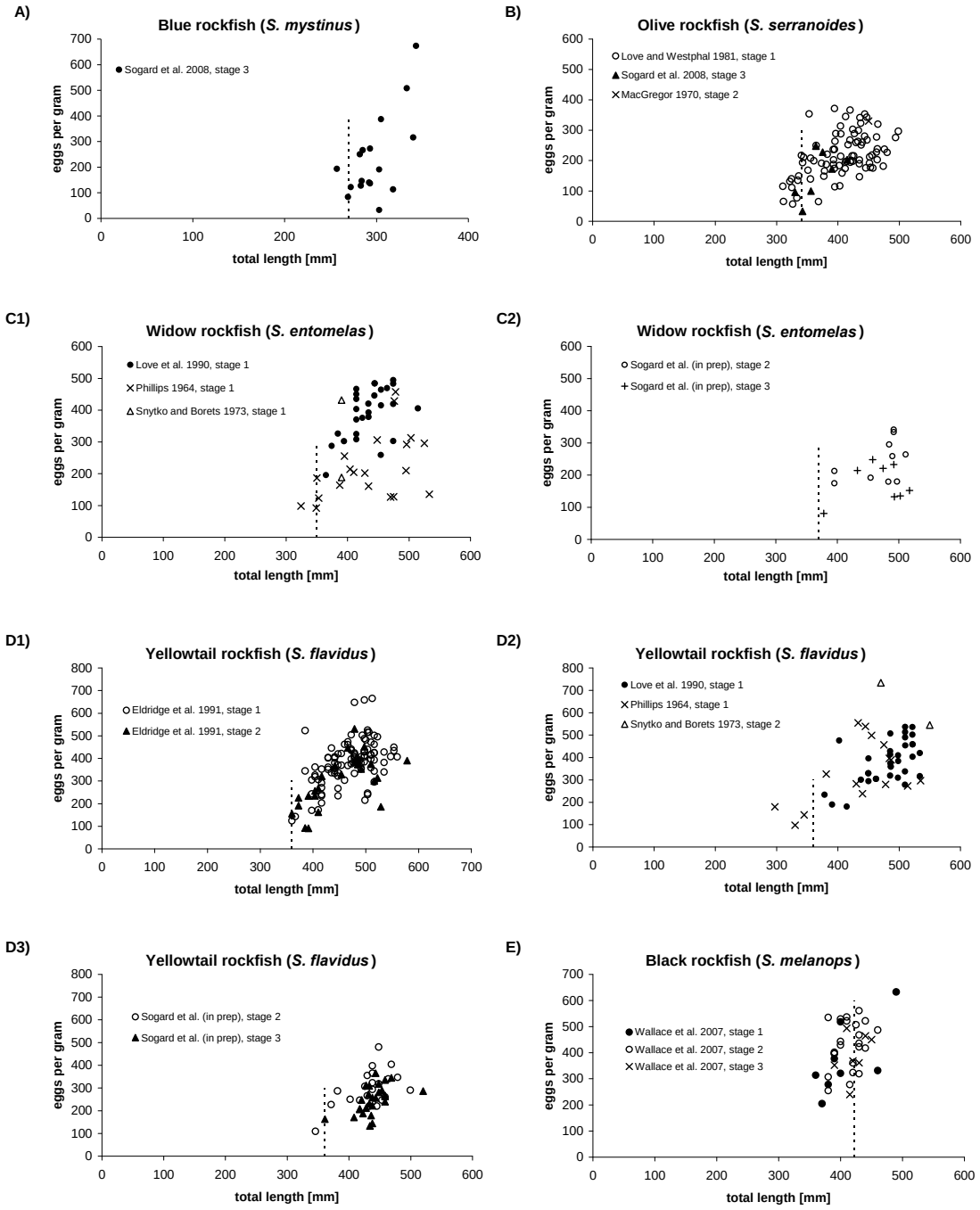

Figure 21. Eggs per gram total body weight versus total length (mm) for species without a named group assignment following Hyde and Vetter (2007), by data source and stage of gonad development. Vertical lines are estimates of length at which 50% of individuals are mature.

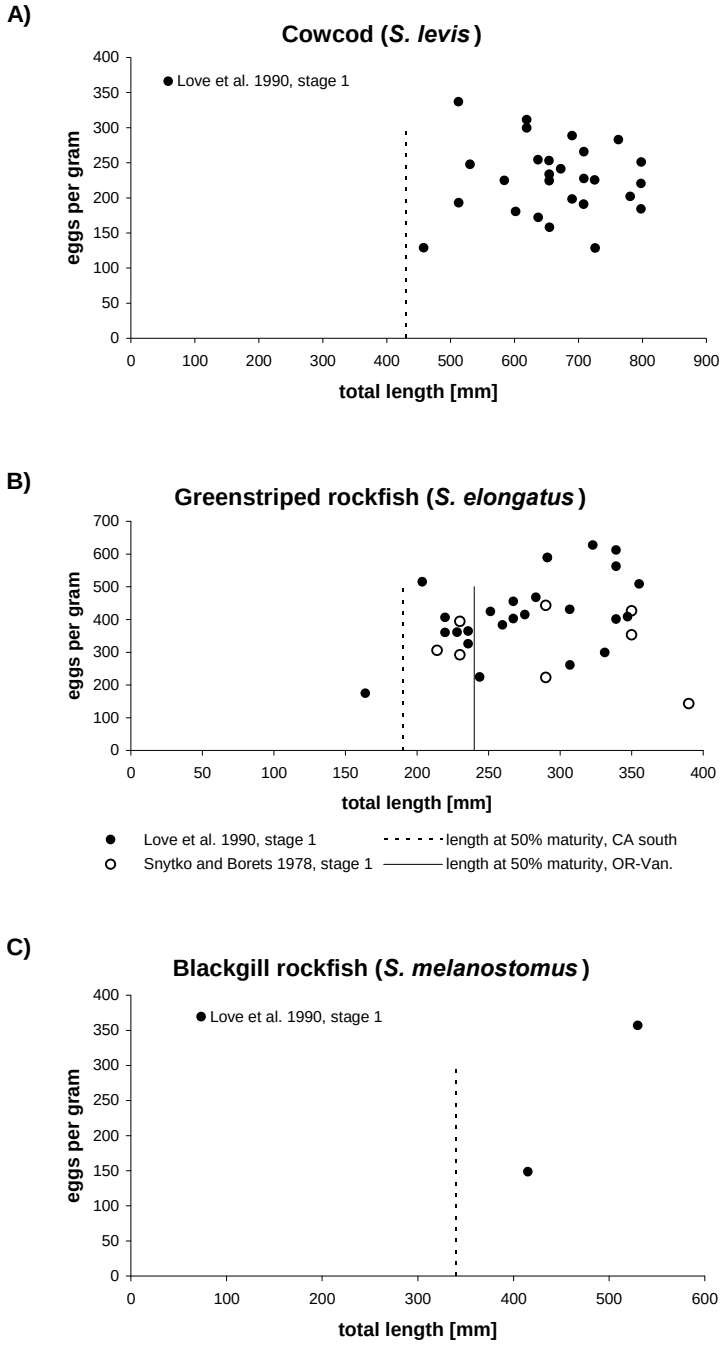

Figure 22. Eggs per gram total body weight for 41 rockfish species, ranked by median values. Sub-generic names are from Hyde and Vetter (2007). Vertical black lines represent median values, boxes are bounded by the first and third quartiles, and whiskers extend to minimum and maximum values.

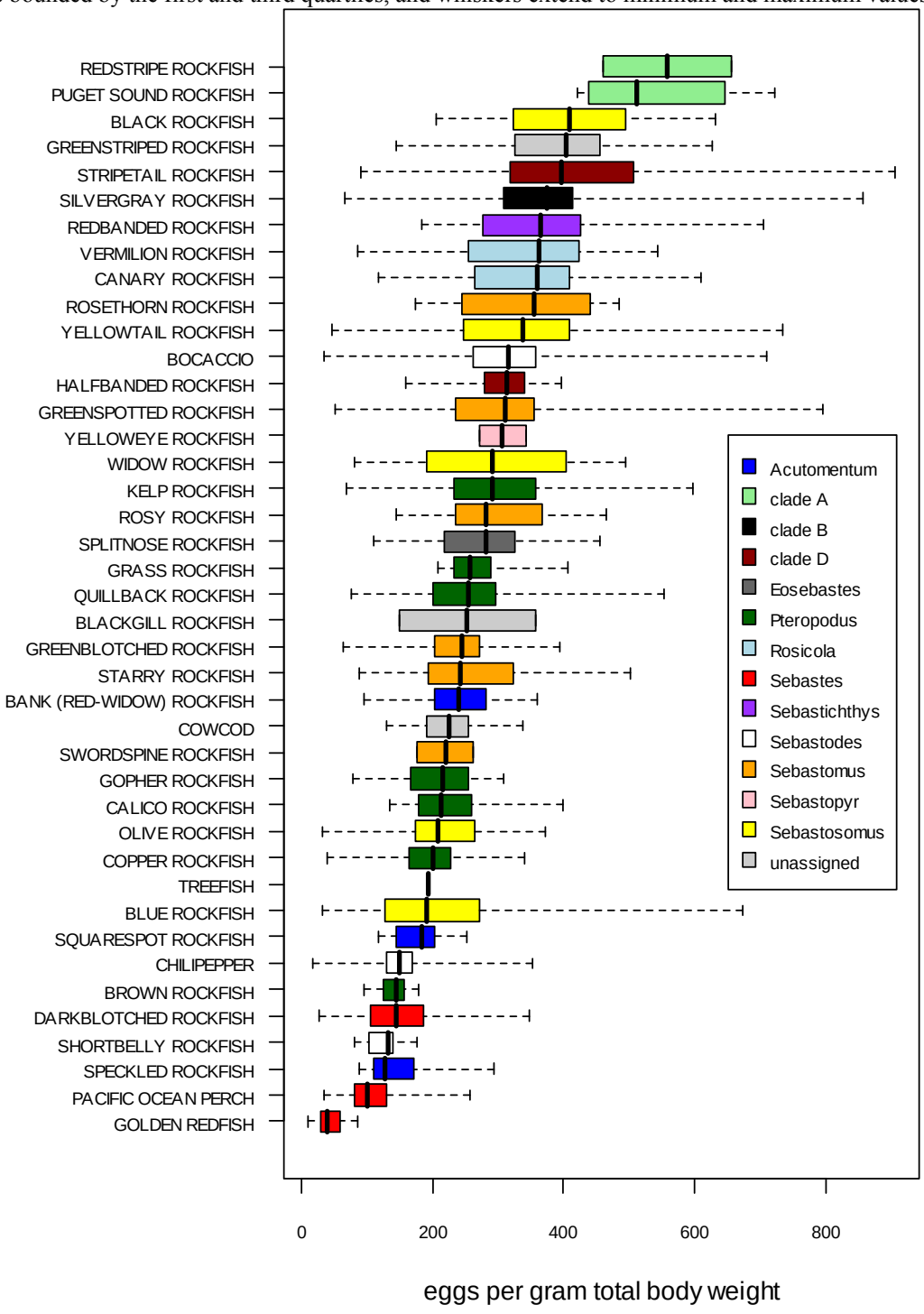

Figure 23. Relative fecundity (eggs per gram total body weight) by gonad maturation stage for 14 *Sebastes* species. Stages 1, 2, and 3 represent pre-fertilized, fertilized (not yet eyed larvae), and eyed larvae.

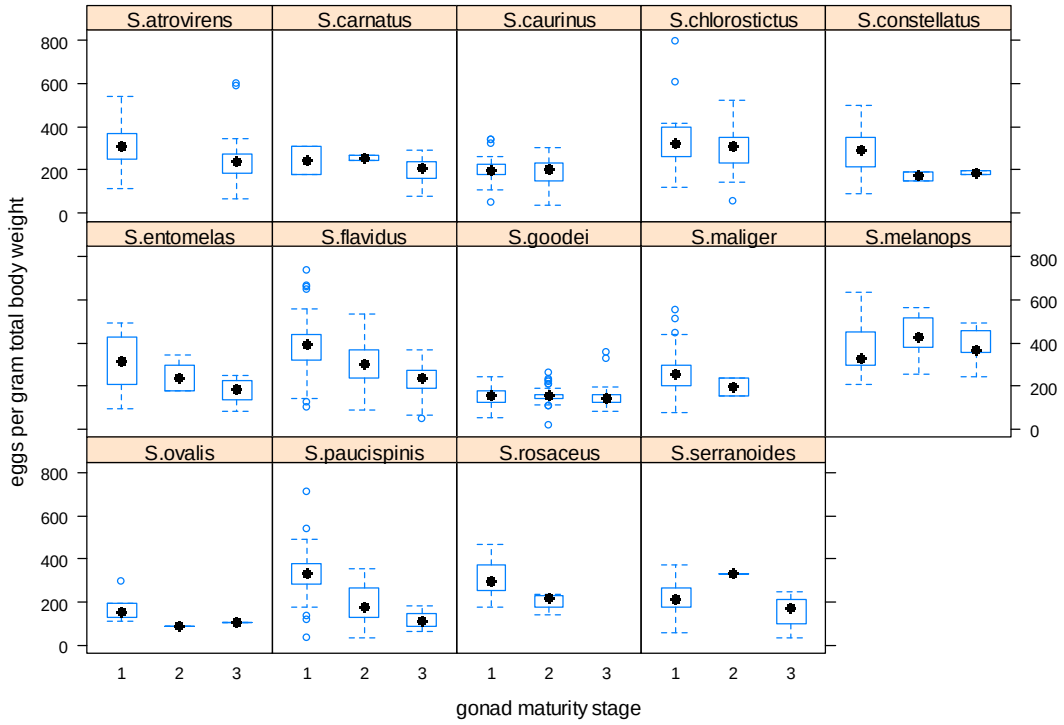

Figure 24. Subgenus *Acutomentum*. Eggs per gram total body weight versus total body weight.

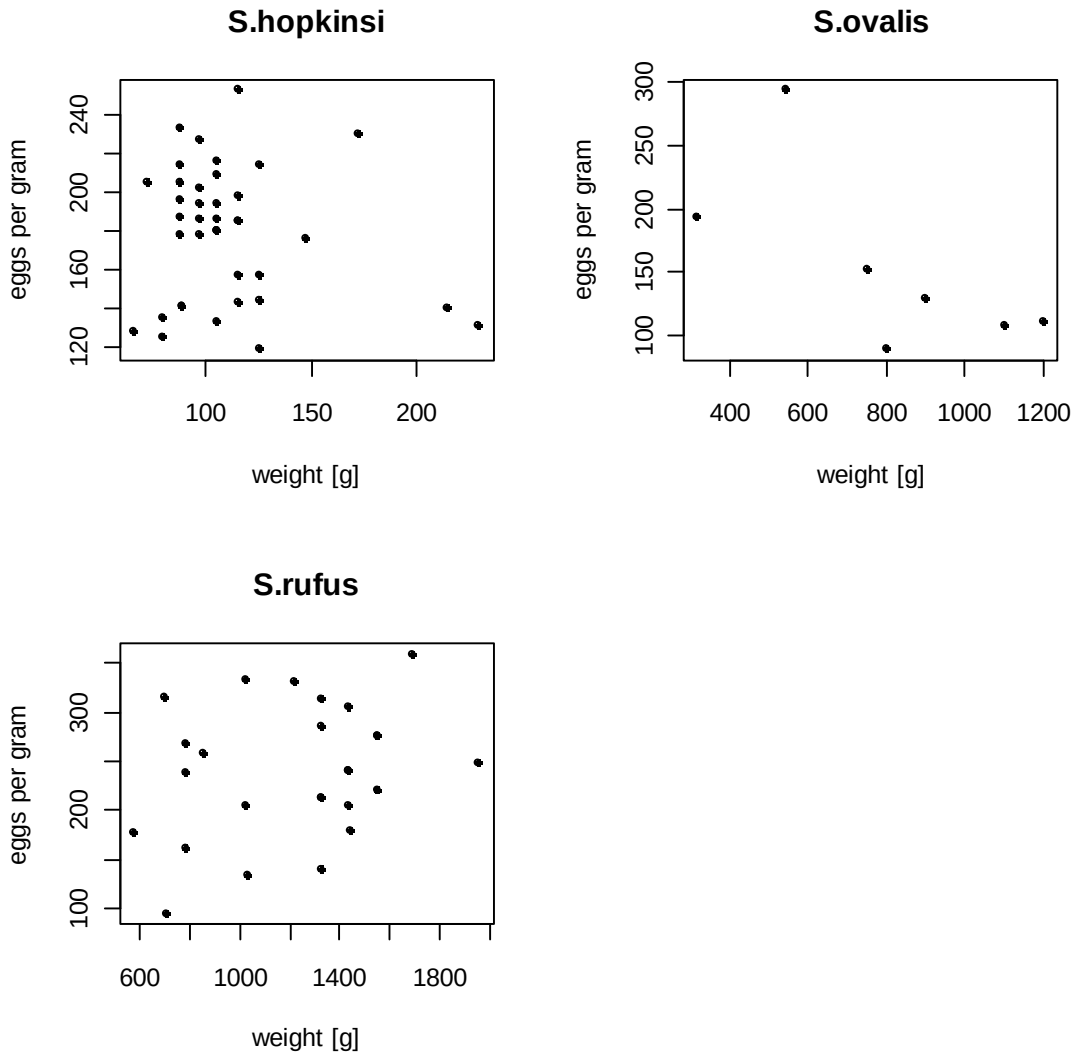

Figure 25. Clade A. Eggs per gram total body weight versus total body weight.

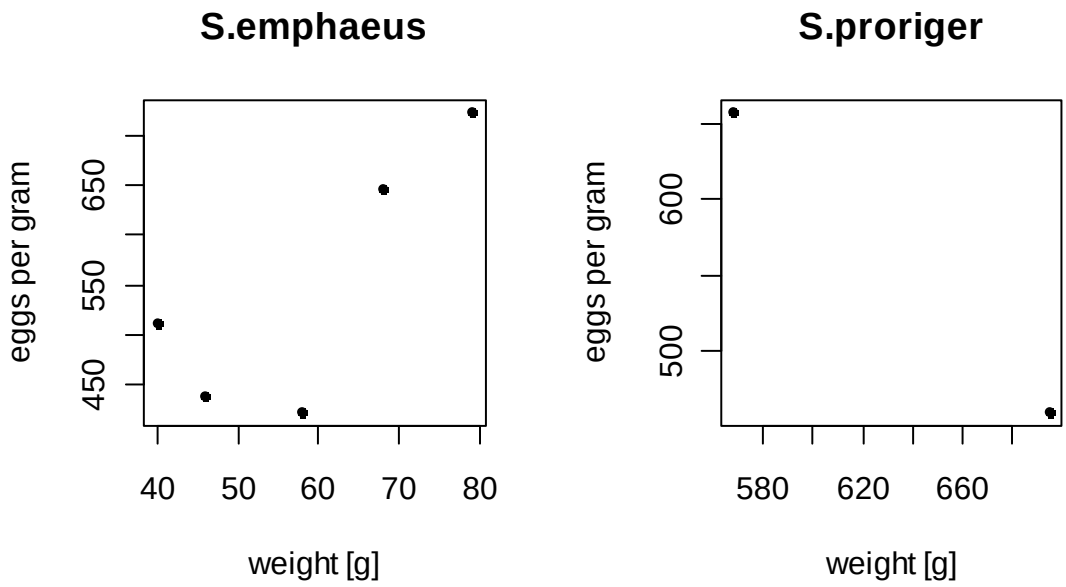

Figure 26. Clade B (*S. brevispinis*). Eggs per gram total body weight versus total body weight.

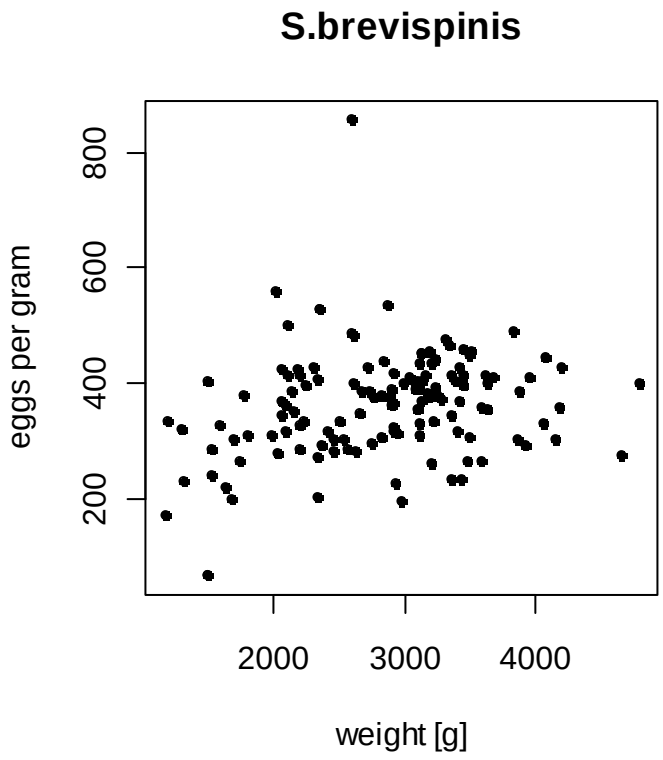

Figure 27. Clade D. Eggs per gram total body weight versus total body weight.

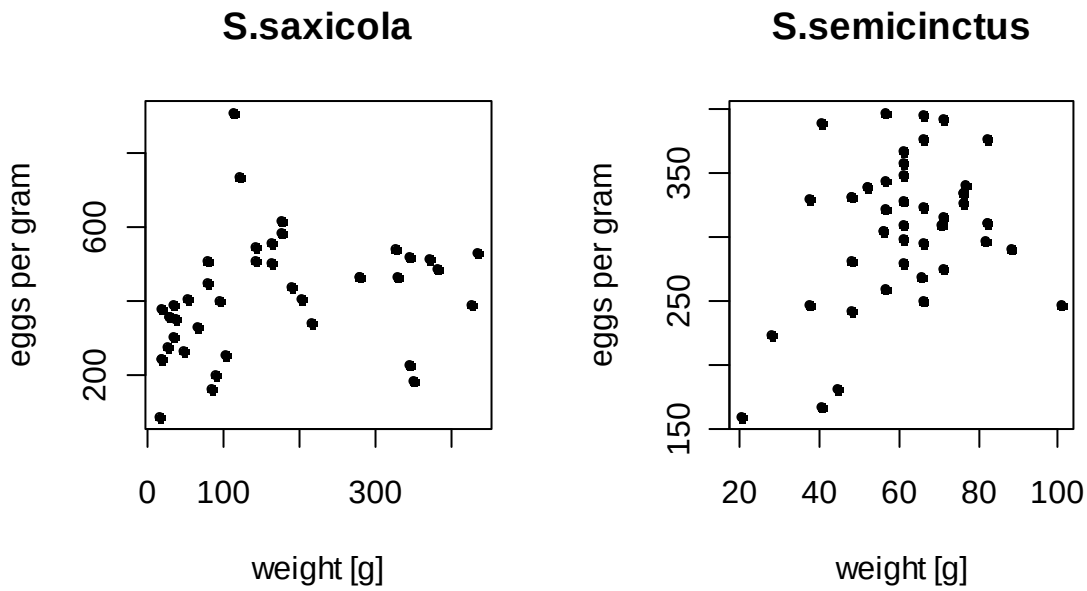

Figure 28. Subgenus *Eosebastes*. Eggs per gram total body weight versus total body weight.

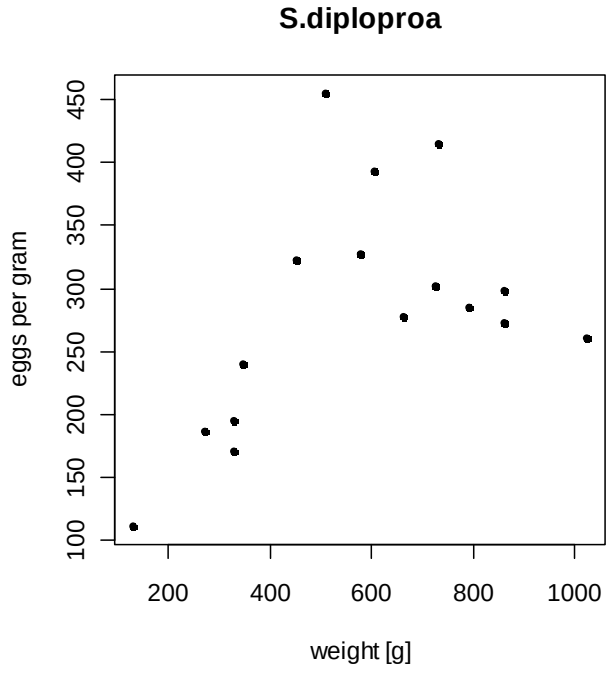

Figure 29. Subgenus *Pteropodus*. Eggs per gram total body weight versus total body weight.

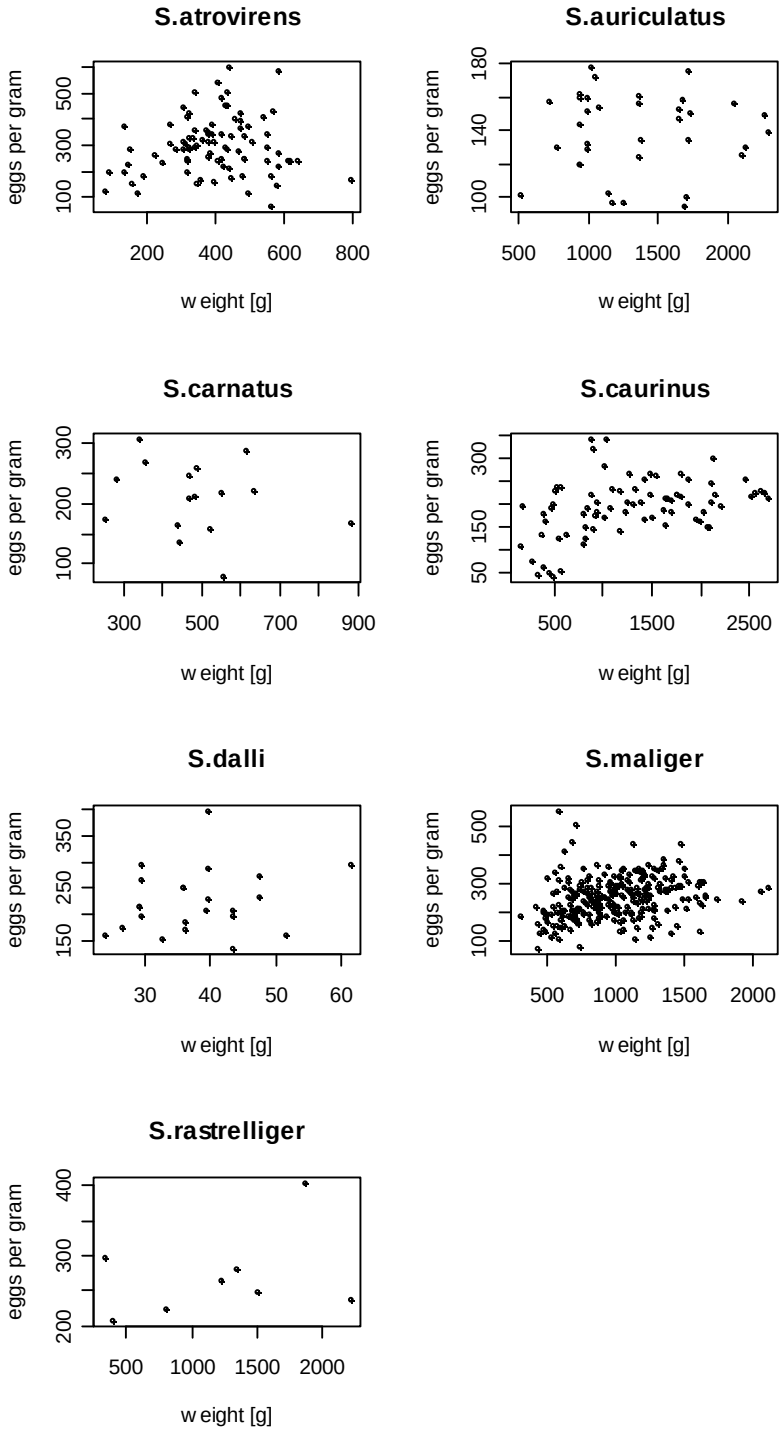

Figure 30. Subgenus *Rosicola*. Eggs per gram total body weight versus total body weight.

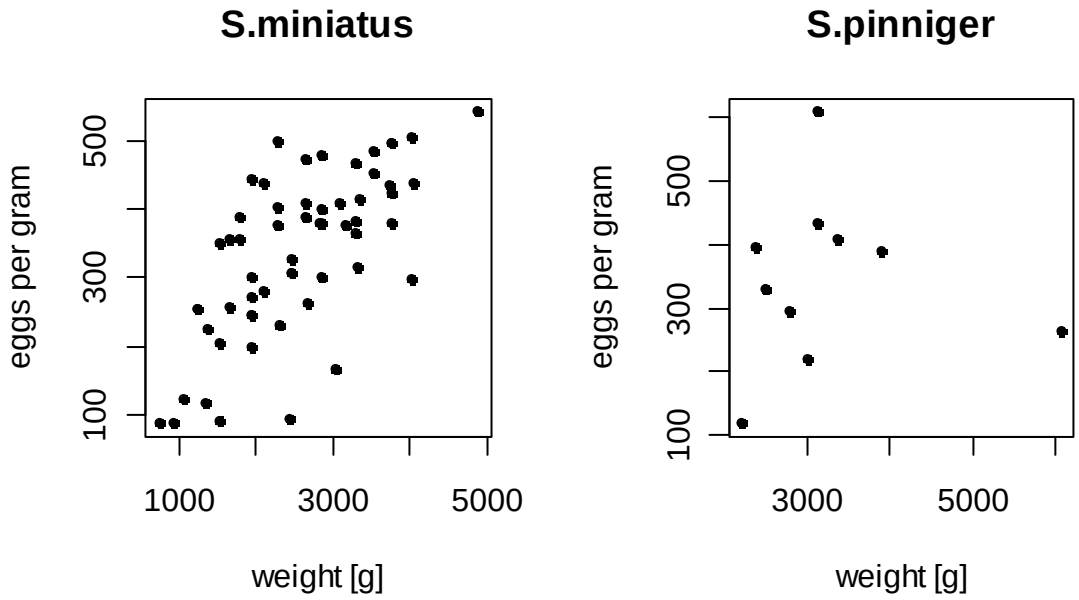

Figure 31. Subgenus *Sebastes*. Eggs per gram total body weight versus total body weight.

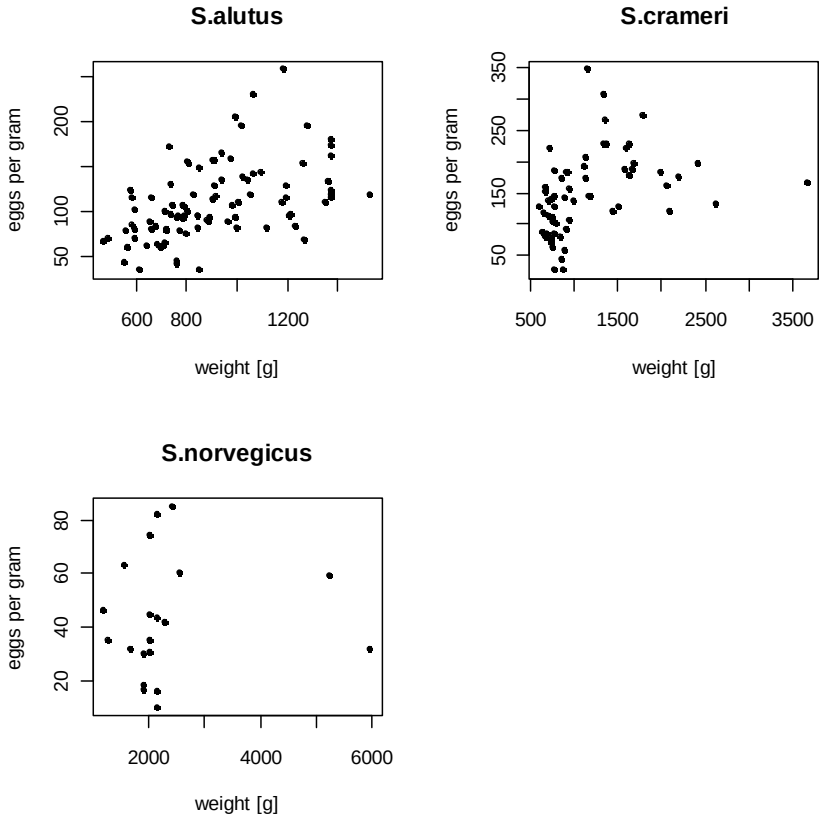

Figure 32. Subgenus *Sebastichthys*. Eggs per gram total body weight versus total body weight.

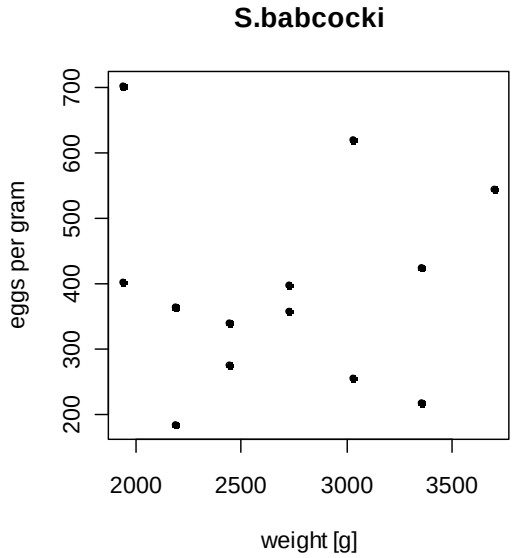

Figure 33. Subgenus *Sebastodes*. Eggs per gram total body weight versus total body weight.

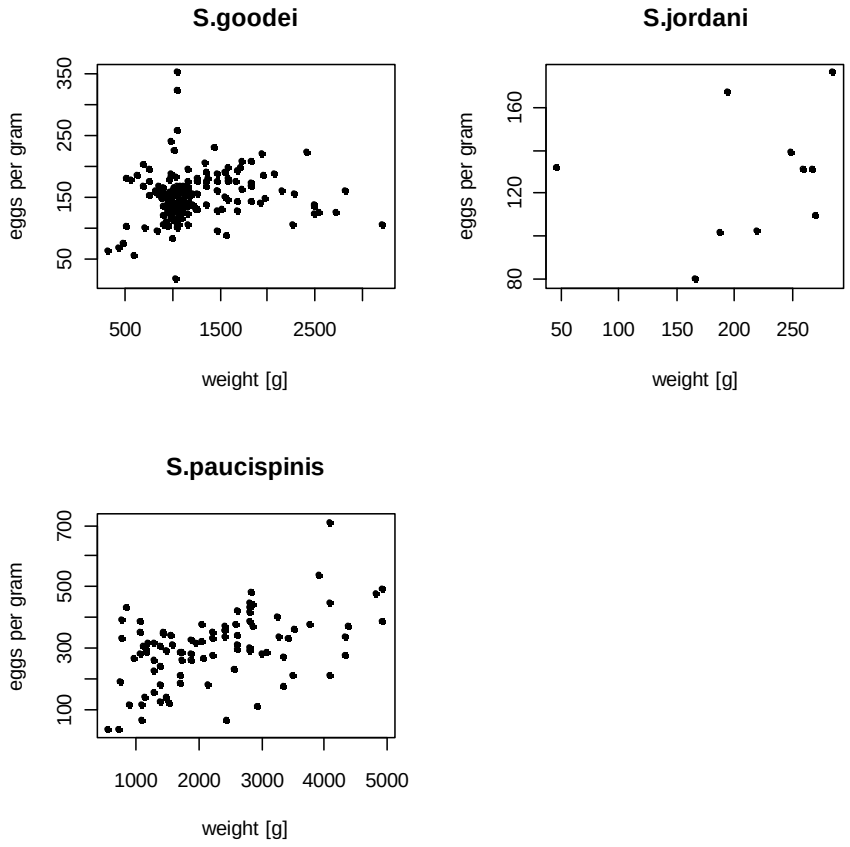

Figure 34. Subgenus *Sebastomus*. Eggs per gram total body weight versus total body weight.

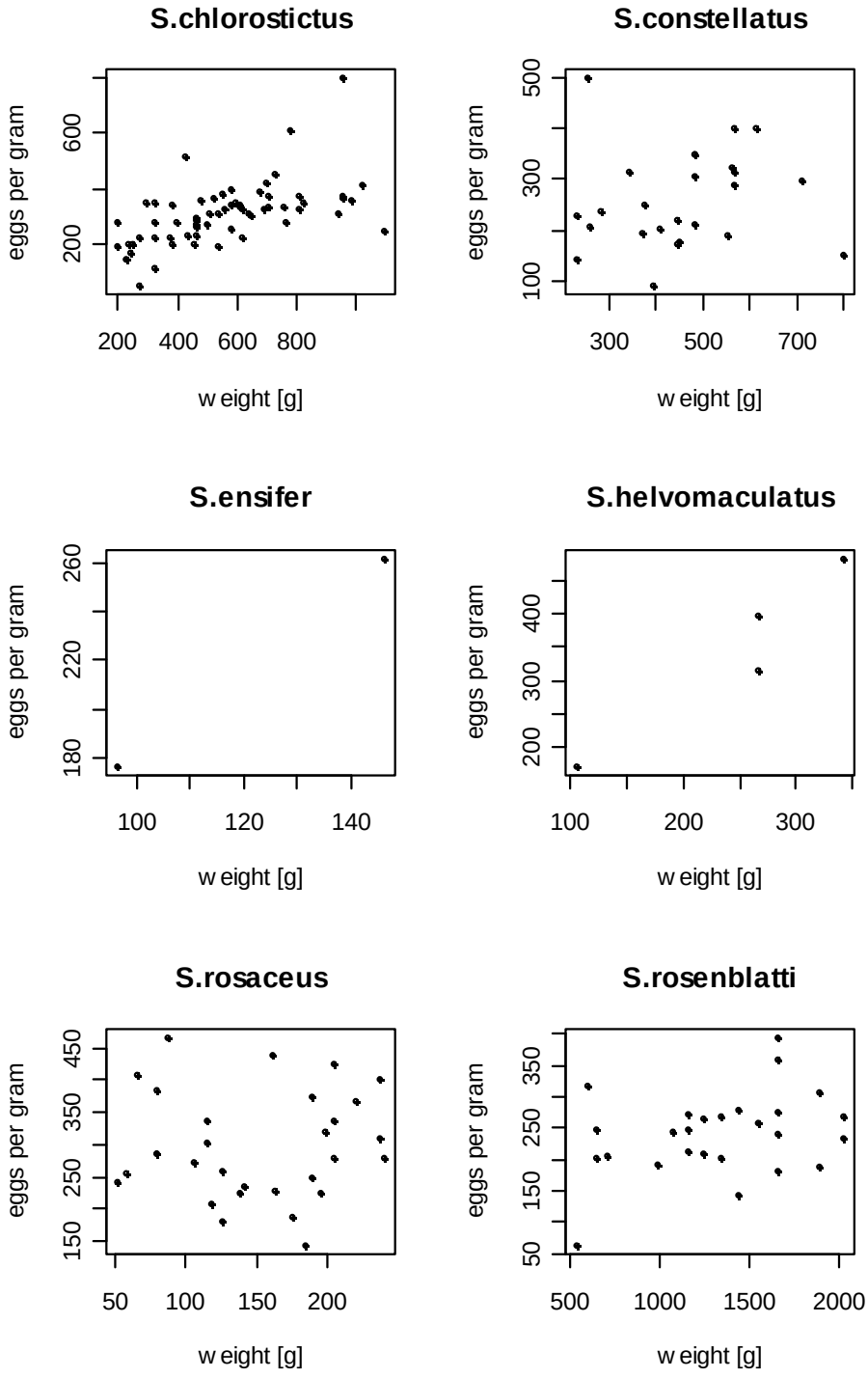

Figure 35. Subgenus *Sebastopyr*. Eggs per gram total body weight versus total body weight.

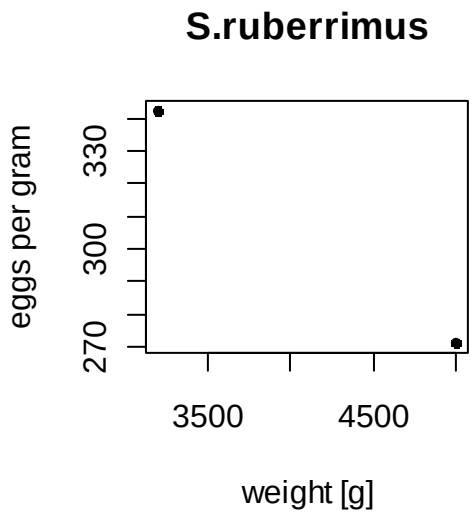

Figure 36. Subgenus *Sebastosomus*. Eggs per gram total body weight versus total body weight.

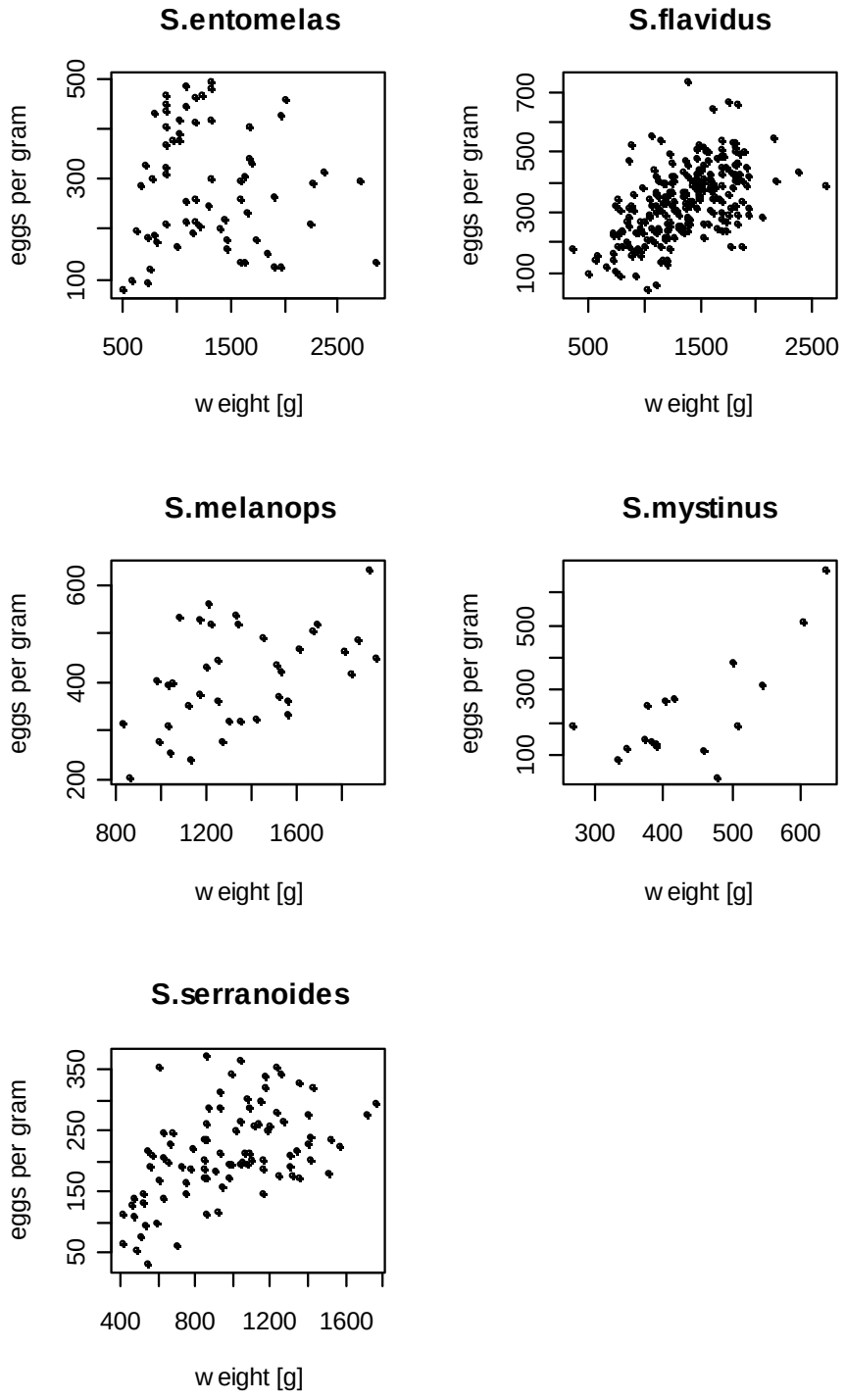

Figure 37. Unassigned species. Eggs per gram total body weight versus total body weight.

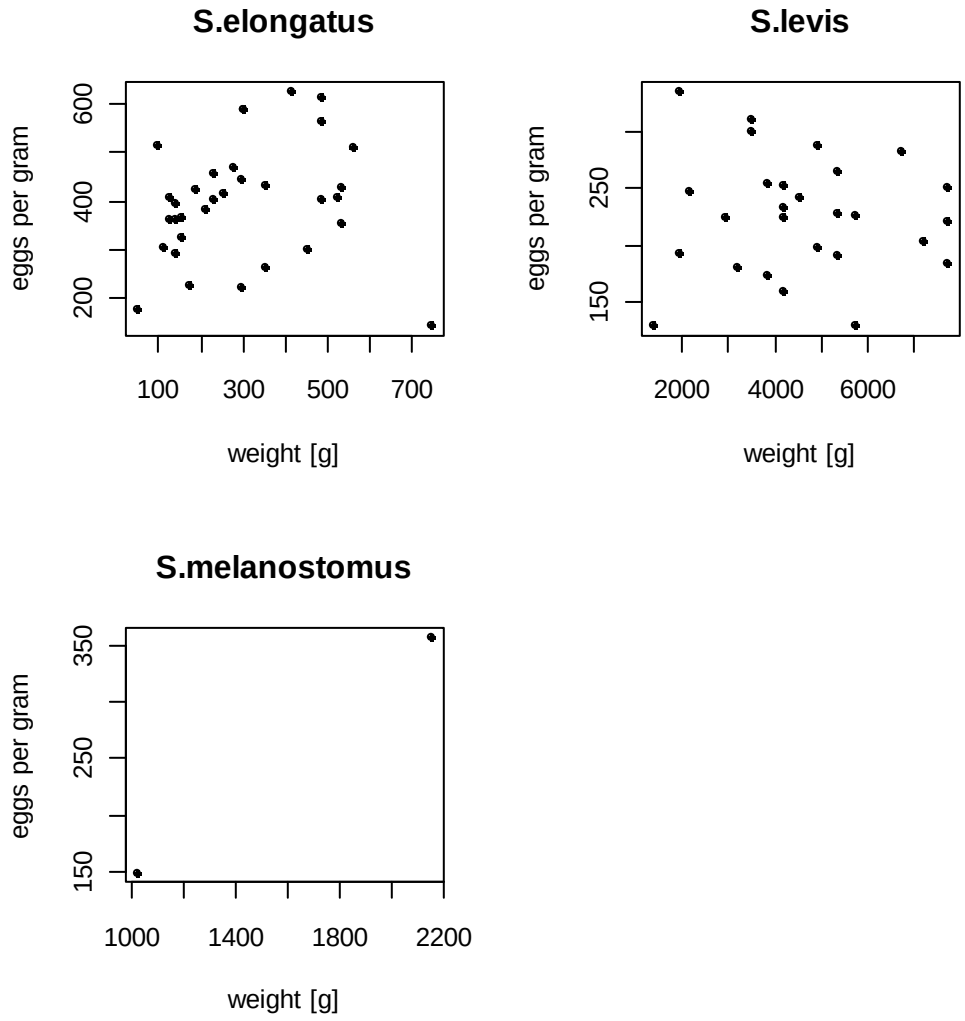

Figure 38. Boxplots (median, interquartile range, and 95% credibility intervals) of posterior slope distributions from model for relative fecundity as a linear function of weight, $\Phi/W = a + bW$. MLEs (circles) are included for comparison. Solid, dashed, and dotted vertical lines are the median, interquartile range, and 95% credibility intervals for the posterior predictive distribution of an unobserved rockfish species. MLEs greater than 0.4 and less than -0.2 are not shown for display purposes (*S. mystinus*, *S. helvomaculatus*, *S. semicinctus*, *S. emphaeus*, *S. ensifer*, *S. dalli*, and *S. proriger*).

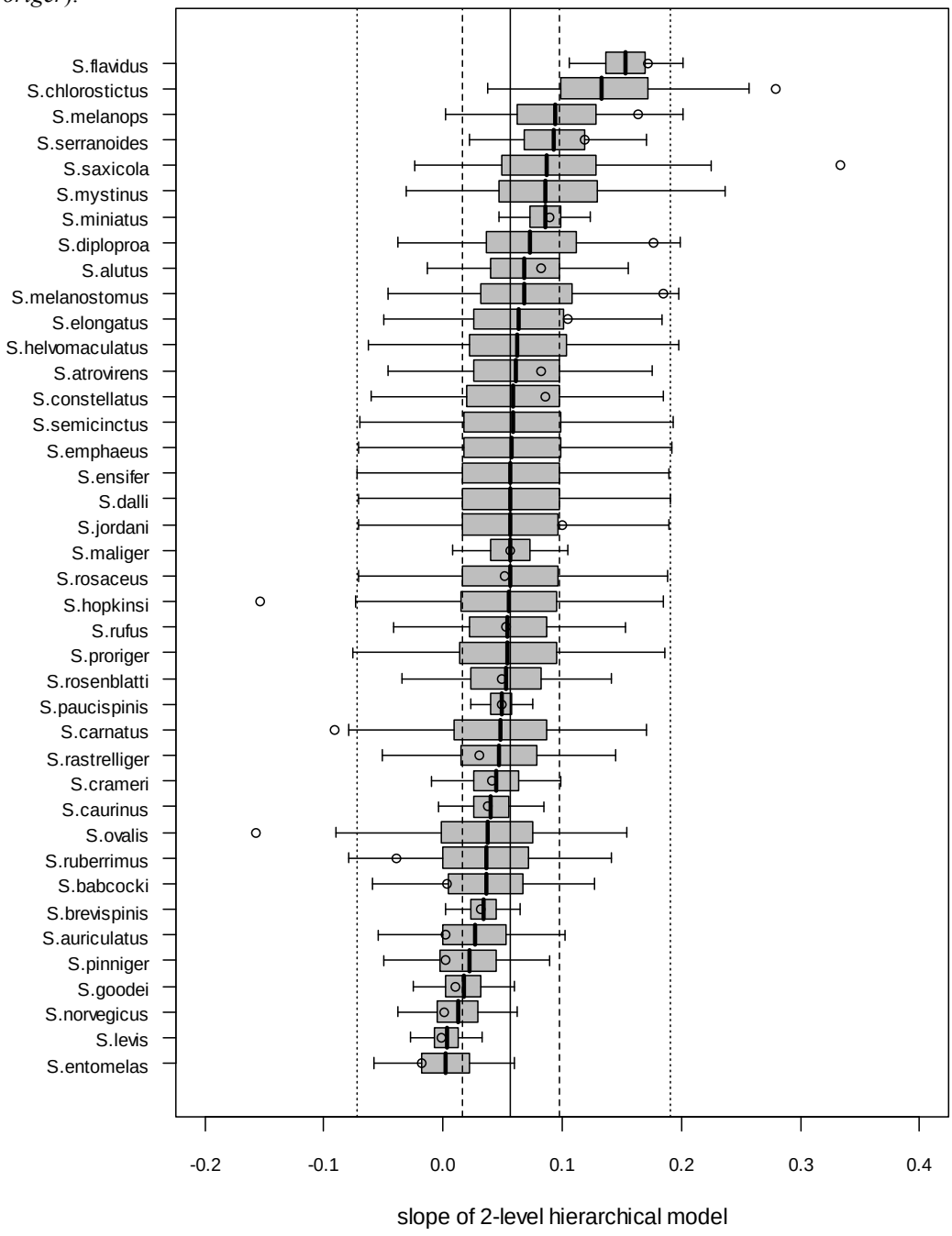

Figure 39. Boxplots (median, interquartile range, and 95% credibility intervals) of posterior intercept distributions from model for relative fecundity as a linear function of weight, $\Phi/W = a + bW$. MLEs (circles) are included for comparison. Solid, dashed, and dotted vertical lines are the median, interquartile range, and 95% credibility intervals for the posterior predictive distribution of an unobserved rockfish species.

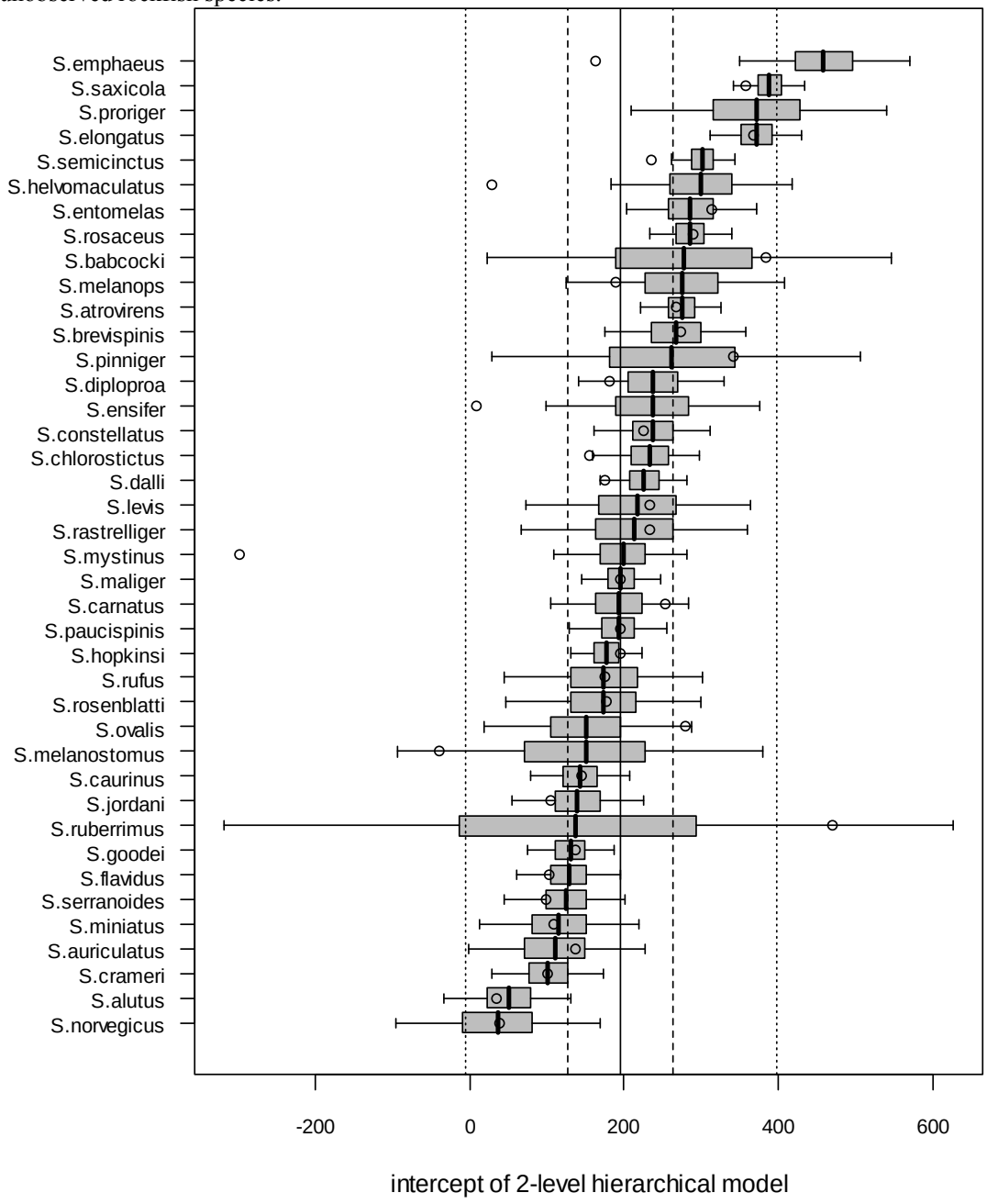

Figure 40. Posterior distributions of variance components from the hierarchical model for relative fecundity as a linear function of total body weight, $\Phi/W = a + bW$. RMSE is root mean squared error, tau.alpha is the variance of the distribution of intercept parameters, and tau.beta is the variance of the distribution of slope parameters.

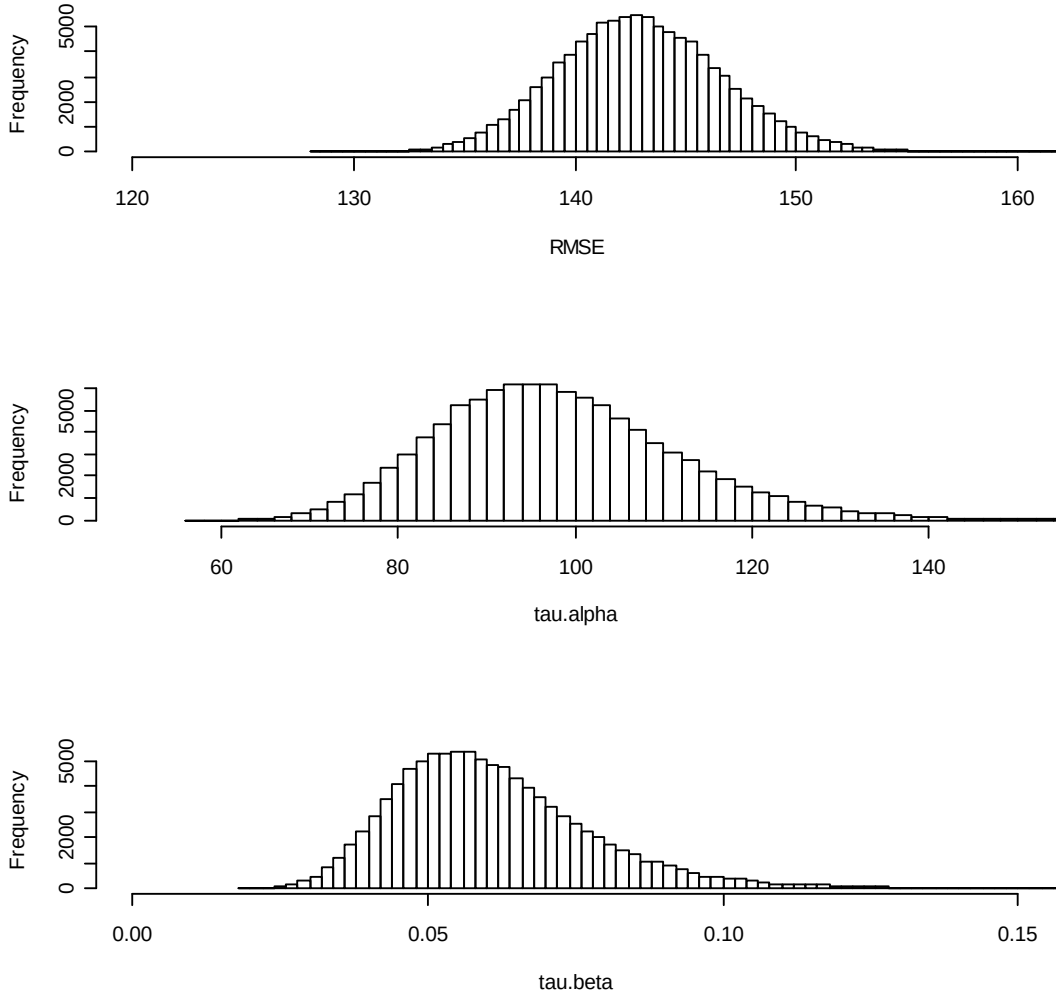

Figure 41. Diagnostic residual plots for maximum likelihood fit to the analysis of covariance model for relative fecundity as a function of total body weight, $\Phi/W = a + bW$.

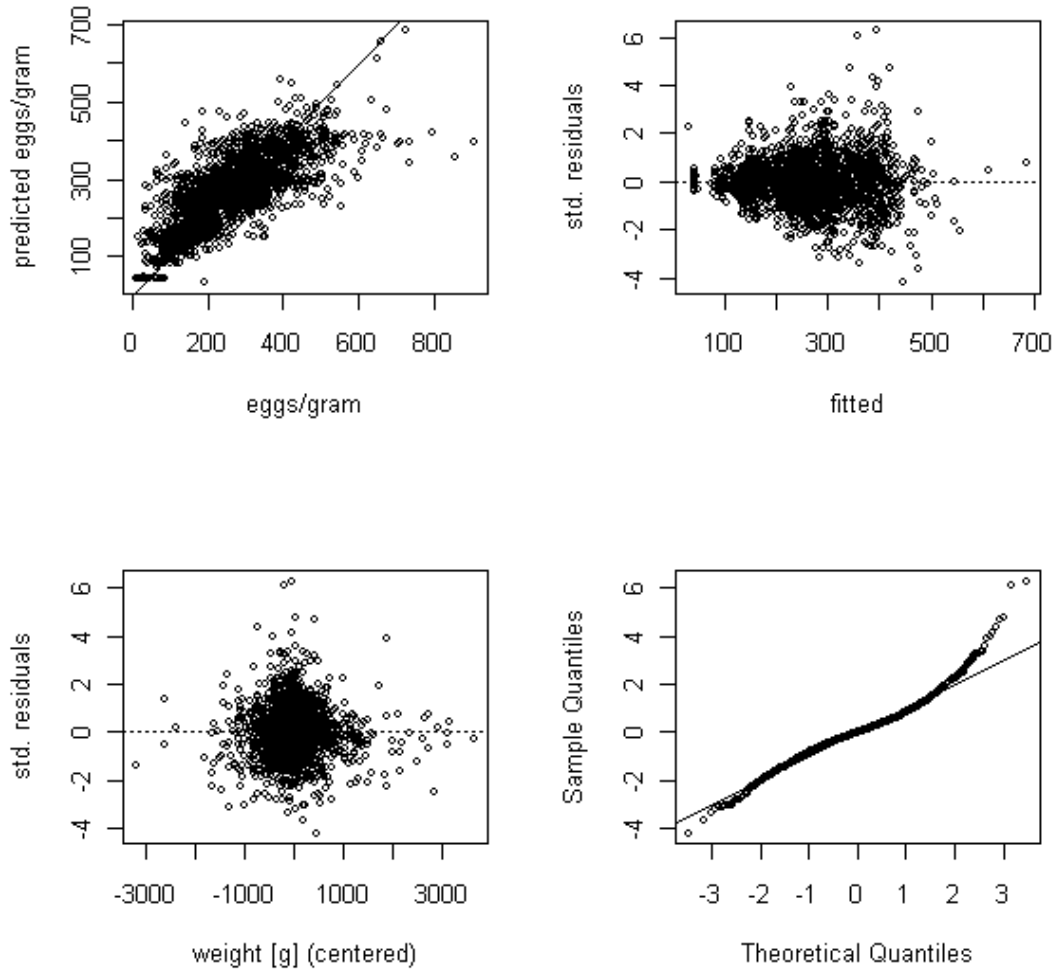

Figure 42. Diagnostic residual plots for maximum likelihood fit to the linearized allometric model of absolute fecundity as a function of total body weight, $\log(\Phi) = \log(c) + d\log(W)$.

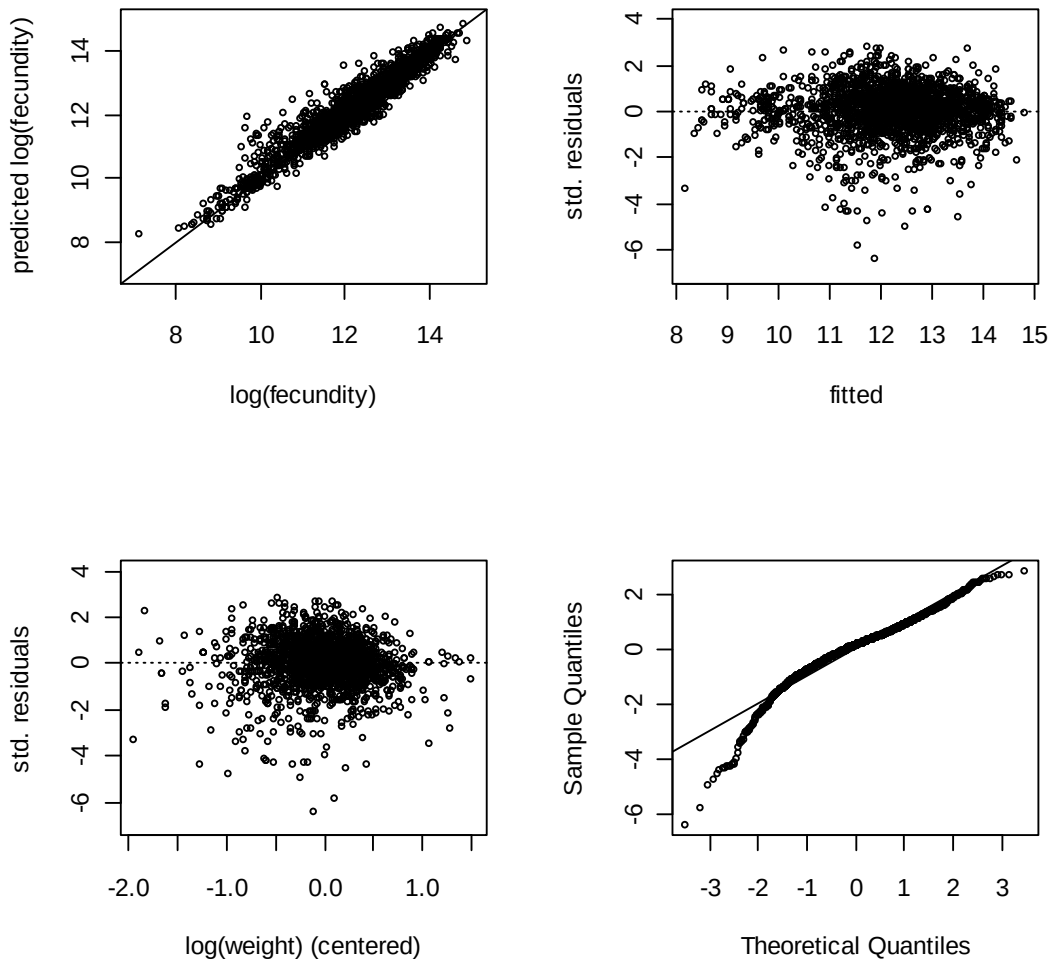

Figure 43. Boxplots (median, interquartile range, and 95% credibility intervals) of posterior slope distributions from model for absolute fecundity as an allometric function of weight, $\log(\Phi) = \log(c) + d\log(W)$. MLEs (circles) are included for comparison. Solid, dashed, and dotted vertical lines are the median, interquartile range, and 95% credibility intervals for the posterior predictive slope distribution of an unobserved rockfish species. The MLE for *S. proriger* is not shown for display purposes, but is reported in Table 13.

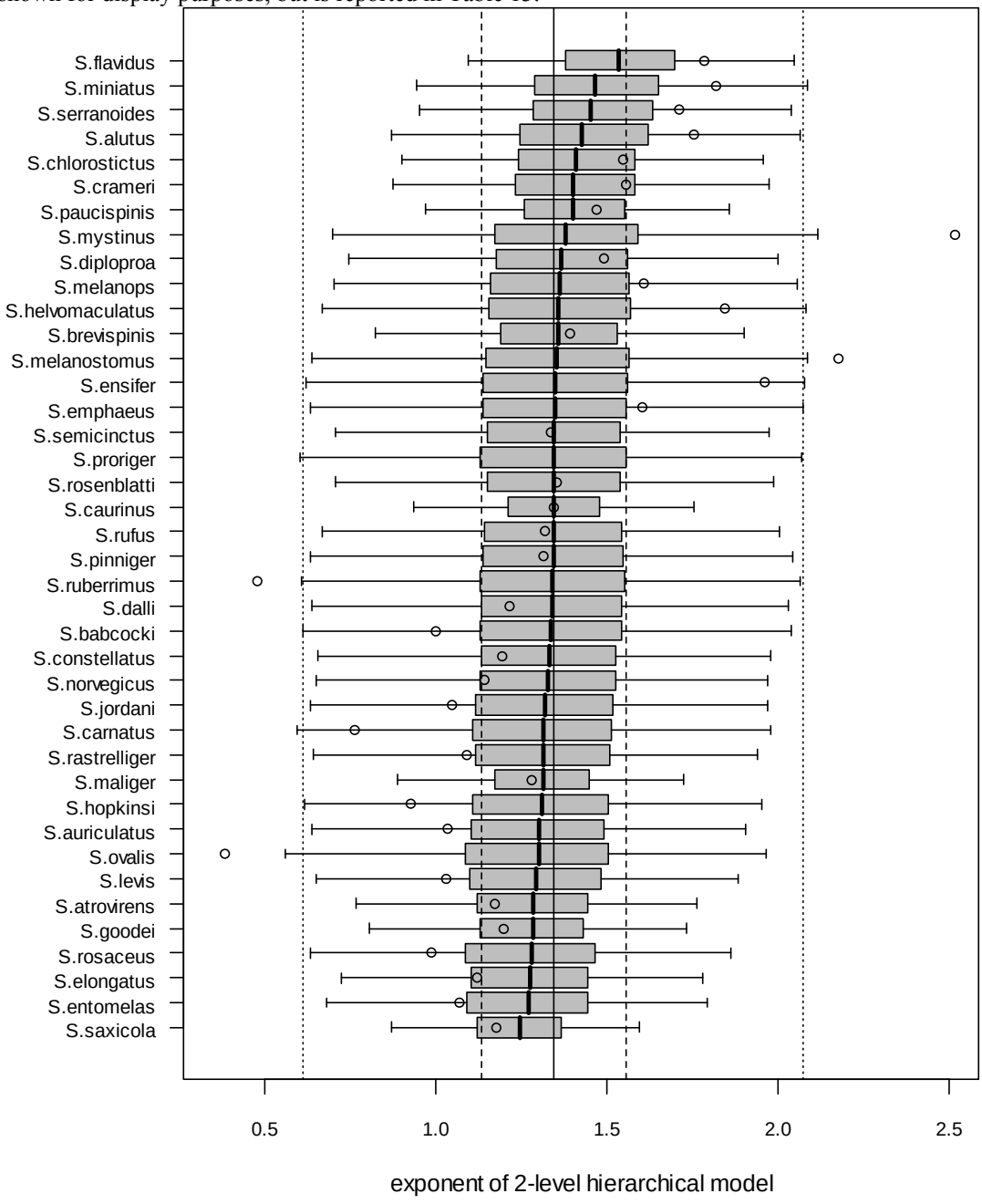

Figure 44. Boxplots (median, interquartile range, and 95% credibility intervals) of posterior intercept distributions (log scale) from model for absolute fecundity as an allometric function of weight, $\log(\Phi) = \log(c) + d\log(W)$. MLEs (circles) are included for comparison. Solid, dashed, and dotted vertical lines are the median, interquartile range, and 95% credibility intervals for the posterior predictive slope distribution of an unobserved rockfish species.

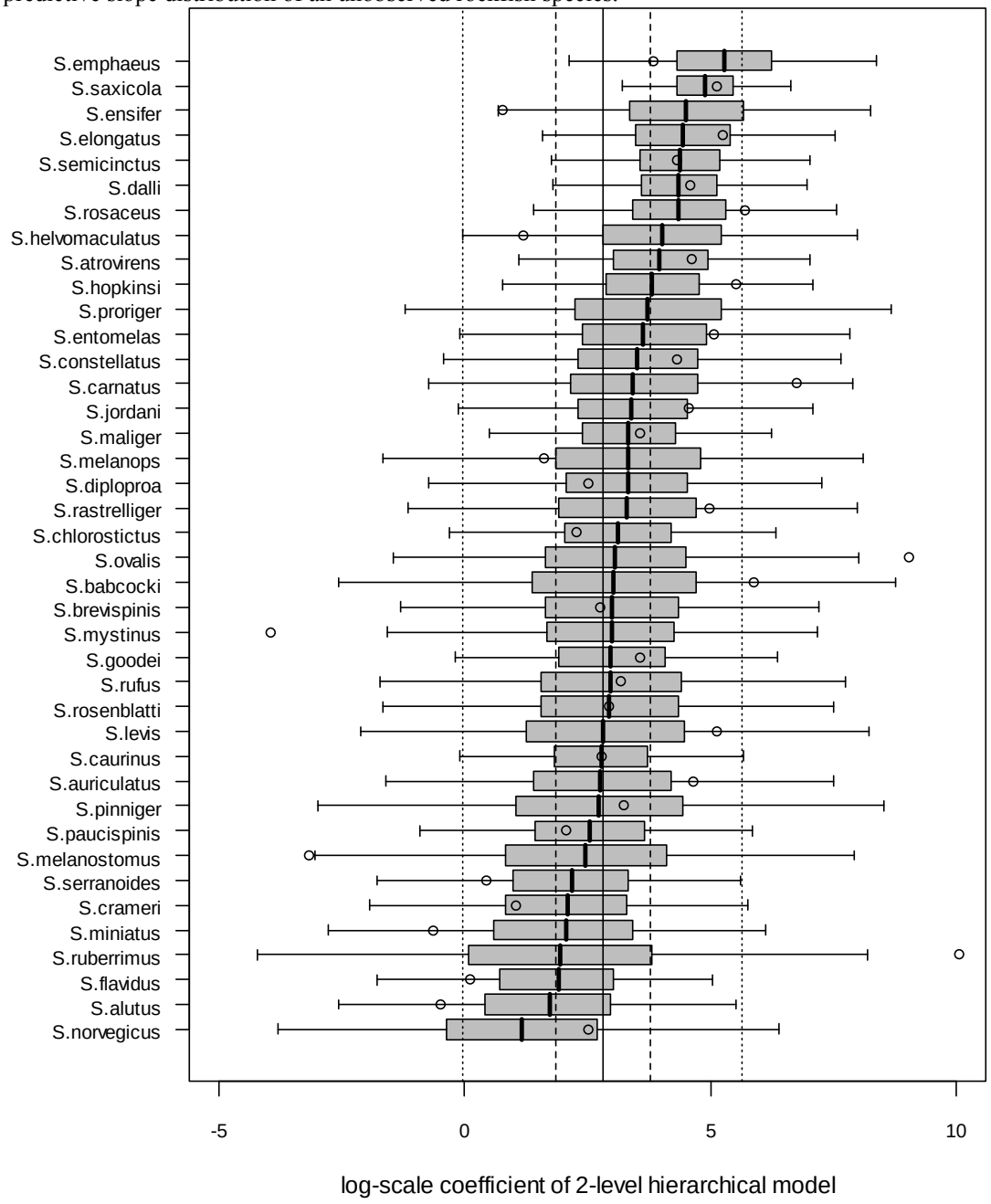

Figure 45. Posterior distributions of variance components from the hierarchical model for absolute fecundity as an allometric function of total body weight, $\log(\Phi) = \log(c) + d\log(W)$. RMSE is root mean squared error (i.e. the data variance), tau.alpha is the variance of the distribution of intercept parameters, and tau.beta is the variance of the distribution of slope parameters.

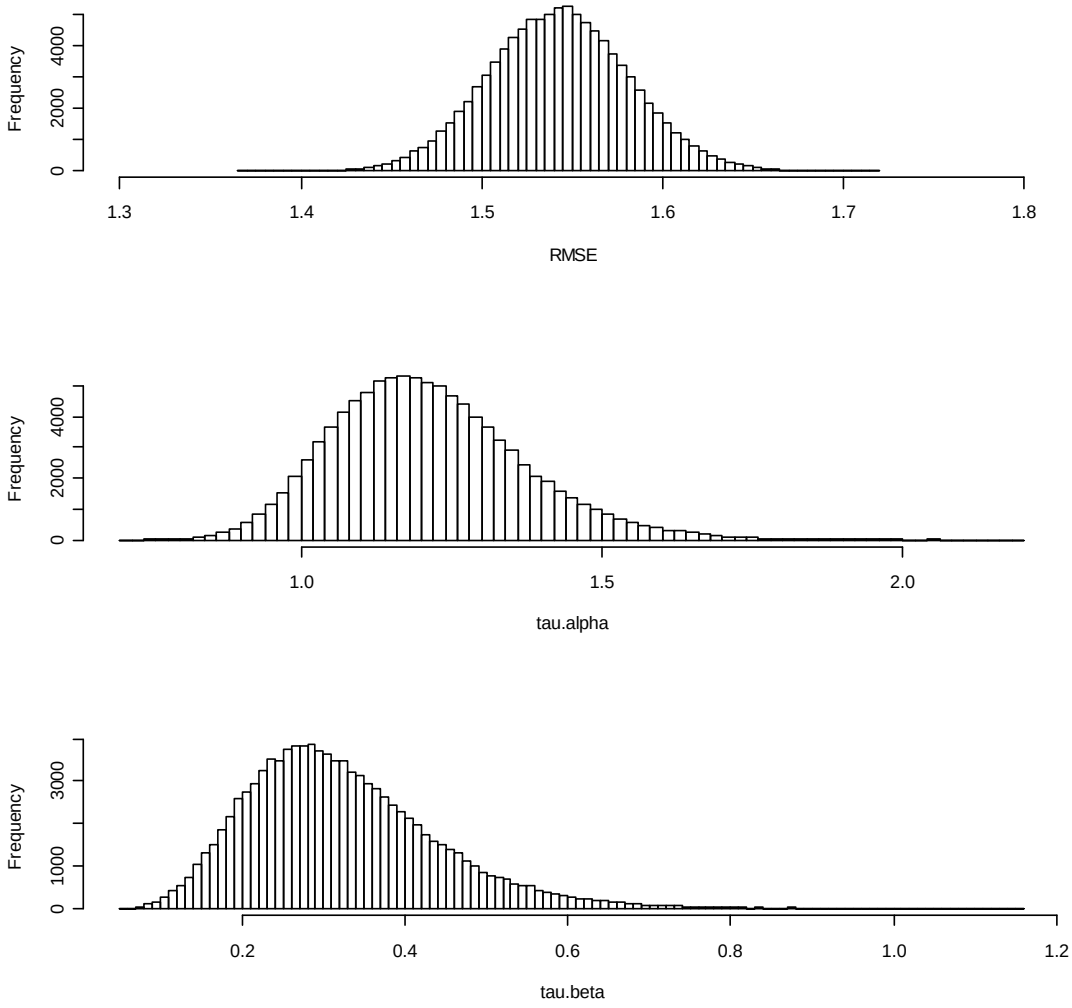

Figure 46. Length increment as a function of length, from four alternative models for the production of surplus energy (ΔW). The growth cost of maturity in the asymptotic production model (Stamps et al., 1998) is set so fish maturing at 1 cm would grow to 33% of the maximum size for immature individuals. Length at maturity is 15 cm, resulting in a maximum potential size for mature fish (no reproduction) of about 88 cm.

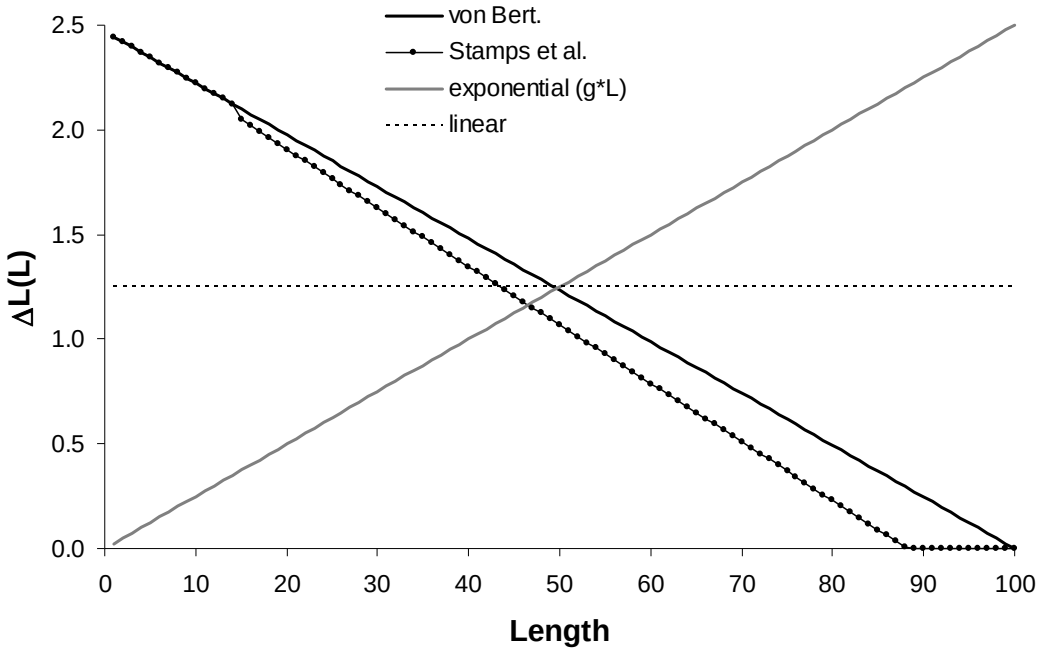

Figure 47. Growth increments in terms of weight corresponding to the length-based increment models shown in Figure 46. ΔW(W) is surplus energy (after maintenance costs) available for allocation to either somatic growth or reproduction. The von Bertalanffy (von Bert.) and Stamps et al. equations limit the ultimate size of an individual that never matures or allocates all surplus energy to growth. The exponential and linear growth models do not constrain immature growth.

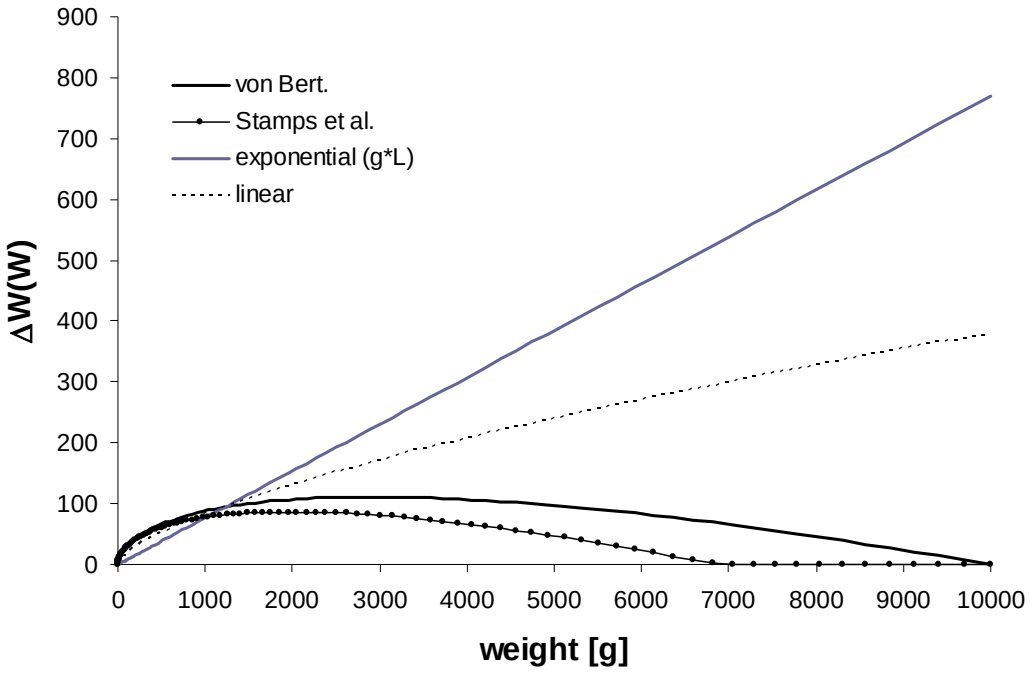

Figure 48. Proportional model for current reproduction as a function of allocation and surplus energy. $R(\rho, \Delta W, \mu=0) = \rho \Delta W e^{-\mu \rho \Delta W}$. The effect of ΔW on R is shown for percentages (10%, 25%, 50%, 75% and 100%) of the maximum value of ΔW (dWmax) generated by the model.

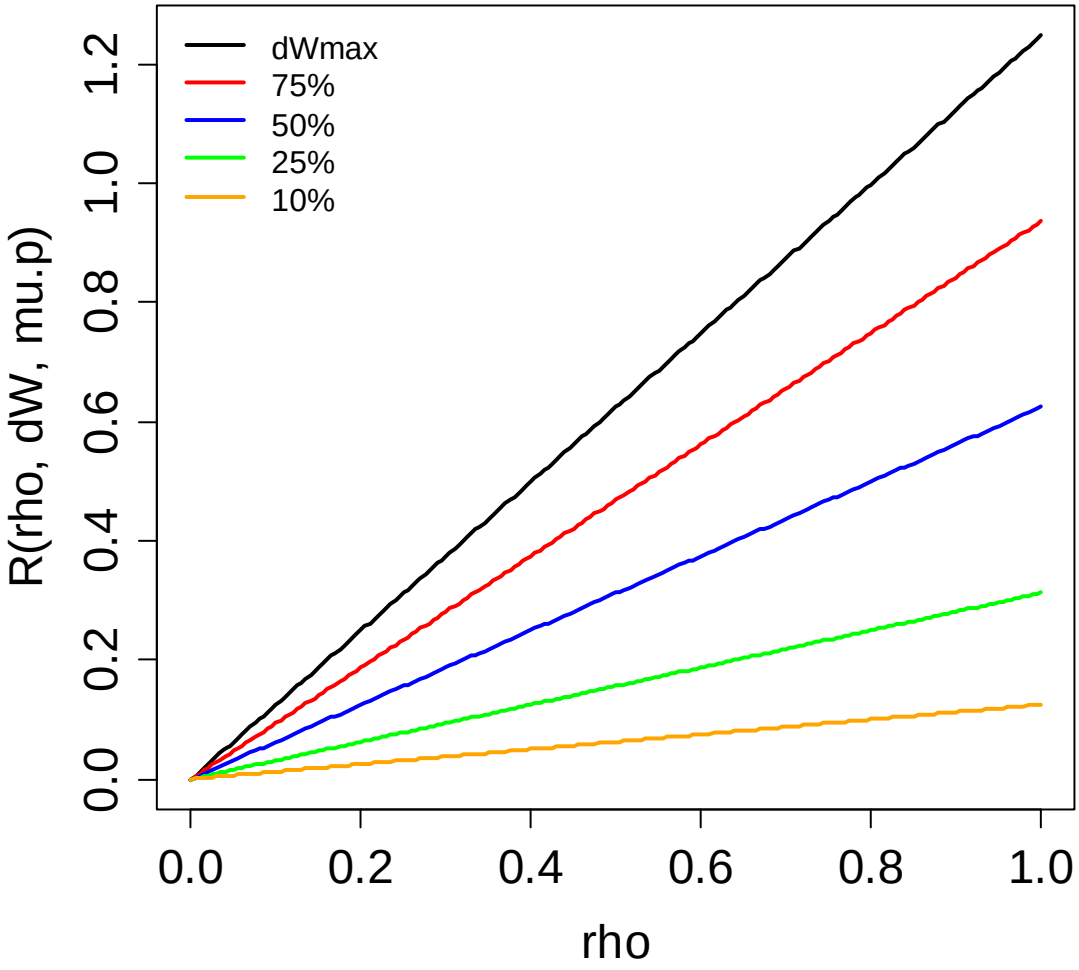

Figure 49. Concave model for current reproduction as a function of allocation and surplus energy. $R(\rho, \Delta W, \mu=0.08) = \rho \Delta W e^{-\mu \rho \Delta W}$. The effect of ΔW on R is shown for percentages (10%, 25%, 50%, 75% and 100%) of the maximum value of ΔW (dWmax) generated by the model.

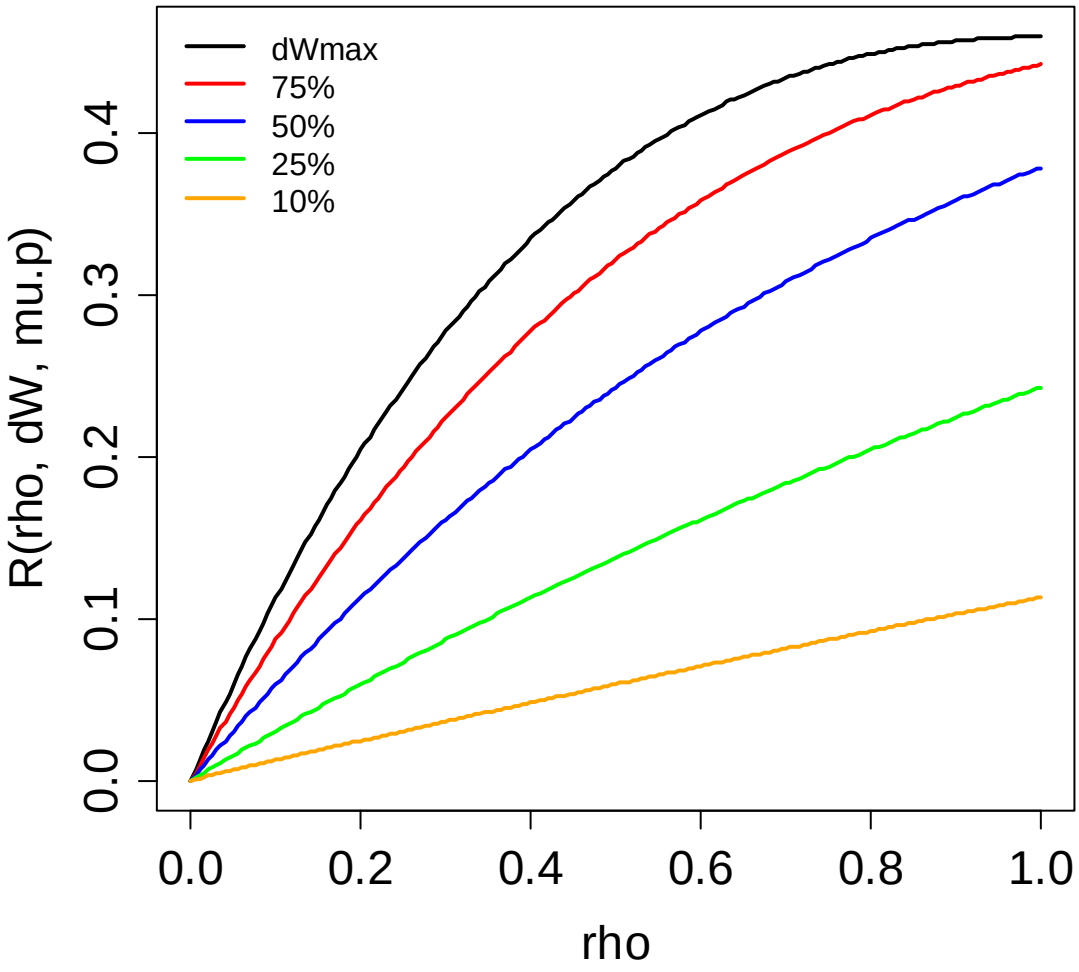

Figure 50. Fraction of potential energy allocated to reproduction as a function of length; predictions from models with exponential, linear, and asymptotic production functions (top, middle, and bottom rows, respectively). Current reproduction is a proportional function (left column) or concave function (right column) of allocation.

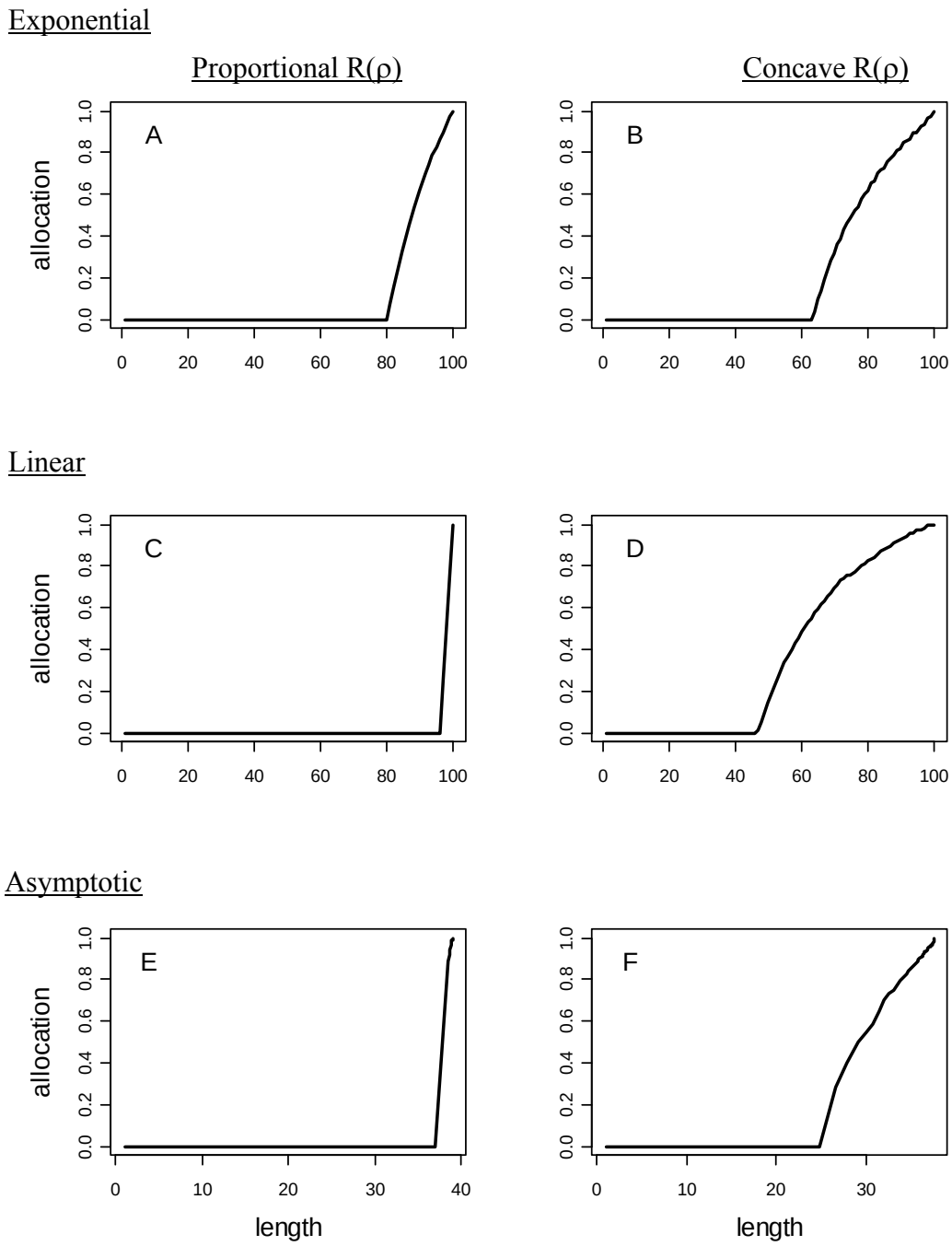

Figure 51. Gonadosomatic index, $\gamma(\rho^*, l, \mu)$, as a function of length; predictions from models with exponential, linear, and asymptotic production functions (top, middle, and bottom rows, respectively). Current reproduction is a proportional function (left column) or concave function (right column) of allocation.

Exponential

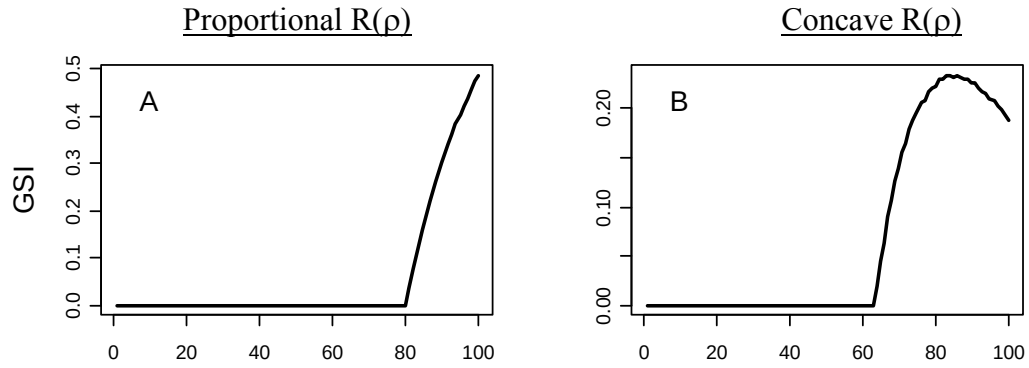

Linear

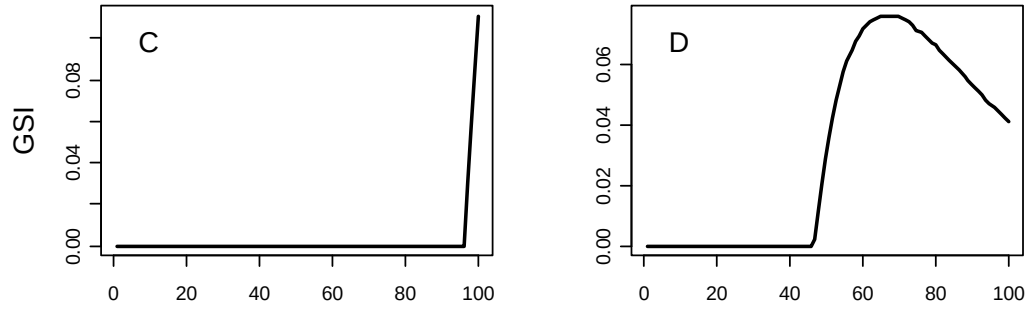

Asymptotic

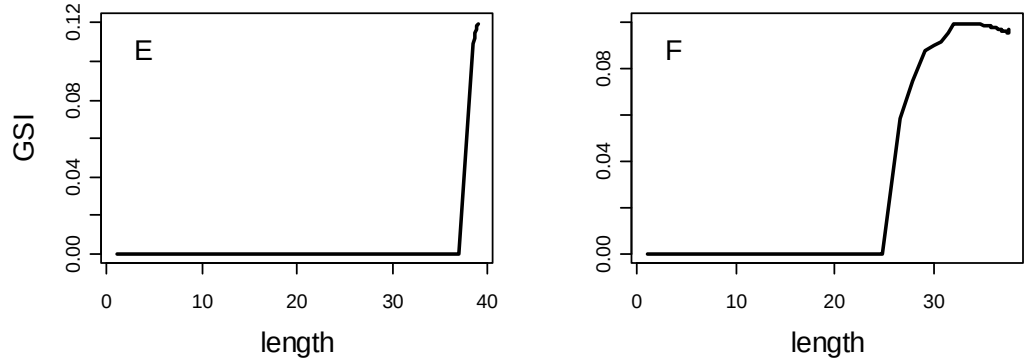

Figure 52. Length at age (solid line) and age at maturity (dotted line); predictions from models with exponential, linear, and asymptotic production functions (top, middle, and bottom rows, respectively). Current reproduction is a proportional function (left column) or concave function (right column) of allocation.

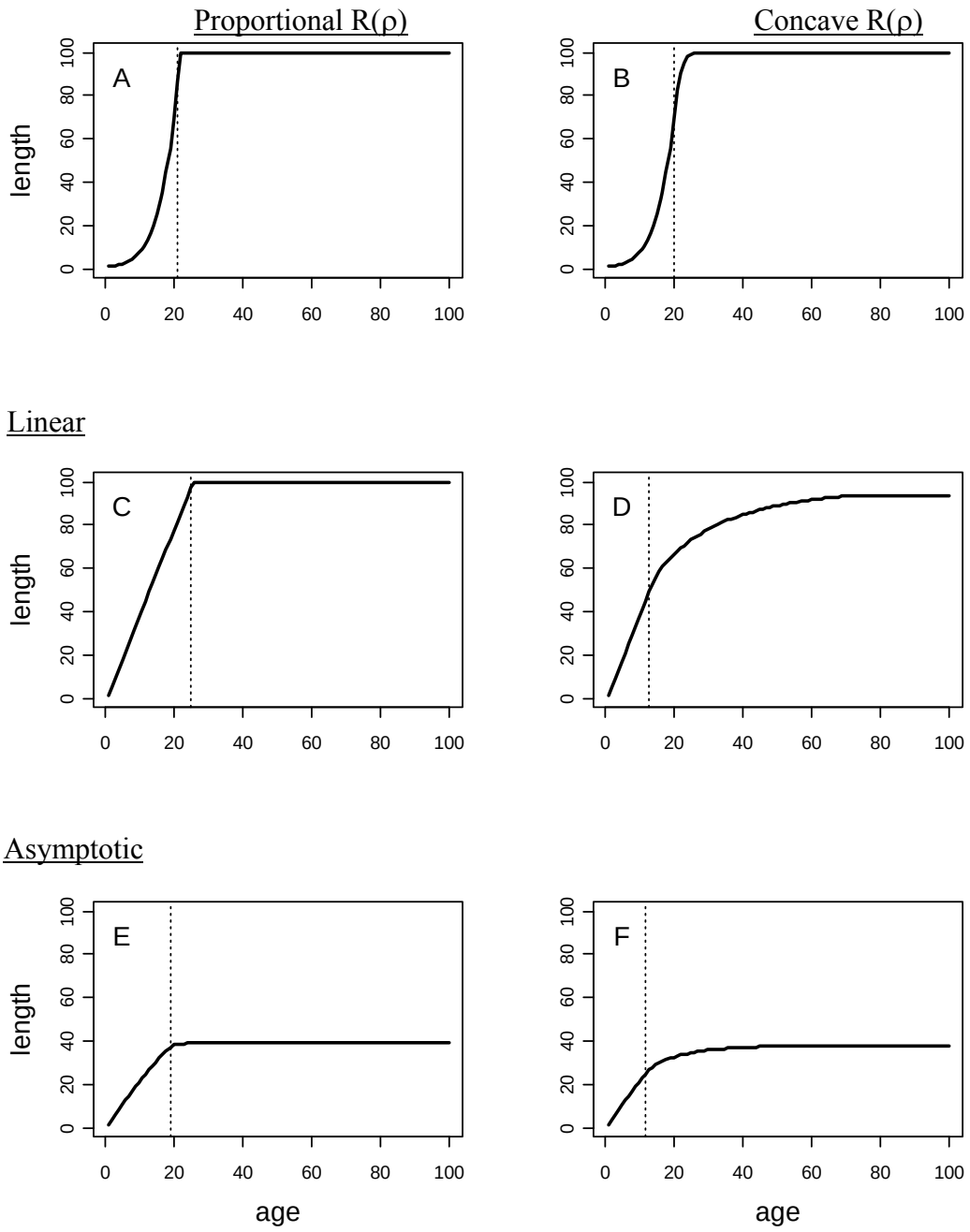

Figure 53. Mortality at age and allocation at length, assuming natural mortality increases as a quadratic function of GSI (Equation 4.29). Reproduction is proportional to potential growth ($R = \rho \Delta W$) in all panels. The production function is linear ($\Delta L(l) = C$) in panels A & C and asymptotic (Equations 4.13 and 4.14) in panels B & D.

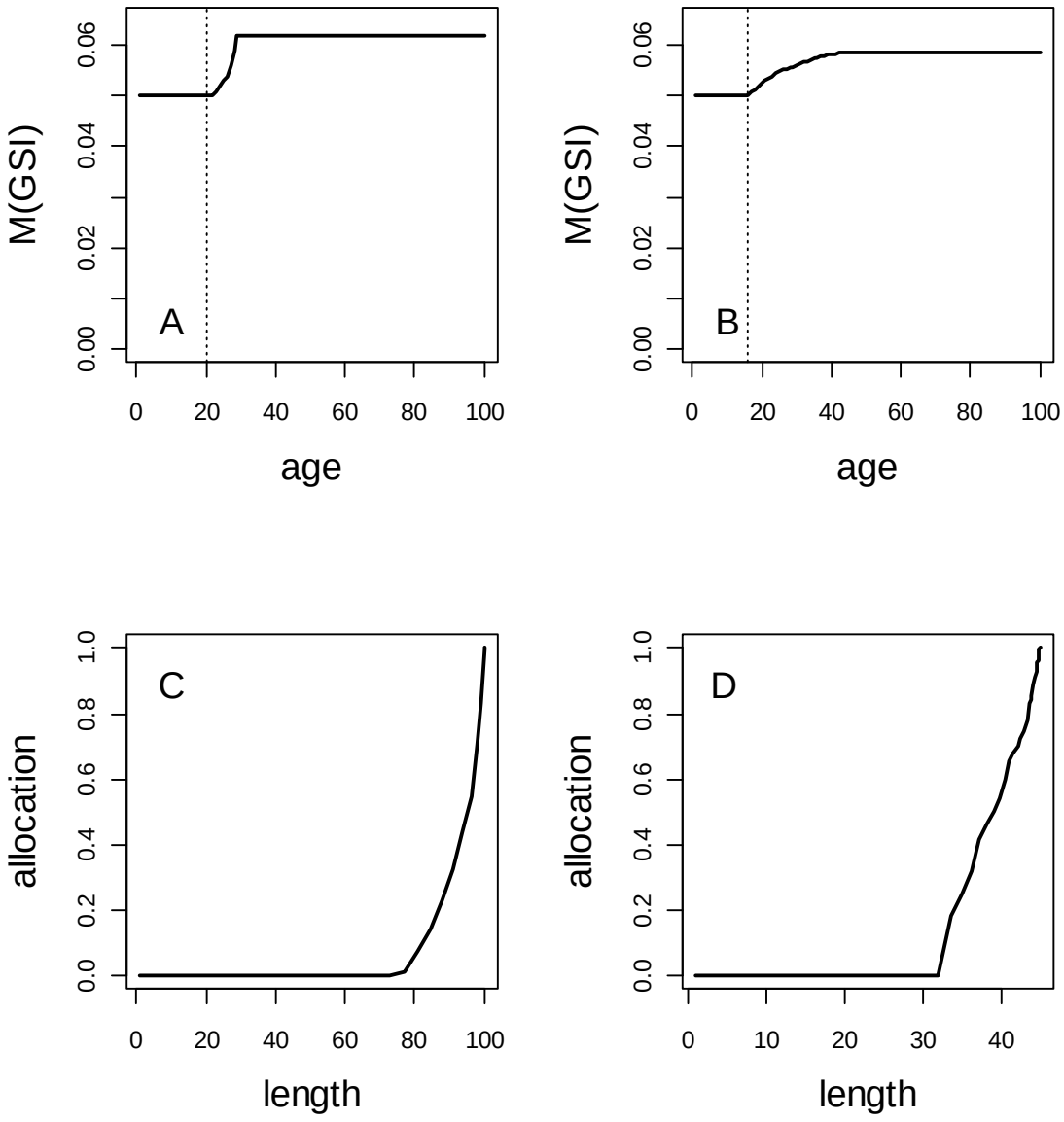

Figure 54. GSI at length and length at age, assuming natural mortality increases as a quadratic function of GSI (Equation 4.29). Reproduction is proportional to potential growth ($R = \rho \Delta W$) in all panels. The production function is linear ($\Delta L(l) = C$) in panels A & C and asymptotic (Equations 4.13 and 4.14) in panels B & D. Age at maturity is shown by the dotted lines in panels C & D.

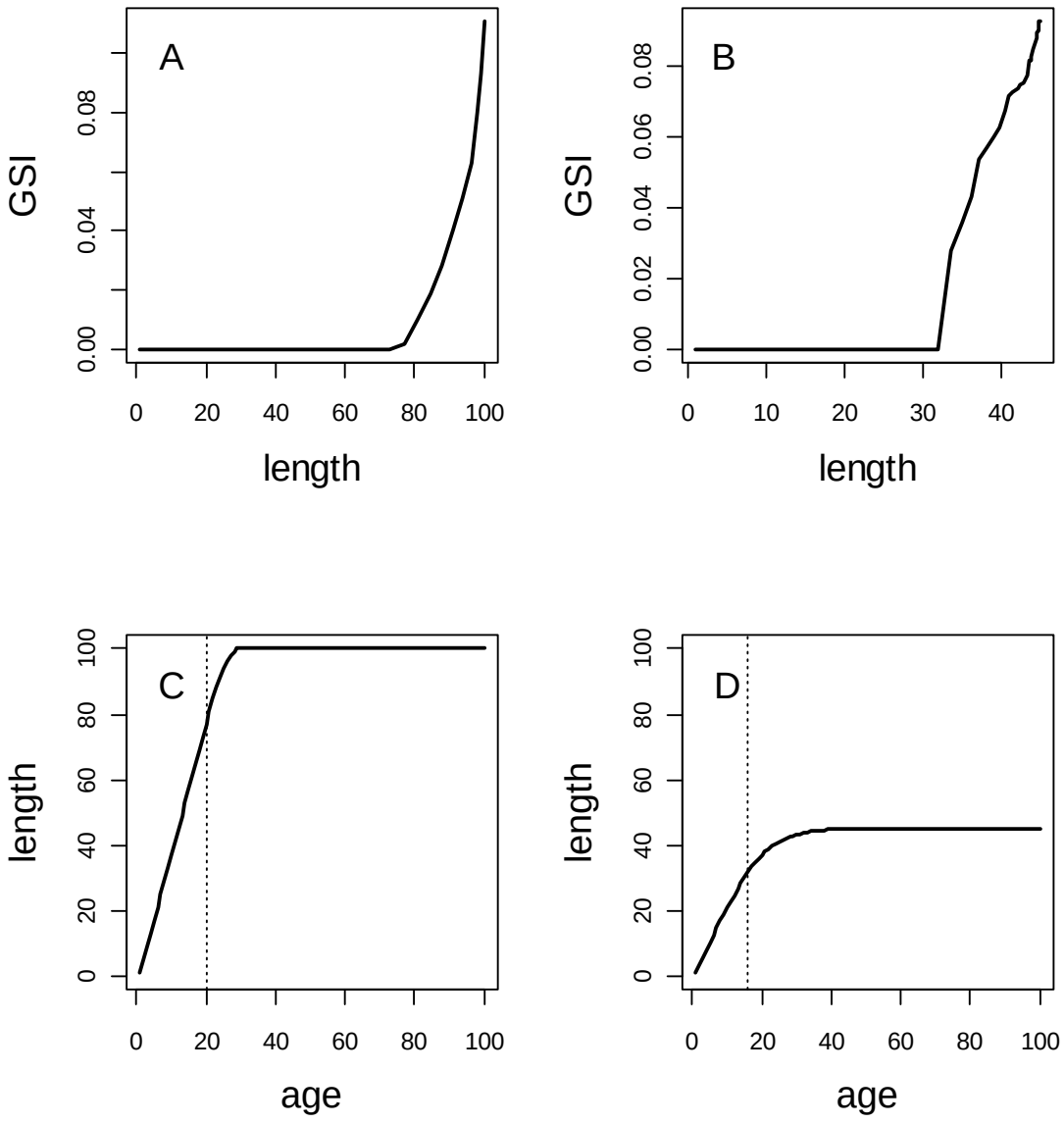

APPENDIX A

METHODS FOR DATA RECOVERY FROM PUBLISHED FIGURES AND COMPARISONS TO REPORTED RESULTS.

Data from three sources were not readily available in numerical format (Love and Westphal, 1981; Romero, 1988; Love *et al*., 1990). I recovered these data from scatterplots of absolute fecundity versus length using a digital scanner and the software program GraphClick (Arizona Software, 2008).

I estimated the parameters of a power function for fecundity in terms of total length for each digitized data set using linear regression following natural-log transformation of the variables (Equations 1.1-1.4 in main text). I then plotted the expected fecundity at length curve with the digitized data, and superimposed the fecundity-length relationship reported in the original publication.

I digitized data on copper rockfish (*S. caurinus*) from Washington *et al*. (1978) because an appendix with the numerical data (referred to in the report) is missing from all the copies we could locate. Dan Ito (NMFS) later located the original data in a report submitted as part of a course taken at the University of Washington (Ito 1977). This data set allowed me to evaluate the accuracy of the digitization procedure by plotting digitized length and fecundity values against the original measurements (Figure A1).

Love *et al*. (1990, their Figure 12) plotted fecundity (1000s of eggs) against total length in cm for 16 rockfish species from the Southern California Bight. They reported fecundity-length parameter estimates, and tabulated minimum and

maximum values of fecundity (eggs) and length (mm) for these sixteen species, plus an additional 3 species. They also report estimated parameters of the weight-length relationship for each species. I compare the digitized data, my fitted fecundity-length curves (Table A1), and the original reported curves in Figures A2 – A17.

Love *et al*. (1990) report the value of the scalar coefficient (*a*) to one significant figure for *S. chlorostictus*, *S. entomelas*, *S. flavidus*, and *S. miniatus*. Discrepancies between the original and digitized fits may be related to this difference in reported precision. The original figure for *S. goodei* in Love *et al*. (1990) has 38 observations, compared to the reported sample size of 37, and the figure for *S. miniatus* has 46 observations, compared to the reported sample size of 45. The reported minimum egg number for this species (158,915) appears to be the second smallest observation in the graph, based on the recovered data. For *S. saxicola*, the reported sample size doesn't match the number of points on the graph (33 versus 30). The observed minimum number of eggs for this species appears to be missing from the figure. I added this value (1,245) to the digitized data set, and the fit to the digitized data very closely matched the reported curve.

I digitized data from Romero (1988) and fit the allometric fecundity-length model described by Equations 2.10 through 2.13 (Figure A18). The fit to the digitized data predicted higher fecundity at length than the curve reported by Romero, which only provides one digit accuracy for the scalar coefficient. The reported value for this parameter is closer to the estimate from the digitized data

prior to applying the bias correction factor (Equation 2.13). The author does not mention use of a bias correction factor in the text, so this may explain the discrepancy between the reported and newly-estimated parameters. The value of the exponent from the digitized fit (4.120) is very similar to the value reported by Romero (4.134).

Love and Westphal (1981) estimated the fecundity of 83 mature olive rockfish. A typographic error is evident in their Figure 10, with respect to the sample size in the figure caption (87, versus 83 described in the text), and the values of the fecundity-length parameters. Plotting predicted values from the reported curve against the data shows that the reported fit underestimates fecundity at length for this sample (Figure A19). Love (1978) reports another set of parameter values for these data, which appear to better represent the relationship between fecundity and length. This curve is consistently lower than the fit to the digitized data, which again may be the result of back-transformation of the scalar coefficient without first including the bias-correction term. Error introduced by the digitization process may also account for the discrepancy.

Table A1: Parameter estimates from allometric fecundity-length model fitted to digitized data from Love *et al*. (1990).

species	RMSE	a	b	R
S. chlorostictus	0.1560	6.33E-06	4.939	0.916
S. constellatus	0.1267	4.96E-05	4.345	0.853
S. dalli	0.1135	3.52E-04	3.906	0.744
S. elongatus	0.1177	2.07E-04	3.963	0.946
S. entomelas	0.0840	1.60E-05	4.514	0.884
S. flavidus	0.0926	5.09E-06	4.769	0.897
S. goodei	0.0961	2.27E-04	3.566	0.904
S. hopkinsi	0.0870	5.01E-03	2.744	0.764
S. levis	0.1072	1.49E-03	3.192	0.885
S. miniatus	0.1189	1.86E-06	5.009	0.922
S. paucispinis	0.0592	7.84E-04	3.368	0.955
S. rosaceus	0.1164	8.67E-04	3.594	0.886
S. rosenblatti	0.1406	4.31E-05	4.201	0.857
S. rufus	0.1307	4.09E-05	4.149	0.817
S. saxicola	0.1249	1.13E-03	3.562	0.973
S. semicinctus	0.0798	2.84E-04	3.929	0.910

Figure A1: Comparison of digitized data from Washington *et al*. (1978) to the original data from Ito (1977). A) length data, B) fecundity data

A)

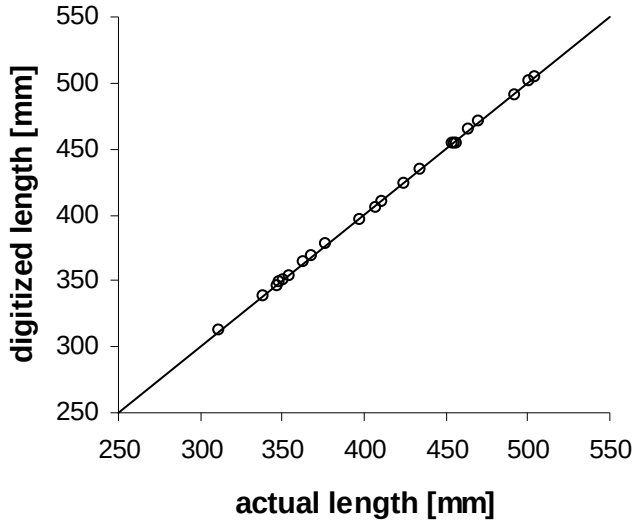

B)

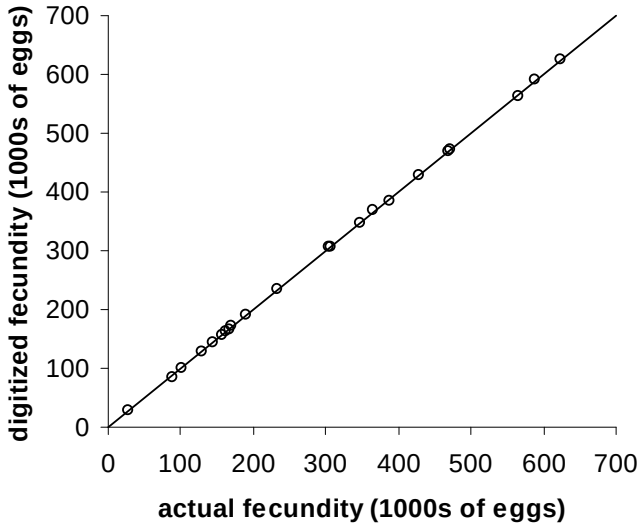

Figure A2. Digitized fecundity and length data for *S. chlorostictus* from Love et al. (1990); lines are reported fecundity-length model (dashed line) and model fit to digitized data (solid line).

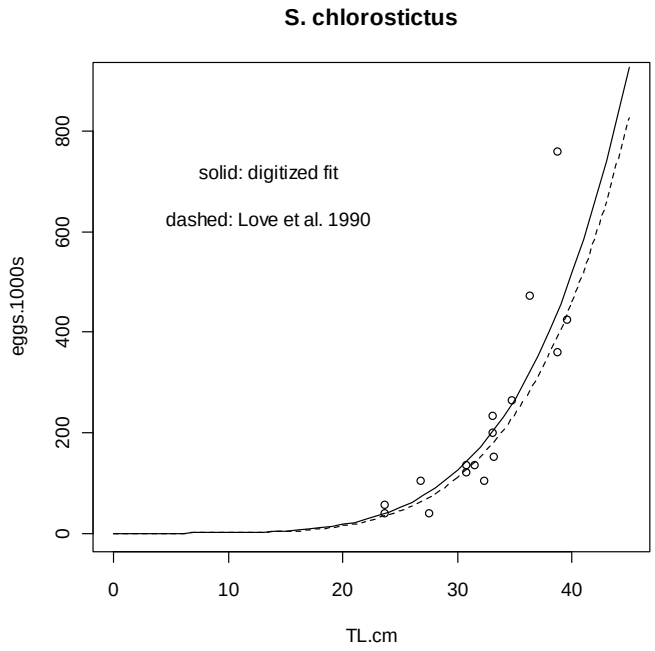

Figure A3. Digitized fecundity and length data for *S. constellatus* from Love et al. (1990); lines are reported fecundity-length model (dashed line) and model fit to digitized data (solid line).

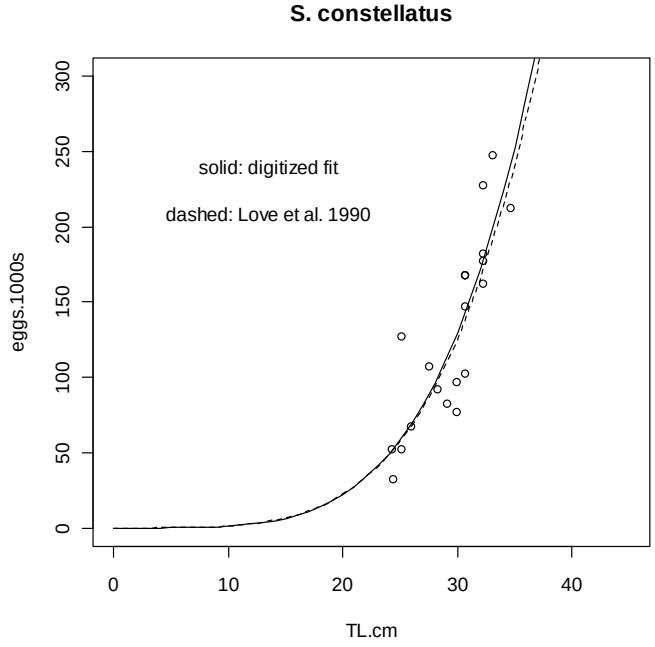

Figure A4. Digitized fecundity and length data for *S. dalli* from Love et al. (1990); lines are reported fecundity-length model (dashed line) and model fit to digitized data (solid line).

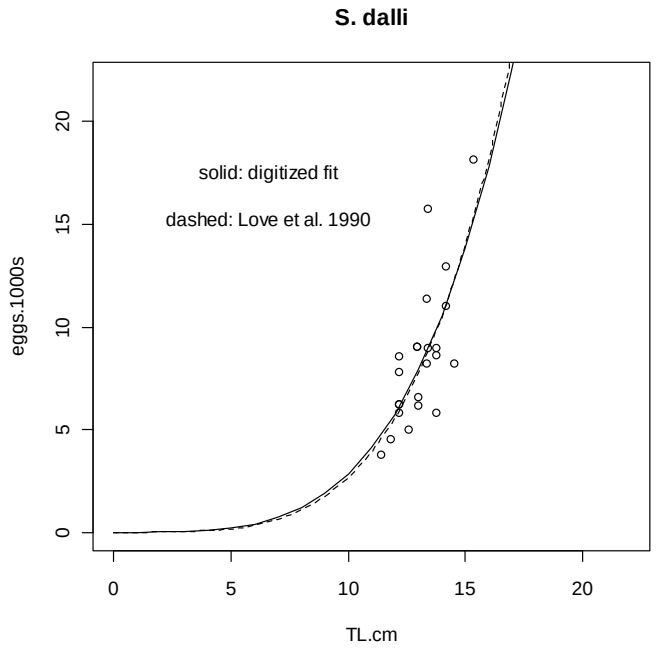

Figure A5. Digitized fecundity and length data for *S. elongatus* from Love et al. (1990); lines are reported fecundity-length model (dashed line) and model fit to digitized data (solid line).

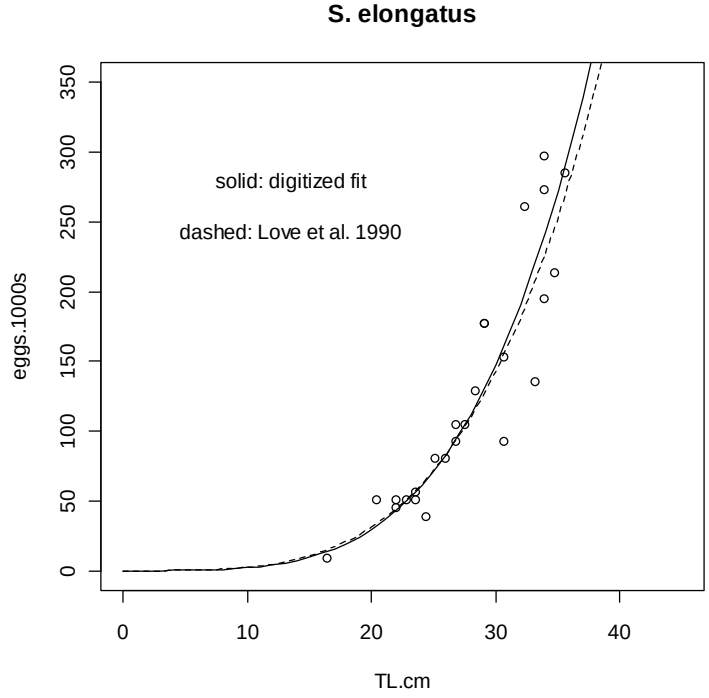

Figure A6. Digitized fecundity and length data for *S. entomelas* from Love et al. (1990); lines are reported fecundity-length model (dashed line) and model fit to digitized data (solid line).

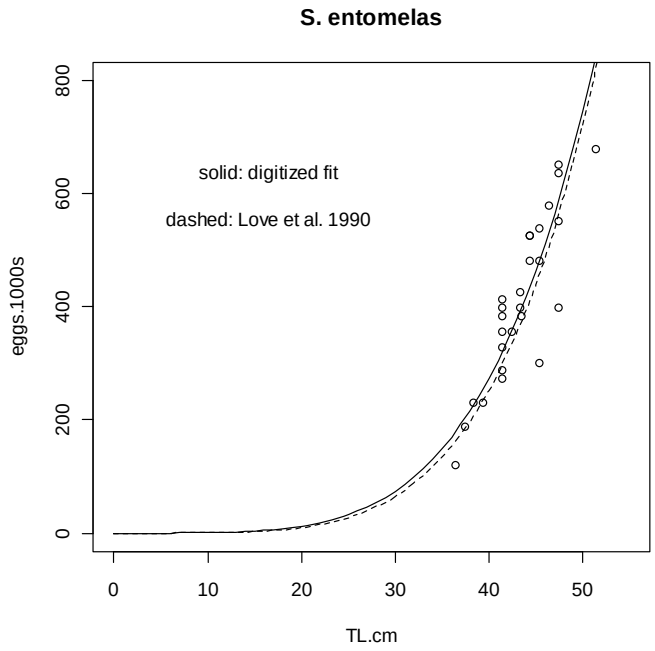

Figure A7. Digitized fecundity and length data for *S. flavidus* from Love et al. (1990); lines are reported fecundity-length model (dashed line) and model fit to digitized data (solid line).

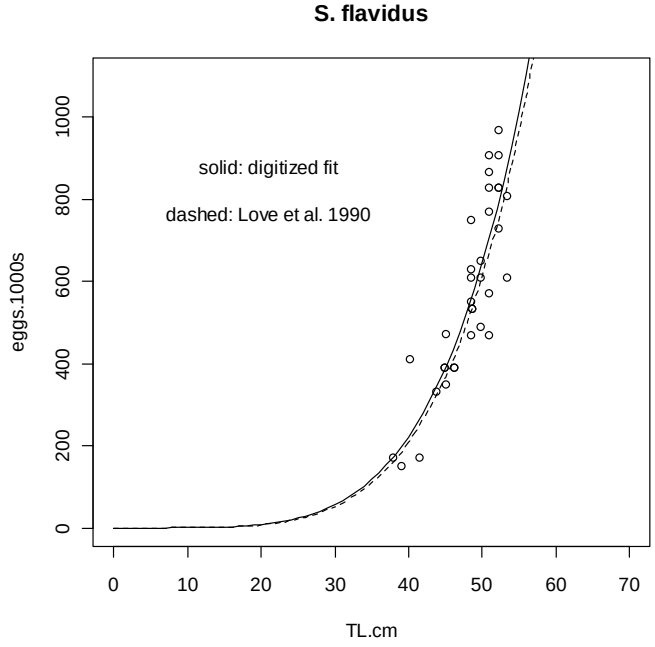

Figure A8. Digitized fecundity and length data for *S. goodei* from Love et al. (1990); lines are reported fecundity-length model (dashed line) and model fit to digitized data (solid line).

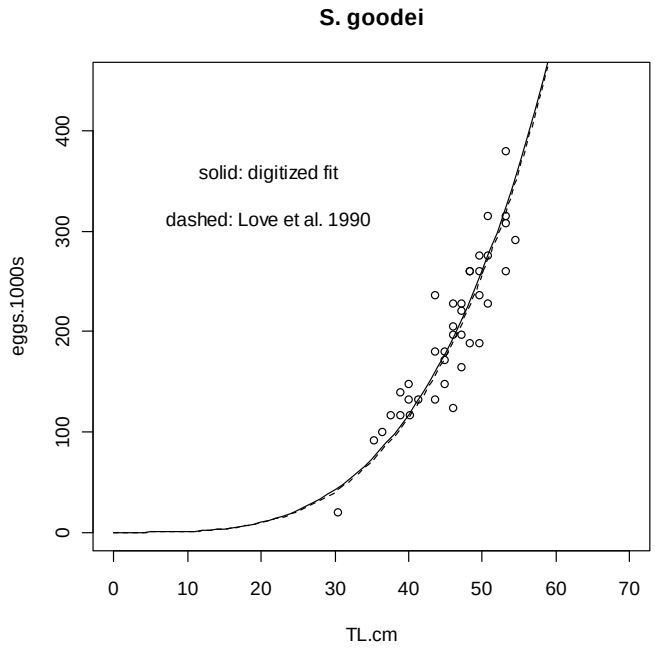

Figure A9. Digitized fecundity and length data for *S. hopkinsi* from Love et al. (1990); lines are reported fecundity-length model (dashed line) and model fit to digitized data (solid line).

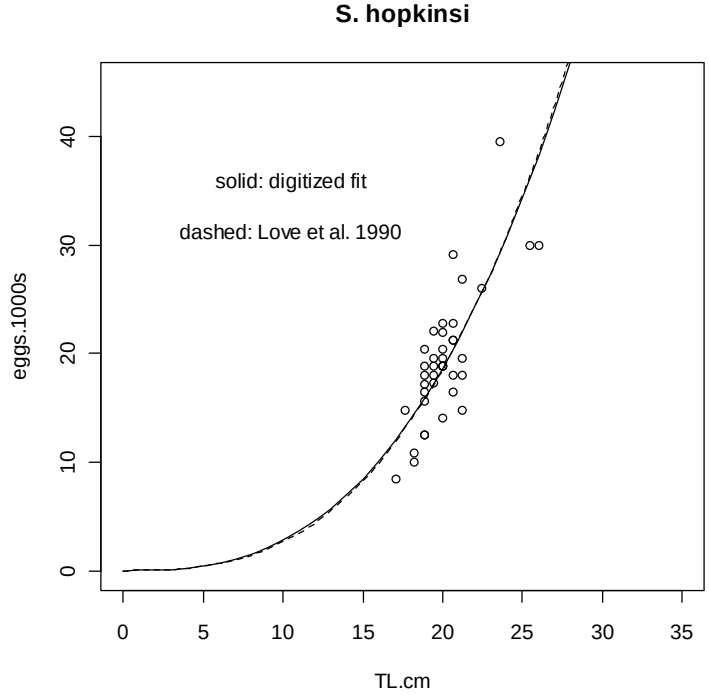

Figure A10. Digitized fecundity and length data for *S. levis* from Love et al. (1990); lines are reported fecundity-length model (dashed line) and model fit to digitized data (solid line).

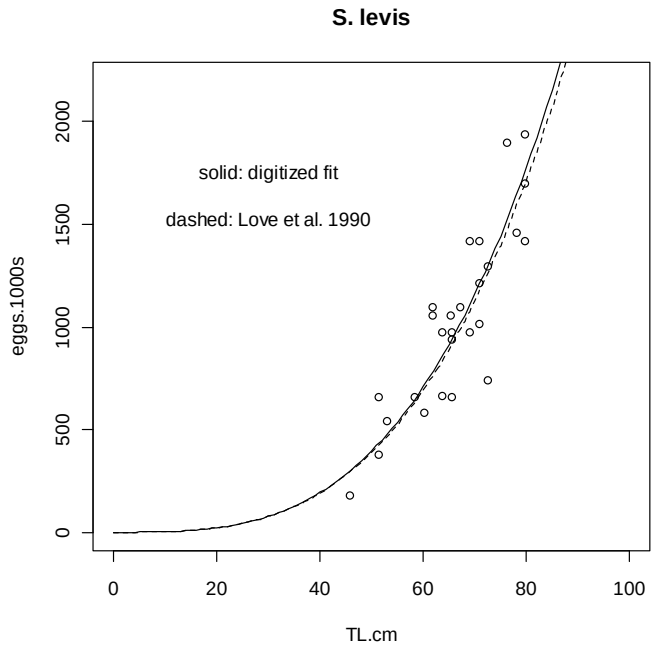

Figure A11. Digitized fecundity and length data for *S. miniatus* from Love et al. (1990); lines are reported fecundity-length model (dashed line) and model fit to digitized data (solid line).

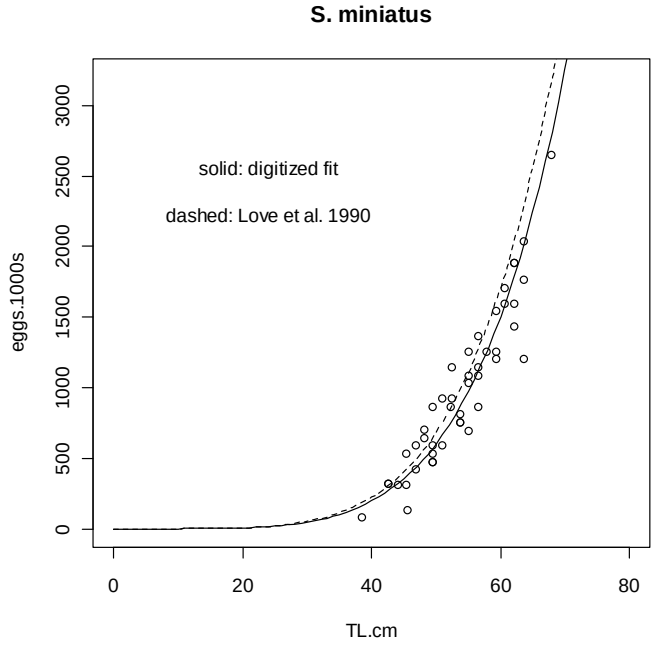

Figure A12. Digitized fecundity and length data for *S. paucispinis* from Love et al. (1990); lines are reported fecundity-length model (dashed line) and model fit to digitized data (solid line).

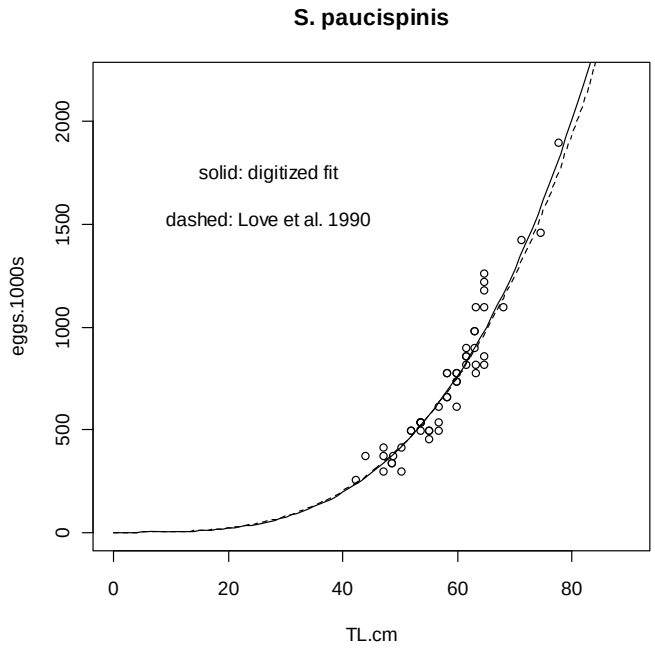

Figure A13. Digitized fecundity and length data for *S. rosaceus* from Love et al. (1990); lines are reported fecundity-length model (dashed line) and model fit to digitized data (solid line).

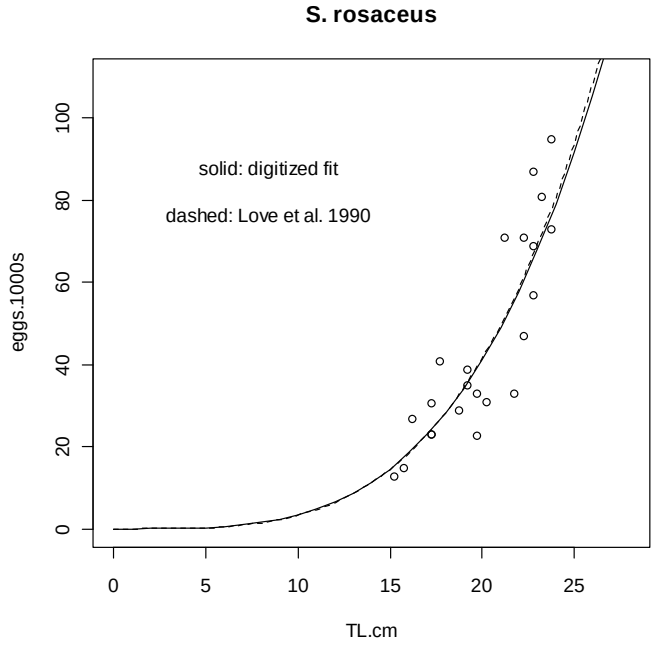

Figure A14. Digitized fecundity and length data for *S. rosenblatti* from Love et al. (1990); lines are reported fecundity-length model (dashed line) and model fit to digitized data (solid line).

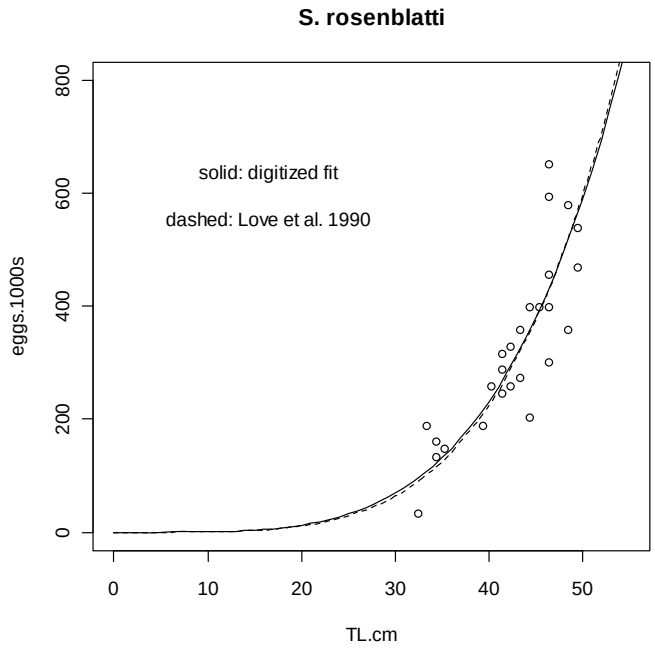

Figure A15. Digitized fecundity and length data for *S. rufus* from Love et al. (1990); lines are reported fecundity-length model (dashed line) and model fit to digitized data (solid line).

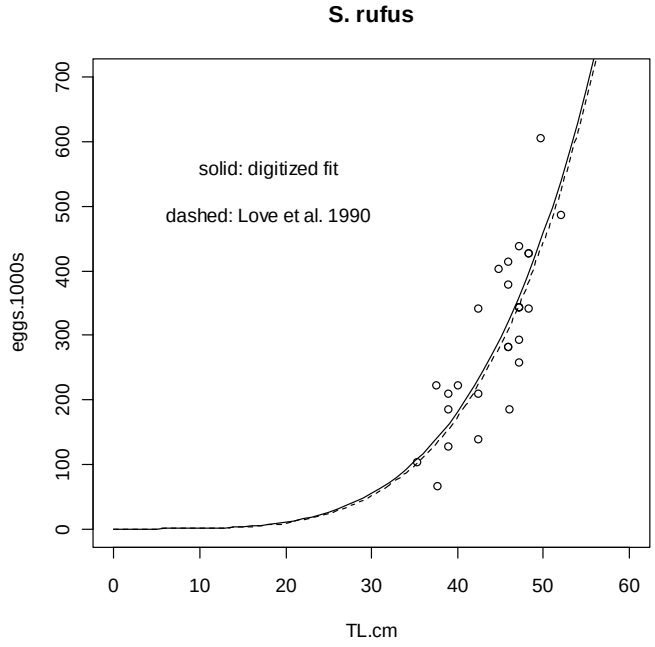

Figure A16. Digitized fecundity and length data for *S. saxicola* from Love et al. (1990); lines are reported fecundity-length model (dashed line) and model fit to digitized data (solid line).

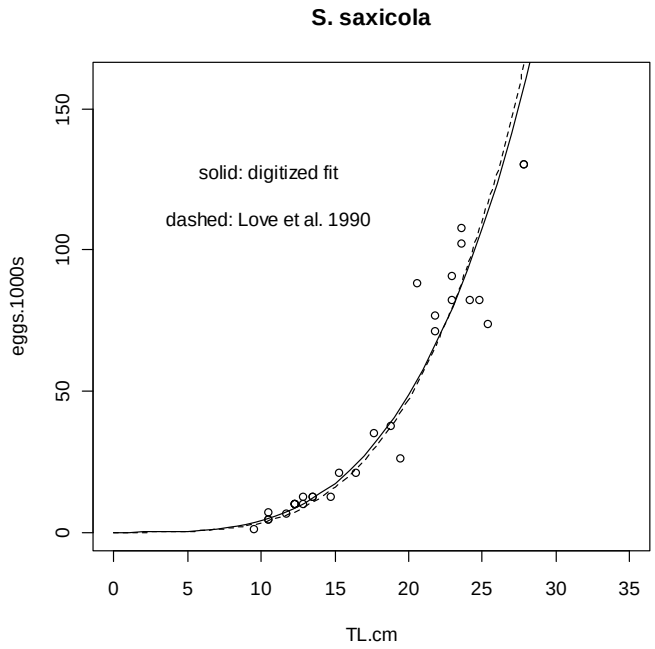

Figure A17. Digitized fecundity and length data for *S. semicinctus* from Love et al. (1990); lines are reported fecundity-length model (dashed line) and model fit to digitized data (solid line).

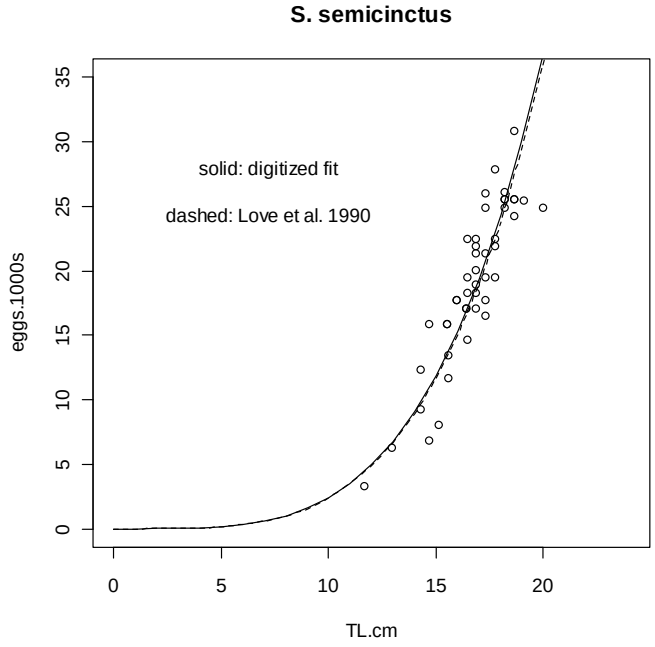

Figure A18. Fecundity versus length data for kelp rockfish (*S. atrovirens*), recovered from Romero (1988).

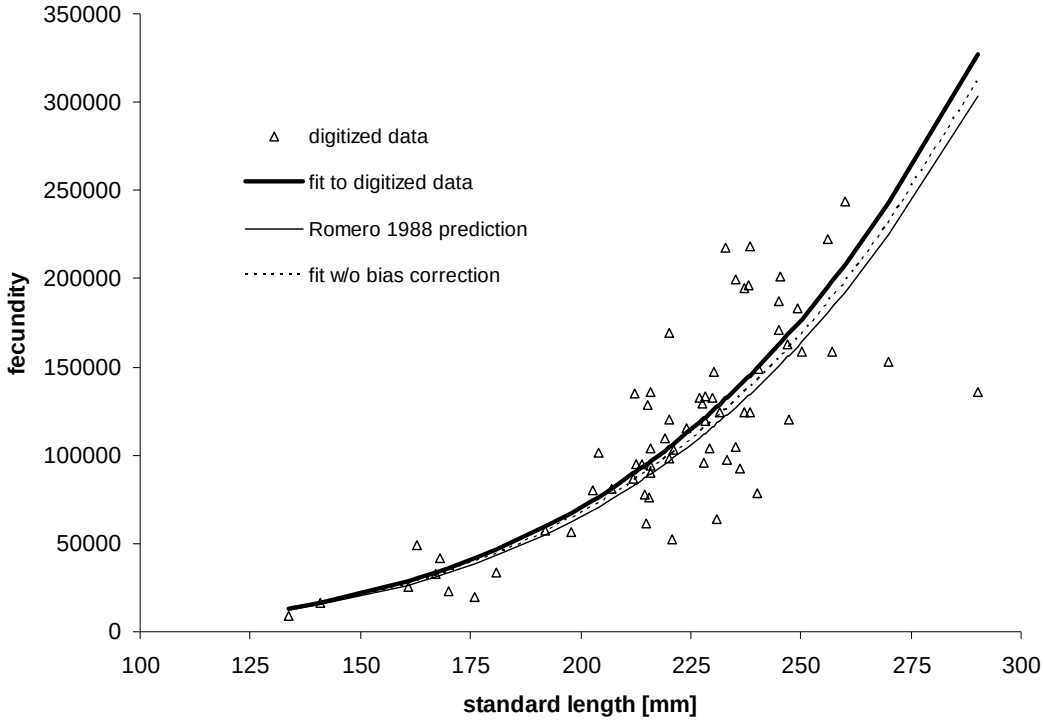

Figure A19. Fecundity versus length data for olive rockfish (*S. serranoides*), recovered from Love and Westphal (1981).

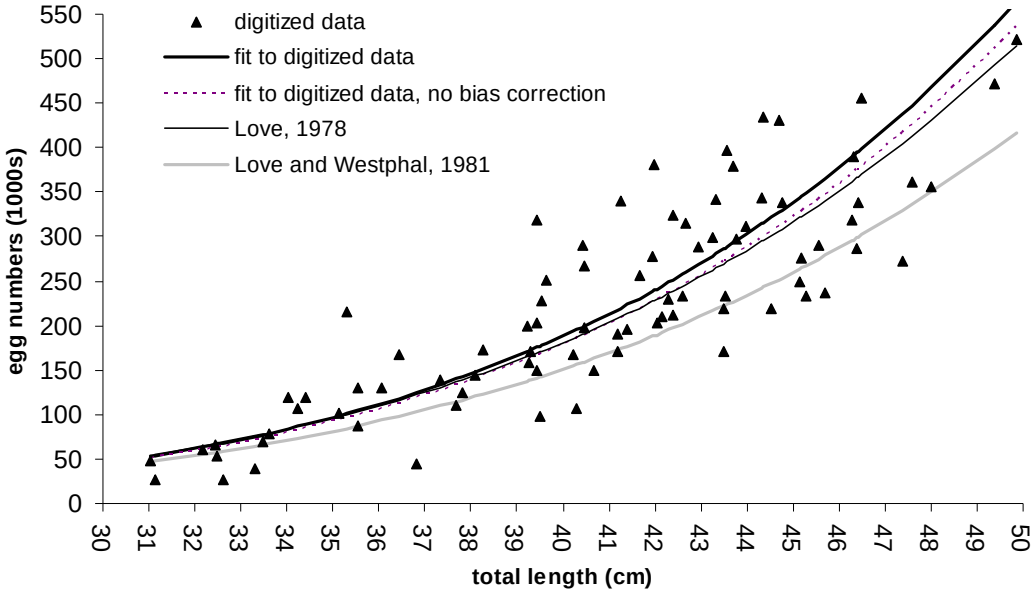

APPENDIX B

MARKOV CHAIN MONTE CARLO (MCMC) DIAGNOSTICS

The Gibbs sampler is a simulation approach to inference about model parameters, and therefore uses random draws to summarize posterior densities. It is impossible to prove that these simulations have converged to the posterior distribution, but we can evaluate properties of the series of random draws ("chains") and determine if they are consistent with a sequence that is approximating the target distribution (Gelman et al., 2004). I used the coda package (M. Plummer, 2009) that is available for the R programming language/environment (R Core Team, 2008) to assess several of these properties for the 2-level hierarchical model for fecundity as an allometric function of weight ($F = aW^b$).

I removed an initial set of 50,000 simulations (the 'burn-in' period) from each chain to minimize the influence of starting values on posterior summaries. Plots of sequentially ordered draws ("traceplots", result not shown) showed that chains initialized over a range of starting values rapidly converged to the same sampling space. The simulations of the intercept and slope parameters were not highly dependent on previous iterations (Figures B1 and B2), but the mean and variance parameters of the population-level slope distributions showed some evidence of autocorrelation (Figure B3). I "thinned" the chains, keeping every 20th iteration, which reduced the dependency between adjacent values of these parameters (Figure B4).

If a chain has converged, then the mean and variance of an early part of the chain should be similar those values computed from a later part of the chain. I calculated Geweke z-scores (Draper, 2005) to test this equality using the coda package (Table B1). The Geweke statistic is testing equality of means for each parameter calculated from the first 10% and last 50% of 100,000 simulations, following the 50,000 simulation 'burn-in' period. The test is repeated for each of two chains. Z-scores with absolute values not much greater than 2 show little evidence of change in mean value over the course of the simulation (Draper, 2005). Two parameters in the 2-level model (bold values in Table B1) have absolute values greater than two, but not consistently among chains.

I initialized the parameter values in the Gibbs sampler from two sets of starting points, to evaluate whether the chains appeared to converge to the same distribution. This approach helps detect possible multi-modality of the posterior distribution, allowing the simulation begin in different areas of parameter space. To assess convergence of the two chains, I used the coda package to calculate Gelman and Rubin shrink factors (Draper, 2005). Values of this statistic that are close to 1 suggest that the chains initialized with overdispersed values relative to the posterior distribution have converged to the same distribution (Table B2). All parameters in the 2-level model had shrink factors equal to 1 based on the 2 chains that I evaluated.

Finally, I used the Raftery and Lewis convergence diagnostics to determine the length of the burn-in period and final simulation length that are necessary to achieve a desired level of accuracy in posterior estimation. Based on the default settings in coda (see Draper (2005) for details), the lengths of the burn-in period (50,000 iterations) and the final set of simulations (100,000) are sufficient (Tables B3, B4, and B5).

Table B1: Geweke z-scores for posterior simulations from the 2-level hierarchical model (see text of Appendix B for details).

	slope (α)		intercept (β)	
	chain 1	**chain 2**	**chain 1**	**chain 2**
S. alutus	-0.47	0.58	0.04	**-2.16**
S. atrovirens	0.16	-0.09	-1.58	0.72
S. auriculatus	-0.48	-0.05	-1.38	0.91
S. babcocki	-0.49	0.89	-0.84	1.35
S. brevispinis	-0.51	-0.14	-1.93	-0.07
S. carnatus	0.21	-0.12	-1.09	-1.71
S. caurinus	-0.15	0.05	-0.06	-0.13
S. chlorostictus	-0.82	-0.32	0.43	-1.04
S. constellatus	-0.07	0.78	-1.23	0.29
S. crameri	-0.43	-0.01	0.08	0.38
S. dalli	-0.17	0.43	-0.10	0.27
S. diploproa	0.05	0.56	0.63	-0.53
S. elongatus	0.79	0.58	-0.33	0.81
S. emphaeus	0.30	0.07	0.98	-0.48
S. ensifer	-0.12	0.86	0.31	0.07
S. entomelas	0.19	-0.12	0.73	0.07
S. flavidus	0.39	0.79	**2.28**	1.39
S. goodei	-0.89	-0.70	-0.09	-0.15
S. helvomaculatus	-0.68	-0.49	-0.38	0.16
S. hopkinsi	0.00	-0.87	-0.79	-0.80
S. jordani	-0.55	0.00	-0.65	-0.05
S. levis	0.06	-0.13	1.29	-0.02
S. maliger	0.60	-0.42	-0.60	1.09
S. melanops	-1.01	0.65	0.73	0.86
S. melanostomus	0.01	-0.17	0.74	-0.73
S. miniatus	-0.28	0.86	0.89	-0.73
S. mystinus	-0.45	1.55	1.77	-0.54
S. norvegicus	0.44	-0.57	0.69	0.33
S. ovalis	0.37	0.06	-0.69	-0.25
S. paucispinis	-0.25	0.94	-0.89	0.15
S. pinniger	0.56	0.87	1.20	0.59
S. proriger	0.40	0.20	-1.29	-0.61
S. rastrelliger	0.56	-0.04	1.16	-0.95
S. rosaceus	-0.81	0.61	0.28	-1.10
S. rosenblatti	1.11	0.53	-1.84	1.07
S. ruberrimus	0.56	0.45	0.30	-0.88
S. rufus	0.57	0.23	0.29	-0.28
S. saxicola	0.53	0.71	0.88	-0.26
S. semicinctus	-0.05	-0.15	0.55	-0.80
S. serranoides	0.53	1.72	-0.55	0.20

	chain 1	**chain 2**
μ_α	-0.47	0.58
μ_β	0.16	-0.09
τ_α	-0.48	-0.05
τ_β	-0.49	0.89
σ^2	-0.51	-0.14

Table B2: Gelman-Rubin shrink factors to check for multi-modality of the posterior intercept distributions in the 2-level hierarchical model. Results are identical for all other model parameters.

Potential scale reduction factors:

	Point est.	97.5% quantile
S. alutus	1	1
S. atrovirens	1	1
S. auriculatus	1	1
S. babcocki	1	1
S. brevispinis	1	1
S. carnatus	1	1
S. caurinus	1	1
S. chlorostictus	1	1
S. constellatus	1	1
S. crameri	1	1
S. dalli	1	1
S. diploproa	1	1
S. elongatus	1	1
S. emphaeus	1	1
S. ensifer	1	1
S. entomelas	1	1
S. flavidus	1	1
S. goodei	1	1
S. helvomaculatus	1	1
S. hopkinsi	1	1
S. jordani	1	1
S. levis	1	1
S. maliger	1	1
S. melanops	1	1
S. melanostomus	1	1
S. miniatus	1	1
S. mystinus	1	1
S. norvegicus	1	1
S. ovalis	1	1
S. paucispinis	1	1
S. pinniger	1	1
S. proriger	1	1
S. rastrelliger	1	1
S. rosaceus	1	1
S. rosenblatti	1	1
S. ruberrimus	1	1
S. rufus	1	1
S. saxicola	1	1
S. semicinctus	1	1
S. serranoides	1	1

Table B3: Raftery and Lewis's diagnostic test for intercept parameters in the 2-level hierarchical model (see text for details).

Quantile (q) = 0.025
Accuracy (r) = +/- 0.005
Probability (s) = 0.95

	Burn-in (M)	Total (N)	Lower bound (Nmin)	Dependence factor (I)
S. alutus	2	3650	3746	0.974
S. atrovirens	2	3741	3746	0.999
S. auriculatus	2	3741	3746	0.999
S. babcocki	2	3680	3746	0.982
S. brevispinis	2	3710	3746	0.990
S. carnatus	2	3650	3746	0.974
S. caurinus	2	3680	3746	0.982
S. chlorostictus	2	3710	3746	0.990
S. constellatus	2	3680	3746	0.982
S. crameri	2	3865	3746	1.030
S. dalli	2	3802	3746	1.010
S. diploproa	2	3620	3746	0.966
S. elongatus	2	3771	3746	1.010
S. emphaeus	2	3771	3746	1.010
S. ensifer	2	3650	3746	0.974
S. entomelas	2	3680	3746	0.982
S. flavidus	2	3834	3746	1.020
S. goodei	2	3788	3746	1.010
S. helvomaculatus	2	3865	3746	1.030
S. hopkinsi	2	3741	3746	0.999
S. jordani	2	3865	3746	1.030
S. levis	2	3865	3746	1.030
S. maliger	2	3680	3746	0.982
S. melanops	2	3771	3746	1.010
S. melanostomus	2	3650	3746	0.974
S. miniatus	2	3802	3746	1.010
S. mystinus	2	3835	3746	1.020
S. norvegicus	2	3771	3746	1.010
S. ovalis	2	3865	3746	1.030
S. paucispinis	2	3590	3746	0.958
S. pinniger	2	3680	3746	0.982
S. proriger	2	3834	3746	1.020
S. rastrelliger	1	3726	3746	0.995
S. rosaceus	2	3834	3746	1.020
S. rosenblatti	2	3771	3746	1.010
S. ruberrimus	2	3711	3746	0.991
S. rufus	2	3650	3746	0.974
S. saxicola	2	3710	3746	0.990
S. semicinctus	2	3680	3746	0.982
S. serranoides	2	3710	3746	0.990

Table B4: Raftery and Lewis's diagnostic test for slope parameters in the 2-level hierarchical model (see text for details).

Quantile (q) = 0.025
Accuracy (r) = +/- 0.005
Probability (s) = 0.95

	Burn-in (M)	Total (N)	Lower bound (Nmin)	Dependence factor (I)
S. alutus	6	12060	3746	3.22
S. atrovirens	4	7600	3746	2.03
S. auriculatus	6	11289	3746	3.01
S. babcocki	6	11232	3746	3.00
S. brevispinis	4	7884	3746	2.10
S. carnatus	9	12243	3746	3.27
S. caurinus	2	3811	3746	1.02
S. chlorostictus	4	7690	3746	2.05
S. constellatus	8	15232	3746	4.07
S. crameri	4	7734	3746	2.06
S. dalli	6	11448	3746	3.06
S. diploproa	6	8106	3746	2.16
S. elongatus	6	8330	3746	2.22
S. emphaeus	6	10917	3746	2.91
S. ensifer	6	12006	3746	3.21
S. entomelas	6	11625	3746	3.10
S. flavidus	2	3785	3746	1.01
S. goodei	2	3840	3746	1.03
S. helvomaculatus	12	15652	3746	4.18
S. hopkinsi	12	16748	3746	4.47
S. jordani	10	19165	3746	5.12
S. levis	6	11964	3746	3.19
S. maliger	2	3780	3746	1.01
S. melanops	6	11064	3746	2.95
S. melanostomus	6	11592	3746	3.09
S. miniatus	4	7746	3746	2.07
S. mystinus	6	11844	3746	3.16
S. norvegicus	9	12249	3746	3.27
S. ovalis	9	12285	3746	3.28
S. paucispinis	2	3782	3746	1.01
S. pinniger	6	11436	3746	3.05
S. proriger	12	17164	3746	4.58
S. rastrelliger	8	15196	3746	4.06
S. rosaceus	6	8462	3746	2.26
S. rosenblatti	6	7776	3746	2.08
S. ruberrimus	8	15056	3746	4.02
S. rufus	6	11592	3746	3.09
S. saxicola	2	3787	3746	1.01
S. semicinctus	6	7866	3746	2.10
S. serranoides	2	3831	3746	1.02

Table B5: Raftery and Lewis's diagnostic test for the hierarchical distribution parameters and data variance (σ^2) in the 2-level hierarchical model (see text for details).

```
Quantile (q) = 0.025
Accuracy (r) = +/- 0.005
Probability (s) = 0.95
```

	Burn-in (M)	Total (N)	Lower bound (Nmin)	Dependence factor (I)
μ_α	6	8036	3746	2.150
μ_β	20	25032	3746	6.680
τ_α	6	8110	3746	2.160
τ_β	48	50616	3746	13.500
σ^2	2	3730	3746	0.996

Figure B1: Autocorrelation plots for intercept parameters from the 2-level hierarchical model.

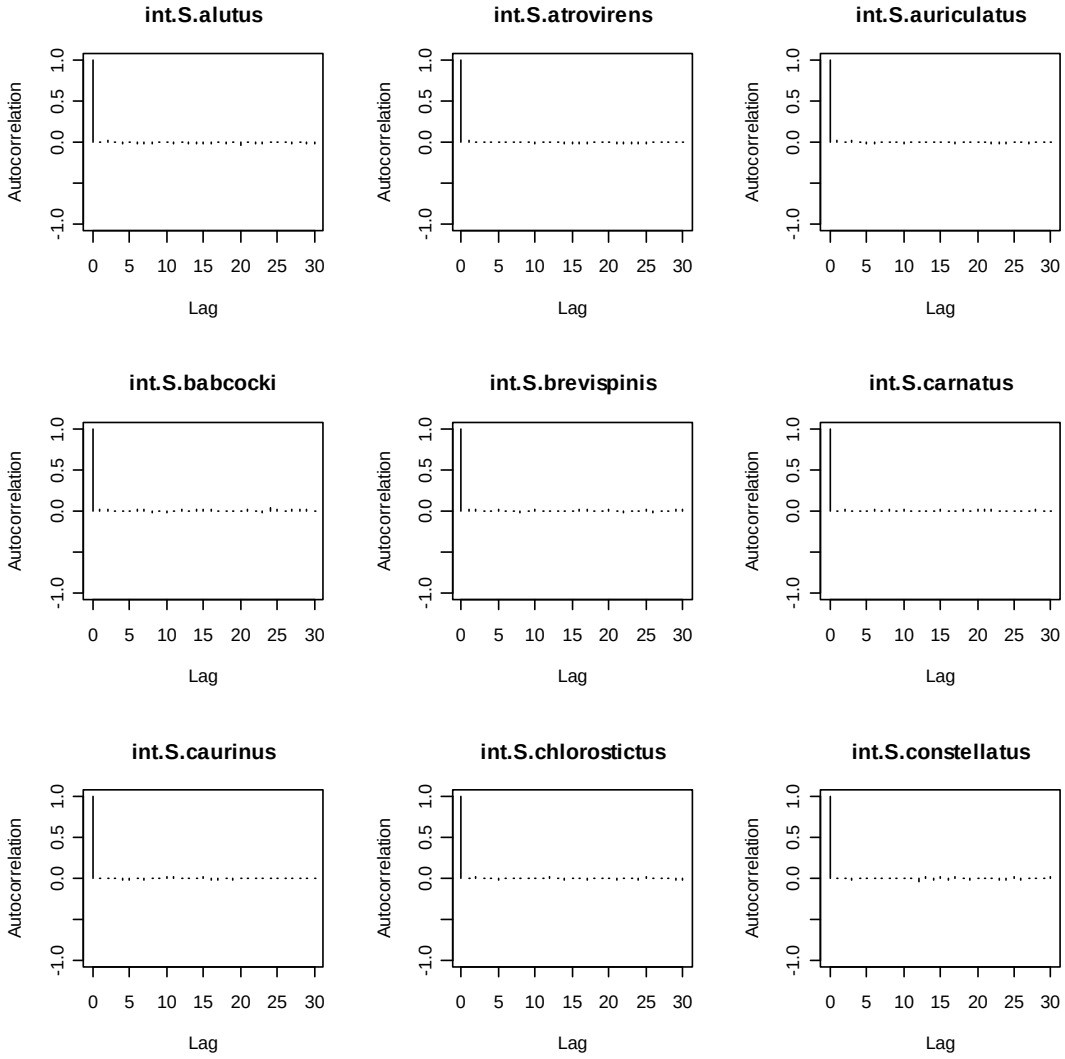

Figure B2: Autocorrelation plots for slope parameters from the 2-level hierarchical model.

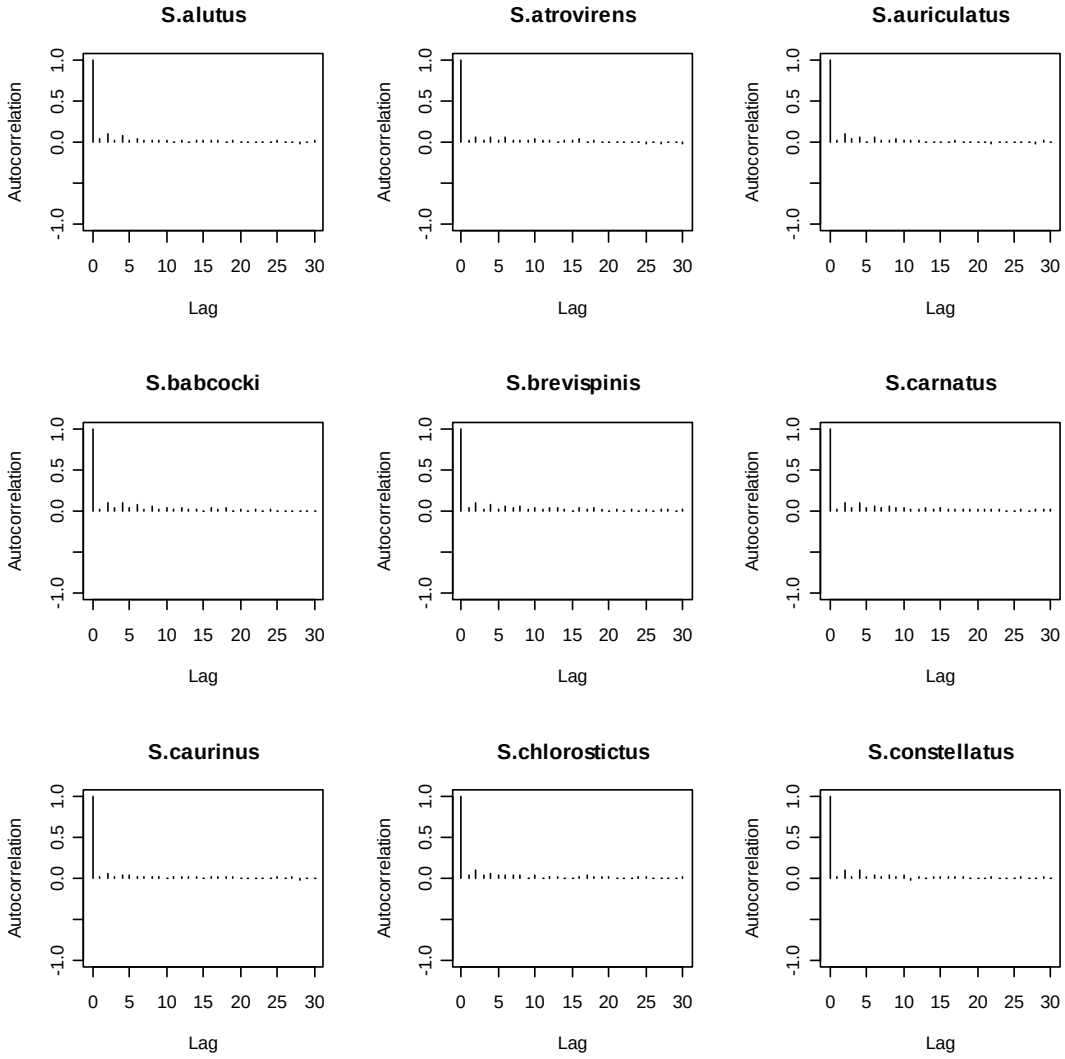

Figure B3: Autocorrelation plots (prior to thinning) for hierarchical distribution parameters and the data variance parameter from the 2-level hierarchical model.

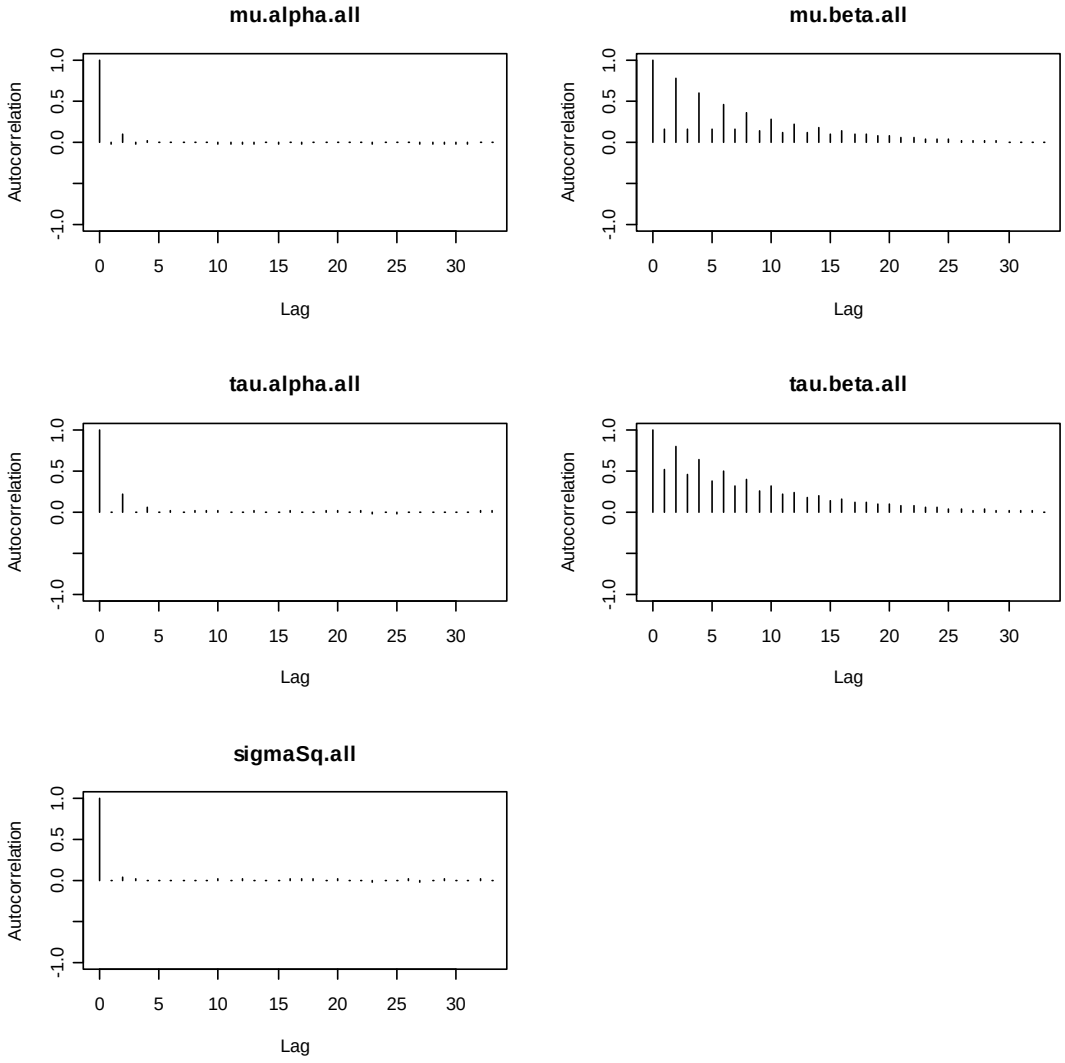

Figure B4: Autocorrelation plots for hierarchical distribution parameters and the data variance parameter from the 2-level hierarchical model. Simulations thinned to every 20^{th} iteration.

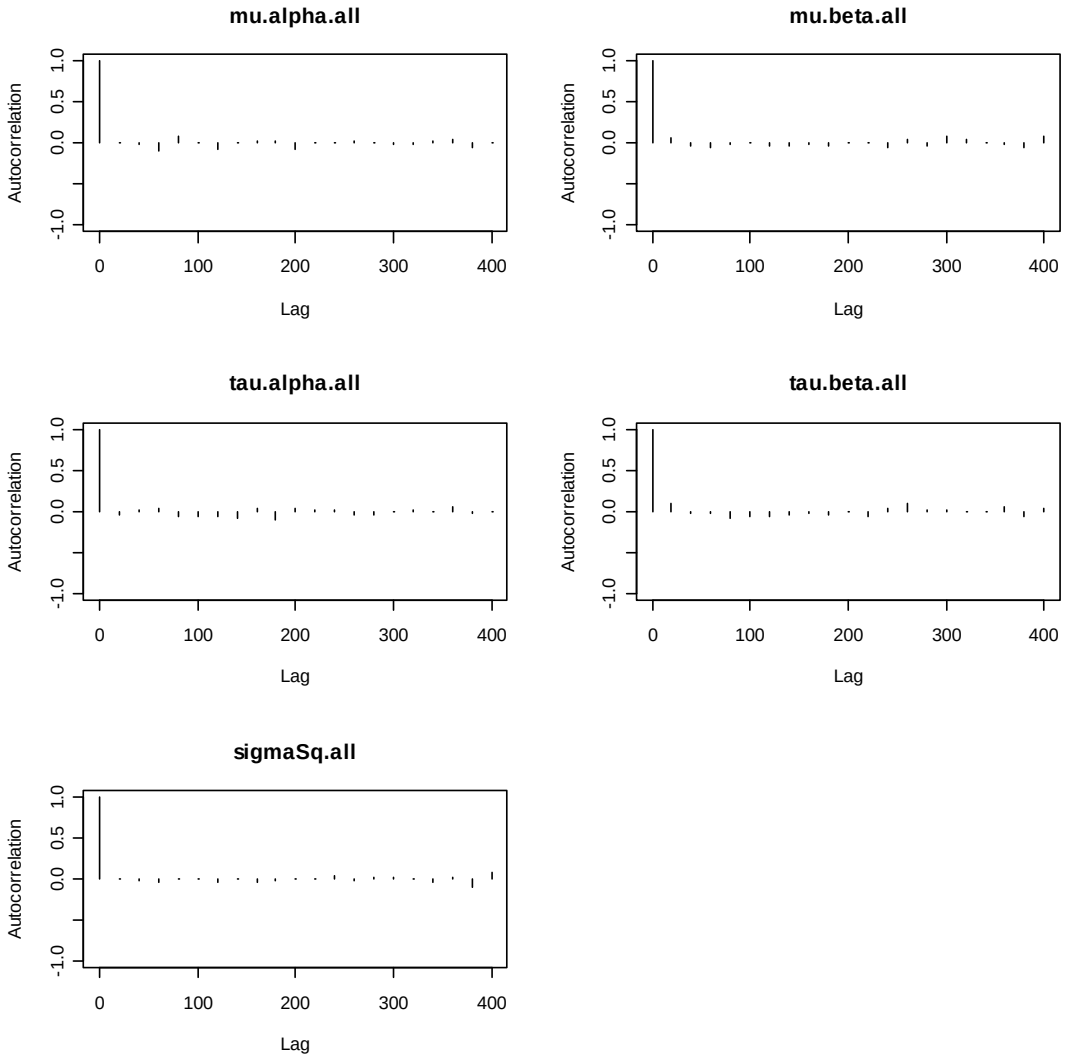

APPENDIX C

LINEAR INTERPOLATION ALGORITHMS

The variables describing the state of the organism take discrete values in the life history models I develop in Chapter 4. Sometimes it is necessary to evaluate a function of the state variable at a value that falls between these discrete values. For example, in the backward iterations of the stochastic dynamic programming algorithm, updated length based on a given allocation decision does not always match a length value for which future fitness is known. Future fitness for this intermediate length can be approximated using a technique called linear interpolation. This approach reduces the dimension of the problem and therefore the required computation time.

If, for a given state variable x ($x = 0, 1, 2, \ldots, n$), we know the value of a function at two values, $f(x_1)$ and $f(x_2)$, then we can approximate the value of the function at an intermediate point, x_c, where $x_1 < x_c < x_2$ and $x_2 - x_1 = 1$ using the algorithm:

1. Calculate the difference $\Delta = x_c - x_1$
2. Approximate $f(x_c) \cong (1-\Delta) \cdot f(x_1) + \Delta \cdot f(x_2)$

This approach can be generalized to multiple dimensions (Clark and Mangel, 2000). The resource allocation models require 2-dimensional interpolation of the allocation decision, which is a function of both current length and length at maturity. Imagine a continuous surface over 2-dimensional, integer-valued grid, and

assume we know the height of the surface at each grid coordinate. The function values (surface heights) at each 'corner' of the grid are already known. Values along the edges, or evaluated at an integer value in one dimension (call it x), only require linear interpolation in the other dimension (call it y), as described above. Values within the boundaries of the grid and between integer grid coordinates (x_c and y_c) require interpolation, which proceeds as follows given $x = 0, 1, 2, \ldots, n_x$ and $y = 0, 1, 2, \ldots, n_y$, and where $x_1 < x_c < x_2$ and $y_1 < y_c < y_2$,

1. Calculate the difference $\Delta x = x_c - x_1$
2. Calculate the difference $\Delta y = y_c - y_1$
3. Approximate f(xc, yc) ≅ (1-Δx)(1 - Δy) f(x1, y1) +

   $(1-\Delta x)(\Delta y)\, f(x_1, y_2)$ +

   $(\Delta x)(1 - \Delta y)\, f(x_2, y_1)$ +

   $(\Delta x)(\Delta y)\, f(x_2, y_2)$

APPENDIX D

R CODE FOR STATE DEPENDENT LIFE HISTORY MODELS

Linear production function with concave reproductive success

```
Tmax <- 100     # time horizon
Lmax <- 100     # max. size [cm]
mu.p <- 0.8     # "concave egg conversion" coefficient

m0 <- 0.05
m1 <- 0.0
m2 <- 0.0

g <- 4     # growth coefficient
dLmax <- g
dL <- g # express constant as fxn. to allow for other increment fxns.
{
   return(g)
}

# mortality is a function of length and reproductive effort
M <- function(L, RepEff)
{
   return( m0 + m1/L + m2*RepEff)
}

# W = a*L^b; weight-length model parameters
a <- 1E-05
b <- 3
Wmax <- a*Lmax^b

# decision variable: prop. of potential mass increment allocated to reprod.
rho <- seq(0, 1, by=0.005)

# initialize fitness matrix to store ELRS at size x and time t
# initialize with zeros --> terminal fitness F(x,T)=0
F.mat <- matrix(NA, nrow=Tmax, ncol=Lmax)
F.mat[Tmax,] <- 0

# store optimal allocation at time t and size x
rho.mat <- matrix(NA, nrow=Tmax, ncol=Lmax)

# matrix to store optimal reproductive output at each time and size
RepEff.mat <- matrix(NA, nrow=Tmax, ncol=Lmax)

# matrix to store optimal GSI at each time and size
GSI.mat <- matrix(NA, nrow=Tmax, ncol=Lmax)

Wrho    <- numeric(length(rho)) # updated somatic weight for allocation j
logLrho <- numeric(length(rho)) # log length for somatic weight j
Lrho    <- numeric(length(rho)) # length [cm] for somatic weight j
Vrho    <- rep(NA,length(rho))
Fnow    <- rep(NA,length(rho))
GSI.vec <- rep(NA,length(rho))
```

```
# save max value of growth increment function for scaling plots
dWmax <- 0

# SDP algorithm
for (z in (Tmax-1):1)
{
   print(z)
   for (i in 1:Lmax)
   {
      # calculate potential growth increment in mass
      Lpot  <- i + dL(i)
      Wpot  <- a*Lpot^b
      Wnow  <- a*i^b
      dWpot <- Wpot-Wnow
      dWmax <- max(dWmax, dWpot) # used to scale axis in plots

      for (j in 1:length(rho))
      {
 # Calculate reproductive success at the current time, size, and allocation
         Fnow[j] <- rho[j]*dWpot*exp(-mu.p*rho[j]*dWpot)
         # Calculate GSI at current time, size and allocation
         GSI.vec[j] <- Fnow[j]/Wpot

         # Calculate updated somatic weight given allocation j
         Wrho[j] <- ifelse(Wnow + (1-rho[j])*dWpot <= Wmax,
                           Wnow + (1-rho[j])*dWpot,
                           Wmax)
         logLrho[j] <- (1/b)*log(Wrho[j]/a)
         Lrho[j] <- exp(logLrho[j])

         # Interpolate future fitness based on current allocation (rho[j])
                                  and new L
         Llow  <- floor(Lrho[j])
         Lhigh <- ifelse(Llow<Lmax, Llow + 1, Lmax)
         dLc   <- Lrho[j] - Llow
         term1 <- (1-dLc) * F.mat[z+1, Llow]
         term2 <- dLc * F.mat[z+1, Lhigh]
         FutureFit <- exp(-M(i,GSI.vec[j]))*(term1 + term2)

         # Reproductive success assuming optimal behavior in the future
         Vrho[j] <-  Fnow[j] + FutureFit

      } # end of allocation loop

      # Store F(x,t)
      F.mat[z,i] <- max(Vrho)

      # store optimal allocation at time z and size i
      rho.mat[z,i] <- rho[which.max(Vrho)]

      # store optimal reproductive output at time z and size i
      RepEff.mat[z,i] <- Fnow[which.max(Vrho)]

      # store optimal GSI for this time and size
      GSI.mat[z,i] <- GSI.vec[which.max(Vrho)]
```

```
   } # end of size loop

} # end of time loop

### FORWARD SIMULATION ###
# initialize objects
Ltru    <- numeric(Tmax)
Ltru[1] <- 1
Wtru    <- numeric(Tmax)
Wtru[1] <- a*Ltru[1]^b
OptRho    <- numeric(Tmax)
OptGSI  <- numeric(Tmax)
OptGonads  <- numeric(Tmax)

for (z in 1:(Tmax-1))
{
   # get optimal allocation (interpolate value based on true size)
   SizeLo <- ifelse(Ltru[z] < Lmax, floor(Ltru[z]), Lmax)
   SizeHi <- ifelse(SizeLo < Lmax, SizeLo+1, Lmax)
   RhoLo  <- rho.mat[z, SizeLo]
   RhoHi  <- rho.mat[z, SizeHi]
   RhoD   <- Ltru[z] - SizeLo
   OptRho[z] <- ifelse(identical(0,RhoD), RhoLo, (1-RhoD)*RhoLo +
                                 RhoD*RhoHi)

   # calculate potential growth
   Lpot  <- Ltru[z] + dL(Ltru[z])
   Wpot  <- a*Lpot^b
   Wnow  <- a*Ltru[z]^b
   dWpot <- Wpot - Wnow

   # calculate updated somatic weight and length given optimal allocation
   Wtru[z+1] <- ifelse( (Wnow+(1-OptRho[z])*dWpot) <= Wmax,
                        Wnow + (1-OptRho[z])*dWpot,
                        Wmax)
   logLtru <- (1/b)*log(Wtru[z+1]/a)
   Ltru[z+1] <- exp(logLtru)

   # interpolate optimal GSI at true size
   GSILo  <- GSI.mat[z, SizeLo]
   GSIHi  <- GSI.mat[z, SizeHi]
   GSIc   <- Ltru[z] - SizeLo
   OptGSI[z] <- ifelse(identical(0,GSIc), GSILo, (1-GSIc)*GSILo +
                                 GSIc*GSIHi)

   # interpolate optimal Gonads at true size
   GonadLo  <- RepEff.mat[z, SizeLo]
   GonadHi  <- RepEff.mat[z, SizeHi]
   Gonad.c   <- Ltru[z] - SizeLo
   OptGonads[z] <- ifelse(identical(0,Gonad.c), GonadLo, (1-
                                 Gonad.c)*GonadLo + Gonad.c*GonadHi)
}
```

Asymptotic production function with convex mortality function

```
Tmax <- 100 # time horizon; try scaling with M (e.g. -log(0.001)/M)
Lmin <- 1   # smallest (integer) length [cm]; must be >= 1
mu.p <- 0.0 # density-dependent effect of predators

# Q/k must be an integer
Q <- 2.5   # maximum growth rate [cm/yr]
k <- 0.025 # growth coefficient [1/yr]
cf <- 0.8  # "cost fraction" (0<cf<1); fish maturing at Lmin grows to
                                  cf*Lpan
d <- k*Lmin*(1/cf-1)   # reparameterize to Stamps et al. version
Lpan <- Q/k            # largest possible length (fish that never matures)

a <- 0.01              # W = a*L^b; weight-length model parameters
b <- 3                 # W = a*L^b; weight in grams, length in cm

m0 <- 0.05  # length-INDEPENDENT mortality
m1 <- 0.0   # length-DEPENDENT mortality
m2 <- 2.0   # mortality associated with reproduction

rho <- seq(0,1,by=0.05)   # fraction of potential growth (mass) allocated
                                  to gonads

##################
### FUNCTIONS ###
##################

# length-increment fxn. for immature fish; fish aren't allowed to shrink
dL0 <- function(L)
{
   n <- length(L)
   out0 <- numeric(n)
   for (i in 1:n)
   {
      out0[i] <- max( (Q/k - L[i]) * (1 - exp(-k)), 0)
   }
   return(out0)
}

# length-increment fxn. for mature fish; fish aren't allowed to shrink
dL1 <- function(L,Lmat)
{
   n <- length(L)
   out1 <- numeric(n)
   k2 <- k + d/Lmat
   for (i in 1:n)
   {
      out1[i] <- max( (Q/k2 - L[i])*(1-exp(-k2)), 0 )
   }
   return(out1)
}

# length-specific mortality function
#M <- function(L,gsi) { m0 + m1/L + m2*gsi }
M <- function(L,gsi) { m0 + m1/L + gsi^m2 }
```

```
# 2-D linear interpolation function (see Clark and Mangel, pg. 52)
# Zmat must have dimensions nrow=length(xmin:xmax) by
                                ncol=length(ymin:ymax)
interp2D <- function(xmin, xmax,
                     ymin, ymax,
                     xtarg, ytarg,
                     Zmat)
{
   xlo <- floor(xtarg)
   ylo <- floor(ytarg)
   dx <- xtarg-xlo
   dy <- ytarg-ylo
   xi <- match(xlo, xmin:xmax) # position of xlo in x vector
   yi <- match(ylo, ymin:ymax) # position of ylo in y vector
   n <- length(xmin:xmax)
   m <- length(ymin:ymax)

   if ( all(identical(xlo,xmin), identical(ylo,ymin)) )
   {
      out <- Zmat[1,1]
   }

   if ( all(xlo<xmax, ylo<ymax) )
   {
      out <- (1-dx)*(1-dy)*Zmat[xi, yi] +
             (1-dx)*dy*Zmat[xi, yi+1] +
             dx*(1-dy)*Zmat[xi+1,yi] +
             dx*dy*Zmat[xi+1,yi+1]
   }

   if ( all(identical(xlo,xmax), ylo<ymax) )
   {
      out <- (1-dy)*Zmat[n, yi] + dy*Zmat[n, yi+1]
   }

   if ( all(xlo<xmax, identical(ylo,ymax)) )
   {
      out <- (1-dx)*Zmat[xi, m] + dx*Zmat[xi+1, m]
   }

   if ( all(identical(xlo,xmax), identical(ylo,ymax)) )
   {
      out <- Zmat[n,m]
   }

   return(out)
}

########################################################
### INITIALIZE OBJECTS AND ASSIGN END CONDITIONS ###
########################################################

Lvec <- Lmin:Lpan
Ldif <- Lmin-1      # offset used for indexing length

# F0 tracks fitness of immature individuals with optimal maturity decision
# dim 1 = time; 1:Tmax
```

```
# dim 2 = length; Lmin:Lpan
F0 <- matrix(NA, nrow=Tmax, ncol=length(Lvec),
             dimnames=list(paste("t",1:Tmax,sep=""),
                           paste("L",Lvec,sep="")))

# terminal fitness function for immature fish
F0[Tmax,] <- 0

# F1 tracks fitness of mature individuals
# dim 1 = time; 1:Tmax
# dim 2 = length; Lmin:Lpan
# dim 3 = length at maturity; Lmin:Lpan
F1 <- array(NA, dim=c(Tmax, length(Lvec), length(Lvec)),
            dimnames=list(paste("t",1:Tmax,sep=""),
                          paste("L",Lvec,sep=""),
                          paste("Lmat",Lvec,sep="")))

F1[Tmax,,] <- 0 # terminal fitness for mature fish

# initialize some objects
Wrho    <- numeric(length(rho))  # updated somatic weight for allocation j
logLrho <- numeric(length(rho))  # log length for somatic weight j
Lrho    <- numeric(length(rho))  # length [cm] for somatic weight j

# matrix to hold fitness values for allocation j and Lmat m
Vrho <- matrix(NA, nrow=length(rho), ncol=length(Lvec),
               dimnames=list(paste("rho",rho,sep=""),
                             paste("Lmat",Lvec,sep="")))

# vector to hold maximum fitness value for length at maturity m
Vmax <- numeric(length(Lvec))
names(Vmax) <- paste("Lmat",Lvec,sep="")

# array to hold optimal value of rho for a given time, length, and length
                                at maturity
rho.arr <- array(NA, dim=c(Tmax, length(Lvec), length(Lvec)),
                 dimnames=list(paste("t",1:Tmax,sep=""),
                               paste("L",Lvec,sep=""),
                               paste("Lmat",Lvec,sep="")))

# array to hold optimal maturity decision for time z and length i
# (1 = mature, 0 = remain immature)
maturity.mat <- matrix(NA, nrow=Tmax, ncol=length(Lvec),
                       dimnames=list(1:Tmax,Lvec))
```

```
####################################
### DYNAMIC PROGRAMMING ALGORITHM ###
####################################

for (z in (Tmax-1):1)      # loop backwards in time
{
   print(paste("Time", z))
   for (i in Lmin:Lpan)    # i indexes length in centimeters
   {
      # loop over possible lengths at maturity that are <= current length
      for (m in Lmin:i)    # m indexes length at maturity
      {
         # loop over different allocation strategies
         for (j in 1:length(rho))  # j indexes values in rho vector
         {
            Lpot   <- i + dL1(i,m) # potential length, Stamps model
            Wnow   <- a*i^b        # current mass
            Wpot   <- a*Lpot^b     # potential mass (somatic + gonadal)
            dW     <- Wpot-Wnow    # potential mass _increment_

            # calculate somatic weight in next time step, given rho
            if (rho[j]<1) # if rho<1, calculate updated length given rho
            {
               Wrho[j] <- Wnow + (1-rho[j])*dW # updated somatic weight
               # back-calculate to log length
               logLrho[j] <- (1/b)*log(Wrho[j]/a)
               # updated length (can't shrink)
               Lrho[j] <- max(exp(logLrho[j]), i)
            }

            if (identical(1,rho[j])) # when rho=1, you don't grow
            {
               Lrho[j] <- i
            }

            # calculate current reproduction
            R.rho <- rho[j]*dW*exp(-rho[j]*dW*mu.p)

            # calculate current GSI
            GSI    <- R.rho/Wpot # GSI; aka relative fecundity

            # interpolate future fitness given length at time z and Lmat m
            if (Lrho[j] < Lpan)  # linear interpolation of fitness
                                 function
            {
               Llow <- floor(Lrho[j])
               Lhigh <- Llow + 1
               dLc  <- Lrho[j] - Llow
               term1 <- (1-dLc) * F1[z+1, Llow-Ldif, m-Ldif]
               term2 <- dLc * F1[z+1, Lhigh-Ldif, m-Ldif]
               Vrho[j,m-Ldif] <- R.rho + exp(-M(i,GSI))*(term1 + term2)
            }
            # if length is already Lpan, fish doesn't grow or reproduce
            if(identical(Lrho[j],Lpan))
            {
               Vrho[j,m-Ldif] <- 0
            }
```

```
   } # end of allocation loop

   # record the maximum fitness for each length at maturity
   Vmax <- apply(Vrho, 2, max)

   # mature fitness for Lmat m is allocation decision that
                          maximizes LERS
   F1[z,i-Ldif, m-Ldif] <- Vmax[m-Ldif]

   # record optimal allocation given time and length for forward
                          simulation
   # get index of largest fitness
   tmp <- apply(Vrho, 2, which.max)[[m-Ldif]]
   # use index to extract optimal rho
   rho.arr[z,i-Ldif,m-Ldif] <- rho[tmp]

} # end of maturity loop

# IF IMMATURE, DECIDE WHETHER TO MATURE
# Vi = value of remaining immature
# Vm = value of maturing

# if length = Lpan, then no growth or reproduction
if (identical(i,Lpan))
{
    Vi <- Vm <- 0
}

# if fish has room to grow,
# first interpolate fitness of remaining immature
if (i < Lpan)
{
   Li <- i + dL0(i)        # updated immature length
   Lilo <- floor(Li)
   Lihi <- Lilo + 1
   u2 <- Li - Lilo
   term3 <- (1-u2) * F0[z+1, Lilo-Ldif]
   term4 <- u2 * F0[z+1, Lihi-Ldif]
   Vi <- exp(-M(i,0))*(term3 + term4) # GSI is zero for immature fish

# next interpolate fitness of maturing at the
# current length and time
# (no allocation to gonads in year of maturation)

   Lm <- i + dL1(i,m)
   Lmlo <- floor(Lm)
   Lmhi <- Lm + 1
   u3 <- Lm - Lmlo
   term5 <- (1-u3) *  F1[z+1, Lmlo-Ldif, m-Ldif]
   term6 <- u3 * F1[z+1, Lmhi-Ldif, m-Ldif]
   # GSI is zero during year of maturation
   Vm <- exp(-M(i,0))*(term5 + term6)
}

# ERS of immature fish is max. value
F0[z, i-Ldif] <- max(Vi, Vm)
```

```
      maturity.mat[z, i-Ldif] <- ifelse(Vi < Vm, 1, 0)

   } # end of length loop
} # end of time loop

############################
### FORWARD SIMULATION ###
############################

N <- 1

# Initialize forward matrices
Ltru <- matrix(NA, nrow=Tmax, ncol=N, dimnames=list(1:Tmax, 1:N))
Ltru[1,] <- Lmin # every fish starts at L.min, for now
Wtru <- matrix(NA, nrow=Tmax, ncol=N, dimnames=list(1:Tmax, 1:N))
Wtru[1,] <- a*Ltru[1,]^b
MatFwd <- matrix(NA, nrow=Tmax, ncol=N, dimnames=list(1:Tmax, 1:N))
AllocFwd <- matrix(NA, nrow=Tmax, ncol=N, dimnames=list(1:Tmax, 1:N))
AllocFwd[1,] <- rho.arr[1, Ltru[1,]-Ldif, Ltru[1,]-Ldif]
Gonads <- matrix(NA, nrow=Tmax, ncol=N, dimnames=list(1:Tmax, 1:N))
dW.T <- matrix(NA, nrow=Tmax, ncol=N, dimnames=list(1:Tmax, 1:N))
Lmat <- rep(0, N)
Mtru <- matrix(NA, nrow=Tmax, ncol=N)

for (z in 1:(Tmax-1))   # z indexes time
{
   for (i in 1:N)       # i indexes fish (not length)
   {
      # get maturity state from closest integer length
      MatFwd[z,i] <- maturity.mat[z, round(Ltru[z,i]-Ldif, 0)]

      # if you're immature, then grow fast
      if (MatFwd[z,i] < 1)
      {
         Ltru[z+1,i] <- Ltru[z,i] + dL0(Ltru[z,i])
         Wtru[z+1,i] <- a*Ltru[z+1,i]^b
         AllocFwd[z+1,i] <- 0
         Gonads[z+1,i] <- 0
      }

      if (all( MatFwd[z,i]>0, MatFwd[z-1,i]<1 ))
      {
         Lmat[i] <- Ltru[z,i]

         # potential true length, mature
         Lpot.T   <- Ltru[z,i] + dL1(Ltru[z,i], Lmat)
         Wpot.T   <- a * Lpot.T^b # potential true mass

         Wrho.T <- Wpot.T   # Somatic true mass in time z+1
         Gonads[z,i] <- 0   # mass allocation to gonads at time z
         # Convert somatic mass to log length
         logLrho.T <- (1/b)*log(Wrho.T/a)
         Ltru[z+1,i] <- max(exp(logLrho.T),Ltru[z,i])
         Wtru[z+1,i] <- Wrho.T

         # 2-D interpolation of allocation (rho) in next time step
         # if Lmat is >= Ltru[z+1,i], no need to interpolate, assign rho=0
```

```
      if (floor(Lmat[i]) >= floor(Ltru[z+1,i]))
      {
         AllocFwd[z+1,i] <- 0
      }

      if (floor(Lmat[i]) < floor(Ltru[z+1,i]))
      {
         AllocFwd[z+1,i] <- interp2D(Lmin, Lpan,
                                     Lmin, Lpan,
                                     Ltru[z+1,i], Lmat[i],
                                     rho.arr[z+1,,])
      }
   }

   # if you're already mature... then use Lmat from the time you matured
   # interpolate optimal allocation based on current length and length
                               at maturity
   if ( sum(MatFwd[1:z,i],na.rm=T)>1 )
   {
      # Calculate updated mature length, given current length and Lmat
      Lpot.T   <- Ltru[z,i] + dL1(Ltru[z,i], Lmat)
      Wnow.T   <- a * Ltru[z,i]^b
      Wpot.T   <- a * Lpot.T^b
      dW.T[z,i] <- Wpot.T - Wnow.T
      Wrho.T <- Wnow.T + (1-AllocFwd[z,i])*dW.T[z,i] # Somatic mass
      Gonads[z,i] <- AllocFwd[z,i]*dW.T[z,i]*exp(-mu.p * AllocFwd[z,i] *
                               dW.T[z,i])
      logLrho.T <- (1/b)*log(Wrho.T/a)
      Ltru[z+1,i] <- max(exp(logLrho.T),Ltru[z,i])
      Wtru[z+1,i] <- Wrho.T

      # 2-D interpolation of allocation (rho)
      if (floor(Lmat[i]) >= floor(Ltru[z,i]))
      {
          AllocFwd[z+1,i] <- 0
      }

      if (floor(Lmat[i]) < floor(Ltru[z,i]))
      {
         AllocFwd[z+1,i] <- interp2D(Lmin, Lpan,
                                     Lmin, Lpan,
                                     Ltru[z+1,i], Lmat[i],
                                     rho.arr[z+1,,])
      }
   }

   # record M(L,GSI) in each time step for each fish
   Mtru[z,i] <- M(Ltru[z,i], Gonads[z,i]/Wtru[z,i])

  } # end of fish loop
} # end of time loop
```

References

Akaike, H. 1973. Information Theory and an Extension of the Maximum Likelihood Principle. In: B. N. Petrov and F. Csaki, eds. Second International Symposium on Information Theory. Budapest: Akademiai Kiado, pp. 267–281.

Arizona Software. 2008. GraphClick. http://www.arizona-software.ch/

Bagenal, T. B. 1957. Annual variations in fish fecundity. Journal of the Marine Biological Association of the U.K. 36:377-382

Bagenal, T. B. 1967. A short review of fish fecundity. *In*: Gerking, S. D. (Ed.) The Biological Basis of Freshwater Fish Production. John Wiley & Sons, Inc., New York. pp. 89-111

Bagenal T. B. 1973. Fish fecundity and its relations with stock and recruitment. Rapports et Procès-Verbaux des Réunions du Conseil International pour l'Exploration de la Mer 164:186–198

Beamish, R. J., G. A. McFarlane, A. Benson. 2006. Longevity overfishing. Progress in Oceanography 68:289-302

Benet, D., E.J. Dick, and D. Pearson. (in prep). Life history aspects of greenspotted rockfish (*Sebastes chlorostictus*) from central California.

Berkeley, S. A., C. Chapman and S. M. Sogard. 2004. Maternal age as a determinant of larval growth and survival in a marine fish, *Sebastes melanops*. Ecology 85(5):1258-1264

Beverton, R. J. H. 1987. Longevity in fish: some ecological and evolutionary considerations. *In* Woodhead, A. D. and K. H. Thompson (Eds.). Evolution of Longevity in Animals. Plenum Press, N.Y.

Beverton, R. J. H. 1992. Patterns of reproductive strategy parameters in some marine teleost fishes. Journal of Fish Biology 41 (Supplement B): 137-160

Beverton, R. J. H. and S. J. Holt. 1957. On the dynamics of exploited fish populations. Crown Copyright, reprinted in 2004 by Blackburn Press.

Beverton, R. J. H. and S. J. Holt. 1959. A review of the lifespans and mortality rates of fish in nature, and their relation to growth and other physiological characteristics. CIBA Foundation Colloquia on Ageing 54:142-180

Bobko, S. J. and S. A. Berkeley. 2004. Maturity, ovarian cycle, fecundity, and age-specific parturition of black rockfish (*Sebastes melanops*). Fishery Bulletin 102:418-429

Boehlert, G. W., W. H. Barss and P. B. Lamberson. 1982. Fecundity of the widow rockfish, Sebastes entomelas, off the coast of Oregon. Fishery Bulletin 80(4):881-884

Boehlert, G. W. and M. M. Yoklavich. 1984. Reproduction, embryonic energetics, and the maternal-fetal relationship in the viviparous genus *Sebastes* (Pisces: Scorpaenidae). Biological Bulletin 167:354-370

Bowers, M. J. 1992. Annual reproductive cycle of oocytes and embryos of yellowtail rockfish *Sebastes flavidus* (Family Scorpaenidae). Fishery Bulletin 90:231-242.

Clemens, W. A. and G. V. Wilby. 1949. Fishes of the Pacific Coast of Canada. Fisheries Research Board of Canada Bulletin 58 (rev.).

Chen, L. 1971. Systematics, variation, distribution, and biology of rockfishes of the subgenus *Sebastomus* (Pisces, Scorpaenidae, *Sebastes*). Bulletin of the Scripps Institute of Oceanography, University of California, San Diego, Volume 18. University of California Press. 115 p.

Chilton, D. E. and R. J. Beamish. 1982. Age determination methods for fishes studied by the groundfish program at the Pacific biological station, Canadian Special Publication of Fisheries and Aquatic Sciences, 60 p.

Clark, W. G. 1991. Groundfish exploitation rates based on life history parameters. Canadian Journal of Fisheries and Aquatic Sciences 48:734-750

Clark, W. G. 2002. $F_{35\%}$ revisited ten years later. North American Journal of Fisheries Management 22:251–257

Clark, C. W. and M. Mangel. 2000. Dynamic State Variable Models in Ecology: Methods and Applications. Oxford University Press.

Clemens, W. A. and G. V. Wilby. 1949. Fishes of the Pacific Coast of Canada. Fisheries Research Board of Canada Bulletin 58 (rev.). 368 p.

Conover, D. and S. B. Munch. 2002. Sustaining fisheries yields over evolutionary time scales. Science 297:94-96

Corlett, J. 1964. Fecundity of redfish from East Greenland. Annales Biol., Copenh. 19:78

Crow, E. L. and K. Shimizu. 1988. Lognormal Distributions: theory and applications. Marcel Dekker, Inc. N.Y.

Day, T. and P. D. Taylor. 1997. von Bertalanffy's growth equation should not be used to model age and size at maturity. The American Naturalist. 149(2):381-393

de Bruin, J-P, R. G. Gosden, C. E. Finch and B. M. Leaman. 2004. Biology of Reproduction 71, 1036–1042

Delacy, A.C., C. R. Hitz, and R.L. Dryfoos. 1964. Maturation, gestation, and birth of rockfish (*Sebastodes*) from Washington and adjacent waters. Washington Department of Fisheries, Research Paper, 2:51-67

Dorn, M. W. 2002. Advice on west coast rockfish harvest rates from Bayesian meta-analysis of stock-recruitment relationships. North American Journal of Fisheries Management 22:280-300

Draper, D. 2005. Bayesian Modeling, Inference and Prediction (Draft 6). Course reader for AMS-206, University of California, Santa Cruz.

Echeverria, T., and W. H. Lenarz. 1984. Conversions between total, fork and standard lengths in 35 species of Sebastes from California. Fishery Bulletin 82:249–251.

Eldridge, M. B., J. A. Whipple, M. J. Bowers, B. M. Jarvis, and J. Gold. 1991. Reproductive performance of yellowtail rockfish, *Sebastes flavidus*. Environmental Biology of Fishes 30:91-102.

Eldridge, M. B. and B. M. Jarvis. 1995. Temporal and spatial variation in fecundity of yellowtail rockfish. Transactions of the American Fisheries Society. 124:16-25.

Fisher, R. A. 1930. A Genetical Theory of Natural Selection. Oxford University Press. 272 p.

Fraser, C. M. 1923. Ichthyological notes. Contrib. Can. Biol. N.S. 1:285-295.

Fulton, T.W. 1898. On the growth and maturation of the ovarian eggs of the teleostean fishes. Fisheries Board of Scotland Annual Report 16:88-124

Fulton, T. W. 1904. The rate of growth of fishes. Fisheries Board of Scotland Annual Report 22 (part 3):141-241, Edinburgh

Gelman, A., J. B. Carlin, H. S. Stern and D. B. Rubin. 2004. Bayesian Data Analysis, 2nd Ed. Chapman and Hall/CRC. 668 p.

Goodyear, C. P. 1993. Spawning stock biomass per recruit in fisheries management: foundation and current use. p. 67-81. *In* S. J. Smith, J. J. Hunt and D. Rivard [ed.] Risk evaluation and biological reference points for fisheries management. Canadian Special Publication of Fisheries and Aquatic Sciences 120.

Gulland, J. A. 1983. Fish Stock Assessment: A Manual of Basic Methods. FAO/Wiley Series on Food and Agriculture, Vol. 1. John Wiley and Sons, 223 p.

Gunderson, D. R. 1976. Population biology of Pacific Ocean Perch (Sebastes alutus) stocks in the Washington-Queen Charlotte Sound Region, and their response to fishing. Ph.D. dissertation, University of Washington. 140 p.

Gunderson, D. R. 1977. Population biology of Pacific Ocean Perch, *Sebastes alutus*, stocks in the Washington-Queen Charlotte Sound region, and their response to fishing. Fishery Bulletin 75(2):369-403

Gunderson, D. R., P. Callahan and B. Goiney. 1980. Maturation and Fecundity of Four Species of *Sebastes*. Marine Fisheries Review 42:74-79.

Gunderson, D. R. 1997. Trade-off between reproductive effort and adult survival in oviparous and viviparous fishes. Canadian Journal of Fisheries and Aquatic Sciences 54:990-998

Haldorson, L. and M. Love. 1991. Maturity and fecundity in the rockfishes, *Sebastes* spp., a review. Marine Fisheries Review 53(2):25-31

Heino, M. and V. Kaitala. 1999. Evolution of resource allocation between growth and reproduction in animals with indeterminate growth. Journal of Evolutionary Biology 12:423-429

Helser, T. E., I. J. Stewart and H. Lai. 2007. A Bayesian hierarchical meta-analysis of growth for the genus *Sebastes* in the eastern Pacific Ocean. Canadian Journal of Fisheries and Aquatic Sciences 64:470-485.

Houston, A. I. and J. M. McNamara. 1999. Models of Adaptive Behaviour: An Approach Based on State. Cambridge University Press. 388 pp.

Hunter, J.R. and B.J. Macewicz. 2003. Improving the accuracy and precision of reproductive information used in fisheries. Report of the Working Group on Modern Approaches to Assess Maturity and Fecundity of Warm- and Cold-water Fish and Squids. Fisken Havet 12:57–68

Hyde, J. R. and R. D. Vetter. 2007. The origin, evolution, and diversification of rockfishes of the genus *Sebastes* (Cuvier). Molecular Phylogenetics and Evolution 44:790-811

Ito, D. H. 1977. Fecundity of the copper rockfish, *Sebastes caurinus* (Richardson) from Puget Sound, Washington. Paper submitted to Professor Bruce Miller as part of project for Fisheries 499, a class at the University of Washington, Seattle. This report does not constitute a publication, and was not peer-reviewed. Used by permission.

Johns, G. C. and J. C. Avise. 1998. Tests for ancient species flocks based on molecular phylogenetic appraisals of *Sebastes* rockfishes and other marine species. Evolution 52(4):1135-1146

Kendall, A. W. 2000. An historical review of *Sebastes* taxonomy and systematics. Marine Fisheries Review 62(2):1-23

Kozlowski, J. 1992. Optimal allocation of resources to growth and reproduction: implications for age and size at maturity. Trends in Ecology and Evolution 7(1):15-19

Kozlowski, J. 1996. Optimal allocation of resources explains interspecific life-history patterns in animals with indeterminate growth. Proceedings of the Royal Society of London B 263:559-566

Kozlowski, J. and J. Uchmanski. 1987. Optimal individual growth and reproduction in perennial species with indeterminate growth. Evolutionary Ecology 1:214-230.

Kozlowski, J., M. Czarnoleski and M. Danko. 2004. Can optimal resource allocation models explain why ectotherms grow larger in cold? Integrative and Comparative Biology 44:480-493

Kusakari, M. 1991. Mariculture of kurosoi, *Sebastes schlegeli*. Environmental Biology of Fishes 30:245-251

Kutner, M. H., C. J. Nachtsheim, J. Neter and W. Li. 2005. Applied Linear Statistical Models, 5th Ed. McGraw-Hill Irwin. 1396 p.

Le Cren, E. D. 1951. The length-weight relationship and seasonal cycle in gonad weight and condition in the perch *Perca fluviatilis*. Journal of Animal Ecology 20:201-219

Lea, R. N., R. D. McAllister, and D. A. VenTresca. 1999. Biological Aspects of Nearshore Rockfishes of the Genus *Sebastes* from Central California With Notes On Ecologically Related Sport Fishes. Scripps Institution of Oceanography Library. Fish Bulletin: 177. http://repositories.cdlib.org/sio/lib/fb/177

Lenarz, W. H. and T. Wyllie Echeverria. 1986. Comparison of visceral fat and gonadal fat volumes of yellowtail rockfish, *Sebastes flavidus*, during a normal year and a year of El Niño conditions. Fishery Bulletin 84(3):743-745

Lester, N. P., B. J. Shuter, and P. A. Abrams. 2004. Interpreting the von Bertalanffy model of somatic growth in fishes: the cost of reproduction. Proceedings of the Royal Society of London B 271:1625-1631

Li, Z., A. K. Gray, M. S. Love, A. Goto and A. J. Gharrett. 2007. Are the subgenera of *Sebastes* monophyletic? p. 185-206 *In* Biology, Assessment, and Management of North Pacific Rockfishes. Alaska Sea Grant College Program. AK-SG-07-01.

Love, M. S. 1978. Aspects of life history of the olive rockfish, *Sebastes serranoides*. Ph.D. thesis, University of California, Santa Barbara, 195 p.

Love, M. S., and W. V. Westphal. 1981. Growth, reproduction, and food habits of olive rockfish, *Sebastes serranoides*, off central California. Fishery Bulletin 79:533–545

Love, M., P. Morris, M. McCrae, and R. Collins. 1990. Life history aspects of 19 rockfish species (Scorpaenidae: *Sebastes*) from the Southern California Bight. NOAA Technical Report NMFS 87: 38 p.

Love, M. and K. Johnson. 1998. Aspects of the life histories of grass rockfish, *Sebastes rastrelliger*, and brown rockfish, S. auriculatus, from southern California. Fishery Bulletin 87: 100-109

Love, M. S., M. Yoklavich and L. Thorsteinson. 2002. The Rockfishes of the Northeast Pacific. University of California Press.

Kusakari, M. 1991. Mariculture of kurosoi, *Sebastes schlegeli*. Environmental Biology of Fishes 30:245-251

MacCall, A. D. 1999. Use of decision tables to develop a precautionary approach to problems in behavior, life history, and recruitment variability. NOAA Tech. Memo. NMFS-F/SPO-40, pp. 53-64

MacFarlane, R. B., E. C. Norton and M. J. Bowers. 1993. Lipid dynamics in relation to the annual reproductive cycle in yellowtail rockfish (*Sebastes flavidus*). Canadian Journal of Fisheries and Aquatic Sciences 50:391-401

MacFarlane, R. B. and M. J. Bowers. 1995. Matrotrophic viviparity in the yellowtail rockfish *Sebastes flavidus*. Journal of Experimental Biology 198:1197-1206

MacGregor, J. S. 1970. Fecundity, multiple spawning, and description of the gonads in *Sebastodes*. United States Fish and Wildlife Service Special Scientific Report, Fisheries No. 596. 12 pp.

Mangel, M. S. 2003. Environment and longevity: The demography of the growth rate. Population and Development Review 29 (Supplement):57-70

Mangel, M. and C. W. Clark. 1988. Dynamic Modeling in Behavioral Ecology. Princeton University Press.

Mangel, M. S. and D. Ludwig. 1992. Definition and evaluation of behavioral and developmental programs. Annual Review of Ecology and Systematics 23:507-536.

Mangel, M., H. K. Kindsvater, and M. B. Bonsall. 2007. Evolutionary analysis of life span, competition, and adaptive radiation, motivated by the Pacific rockfishes (*Sebastes*). Evolution 61(5):1208-1224

Methot, R. D. 2005. Technical description of the Stock Synthesis II assessment program.

Miller, D. J. and J. J. Geibel. 1973. Summary of Blue Rockfish and Lingcod Life Histories; A Reef Ecology Study; And Giant Kelp, *Macrocystis Pyrifera*, Experiments In Monterey Bay, California. Scripps Institution of Oceanography Library. Fish Bulletin: 158. http://repositories.cdlib.org/sio/lib/fb/158

Miller, T. E. X., B. Tenhumberg, and S. M. Louda. 2008. Herbivore-mediated ecological costs of reproduction shape the life history of an iteroparous plant. The American Naturalist 171(2):141-149

Morgan, M. J. 2008. Integrating reproductive biology into scientific advice for fisheries management. Journal of Northwest Atlantic Fishery Science 41: 37–51

Moser, H. G. 1967. Reproduction and development of *Sebastodes paucispinis* and comparisons with other rockfishes off Southern California. Copeia 4:773:797

Moulton, L. L. 1975. Life history observations on the Puget Sound Rockfish, *Sebastes emphaeus* (Starks, 1911). Journal of the Fisheries Research Board of Canada 32:1439-1442.

Murawski, S. A., P. J. Rago and Trippel, E. A. 1999. Impacts of demographic variation in spawning success on reference points for fishery management. NOAA Tech. Memo. NMFS-F/SPO-40, pp. 77-85.

Murphy, G. I. 1968. Pattern in life history and the environment. The American Naturalist 102:391-403

Murua, H. and F. Saborido-Rey. 2003. Female reproductive strategies of marine fish species of the North Atlantic. Journal of Northwest Atlantic Fishery Science 33:23-31

Murua, H., G. Kraus, F. Saborido-Rey, P. R. Witthames, A. Thorsen, and S. Junquera. 2003. Procedures to estimate fecundity of marine fish species in relation to their reproductive strategy. Journal of Northwest Atlantic Fishery Science 33: 33-54.

Myers, R. A. and R. W. Doyle. 1983. Predicting natural mortality rates and reproduction-mortality trade-offs from life history data. Canadian Journal of Fisheries and Aquatic Sciences. 40:612-620

Mylius, S. D. and O. Diekmann. 1995. On evolutionarily stable life histories, optimization and the need to be specific about density dependence. Oikos 74:218-224

Nichol, D. G. and E. K. Pikitch. 1994. Reproduction of darkblotched rockfish off the Oregon coast. Transactions of the American Fisheries Society 123: 469-481.

Noren, D.P. and M. Mangel. 2004. Energy reserve allocation in fasting Northern Elephant Seal Pups: inter-relationships between body condition and fasting duration. Functional Ecology 18:233-242

Parker, R. R. and P. A. Larkin. 1959. A concept of growth in fishes. Journal of the Fisheries Research Board of Canada 16(5):721-745

Perrin, N. and R. M. Sibly. 1993. Dynamic models of energy allocation and investment. Annual Review of Ecology and Systematics 24:379-410

Perrin, N., R. M. Sibly and N. K. Nichols. 1993. Optimal growth strategies when mortality and production rates are size-dependent. Evolutionary Ecology 7:576-592

PFMC (Pacific Fishery Management Council). 2006. Pacific Coast Groundfish Fishery Management Plan for the California, Oregon, and Washington groundfish fishery as amended through Amendment 19. Pacific Fishery Management Council, Portland, OR, USA.

Phillips, J. B. 1964. Life history studies on ten species of rockfish (genus *Sebastodes*). California Department of Fish and Game, Fish Bulletin 126. 158 pp.

Plummer, M., N. Best, K. Cowles and K. Vines. 2008. coda: Output analysis and diagnostics for MCMC. R package version 0.13-3.

Prager, M. 2006. 4D contour plot. http://addictedtor.free.fr/graphiques/graphcode.php?graph=90.

Quinn, T. J. and R. B. Deriso. 1999. Quantitative Fish Dynamics. Oxford University Press. 560 p.

R Development Core Team. 2008. R: A language and environment for statistical computing. R Foundation for Statistical Computing, Vienna, Austria. ISBN 3-900051-07-0, URL http://www.R-project.org.

Raitt, D. S. 1933. The fecundity of the haddock. Scientific Investigations of the Fishery Board for Scotland, 40 p.

Raitt, D. S. and W. B. Hall. 1967. On the fecundity of the redfish, *Sebastes marinus* (L.). Journal du Conseil International pour l'Exploration de la Mer 31(2):237-245

Ralston, S. 1998. The Status of Federally Managed Rockfish on the U.S. West Coast, In: Marine Harvest Refugia for West Coast Rockfish, A Workshop, Mary M. Yoklavich, Ed. NMFS Pacific Fishery Environmental Laboratory. NOAA Technical Memorandum NOAA-TM-NMFS-SWFSC-255. pp. 6-16.

Ralston, S. 2002. West coast groundfish harvest policy. North American Journal of Fisheries Management 22:249-250.

Ralston, S. and D. F. Howard. 1995. On the development of year-class strength and cohort variability in two northern California rockfishes. Fishery Bulletin 93:710-720

Ralston, S. and B. R. MacFarlane. (in prep.). Population estimation of bocaccio (*Sebastes paucispinis*) based on larval production in the southern California Bight.

Richards, L. J. and B. Emmett. 1988. Methods used for fecundity estimation of rockfish and lingcod ovaries. Canadian Data Report of Fisheries and Aquatic Sciences No. 707. 44 p.

Richards, L. J. and J. T. Schnute. 1990. Use of a general dose-response model for rockfish fecundity-length relationships. Canadian Journal of Fisheries and Aquatic Sciences 47:1148-1156

Rocha-Olivares, A., C. A. Kimbrell, B. J. Eitner and R. D. Vetter. 1999a. Evolution of a mitochondrial cytochrome b gene sequence in the species-rich genus *Sebastes* (Teleostei, Scorpaenidae) and its utility in testing the monophyly of the subgenus *Sebastomus*. Molecular Phylogenetics and Evolution 11(3):426-440

Rocha-Olivares, A., R. H. Rosenblatt and R. D. Vetter. 1999b. Molecular evolution, systematics, and zoogeography of the rockfish subgenus *Sebastomus* (*Sebastes*, Scorpaenidae) based on mitochondrial cytochrome b and control region sequences. Molecular Phylogenetics and Evolution 11(3):441-458

Roff, D. A. 1983. An allocation model of growth and reproduction in fish. Canadian Journal of Fisheries and Aquatic Sciences 40:1395-1404

Roff, D. A. 1984. The evolution of life history parameters in teleosts. Canadian Journal of Fisheries and Aquatic Sciences 41:989-1000

Roff, D. A., E. Heibo and L. A. Vøllestad. 2006. The importance of growth and mortality costs in the evolution of optimal life history. Journal of Evolutionary Biology 19(6):1920-1930

Romero, M. 1988. Life history of the kelp rockfish, *Sebastes atrovirens* (Scorpaenidae). Masters thesis, San Francisco State University, 49 pp.

Rothschild, B. J. and M. J. Fogarty. 1989. Spawning-stock biomass: a source of error in recruitment/stock relationships and management advice. Journal du Conseil International pour l'Exploration de la Mer 45:131-135

Sars, G. O. 1876. On the spawning and development of the cod-fish. Report of the United States Fish Commission, 3 (Appendix): 213–222.

Sibly, R., P. Calow, and N. Nichols. 1985. Are patterns of growth adaptive? Journal of Theoretical Biology 112:553-574

Simpson, A. C. 1951. The fecundity of the plaice. Fish. Invest. Ser. 2, Vol. 17, No. 5, 27 pp.

Sissenwine, M. P. and J. G. Shepherd. 1987. An alternative perspective on recruitment overfishing and biological reference points. Canadian Journal of Fisheries and Aquatic Sciences 44:913-918.

Sogard, S. M., S. A. Berkeley and R. Fisher. 2008. Maternal effects in rockfishes *Sebastes* spp.: a comparison among species. Marine Ecology Progress Series 360:227-236

Sogard, S. M., D. Stafford and N. Kashef. Unpublished data.

Snytko, V. A., and L. A. Borets. 1973. Some data on the fecundity of ocean perch in the Vancouver-Oregon region. (translated from Russian). Fisheries Research Board of Canada Translation Series No. 2502. 5 p.

St.-Pierre, J-F, and Y. de Lafontaine. 1995. Fecundity and reproduction characteristics of beaked redfish (*Sebastes fasciatus* and *S. mentella*) in the Gulf of St. Lawrence. Canadian Technical Report of Fisheries and Aquatic Sciences 2059. 32 p.

Stamps, J. A., M. S. Mangel, and J. A. Phillips. 1998. A new look at the relationships between size at maturity and asymptotic size. The American Naturalist. 152(3):470-479

Stanley, R. D. and A. R. Kronlund. 2005. Life history characteristics for silvergray rockfish (Sebastes brevispinis) in British Columbia waters and the implications for stock assessment and management. Fishery Bulletin 103:670-684.

Stearns, S. C. 1992. The Evolution of Life Histories. Oxford University Press.

Svärdson, G. 1949. Natural selection and egg number in fish. Report of the Institute of Freshwater Research, Drottningholm 29:115-122

Taylor, H. M., R. S. Gourley, C.E. Lawrence, and R. S. Kaplan. 1974. Natural selection of life history attributes: an analytical approach. Theoretical Population Biology 5:104-122

Tomkiewicz, J., M. J. Morgan, J. Burnett, and F. Saborido-Rey. 2003. Available information for estimating reproductive potential of Northwest Atlantic Groundfish Stocks. Journal of Northwest Atlantic Fishery Science 33: 1-21

Trippel, E. A., O. S. Kjesbu and P. Solemdal. 1997. Effects of adult age and size structure on reproductive output in marine fishes. pp. 31-62 *In* Early Life History and Recruitment in Fish Populations, Chapman and Hall, 596 p.

Trippel, E. A. 1999. Estimation of stock reproductive potential: history and challenges for Canadian Atlantic gadoid stock assessments. Journal of Northwest Atlantic Fishery Science 25:61-81

VenTresca, D. A., R. H. Parrish, J. L. Houk, M. L. Gingras, S. D. Short and N. L. Crane. 1995. El Niño effects on the somatic and reproductive condition of blue rockfish, *Sebastes mystinus*. CalCOFI Reports 36:167-174

von Bertalanffy, L. 1938. A quantitative theory of organic growth (inquiries on growth laws. II). Human Biology 10(2):181-213

Wallace, F., Y. W. Cheng, T. Tsou. 2008. Status of the black rockfish resource north of Cape Falcon, Oregon to the U.S.-Canadian border in 2006. Status of the Pacific Coast groundfish fishery through 2007, Stock assessment and fishery evaluation Stock Assessments and Rebuilding Analyses. 2008. Portland, Oregon, PFMC.

Waples, R. S., A. E. Punt, and J. M. Cope. 2008. Integrating genetic data into management of marine resources: how can we do it better? Fish and Fisheries 9:423-449

Ware, D. M. 1980. Bioenergetics of stock and recruitment. Canadian Journal of Fisheries and Aquatic Sciences 37:1012-1024

Washington, P.M., R. Gowan, and D.H. Ito. 1978. A biological report on eight species of rockfish (*Sebates* spp.) from Puget Sound, Washington. Northwest and Alaska Fisheries Centers Proc. Reprot. Natinal Marine Fisheries Service, Seattle, Washington. 50 p.

Westrheim, S. J. 1958. On the Biology of the Pacific Ocean Perch, *Sebastodes alutus* (Gilbert). University of Washington Masters Thesis. 106 p.

Westrheim, S. J. 1975. Reproduction, maturation, and identification of larvae of some *Sebastes* (Scorpaenidae) species in the Northeast Pacific Ocean. Journal of the Fisheries Research Board of Canada 32:2399-2411.

Wooton, R. J. 1979. Energy costs of egg production and environmental determinants of fecundity in teleost fishes. Symposia of the Zoological Society of London 44:133-159

Wooton, R. J. 1998. Ecology of Teleost Fishes, 2nd ed. Fish and Fisheries Series 24, Kluwer Academic Publishers, 386 p.

Wyllie Echeverria, T. 1987. Thirty-four species of California rockfishes: maturity and seasonality of reproduction. Fishery Bulletin 85(2):229-250

Yoklavich, M. (Ed.). 1998. Marine harvest refugia for west coast rockfish: a workshop. NOAA, NMFS Tech. Memo. NOAA-TM-NMFS-SWFSC-255. 159 p.